TWO-POINT VARIABILITY OF WIND

by

C. Eugene Buell

VOLUME TWO

Report No. KN-173-62-2(FR)

Final Report
Contract No. AF19(604)7282
July, 1962

Project 8624
Task 862402

GEOPHYSICS RESEARCH DIRECTORATE
AIR FORCE CAMBRIDGE RESEARCH LABORATORIES
OFFICE OF AEROSPACE RESEARCH
UNITED STATES AIR FORCE
BEDFORD, MASSACHUSETTS

Kaman Nuclear
COLORADO SPRINGS, COLORADO
A DIVISION OF KAMAN AIRCRAFT CORPORATION

DISCLAIMER NOTICE

THIS DOCUMENT IS BEST QUALITY PRACTICABLE. THE COPY FURNISHED TO DTIC CONTAINED A SIGNIFICANT NUMBER OF PAGES WHICH DO NOT REPRODUCE LEGIBLY.

AFCRL-62-889 (II)

TWO-POINT VARIABILITY OF WIND

by

C. Eugene Buell

Kaman Nuclear
Colorado Springs, Colorado

VOLUME TWO

Report No. KN-173-62-2(FR)

Final Report
Contract No. AF19(604)7282

July, 1962

Project 8624
Task 86242

GEOPHYSICS RESEARCH DIRECTORATE
AIR FORCE CAMBRIDGE RESEARCH LABORATORIES
OFFICE OF AEROSPACE RESEARCH
UNITED STATES AIR FORCE
BEDFORD, MASSACHUSETTS

NOTICES

"Requests for additional copies by Agencies of the Department of Defense, their contractors, and other Government agencies should be directed to the:

ARMED SERVICES TECHNICAL INFORMATION AGENCY
ARLINGTON HALL STATION
ARLINGTON 12, VIRGINIA

Department of Defense contractors must be established for ASTIA services or have their 'need to know' certified by the cognizant military agency of their project or contract."

"All other persons and organizations should apply to the:

U.S. DEPARTMENT OF COMMERCE
OFFICE OF TECHNICAL SERVICES
WASHINGTON 25, D.C."

TABLE OF CONTENTS

VOLUME TWO

* * * PART THREE * * *

LIST OF FIGURES

VOLUME TWO

TWO-POINT VARIABILITY OF WIND

by

C. Eugene Buell

Kaman Nuclear
Colorado Springs, Colorado

VOLUME TWO

The reason for dividing this report into three volumes is to keep the bulk of paper in each within reasonable limits. The text material of Volumes One and Two is continuous and neither volume is complete without the other. Volume Three contains the Appendices of the B-series. These are extensive tables which are not required except as a record for those who would care to investigate the subject more extensively.

* * * PART TWO * * *

CHAPTER VI

SYNOPTIC SCALE VARIABILITY OF WINDS WITH TIME AND HEIGHT DIFFERENCES AS PARAMETERS

Chapter VI is devoted to extending the analysis of wind variability from the case in which the two points concerned are located on an isobaric surface and winds are observed simultaneously to the more general case in which the winds are observed at two points that are on different isobaric surfaces and may be measured at significantly different times.

The wind variability in such cases has been studied extensively for the particular cases of the variability in time at a particular point. Another important special case that has been studied extensively is that of the variability of wind with height at a given location (essentially simultaneous measurements of winds over a fixed point at different levels). The references available on these two special cases are extensive and are well summarized by Major Hugh W. Ellsaesser.(1) The correlation of winds obtained in each of these two special cases show peculiarities which require some explanation. This explanation is far from obvious when these special cases are considered separately, but when the whole picture is considered the major variation of the observed correlations fit a reasonably straightforward analysis. In other words, to explain the phenomena observed in the variability of winds with time and with height requires a complete four-dimensional analysis of the variability of wind, three space co-ordinates and a time co-ordinate.

There is a tendency to "equate" time variability of wind and variability of wind with distance.[1-2] Though such a rough and ready relation is handy for some purposes, it will be seen that the phenomena concerned is somewhat too complex and that a more detailed separation of the influences is required.

A. VERBAL DESCRIPTION OF STRUCTURE OF CORRELATION TENSOR COMPONENTS

The basic item to consider in treating the two-point variability of wind in space and time is the structure of the components of the wind correlation tensor. The form of the components of this tensor was discussed extensively in Chapter III and the relation to the height correlation functions was given in equation (7). An ideal description of the components of the wind correlation tensor was presented in Fig. III-3 for the case of the two points on an isobaric surface.

1. Variation in the Vertical

To introduce a third dimension into this description one starts by depicting a family of illustrations like Fig. III-3 stacked on top of each other. The point P is located at the origin of co-ordinates (in the case of each individual component) on the "center" sheet of the stack. The point P′ is located on some other sheet of the stack.

So far, all sheets of the stack are identical. Now modify somewhat all sheets (except the center sheet containing P) working up and down from the center sheet in a roughly symmetrical manner. The first modification is to "degrade" the correlation coefficient values, i.e. reduce the numerical value. This is done progressively outward from the center sheet. In our original stack, the surfaces of constant correlation coefficients were vertical cylinders. When the correlation coefficient values are "degraded", these cylinders become closed over at "top" and "bottom" to become somewhat like ellipsoids.

The second modification that should be made is to tilt the stack or to introduce a shear in the sheets. This corresponds to the well-known tilt of axis of highs and lows in the atmosphere. The direction of shear is predominantly in the east-west direction (though not necessarily exactly so).

At this point, one may begin to see one of the characteristics of the behavior of wind component correlations in the vertical. In modifying the components of the wind correlation tensor, each component was modified in the same manner. But in Fig. III-3 the correlation contours for r_{11} and for r_{22} (for the east pointing and the north pointing components at both P and P′ respectively) are rotated at right angles to each other. The introduction of some tilt or shear in the east-west direction affects these two components of the correlation tensor quite differently. In the case of r_{11} the shear is in the same direction as the longest direction of the ovals of equal correlation value while in the case of r_{22} the direction of shear is in the direction of the shortest dimension of the ovals of equal correlation value. As a result, as one progresses upward (or downward) from the central sheet the value of r_{22} will decay slightly more rapidly than the value of r_{11}. (This is more pronounced in the lower troposphere where the tilt of highs and lows is greatest.)

2. Variation with Time

The addition of time as a variable (to the case of P and P′ on the same isobaric surface) may be depicted in an

analogous manner. First one considers a transparent overlay for Fig. III-3 which contains the four sets of co-ordinate axes. The point P is the origin of co-ordinate for each of these sets of axes, one for each component of the wind correlation tensor.

The remaining steps are similar to those described in connection with the wind correlation in the vertical, degradation and shift. First, consider the correlation contour values to be reduced (in magnitude) with the passage of time. Second, consider the degraded contours to be shifted eastward (roughly) with the passage of time. The correlation coefficient of a wind component at P with a wind component at P′ is indicated by the degraded and shifted correlation contour patterns. Note that the geographical locations of P and P′ are fixed so that these two points are located on the overlay that has the co-ordinate axes.

The correlation coefficients that would be obtained in considering the variation of wind at a single point are given when P′ lies at the origin of co-ordinates (coincident with P). In this instance, it is readily seen that the value of r_{11} drops off more slowly than r_{22} because the direction of shift of the pattern with the passage of time is roughly in the direction of the elongated contours of r_{11} and transverse to the direction of elongation of the contours of r_{22}.

The situation for observations made at the points P′ 24 hours ahead of that at P (Columbia, Mo., at the Star) is illustrated in Fig. VI-1 in the case of components r_{11} and r_{22} (Winter, 100 mb).

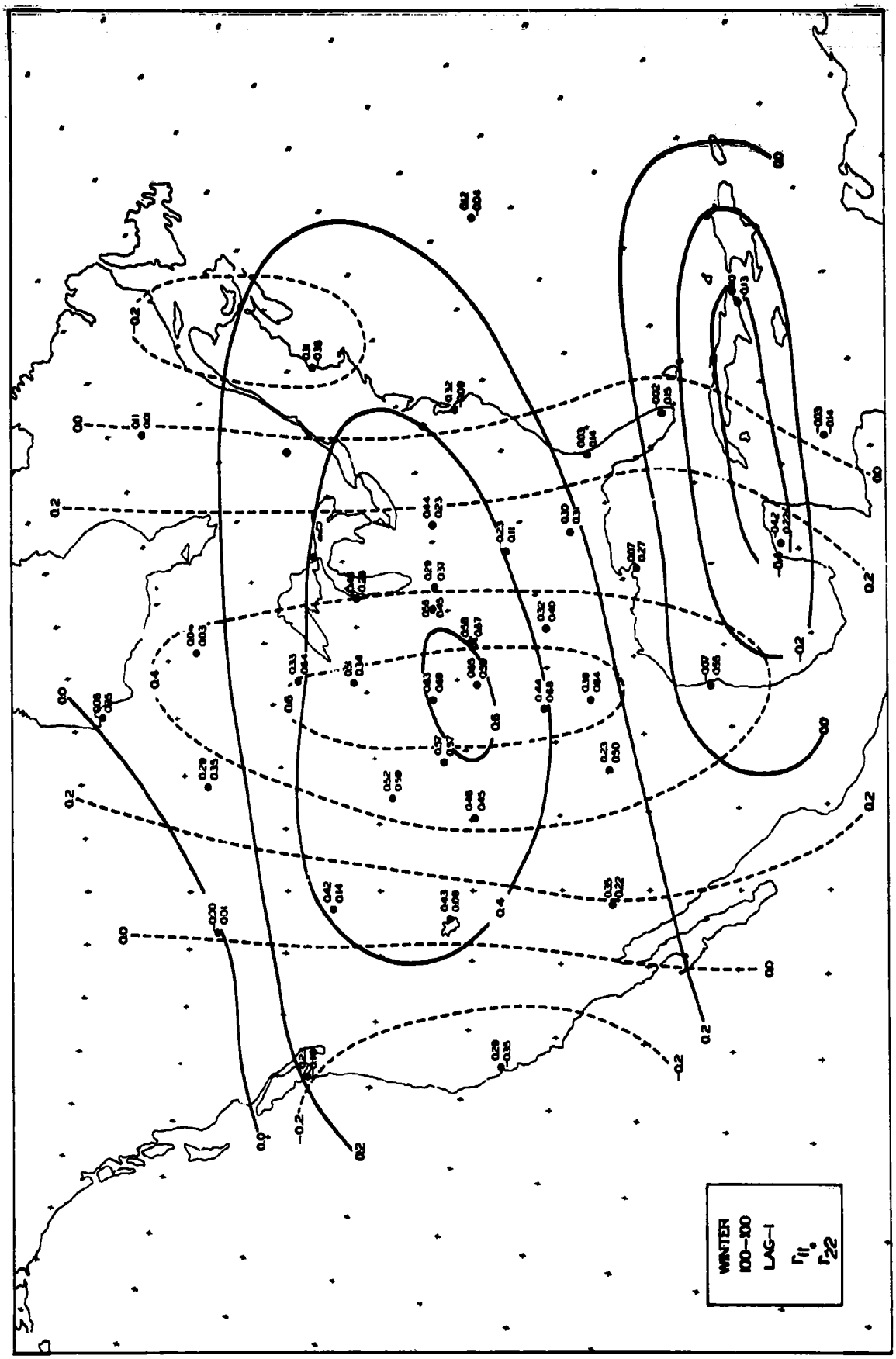

Fig. VI-1 Contours of r_{11} (full) and r_{22} (dashed), 100 mb, Winter, ABMA Data. Observations at P' made 24 hours before those at P (Columbia, Mo.)

If one combines variation with time and distance, then the points P and P′ are separate. The point P is at the origin of co-ordinates. The correlation values for each component are read at the location of P′ (not P) from the shifted and degraded correlation contours.

The situation becomes extremely complex when time variability at a point is considered and the correlations are computed along and across the wind direction. However, even in such cases, for the upper air, the wind direction is sufficiently consistent to show a more rapid decrease in the cross-wind component correlations than in that along the wind.

3. Some Further Considerations

In the preceding verbal description of the construction of the components of the wind correlation tensor as functions of differences in level and time, only the most elementary aspects of the situation are described. It will be noted that reference is made to Fig. III-3 and not to Fig. III-4 where the tensor components are in terms of transverse and longitudinal wind components. When the height and time variables are introduced, the concept of longitudinal and transverse wind components become unnecessarily complex, more complex than reverting back to the fact that the point of maximum correlation departs appreciably from the location of the point P. In order to maintain the idea of longitudinal and transverse wind components, it would be necessary to measure these along and across the direction joining the point of maximum correlation to the point P′. This direction

is not known before the fact. Further, even when the point of maximum correlation is known, the fact that it is not at P makes the practical usefulness of the concept less convenient than the reference ordinary geographical co-ordinates.

In the case of P and P′ on the same isobaric surface, the fact that the standard deviation of the wind components is a function of geographical location introduced only some rather minor terms into expressions for the two components of the wind correlation tensor. The variation of the standard deviation of the wind component in the vertical is several times larger than in the horizontal. Consequently, this non-homogeneous structure of the atmospheric wind field brings about some important modifications when P and P′ are separated in the vertical.

B. VALIDITY OF PREVIOUS RESULTS IN GEOSTROPHIC WIND CASE

The basic equation relating the wind covariance tensor components to the height correlation function is of the same form as that of (7) in Chapter III. The justification for this same form is easily seen by considering its derivation in Appendix A-I. We repeat here only the modifications that would have to be made in the arguments of Appendix A-I to show the relatively trivial changes involved.

Equation (7) of Chapter III is repeated for convenience here.

$$\frac{\lambda\lambda'}{g^2}\overline{(u_i u_j')} = \sigma\sigma'\left\{\left(\frac{\partial^2 R_{hh}}{\partial r^2} - \frac{1}{r}\cdot\frac{\partial R_{hh}}{\partial r}\right)\nu_i\nu_j + \frac{\partial^2 R_{hh}}{\partial s^2}\lambda_i\lambda_j + \frac{\partial^2 R_{hh}}{\partial r\,\partial s}(\nu_i\lambda_j + \nu_j\lambda_i)\right\}$$

$$+ \frac{\partial R_{hh}}{\partial r}\left[\sigma|\nabla\sigma'|\nu_j\mu_i' - \sigma'|\nabla\sigma|\nu_i\mu_j\right] \qquad (1)$$

$$+ \frac{\partial R_{hh}}{\partial s}\left[\sigma|\nabla\sigma'|\lambda_j\mu_i' - \sigma'|\nabla\sigma|\lambda_i\mu_j\right] - |\nabla\sigma||\nabla\sigma'|R_{hh}\mu_j\mu_i'$$

$$+ \delta_{ij}\left\{-\sigma\sigma'\left[\frac{\partial^2 R_{hh}}{\partial r^2} + 2\frac{\partial^2 R_{hh}}{\partial r\,\partial s}\nu_k\lambda_k + \frac{\partial^2 R_{hh}}{\partial s^2}\right] + |\nabla\sigma||\nabla\sigma'|R_{hh}\mu_k\mu_k'\right.$$

$$- \frac{\partial R_{hh}}{\partial r}\left[\sigma|\nabla\sigma'|\nu_k\mu_k' - \sigma'|\nabla\sigma|\nu_k\mu_k\right]$$

$$\left. - \frac{\partial R_{hh}}{\partial s}\left[\sigma|\nabla\sigma'|\lambda_k\mu_k' - \sigma'|\nabla\sigma|\lambda_k\mu_k\right]\right\}.$$

The significance of the quantities appearing here is the same as that tabulated on Page III-7. The geometrical relations involved are illustrated in Figs. III-2 and VI-2(a).

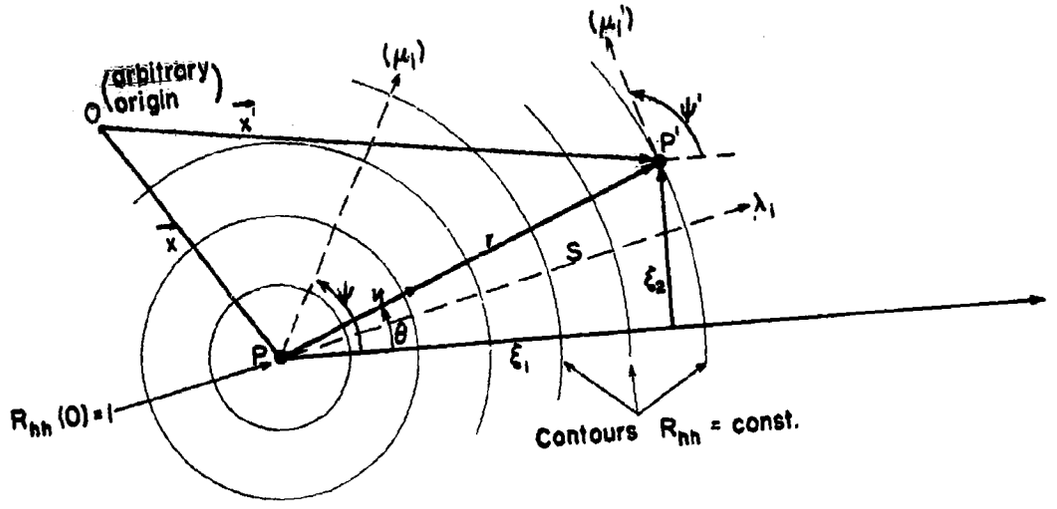

(a) Locations of P, P', and R_{hh} = constant if P and P' on same isobaric surface and observations made simutaneously.

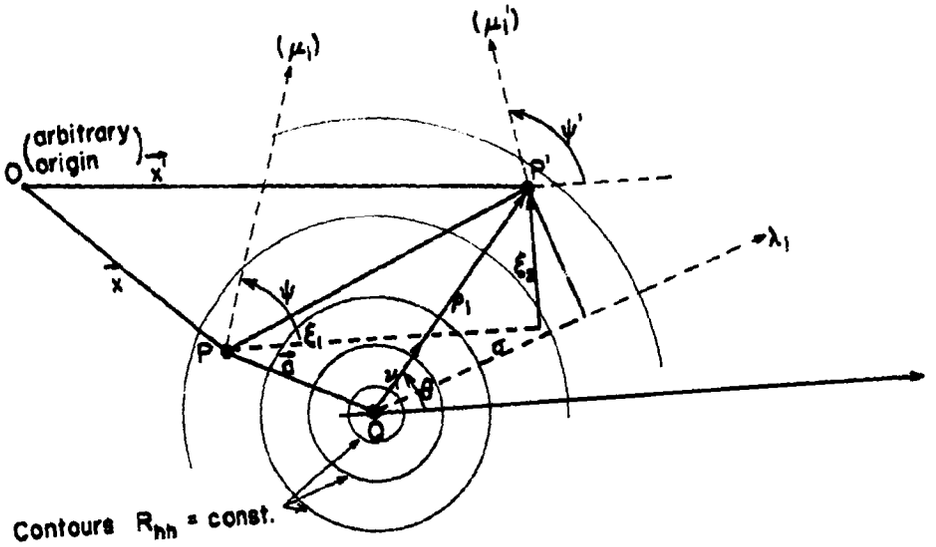

(b) Locations of P, P', and R_{hh} = constant if P and P' not necessarily on same isobaric surface and observations not necessarily simultaneous.

Fig. VI - 2. Geometric relations of the parameters appearing in equation (1).

The basic equation from (8) of Appendix A-I

$$e_{i3k}e_{j3\ell}\lambda_3\lambda_3'\overline{(u_k u_\ell')} = g^2\left\{\sigma\sigma'\frac{\partial^2 R_{hh}}{\partial\xi_i\,\partial\xi_j} + \frac{\partial\sigma}{\partial x_i}\sigma'\frac{\partial R_{hh}}{\partial\xi_j} - \sigma\frac{\partial\sigma'}{\partial x_j'}\cdot\frac{\partial R_{hh}}{\partial\xi_i}\right.$$
$$\left. + \frac{\partial\sigma}{\partial x_i}\cdot\frac{\partial\sigma'}{\partial x_j'}R_{hh} + \sigma\left[\frac{\partial\sigma'}{\partial x_j'}\cdot\frac{\partial R_{hh}}{\partial x_i} + \sigma'\frac{\partial^2 R_{hh}}{\partial\xi_j\,\partial x_i}\right]\right\} \qquad (2)$$

in which e_{i3k} (and $e_{j3\ell}$) = the alternating tensor and has the value 1 if i = 1, k = 2; - 1 if i = 2, k = 1; 0 otherwise. u_k = wind components at P, k = 1, 2; u_ℓ = wind components at P′. The symbol $\overline{(u_k u_j')}$ is the mean value of the product, and the factors of the product are departures from their respective means (these are the components of the wind covariance tensor). g = acceleration of gravity; σ, σ′ are standard deviations of height at P and P′ respectively; R_{hh} = height correlation function, the correlation coefficient relating height of an isobaric surface at P to that at P′; x_i = co-ordinates at P and x_j' = co-ordinates at P′.

The basic idea at this point was (in Appendix A-I), that R_{hh} is a function of the relation of P′ to P and only secondarily a function of the location of P itself.

Symbolically

$$R_{hh} = R_{hh}(x_1, x_2; x_1', x_2') = R_{hh}(\xi_1, \xi_2; x_1, x_2) \cong R_{hh}(\xi_1, \xi_2)$$

where

$$\xi_1 = x_1' - x_1$$
$$\xi_2 = x_2' - x_2.$$

Some assumptions about the particular relation $R_{hh}(\xi_1, \xi_2)$ were then made. It was found that if $r^2 = \xi_1^2 + \xi_2^2$ = square of distance from P to P′ and $R_{hh} = R_{hh}(r)$, the expressions for $\overline{(u_k u_\ell')}$

were particularly simple. (See Fig. III-3 and equation (13) of Chapter III.)

Four new variables have been introduced when height and time separation are involved. These are z, z′, t, t′; height and time for P and P′. We will not introduce these specifically in the symbolism since differentiation with respect to these are not involved in (1). The presence of these variables implies that the largest correlation between height at P and height at P′ is no longer reached if P′ ≡ P. (Formerly $R_{hh}(0,0) = 1$.) Let the largest value of R_{hh} be attained at some point Q (see Fig. VI-2(b)). Let the vector PQ be given by $\vec{a} = (a_1, a_2)$. And let the vector QP′ be given by $\vec{\rho} = (\rho_1, \rho_2)$. Then (Fig. VI-2)

$$\vec{x}' = \vec{x} + \vec{a} + \vec{\rho}, \quad \text{or} \quad \begin{aligned} x_1' &= x_1 + a_1 + \rho_1, \\ x_2' &= x_2 + a_2 + \rho_2. \end{aligned}$$

It is now convenient to describe the correlation contours of R_{hh} = constant in terms of a co-ordinate pair (ρ, σ) where

$$\rho^2 = \rho_1^2 = \rho_1^2 + \rho_2^2 \quad \text{and} \quad \sigma = \rho_i \lambda_i$$

$$= \rho^2(\nu_i^2)$$

where ν_i is a unit vector giving the azimuth of P′ from Q; λ_i is a preferred reference direction (an axis of symmetry of R_{hh} = constant, for example). ($\lambda_i = (\lambda_1, \lambda_2)$ has nothing to do with λ_3, λ_3', values of the Coriolis parameter; σ here is temporarily used as a co-ordinate, projection of QP′ on the reference direction, and has nothing to do with standard deviation of height.)

Now

$$\frac{\partial R_{hh}}{\partial \xi_i} = \frac{\partial R_{hh}}{\partial \rho} \cdot \frac{\partial \rho}{\partial \xi_i} + \frac{\partial R_{hh}}{\partial \sigma} \cdot \frac{\partial \sigma}{\partial \xi_i} .$$

Since

$$\rho^2 = (\xi_1 - a_1)^2 + (\xi_2 - a_2)^2 \quad \text{and} \quad \sigma = (\xi_1 - a_1)\lambda_1 + (\xi_2 - a_2)\lambda_2$$

then

$$\frac{\partial \rho}{\partial \xi_i} = \frac{\rho_i}{\rho} = \nu_i , \qquad \frac{\partial \sigma}{\partial \xi_i} = \lambda_i$$

where ν_i is the vector giving the azimuth of P′ from Q. Then

$$\frac{\partial R_{hh}}{\partial \xi_i} = \frac{\partial R_{hh}}{\partial \rho}\nu_i + \frac{\partial R_{hh}}{\partial \sigma}\lambda_i$$

which is exactly the same as (9) of Appendix A-I except that (ρ,σ) replaced (r,s). The remainder of the transformation is only tedious and involves no new ideas not already covered. The end result is that to estimate the wind covariance components, equation (1) is valid provided that the center of the co-ordinates (r,s) is at Q, a "floating point" not specified exactly a priori, and is that point where R_{hh} has its maximum value.

To rotate co-ordinates along which wind components are resolved into longitudinal and transverse form it is required to multiply (1) by the proper unit vectors. In (1) the unit vector ν_i gives the azimuth of P′ with respect to Q, the center of maximum R_{hh}. If one multiplies (1) by $\nu_i \nu_j$ and sums over the subscripts i and j (since they are now repeated), the same results are obtained as before as far as their form is concerned. This gives the covariance form $\overline{(u_\ell u'_\ell)}$. The geometrical interpretation is a bit awkward, however. As shown in Fig. VI-3, the direction of the longitudinal component is QP′ (and the

direction of the transverse component would be perpendicular thereto). This is by no means the direction $\overline{PP'}$. The longitudinal and transverse component form was convenient because, among other things, these could be thought of as head-wind and cross-wind components along a flight path. This would be true now only if P, Q, P′ were colinear.

If winds are resolved along and across PP′, other difficulties arise. Let $\hat{v}_i$ be the unit vector from P to P′. Multiplying (1) by $\hat{v}_i \hat{v}_j$ one obtains $\overline{(u_\ell u'_\ell)}$ on the left-hand side, but the direction factor in the product on the right-hand side in the case of the first term becomes

$$v_i v_j (\hat{v}_i \hat{v}_j) = (v_i \hat{v}_j)(v_j \hat{v}_j) = \cos^2(\theta - \theta^*)$$

where θ is the azimuth of P′ with respect to Q and where θ^* is the azimuth of P′ with respect to P (see Fig. VI-3). In a similar manner, the term in δ_{ij} will have the factor $\delta_{ij} \hat{v}_i \hat{v}_j = \cos^2\theta^*$. Thus on the whole the terms on the right of (1) become strongly direction dependent even when $R_{hh} = R_{hh}(\rho)$ is a function of radial distance only. As a consequence, the simplifications that were present when P and P′ were on the same isobaric surface are completely lost.

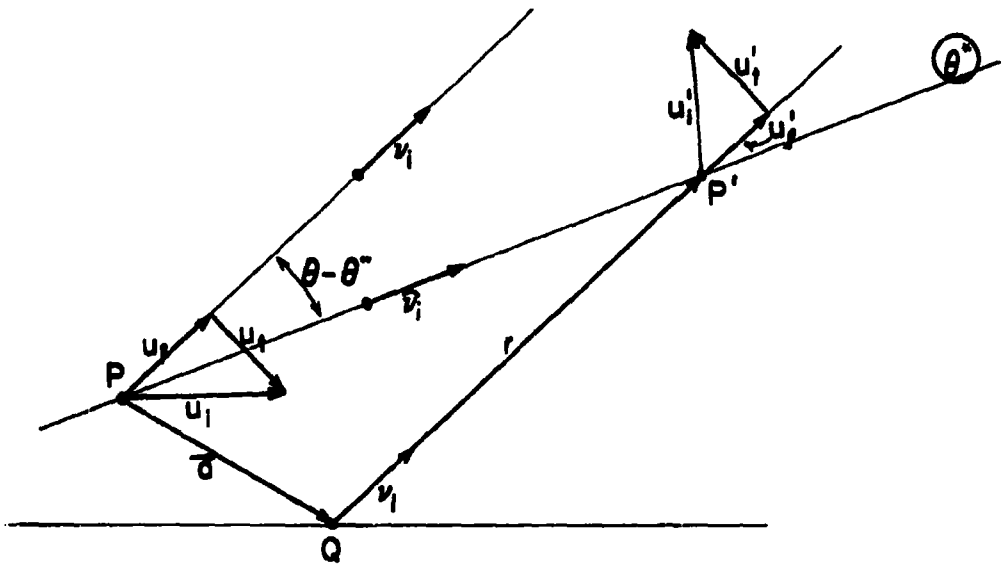

Fig. VI-3 Geometric Relations Between the Locations of P, Q, and P' when Winds are not Observed Simultaneously or on the Same Isobaric Surface, or both

C. HEIGHT CORRELATION FUNCTION WHEN DIFFERENCES IN LEVELS AND TIME

In order to use (1) to estimate the form of the components of the wind correlation tensor (covariance) components or the corresponding wind component correlations, it is necessary to estimate the form of the height correlation function R_{hh}. This is done in only a very simplified case.

When P and P′ lie on the same isobaric surface, a simple reasonable estimate of R_{hh} appeared to be

$$R_{hh} = ke^{-\alpha^2 r^2/2}$$

where $0 < k \leq 1$ and $L = \alpha^{-1}$ = constant = size parameter. This particularly simple form is now modified into a form like

$$R_{hh} = k_o\left(1 - \frac{t^2}{\tau^2}\right)\left(1 - \frac{z^3}{\zeta^3}\right)e^{-\alpha^2 r^2/2}e^{-z^2/2D^2}$$

$$\alpha^2 r^2 = \frac{(x_1'-x_1-a_1 t-b_1 z)^2 + (x_2'-x_2-a_2 t-a_2 z)^2}{[L(t,z)]^2}. \qquad (3)$$

The many factors in this function form serve only the purpose of introducing effects that are likely to be encountered. It is perhaps too much to ask that the details of such an expression be confirmed.

The factor k_o, $0 < k_o \leq 1$ is introduced to take into account errors of measurement and effects of small scale motions that are too small to be adequately accounted for in the network of data points that are available.

The factor $(1 - t^2/\tau^2)$ is indicative of the degradation of correlation at its maximum point on an isobaric surface with the passage of time.

The factor, $e^{-z^2/2D^2}$ is indicative of the degradation of the maximum correlation value when P and P′ are separated by a height difference z.

The factor $(1 - z^3/\zeta^3)$ is to account for the fact that the correlations are not degraded symmetrically above and below the level z = 0 (level of P). This is due to the fact that the standard deviation of height increases to a maximum and then decreases. The rate of decrease and increase are large enough to materially affect the shape of the correlation function. (See Appendix A-III where the subject is discussed in detail.)

The terms in $a_1 t + b_1 z$ allow for the drift of the center of correlation maximum as a function of time and also the tilt as a function of the difference between the levels of P and P′.

The factor L(t,z) allows for spreading of the correlation pattern as a function of the time lags and height lags (differences).

None of the differentiations in (1) is with respect to z or t so that all of the factors containing these quantities may be treated as constants. This means that one may actually ignore the conjectures made in the specific formulation of (3) and write it in the form

$$R_{hh} = Ke^{-\alpha^2 r^2/2}$$
$$\alpha^2 r^2 = \left[(x_1' - x_1 - A_1)^2 + (x_2' - x_2 - A_2)^2\right]/L^2 \qquad (3a)$$

in which K, L, A_1, A_2 are all functions of t and z. In particular,

one would expect that

$$\begin{aligned} K &\sim k\left(1 - \frac{t^2}{\tau^2}\right)\left(1 - \frac{z^3}{\zeta^3}\right)e^{-z^2/2D^2} \\ A_1 &\sim a_1 t + b_1 z \\ A_2 &\sim a_2 t + b_2 z \\ L &\sim L(t,z) \end{aligned} \tag{3b}$$

The form of (1) is much too complex for direct substitution of (3a) to yield reasonably tractable results. Only the terms of primary importance are retained. These, as was pointed out in Chapter III, consist of the terms underlined thrice in (1). We also retain the terms underlined twice in (1) but with the assumption that the gradient of the standard deviation of height is small and uniform, i.e. that $\sigma \cong \sigma'$, $|\nabla\sigma| = |\nabla\sigma'|$, $\mu_i = \mu_i'$. Then substituting the values of 1 and 2 for the subscripts one obtains

$$\frac{\lambda\lambda'}{g^2}\overline{(u_1 u_1')} = -\sigma\sigma'\left[\frac{1}{r}\cdot\frac{\partial R_{hh}}{\partial r}\cos^2\theta + \frac{\partial^2 R_{hh}}{\partial r^2}\sin^2\theta\right] + |\nabla\sigma|^2 R_{hh}\sin^2\psi, \tag{4a}$$

$$\frac{\lambda\lambda'}{g^2}\overline{(u_2 u_2')} = -\sigma\sigma'\left[\frac{1}{r}\cdot\frac{\partial R_{hh}}{\partial r}\sin^2\theta + \frac{\partial^2 R_{hh}}{\partial r^2}\cos^2\theta\right] + |\nabla\sigma|^2 R_{hh}\cos^2\psi, \tag{4b}$$

$$\begin{aligned} \frac{\lambda\lambda'}{g^2}\overline{(u_1 u_2')} = -\sigma\sigma'\Bigg[&\frac{\partial^2 R_{hh}}{\partial r^2}\cdot\frac{1}{r}\cdot\frac{\partial R_{hh}}{\partial r}\sin\theta\cos\theta + \left|\frac{\nabla\sigma}{\sigma}\right|^2 R_{hh}\sin\psi\cos\psi \\ &+ \left|\frac{\nabla\sigma}{\sigma}\right|\frac{\partial R_{hh}}{\partial r}\sin(\theta-\psi)\Bigg], \end{aligned} \tag{4c}$$

$$\begin{aligned} \frac{\lambda\lambda'}{g^2}\overline{(u_2 u_1')} = -\sigma\sigma'\Bigg[&\frac{\partial^2 R_{hh}}{\partial r^2} - \frac{1}{r}\cdot\frac{\partial R_{hh}}{\partial r}\sin\theta\cos\theta + \left|\frac{\nabla\sigma}{\sigma}\right|^2 R_{hh}\sin\psi\cos\psi \\ &- \left|\frac{\nabla\sigma}{\sigma}\right|\frac{\partial R_{hh}}{\partial r}\sin(\theta-\psi)\Bigg], \end{aligned} \tag{4d}$$

where θ is the azimuth of P′ with respect to Q and ψ is the azimuth of the gradient of the standard deviation of height, $\nabla\sigma$.

Note that when (4a) and (4b) are added and subtracted, one obtains

$$\frac{\lambda\lambda'}{g^2\sigma\sigma'}\left[\overline{(u_1 u_1')} + \overline{(u_2 u_2')}\right] = -\left(\frac{1}{r}\cdot\frac{\partial R_{hh}}{\partial r} + \frac{\partial^2 R_{hh}}{\partial r^2}\right) + \left|\frac{\nabla\sigma}{\sigma}\right|^2 R_{hh} \qquad (5a)$$

and

$$\frac{\lambda\lambda'}{g^2\sigma\sigma'}\left[\overline{(u_1 u_1')} - \overline{(u_2 u_2')}\right] = -\left(\frac{1}{r}\cdot\frac{\partial R_{hh}}{\partial r} - \frac{\partial^2 R_{hh}}{\partial r^2}\right)\cos 2\theta + \left|\frac{\nabla\sigma}{\sigma}\right|^2 R_{hh}\cos 2\psi. \qquad (5b)$$

It is worthy of note that (5a) is very closely related to the stretch vector correlation coefficient[2] and is seen to be independent of the azimuth of P with respect to Q when R_{hh} is also independent of ϑ. On the other hand, even when R_{hh} is independent of ϑ, the factor $\cos 2\theta$ makes (5b) highly dependent on the azimuth of P′ with respect to Q.

The sum and difference of (4c) and (4d) likewise have distinct characteristics. Thus,

$$\frac{\lambda\lambda'}{g^2\sigma\sigma'}\left[\overline{(u_1 u_2')} + \overline{(u_2 u_1')}\right] = -\left(\frac{\partial^2 R_{hh}}{\partial r^2} - \frac{1}{r}\cdot\frac{\partial R_{hh}}{\partial r}\right)\sin 2\theta - \left|\frac{\nabla\sigma}{\sigma}\right|^2 R_{hh}\sin 2\psi \qquad (5c)$$

and

$$\frac{\lambda\lambda'}{g^2\sigma\sigma'}\left[\overline{(u_1 u_2')} - \overline{(u_2 u_1')}\right] = 2\left|\frac{\nabla\sigma}{\sigma}\right|\frac{\partial R_{hh}}{\partial r}\sin(\theta-\psi). \qquad (5d)$$

In (5c) it is readily seen that the first term on the right is highly direction dependent while the second term on the right is independent of direction and is small if $|\nabla\sigma/\sigma|$ is small. The expression (5d) is dependent on $|\nabla\sigma/\sigma|$ and would become zero if the gradient of the standard deviation of height were completely negligible.

If we use (3a) for R_{hh} and convert to correlation coefficients rather than to using covariances, one obtains (on retaining only the most important terms*)

$$S^* = r_{11} + r_{22} = 2K(1-\hat{r}^2/2)e^{-\hat{r}^2/2}, \tag{6a}$$

$$D^* = r_{11} - r_{22} = K(\hat{r}_1^2-\hat{r}_2^2)e^{-\hat{r}^2/2}, \tag{6b}$$

$$S = r_{12} + r_{21} = 2K(\hat{r}_1\hat{r}_2+A)e^{-\hat{r}^2/2}, \tag{6c}$$

$$D = r_{12} - r_{21} = 2K(B\hat{r}_2+C\hat{r}_1)e^{-\hat{r}^2/2}, \tag{6d}$$

where

$$\hat{r}_1 = (x_1'-x_1-A_1)/L, \quad \hat{r}_2 = (x_2'-x_2-A_2)/L, \quad \hat{r}^2 = \hat{r}_1^2 + \hat{r}_2^2.$$

Thus, the four relations (6a), ---, (6d) contain seven undetermined parameters. Four of these arise from the assumptions regarding the form of R_{hh}: K, L, A_1, A_2; and three depend on the fact that the horizontal gradient of height is not entirely negligible: A, B, C. Thus,

$$2KA \cong L^2\left|\frac{\nabla\sigma}{\sigma}\right|^2 \sin 2\psi \tag{7a}$$

$$2KB \cong -L\left|\frac{\nabla\sigma}{\sigma}\right| \cos\psi \tag{7b}$$

$$2KC = L\left|\frac{\nabla\sigma}{\sigma}\right| \sin\psi \tag{7c}$$

One should note that in assigning meaning to A, B, and C in the above one has only retained here the effect of the nonvanishing

---

*The arithmetic of the reduction is tedious. In carrying out the reduction it is necessary to go to the forms (4a), ---, (4d) and to account for the component standard deviations by using the limit relations for $P' \to P$, $Q \to P$ at $t = z - 0$.

of the gradient of the standard deviation of height. This serves merely to justify the fact that such terms should be retained in S and D. Actually, parameters A, B, C pick up contributions due to the fact that R_{hh} may be of an elliptical shape, that the standard deviation of height may be non-uniform, etc. Consequently, one is inclined to look on A, B, and C as three empirical factors that should be retained and to de-emphasize any meaning that might be ascribed to them in the initial analysis.

The individual correlation coefficient has the forms

$$\begin{aligned} r_{11} &\cong K(1 - \hat{f}_2^2)e^{-\hat{f}^2/2} \\ r_{22} &\cong K(1 - \hat{f}_1^2)e^{-\hat{f}^2/2} \\ r_{12} &\cong K\left[\hat{f}_1\hat{f}_2 + A + B\hat{f}_1 + C\hat{f}_2\right]e^{-\hat{f}^2/2} \\ r_{21} &\cong K\left[\hat{f}_1\hat{f}_2 + A - B\hat{f}_1 - C\hat{f}_2\right]e^{-\hat{f}^2/2} \end{aligned} \tag{8}$$

The first pair is by far the most important. Both r_{12} and r_{21} are small and their expressions are somewhat complex for practical purposes.

D. REDUCTION OF THE DATA

The values of K, L, A_1, and A_2 were estimated from (6a) and (6b) by minimizing the sum of the squares of the differences between S* and D* as computed and as determined from the correlations actually observed. The method used was that of Gauss for determining parameters that appear in a non-linear form (see Appendix A-IV for a similar example).

The values of A, B, and C appear linearly in (6b) and (6d). They were estimated by standard least squares methods from these expressions after the values of K, L, A_1, and A_2 from (6a) and (6b) had been obtained.

The correlation data used throughout were those computed by the Sandia Corporation using serially complete wind data prepared by the U.S. Weather Bureau for the Federal Civil Defense Agency covering a period of five years.(3)

E. THE EMPIRICAL PARAMETERS

Figs. VI-4 through VI-45 illustrate the results of the numerical estimates of the parameters K, L, A_1, A_2, A, B, and C. These illustrations are divided into seven groups, one for each parameter. These groups each contain 6 figures and are divided into three illustrations of summer conditions and three for winter conditions. There are three "master levels" or levels for the point P, 500 mb, 300 mb, and 100 mb.

The 500 mb level illustrates conditions in the lower tropopause where the gradient of standard deviation is increasing rapidly with height, the 300 mb level represents conditions in the upper troposphere where the standard deviations are near their maximum, the 100 mb level represents conditions in the lower stratosphere where the standard deviations are decreasing with heights.

Each illustration is divided into three parts, one representing conditions with Washington, D.C. as the point P or "master station", the next with Omaha, Nebraska, and the third with Oakland, California, serving in this role. The identity of the master station has been preserved not only to show the distinction between conditions centered at these locations, but also to emphasize the great similarities that occur.

The characteristics of each parameter as functions of z, height difference, and t, time difference, are discussed in turn with the exception of A_1 and A_2 (which represent a displacement vector) and of B and C (which also represent vector components).

In all cases, the functions of z and t have been determined at 25 points each, 5 time lags of -2, -1, 0, +1, and +2 days and 5 height lags (which amounts to roughly -4, -2, 0, +2, +4 kilometers, but which differ from one master level to another since winds on standard isobaric surfaces are used.*

1. Characteristics of Parameter k

The variation of the parameter k with height and time lag is illustrated in Fig. VI-4 through VI-9. There are common characteristics present in all of these figures. The most important is the decay of the value of k with both height and time lags. The largest value is, of course, that for zero height and time lag located at the "center" of the 5 x 5 array of points.

(a) 100 mb Level

The most important property that is typical of the 100 mb level is the somewhat more rapid decay of k for P′ located above P as compared with the location of P′ below P. This characteristic is prominent at all locations and seasons, though somewhat more noticable in summer (Fig. VI-4) than in winter (Fig. VI-5). This is one of the effects brought about by the non-homogeneity of the wind field in the vertical; specifically, the fact that at the 100 mb level in both seasons the standard deviation of wind is decreasing with height.

*The "slave levels" for each master level are:

Master Level (P)	Slave Level (P′)
500 mb	850, 700, 500, 400, 300 mb
300 mb	500, 400, 300, 250, 200 mb
100 mb	200, 150, 100, 80, 50 mb

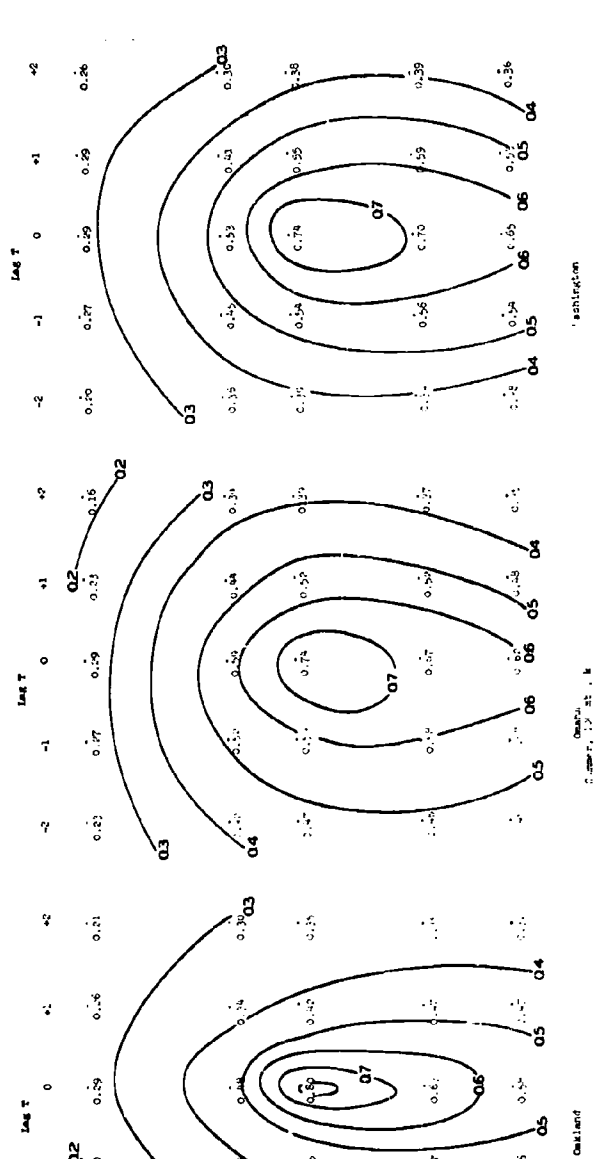

Fig. VI-4

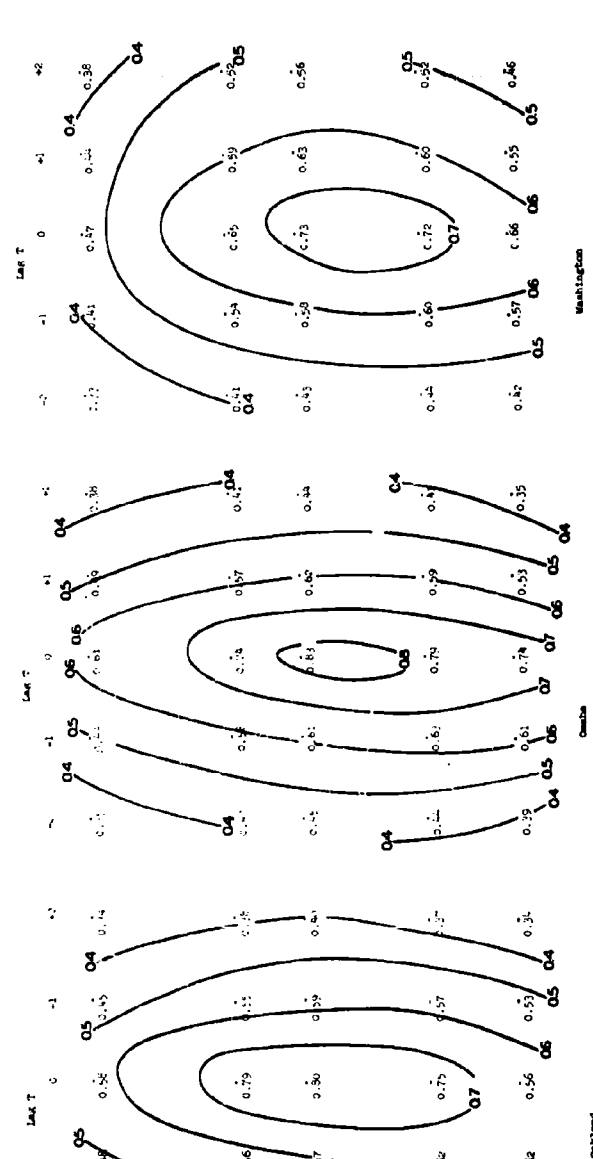

Winter, 100 mb., K

Fig. VI-5

(b) 300 mb Level

The 300 mb level, located reasonably close to the level of maximum wind and of the maximum standard deviation of wind, displays the characteristic that the decrease of k with increasing numerical value of time lag is nearly the same for both positive and negative values (P' above or below P). The values of k for both summer (Fig. VI-6) and winter (Fig. VI-7) appear to behave in much the same way so that seasonal changes appear to be minor.

(c) 500 mb Level

At the 500 mb level in both summer (Fig. VI-8) and winter (Fig. VI-9) the change of k with height lag is just the reverse of that illustrated at the 100 mb level. At the 500 mb level the value of k drops off more rapidly for negative height lags (P' below P) than for positive height lags. This is, of course, due to the fact that at 500 mb the standard deviation of wind is increasing with height in both seasons.

2. Characteristics of Parameter L

The major over-all characteristic of the parameter L, the size parameter in the horizontal, that appears to some extent in Figs. VI-10 through VI-15 is the apparent uniformity. There appears to be a trend for L to be larger as the magnitude of the time difference between observations increases, but this is not invariably observed. The behavior of L in detail is characterized primarily by the level of the point P. The three particular cases are discussed separately.

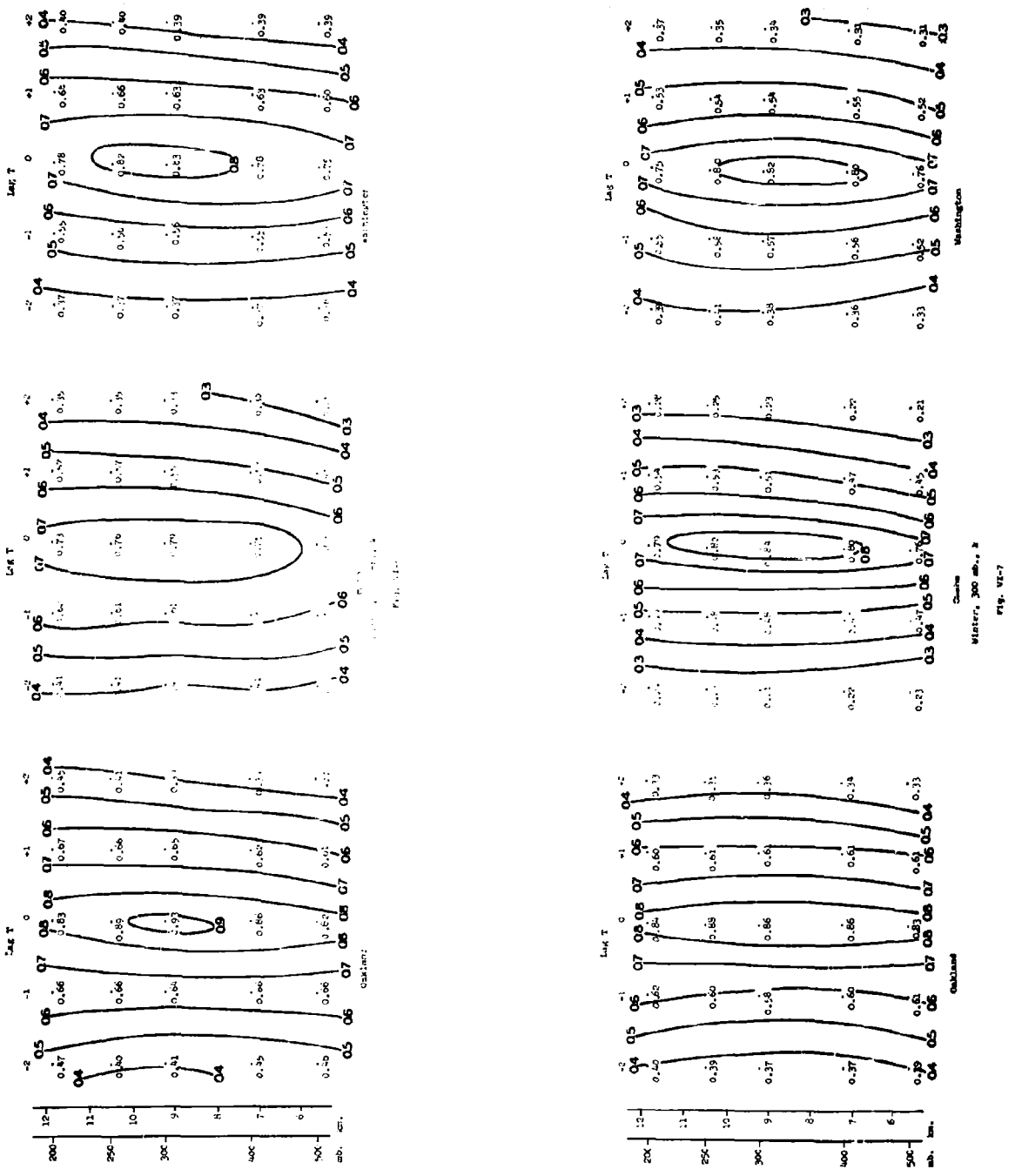

Winter, 300 mb., K

Fig. VI-7

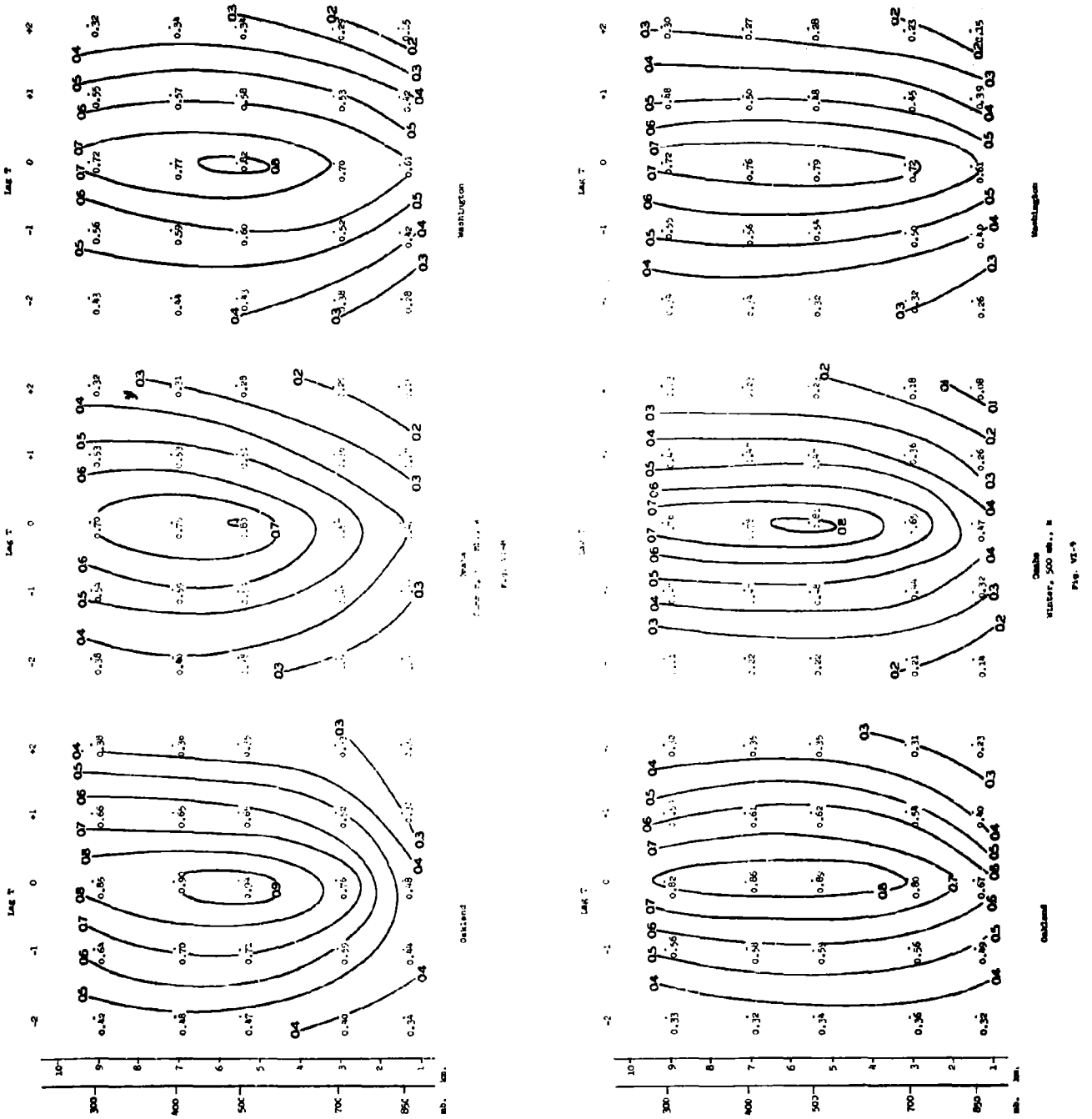
Lag T
Oakland
Washington
km.
mb.

One characteristic that appears at each level to a greater or less degree, and which warrants special mention is the tendency of the size parameter to increase somewhat more rapidly with negative time lag at Oakland than it does when time lags are positive. In contrast with this at Washington the value of L tends to increase more rapidly with positive time lags than with negative. This unsymmetrical change of L with time lag at these locations may be a phenomena introduced by the geometrical relation of the family of points P′ with respect to the point P. The points P′ are in each instance radiosonde (rawinsonde) locations in North America. As discussed in the next section, the location of the correlation "center" (the point of maximum correlation for r_{11} and r_{22}) lies to the west of the point P for negative time lags and to the east of P for positive lags. The distance is roughly proportional to the lag magnitude. This means that, with negative lags at Oakland and positive lags at Washington, the "center of correlation" lies to sea from the data used to estimate the parameters. This indicates that instead of estimating L from data points surrounding the "center of correlation", all of the available data lie to one side of the center. It may well be that this situation has had a tendency to produce values of L which are larger than would be really present if data had been available surrounding the center of correlation maximum symmetrically. (The same uncertainty is present in the calculation of values for A_1 and A_2, the co-ordinates of the center of correlation maximum for r_{11} and r_{22}.)

(a) 100 mb Level

The variation of the parameter L with height and time lags is illustrated in Figs. VI-10 and VI-11 for summer and winter respectively. In both summer and winter the size parameter (L) tends to increase with increasing height lag, the rapid rate increase taking place at the positive height lags. The situation is much more pronounced in summer (Fig. VI-10) than in winter (Fig. VI-11). It is interesting to note that such a shift of the size parameter implies that the fundamental dynamics of the air motions are undergoing a fundamental change (or are about to undergo such a change) at the levels where such a change in size parameter appears.

The strong tendency for unusually large L with large negative time lags at Oakland and large positive time lags at Washington shows up strongly in Fig. VI-11. It is not without interest to note that the situation at Omaha is at the same time unsymmetrical and corresponds to the situation at Washington. This lack of symmetry at Omaha cannot be explained by the lack of data eastward of Omaha because this is the area in which the data density is greatest. One might conjecture that the effect of the mountain region lying between Oakland on the west and Omaha and Washington on the east may contribute to this effect, but the detailed mechanism to account for this is by no means clear.

(b) 300 mb Level

The variation of L with time and height lags for summer (Fig. VI-12) and winter (Fig. VI-13) at the 300 mb level

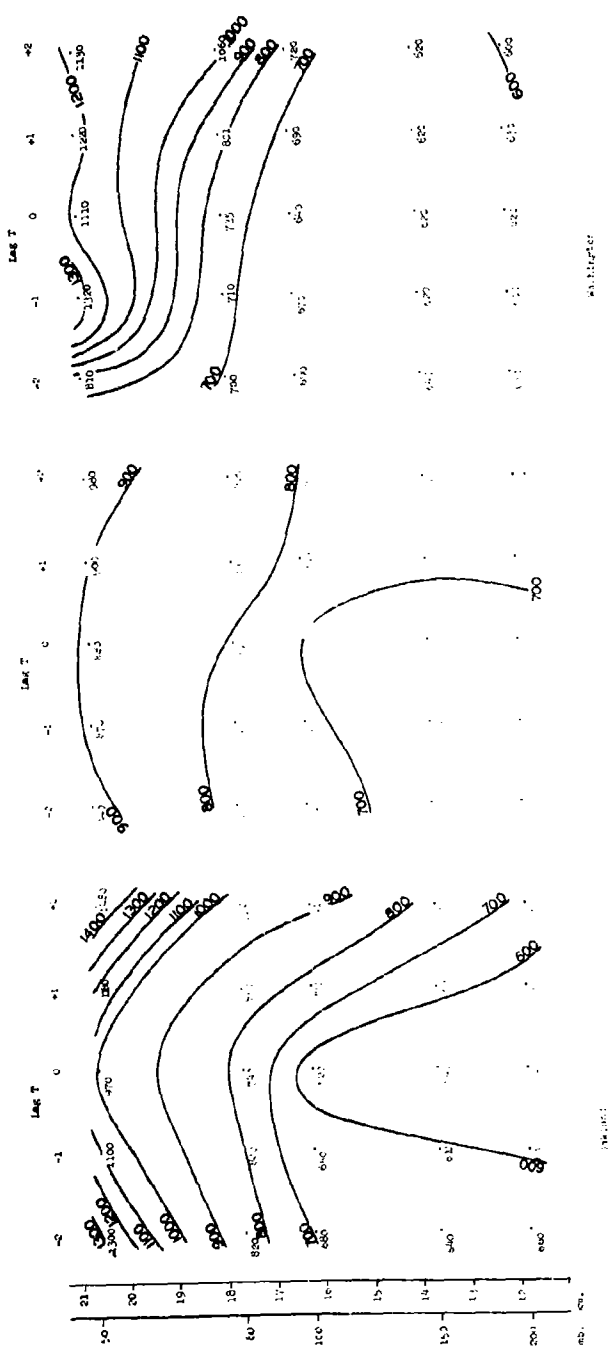

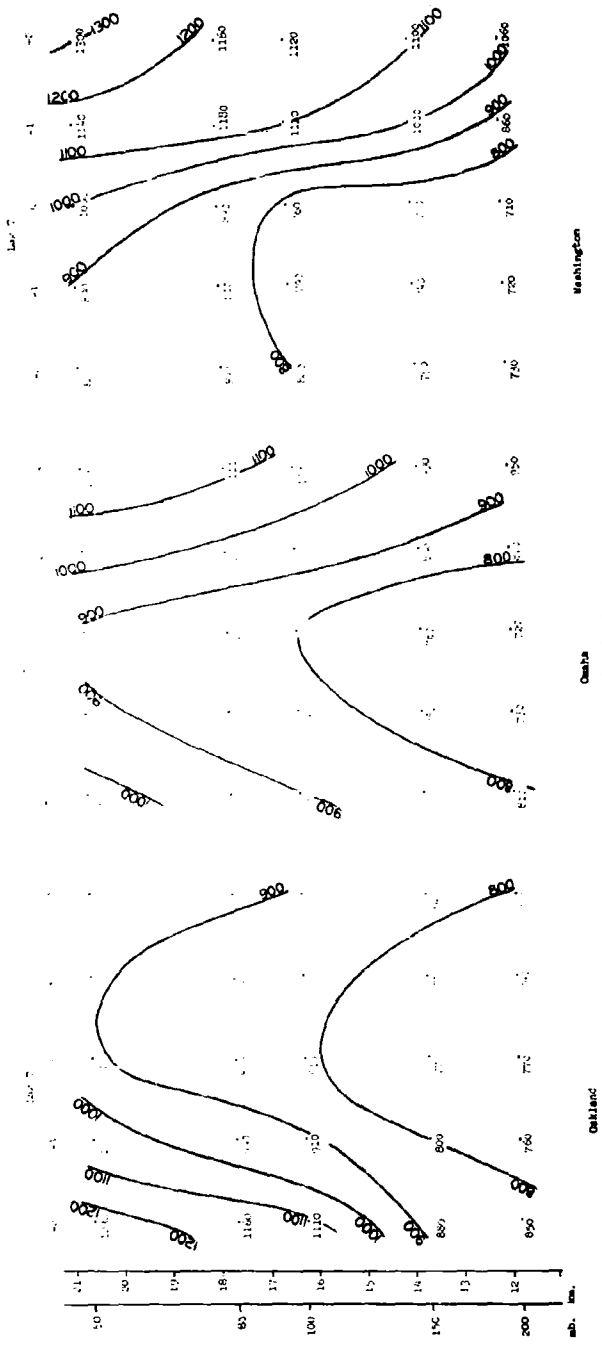

Fig. VI-11

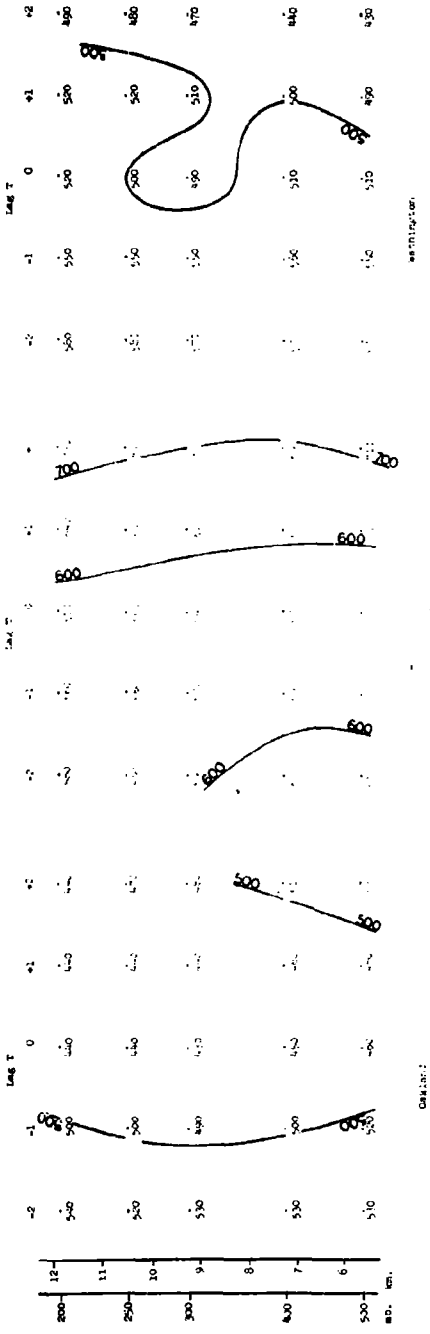

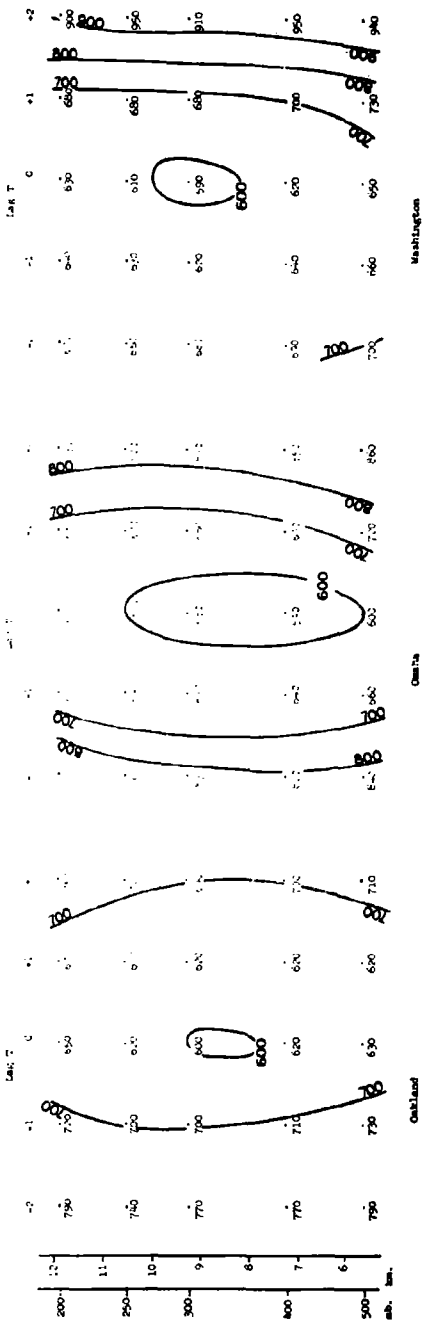

Fig. VI-13

are the least interesting of the three levels. The value of L increases slowly with the magnitude of the time lags and shows little variation with height lag.

(c) 500 mb Level

Both the summer and winter situations of Figs. VI-14 and VI-15 respectively indicate a tendency for larger values of L at the negative height lags (near the surface). This is just the opposite to the situation encountered at the 100 mb level. This, of course, corresponds to the difference in structure of atmospheric disturbances in the surface layers and that of the middle troposphere where surface effects have lost a great deal of this effectiveness.

It should be pointed out that the variation of correlations r_{11} and r_{22} in the vertical include an "interaction" between the variation of both the parameters k and L as functions of height.

3. Characteristics of Parameters A_1 and A_2

The parameters A_1 and A_2 are discussed together since they are the components of the displacement for the center of maximum correlation r_{11} and r_{22} from the point P. The major feature of the displacement is the movement from west to east through P with increasing time lag. There is a pronounced tendency for displacement from east to west with increasing height lag. This is particularly prominent at the 500 mb level.

The situation of the "center of correlation" and the data area, mentioned in connection with the parameter L, should be kept in mind. Generally for negative lags the center of correlation at Oakland is well west of the area of data while at

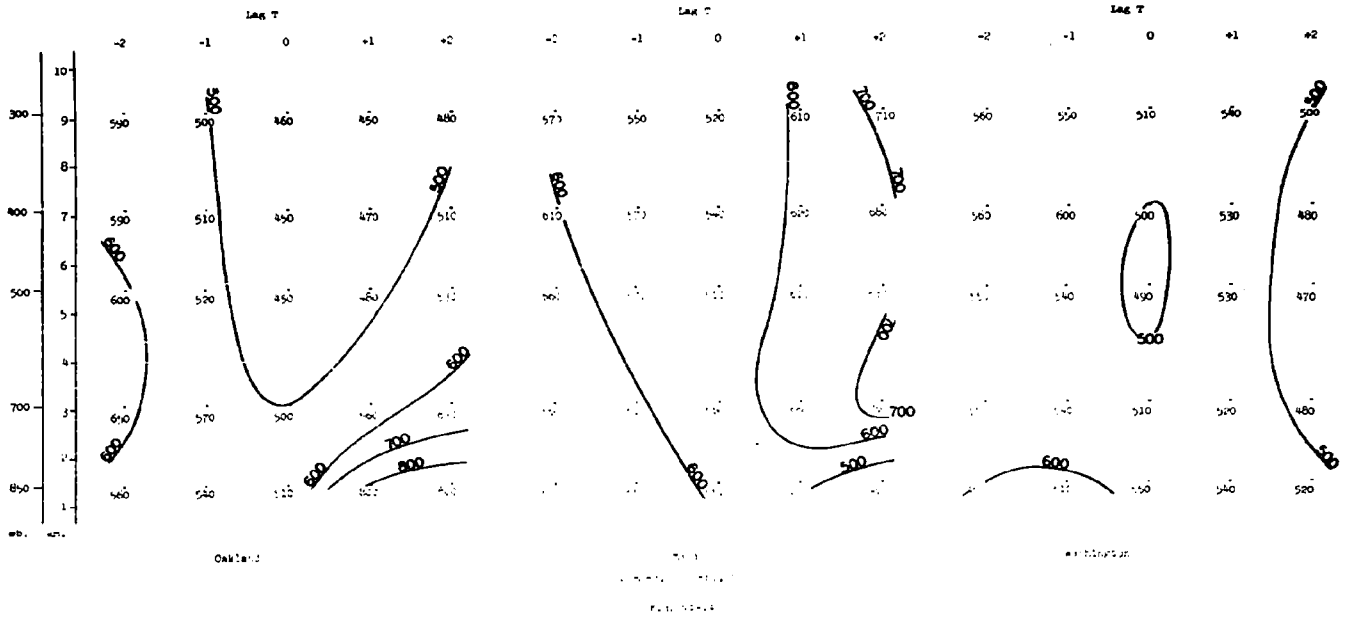

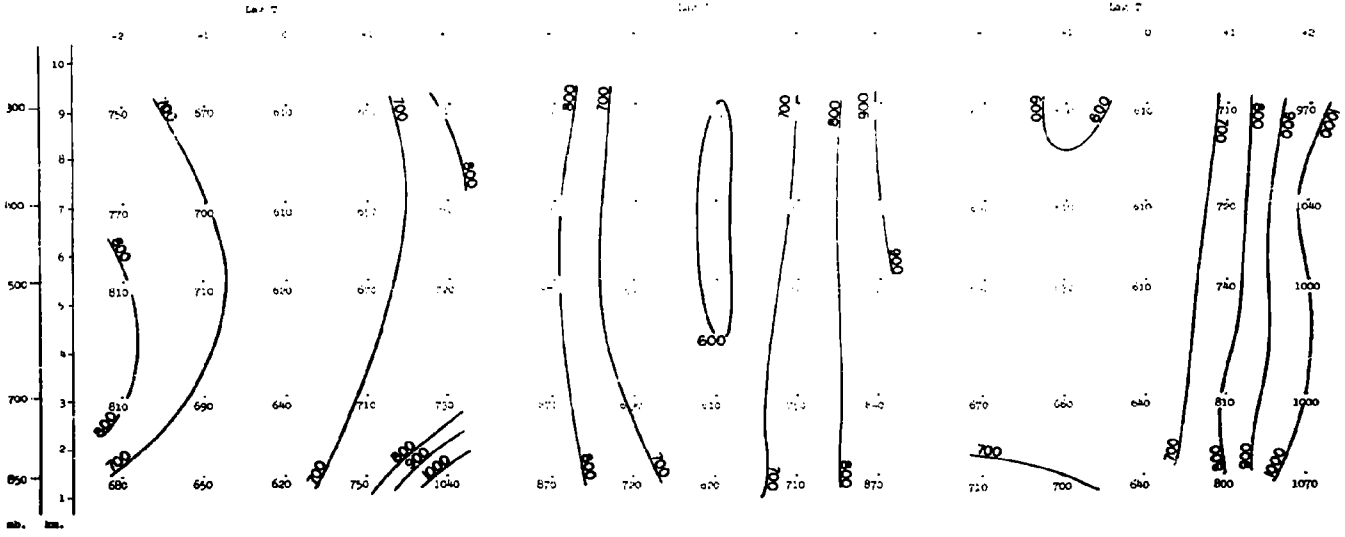

Winter, 500 mb., L

Fig. VI-15

Washington with positive lags the center is well east of the area of data. In these cases it is felt that the displacement values A_1, A_2 (and all other parameters, for that matter) may be unreliable.

In the case of parameter A_2, many cases occur where the values are quite small. In such cases the reality of any trend with height or time lag is seriously questioned. Such trends may be entirely due to the errors in the basic data and may not be real. An estimate of the error in the values of A_1 and A_2 may be obtained from the values listed in the figures at lag zero in time and height. For zero height and time lags the center of maximum correlation in r_{11} and r_{22} should be at P, i.e. $A_1 = A_2 = 0.0$. The computing program, however, did not supply this information. Consequently, the computing procedure computed what A_1, A_2 should be even in this case from the correlation values. The root mean square values of A_1 and A_2 together is 34 n mi and is considered as measure of the error included in these parameters.

(a) 100 mb Level

The summer displacements at 100 mb, Figs. VI-16 and VI-17, tend to be somewhat anomalous. The trend for eastward displacement (A_1) of about 100 n mi/day appears generally, but there are pronounced exceptions. For positive height lags at Oakland the displacements are of the wrong sign for positive time lags. These particular values are also associated with unusually large values of L (see Section 2a).

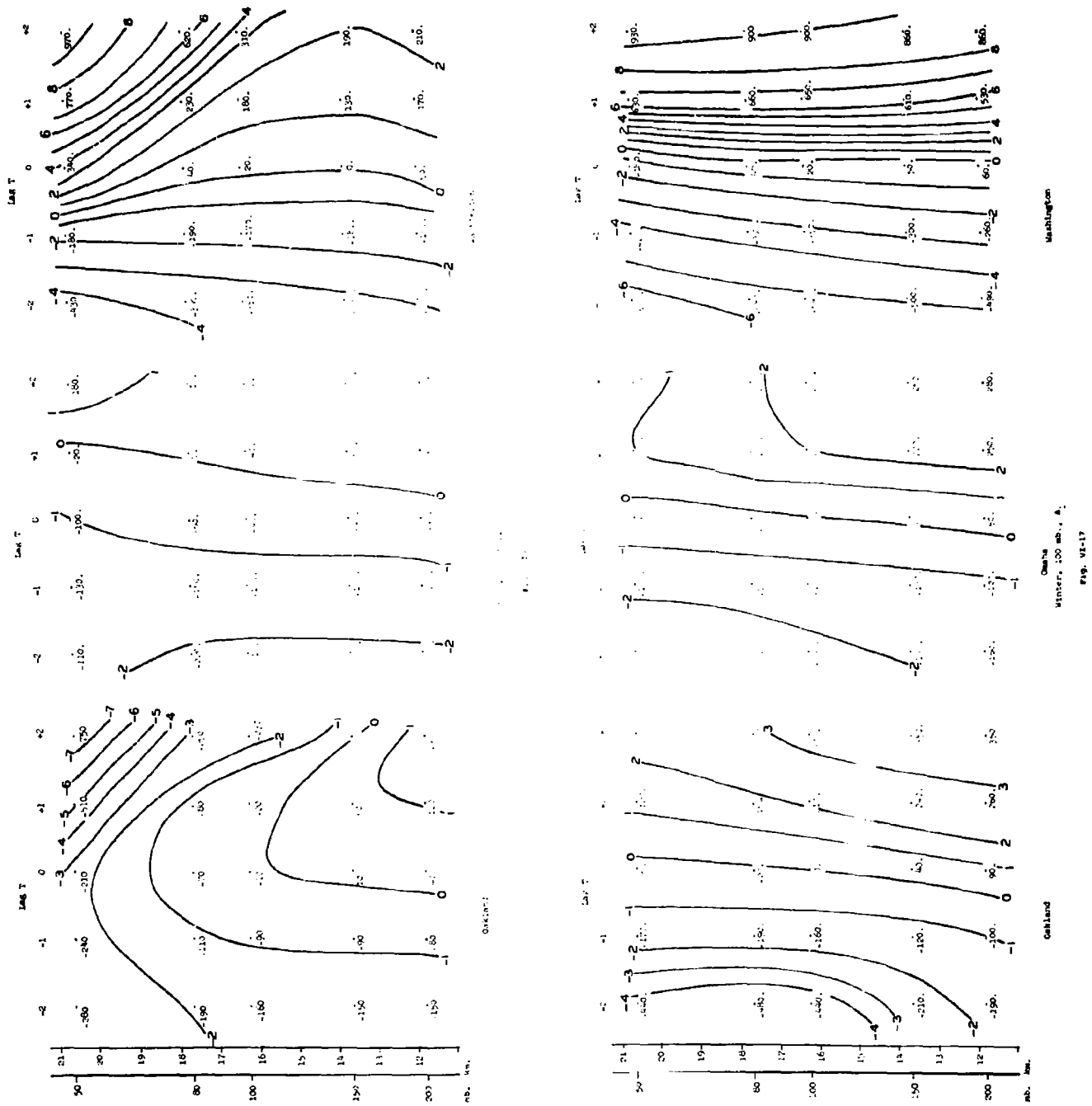

Winter, 100 mb. A.

Fig. VI-17

The values of A_2 in this instance are also anomalous, tending to be negative and large too. The values of A_2, except at Washington, tend to be increasingly negative for both positive and negative time lags. This would lead to a curved path for the center of correlation. Only at Washington is the displacement of the center of correlation definitely from the northwest to the southeast. (This case is exceptional at height lag of +2.)

The winter picture in Figs. VI-18 and VI-19 is much more definite. The value of A_1 shows rapid eastward displacement of the center of correlation. The rate appears to be more rapid at Washington and least at Omaha (near 350 and 170 n mi/day respectively with a value near 220 n mi/day at Oakland). There also appears to be a tendency for more rapid movement in the interval from lag -1 day to lag +1 day than in the outlying lag intervals.

All of the values of A_2 (Fig. VI-19) are positive (as contrasted to negative values in the summer) with a strong tendency for the larger values at the larger numerical time lags. This would indicate that as the center of correlation moves from west to east it approaches from the north of west (negative time lags) and departs (positive time lags) toward the north of east.

(b) <u>300 mb Level</u>

The trend of the center of correlation at the 300 mb level is much more definite in both summer and winter. The summer situation, Figs. VI-20 and VI-21, shows a moderate west

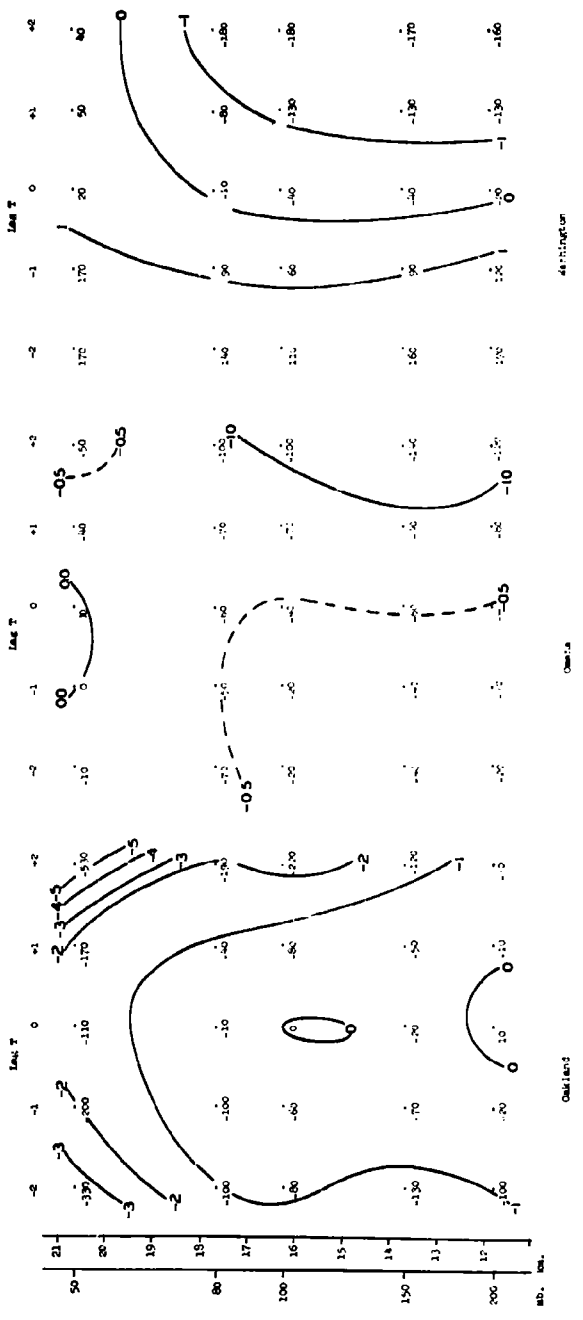

Fig. VI-18

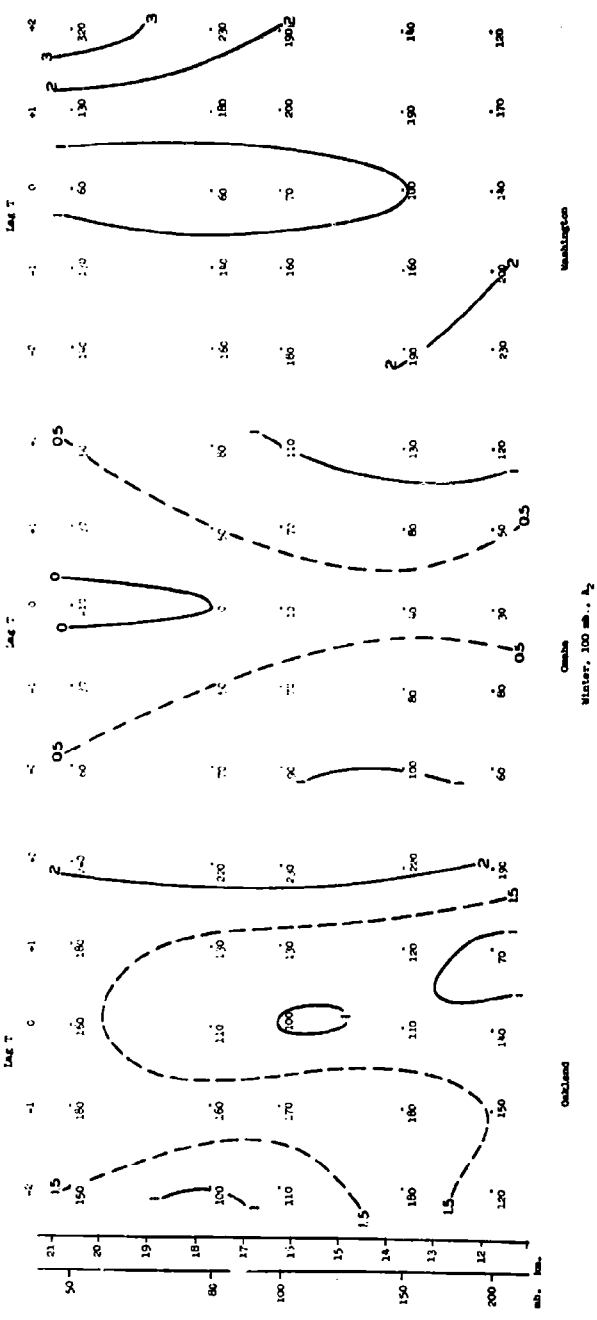

Fig. VI-19

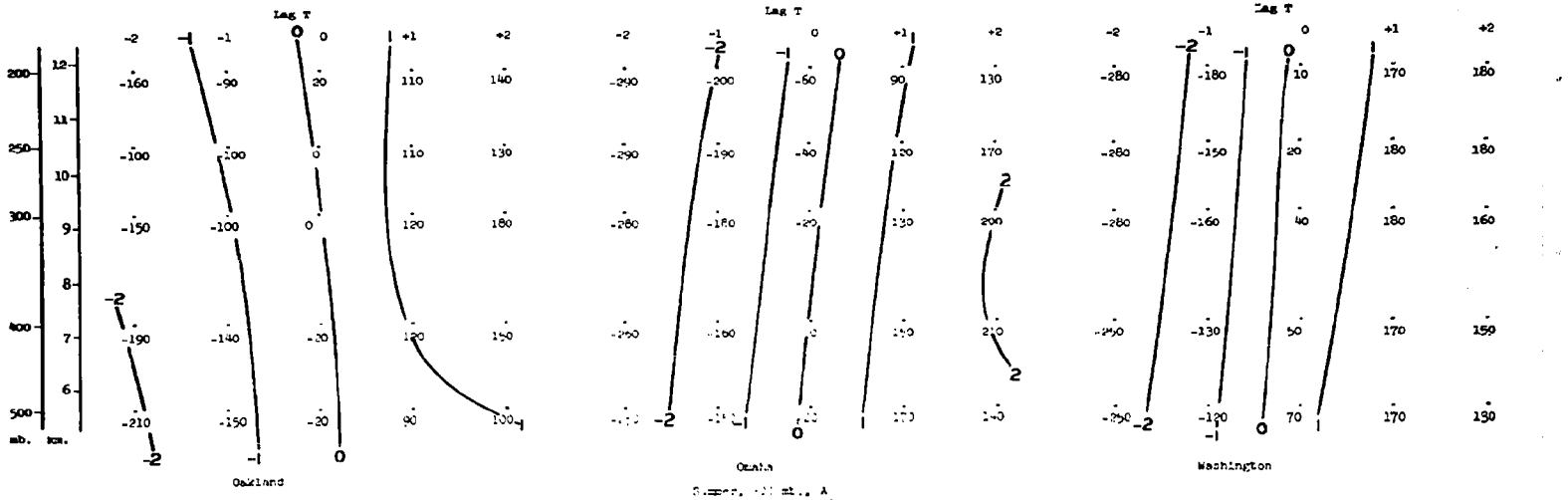

Winter, 300 mb., A

Fig. VI-20

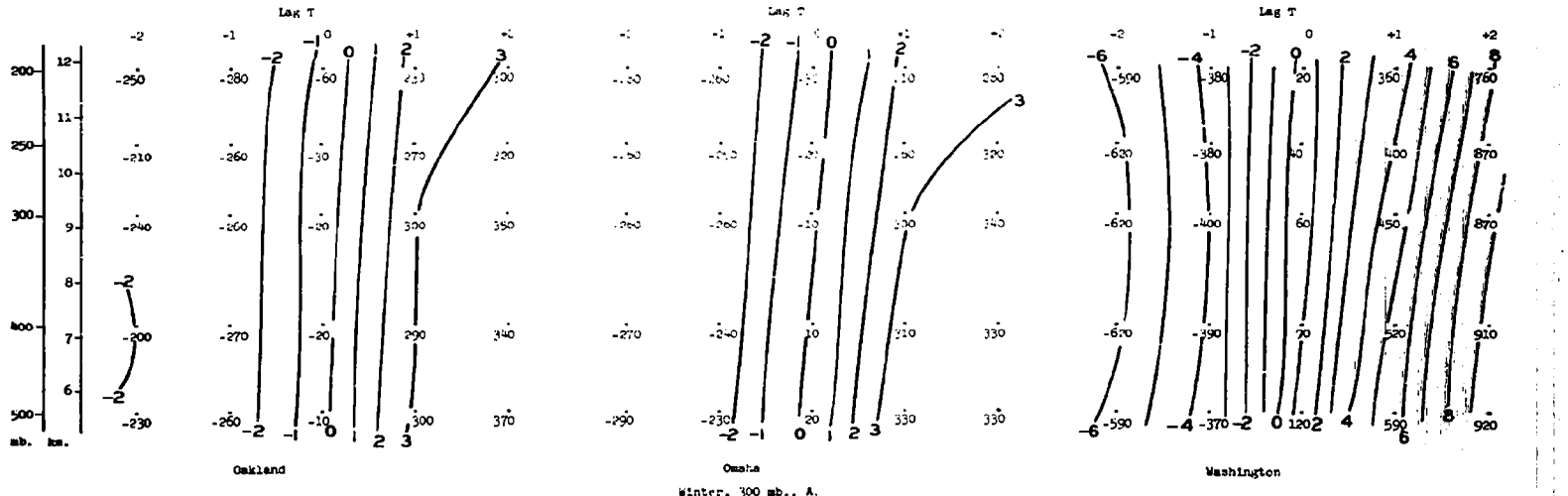

Winter, 300 mb., A

Fig. VI-21

to east motion of near 150 n mi/day (again more rapid near time lag zero than for larger numerical values). The vertical displacement at Oakland appears to be slightly toward the east while at Washington and Omaha it appears to be tilted toward the west (expected). The values of A_2 (Fig. VI-21) indicate a trend from north to south with time lag and from south to north with height lag. This trend at Oakland is particularly small. As a consequence, the center of correlation moves from somewhat north of west to somewhat south of east. The systems are tilted from southeast to northwest.

In the winter (Figs. VI-22 and VI-23) the same situation prevails except with a greatly increased speed of movement in the eastward direction. The decreased rate of movement from -2 to -1 and +1 to +2 is particularly pronounced (Fig. VI-22). The north-south displacement with time lag is also smaller than in summer except in the case of Washington when the sign of the time displacement is reversed, being from south to north.

(c) 500 mb Level

The situation at 500 mb is similar to that at 300 mb in its general aspect. The summer situation (Figs. VI-24 and VI-25) shows the eastward movement of the center of correlation with a tendency to move also from somewhat north of west to definitely south of east. The tilt is reasonably strong from southeast to northwest. (The value of A_1 at height lag -1 and time lag +2 at Omaha is definitely anomalous. The same appears to be true of the values of A_1 at Oakland for height lag of -1,

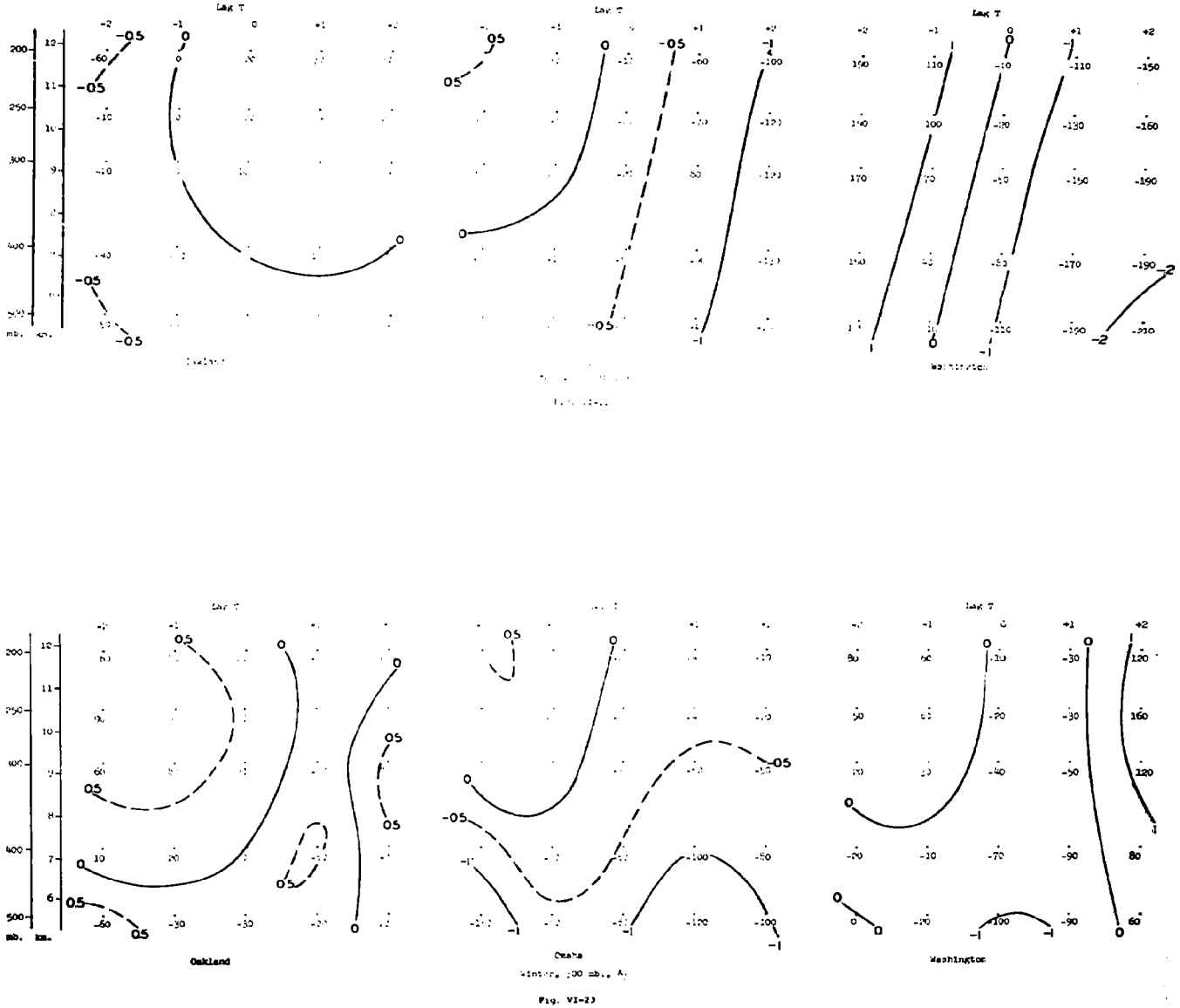

Fig. VI-23

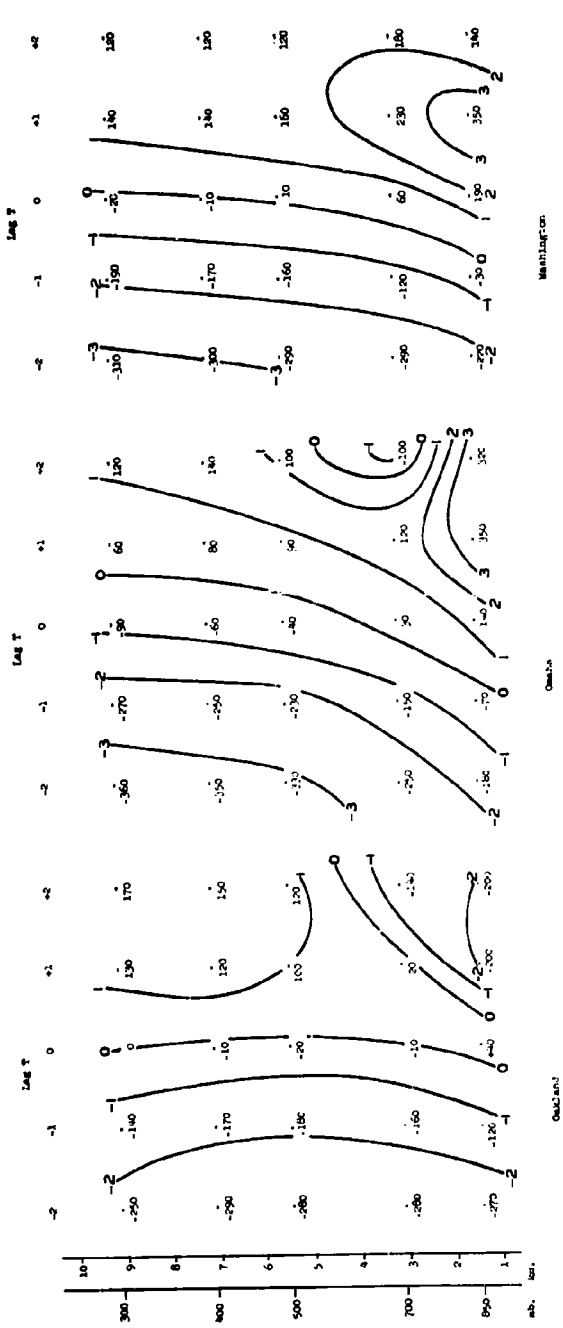

Fig. VI-24

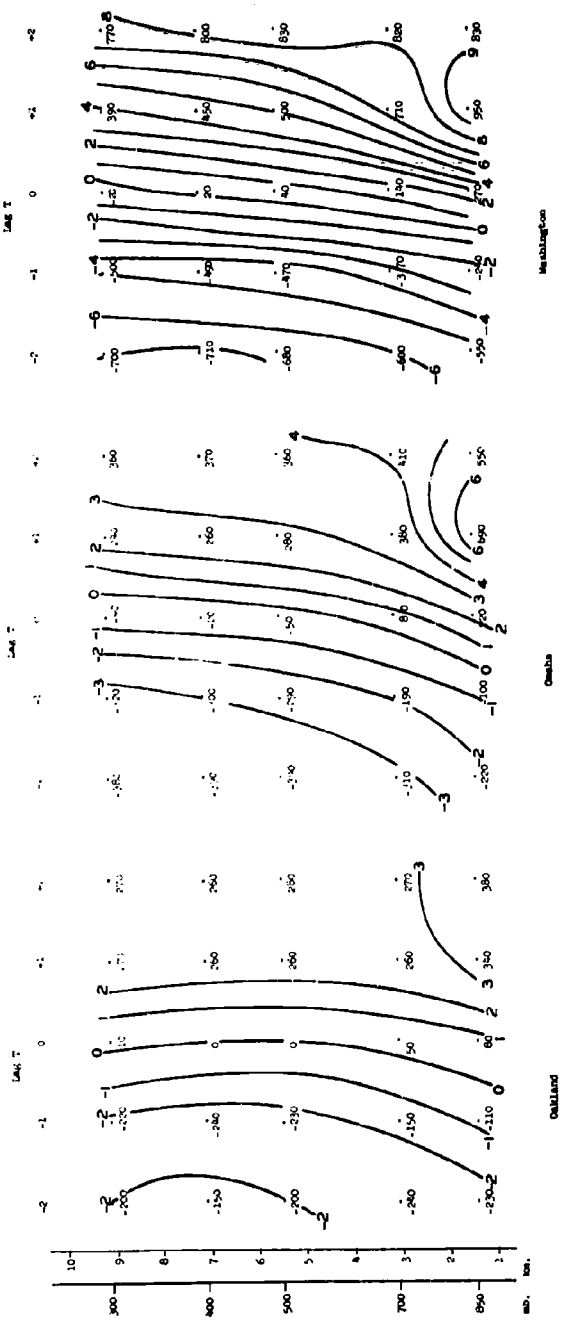

Fig. VI-25

time lag +2 and height lag -2 and time lags -1 and -2. These values were carefully checked, but the source of the error was not located.) In the case of Oakland, the north-south component of motion is much smaller than at the other locations.

The winter situation, Figs. VI-26 and VI-27, appears to be analogous to that at 300 mb in general. At Oakland the movement of the center of correlation is from west to east at about 200 n mi/day with a tilt from southeast to northwest. The same situation prevails at Omaha with a much more pronounced tilt. At Washington the motion is much more rapid, near 400 n mi/day, and with a trend toward a curved path from near west-east curving to the northward for positive time lags. At Washington the tilt tends to be from south to north with little west-east component except for the largest negative height lags.

In Table I the values of the parameters a and b are broken down on the basis of a least squares fit to the form

$$A_1 = a_1 t + b_1 z$$

$$A_2 = a_2 t + b_2 z$$

i.e. strictly linear translation of the center of the correlation pattern with time and linear tilt with height.

(a_1, a_2) = Components of horizontal translation with time (n mi per day)

(b_1, b_2) = Component of tilt with height (n mi per kilometer)

The fit was made in two ways, first for all five time lags, -2 to +2 days, then with only the three central time lags, -1 to +1 days. The speed of translation is larger in this last

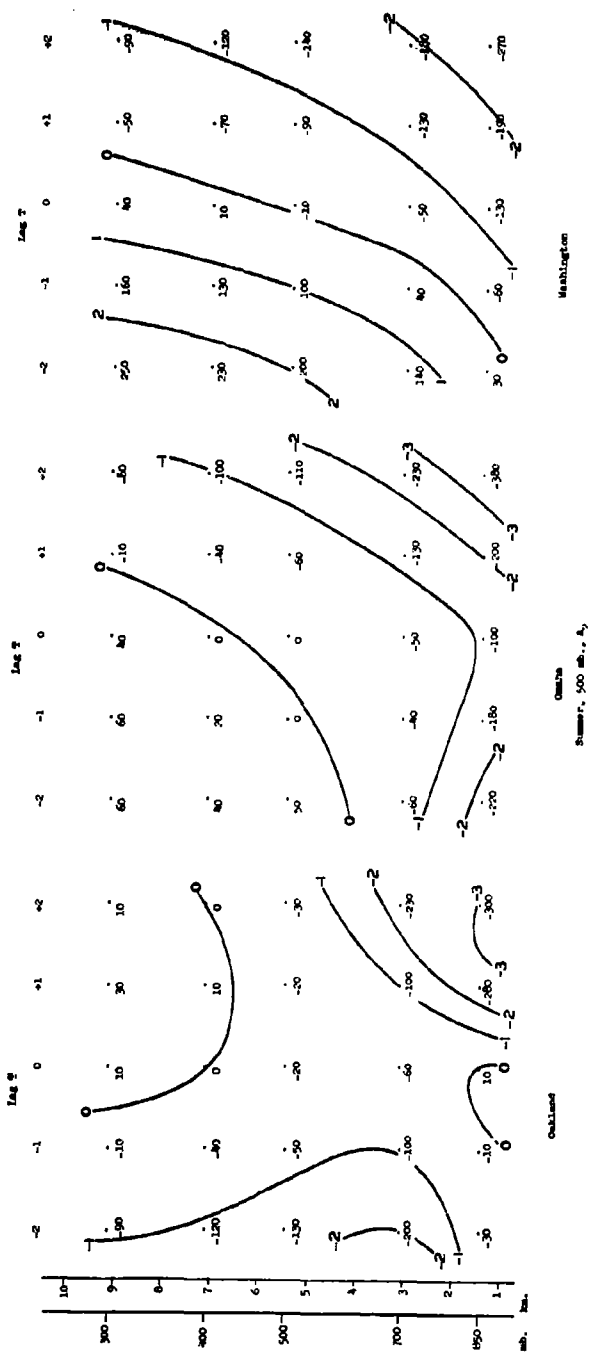
Lag T
Omaha
Summer, 500 mb., A_g
Fig. VI-26
Oakland
Washington

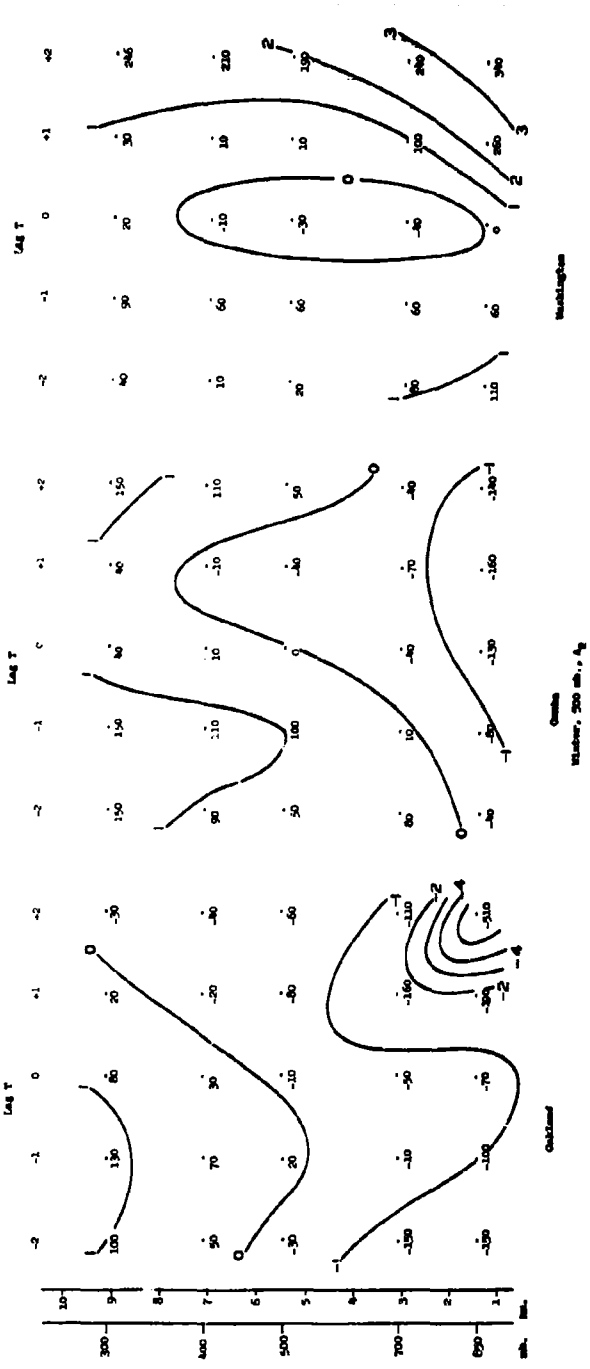
Lag T
Omaha
Winter, 500 mb., A_g
Fig. VI-27
Oakland
Washington

TABLE I

DISPLACEMENT AND TILT RATES
OF THE CORRELATION CENTERS

Master	Season	Level (mb)	-2 ≤ Lag T ≤ +2						-1 ≤ Lag T ≤ +1						$\bar{U}$ (kts)	$\bar{V}$ (kts)
			a_1	b_1	RMS Error	a_2	b_2	RMS Error	a_1	b_1	RMS Error	a_2	b_2	RMS Error		
Wash.	W	100	385	-8.7	156	5	-14.3	163	478	-7.2	93	7	-10.5	111	52.5	1.8
		300	380	-20.2	97	8	12.8	62	428	-20.7	45	-41	15.8	22	75.5	3.5
		500	392	-36.7	132	38	-12.2	116	506	-49.1	79	5	-8.6	61	49.0	0.8
	S	100	208	33.8	164	-75	8.8	49	221	32.1	113	-96	9.4	29	11.0	-4.9
		300	118	-1.7	52	-91	14.5	34	162	-6.4	19	-107	17.5	31	25.8	-5.4
		500	117	-16.7	76	-84	23.0	26	169	-24.7	35	-88	22.7	19	18.7	-4.7
Omaha	W	100	119	-13.9	44	4	-6.5	66	169	-12.2	14	-2	-5.8	37	38.5	-2.4
		300	171	-8.0	71	-12	19.4	41	266	-10.7	15	-38	15.2	26	54.1	-7.9
		500	209	-32.3	99	-18	24.5	52	304	-38.9	62	-52	23.3	21	33.9	-6.9
	S	100	67	3.5	72	-18	5.7	55	78	-3.6	45	-21	5.2	35	12.0	-0.6
		300	119	-6.0	48	-36	10.3	40	154	-9.1	21	-45	9.0	22	31.0	-1.9
		500	115	-20.6	102	-33	30.1	81	165	-26.8	40	-30	24.2	38	19.4	-0.3
Oakland	W	100	168	-17.5	47	13	0.0	158	174	-13.2	19	-20	1.5	110	30.5	-6.8
		300	171	-5.1	86	-7	8.3	42	273	-5.4	17	-33	9.8	21	39.6	-10.8
		500	147	-8.8	80	-33	33.8	83	234	-12.5	33	-54	25.2	19	24.5	-7.8
	S	100	-3	-39.5	197	-12	-20.5	146	16	-33.2	101	9	-13.1	57	12.4	5.7
		300	82	7.4	28	12	7.6	16	112	6.2	8	14	7.8	6	26.0	9.0
		500	77	20.1	114	-1	19.8	101	94	11.7	62	-16	16.1	54	13.5	5.0

case and more representative of a speed value. The root mean square error is also tabulated in each case. The mean wind components are shown in the last two columns.

The association between the mean wind and the values of a_1 and a_2 may be estimated by means of the following relations:

at the 100 mb level displacement = 0.30 x 24-hour average wind movement

at the 300 mb level displacement = 0.23 x 24-hour average wind movement

at the 500 mb level displacement = 0.40 x 24-hour average wind movement with RMS errors of 68, 36, and 26 n mi respectively

(If the displacement is related to 24-hour wind movement by a two-term regression of the form $\alpha + \beta(\overline{U}x24)$, $\overline{U}$ x 24 = movement of wind in 24 hours, then

α	β	RMS Error
-8 n mi	0.31	68 n mi
-23	0.25	31
-18	0.42	21

and it is seen that the additional refinement in $\alpha \neq 0$ is scarcely worth while.)

4. Characteristics of Parameter A

Figs. VI-28 through VI-33 show the variation of the parameter A with height lag and time lag. The general characteristics of this variation is that the parameter A has its maximum value near height and time lag zero and decreases as the height and time lags depart from zero.

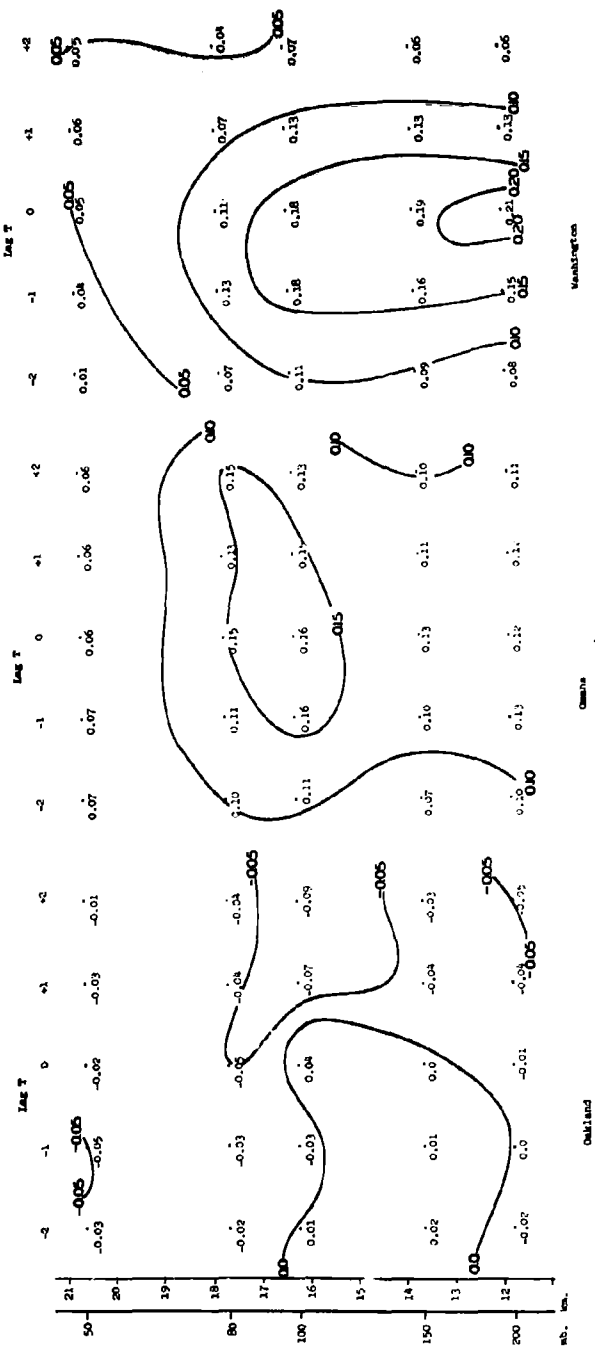

Fig. VI-28

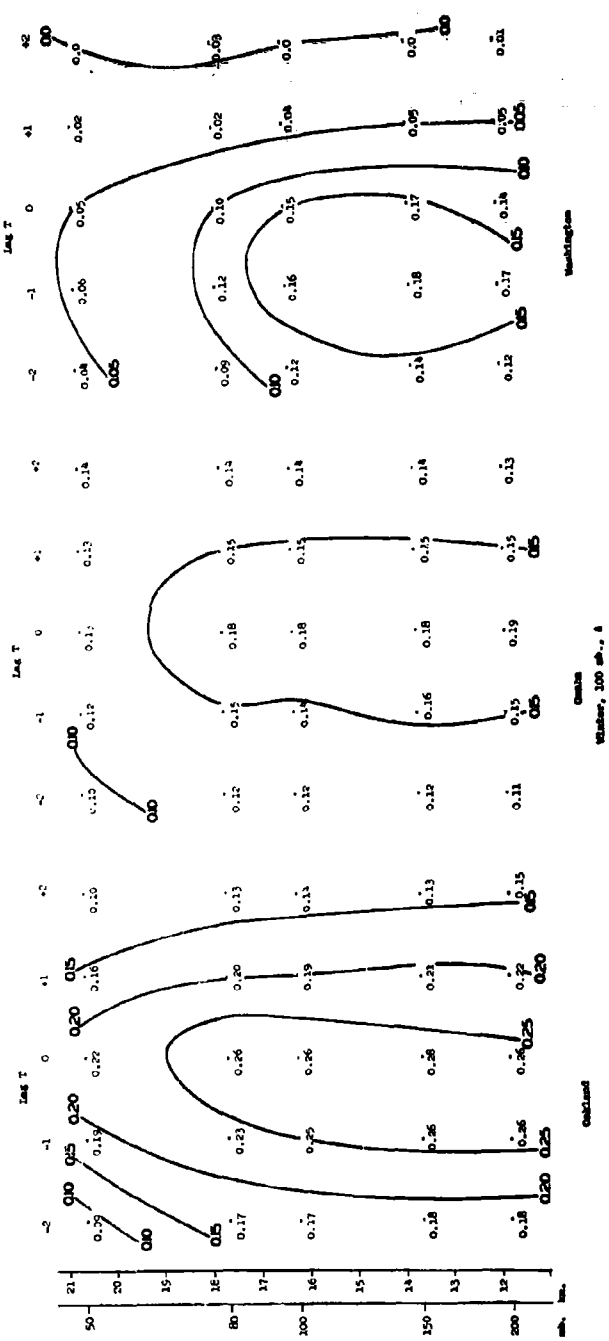

Fig. VI-29

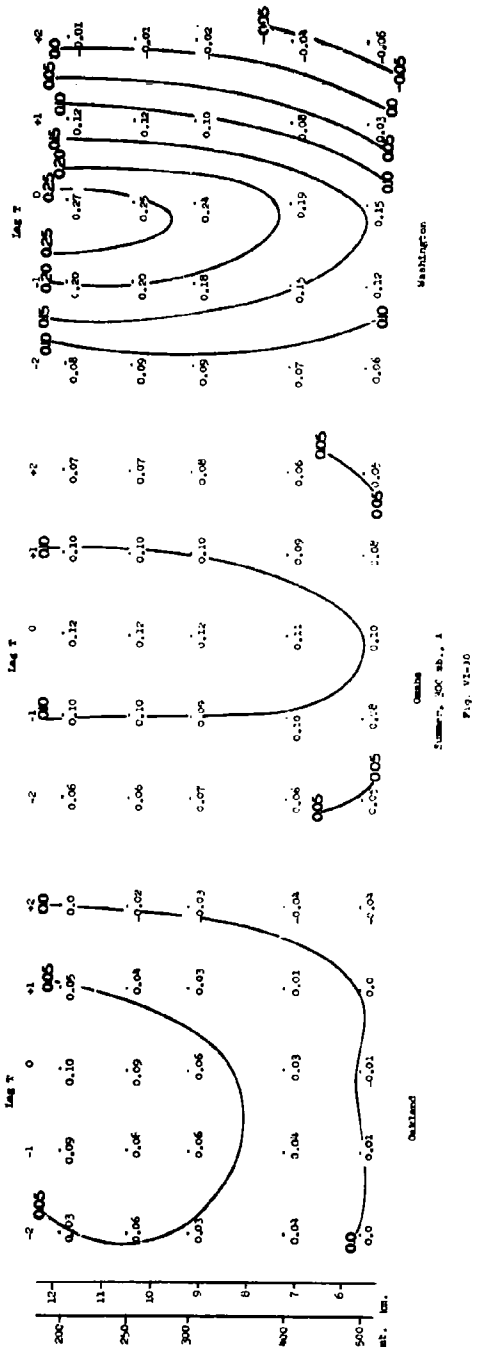
Lag T
Oakland
Washington
Omaha
Summer, 300 mb., A
Fig. VI-30

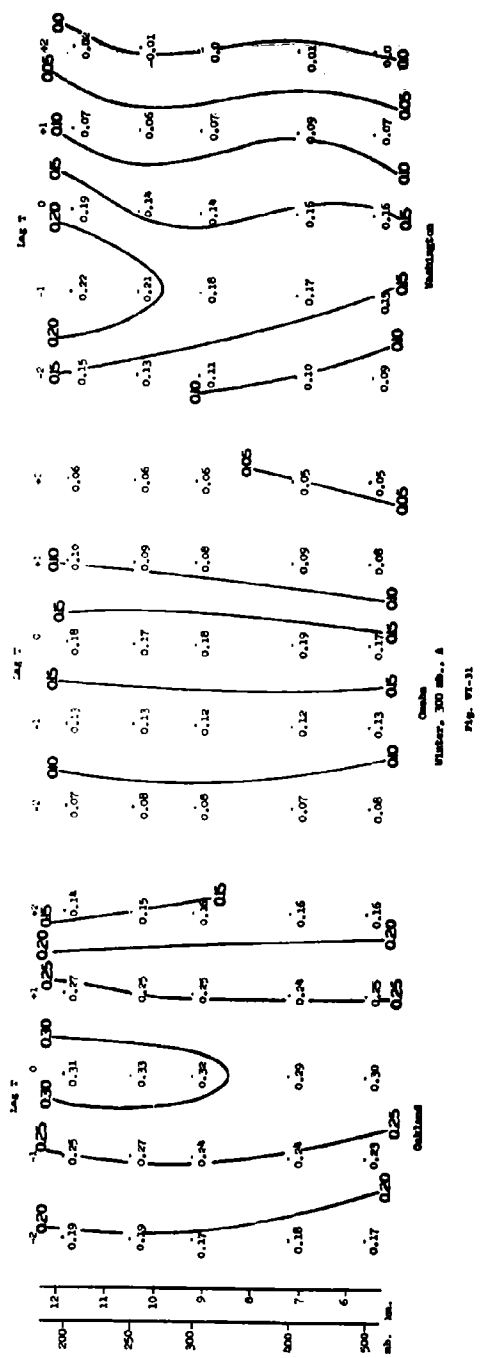
Lag T
Oakland
Washington
Omaha
Winter, 300 mb., A
Fig. VI-31

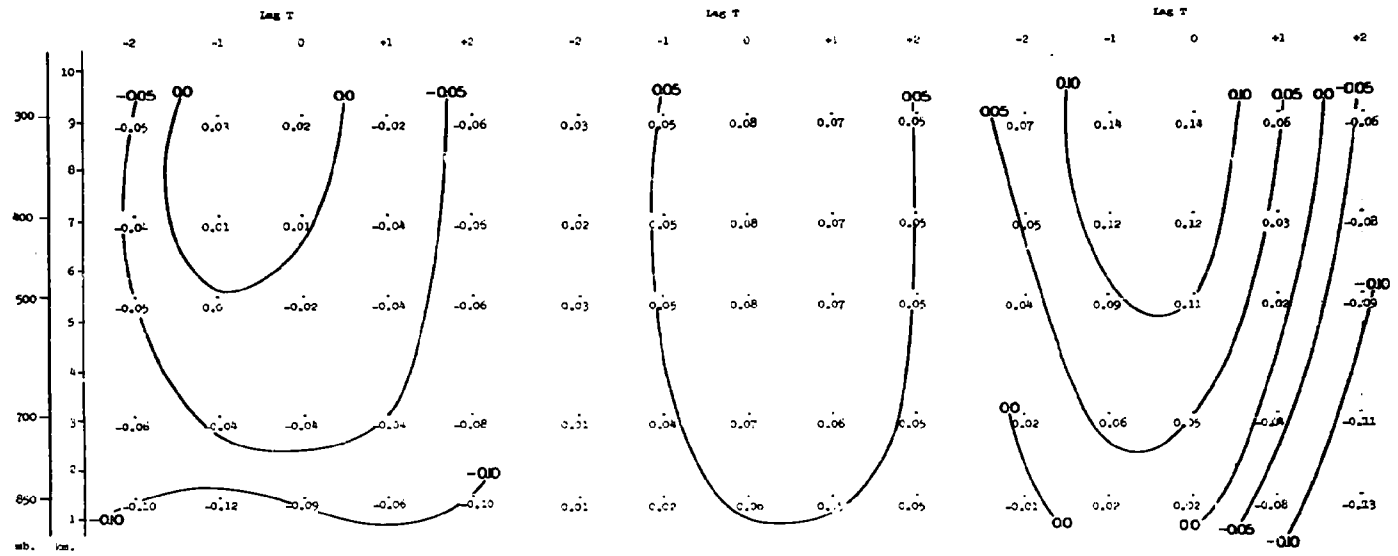

Fig. VI-32

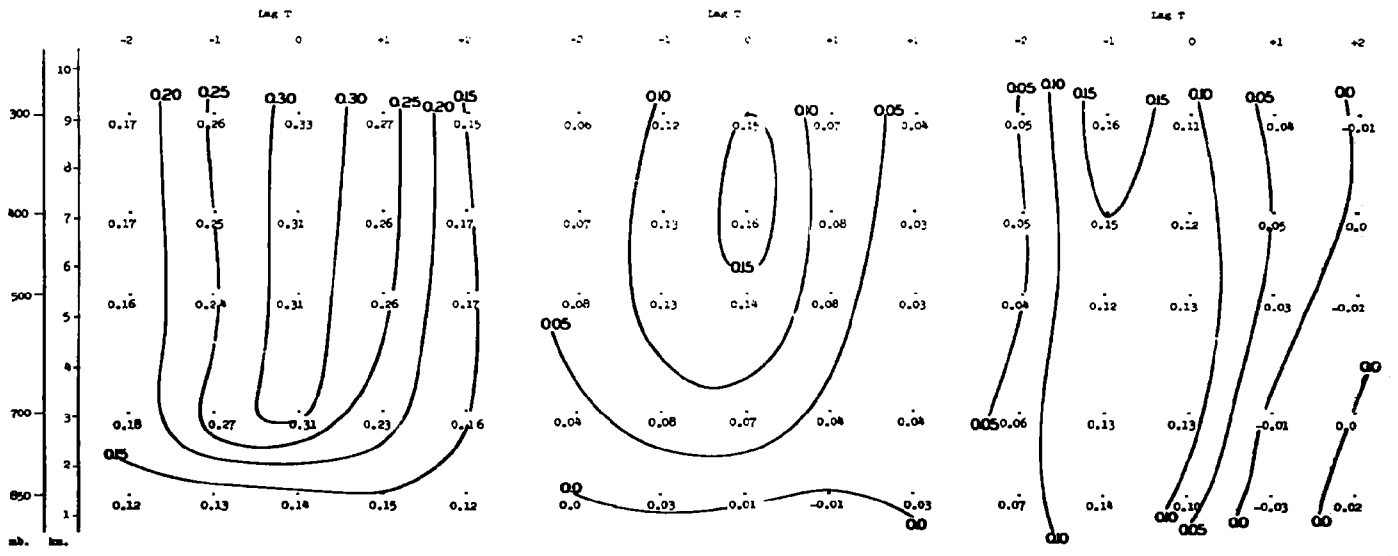

Fig. VI-33

From equation (7a) it is seen that the value of A depends on i) the direction and orientation of the gradient of the standard deviation of height, ii) the square of the size parameter L.

The direction and orientation of the gradient of the standard deviation of height is constant with respect to time lag so that the time variation of A should be a reflection of that of L. Since L tends to increase with time lag the reflected variation with respect to time as it appears in A would be such as to make A increase with time lag. This is just the reverse of the variation actually experienced. One can only conclude that the simplified assumptions that enter into the deviation of the estimate of the form of equation (6c) are inadequate.

The decrease in the parameter k with time lag is ignored since it would be expected that the correlations entering the equations carry with them such a factor which will account for the degradation of correlation due to the various factors involved in the parameter k.

The form of the expression (6c) was derived on the basis of the assumption that the major contribution to the departure from a strictly ideal situation consists of the non-zero gradient of the standard deviation of height. It has been pointed out that the effects of the non-circularity of the height correlation contours may be detected in the structure of the components of the correlation tensor. This and other effects such as other departures from homogeneity in the correlations themselves (the

fact that parameters in the description of the correlation function also have gradients) may well contribute to the anomalous behavior of parameter A.

5. Characteristics of Parameters B and C

Figs. VI-34 through VI-45 show the behavior of the parameters B and C as functions of height lag and time lag. The illustrations in this sequence are ordered like those for parameters A_1 and A_2 since B and C are related to vector components; i.e. illustration for B and C are in successive pairs for each season and elevation.

The parameters B and C are related (see equations (7a) and (7b)) to the components of the gradient of the standard deviation of height and as such they should be independent of the time lag. Descriptions of Figs. VI-34 through VI-45 clearly indicate a time lag dependence in these parameters. On the other hand, equations (7a) and (7b) contain the time lag dependent parameter L which increases with time lag; but, the nature of the variation of B and C with time could hardly be attributed to a reflection of the variation of the parameter L

The situation with regard to parameters B and C appears to be similar to that encountered in the case of parameter A; there appear to have been so many simplifying assumptions made in the derivation of the form of equation (6d) that contact with the actual situation has been largely lost.

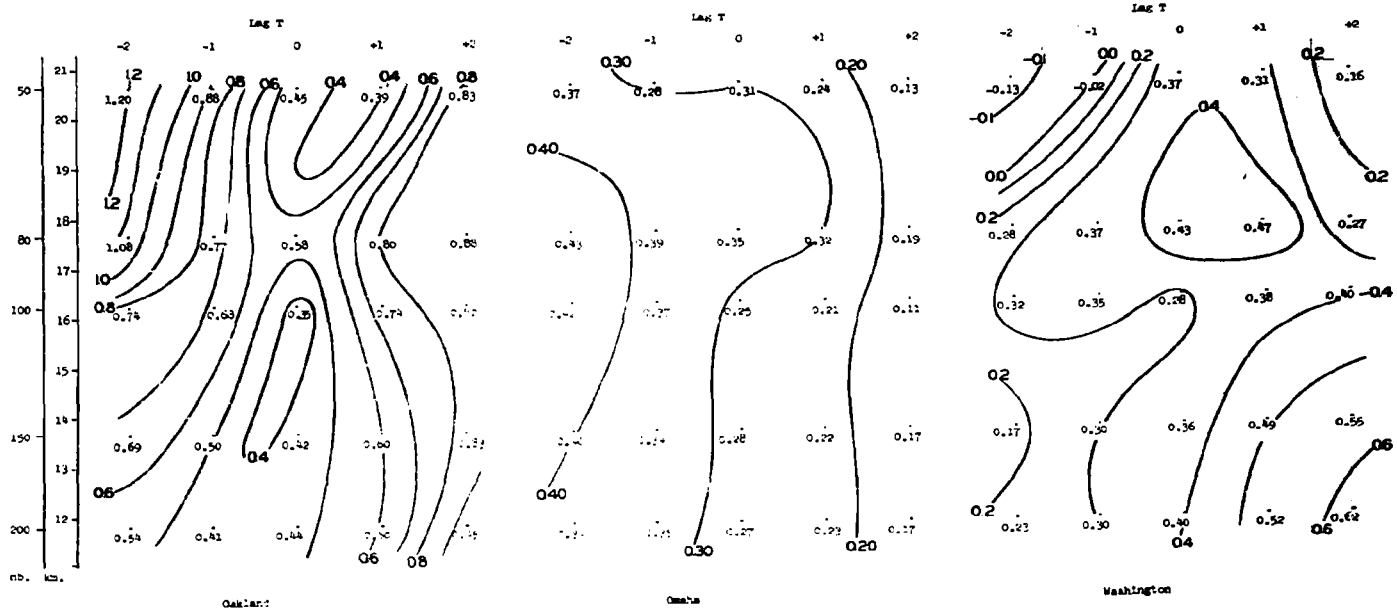

Fig. VI-34

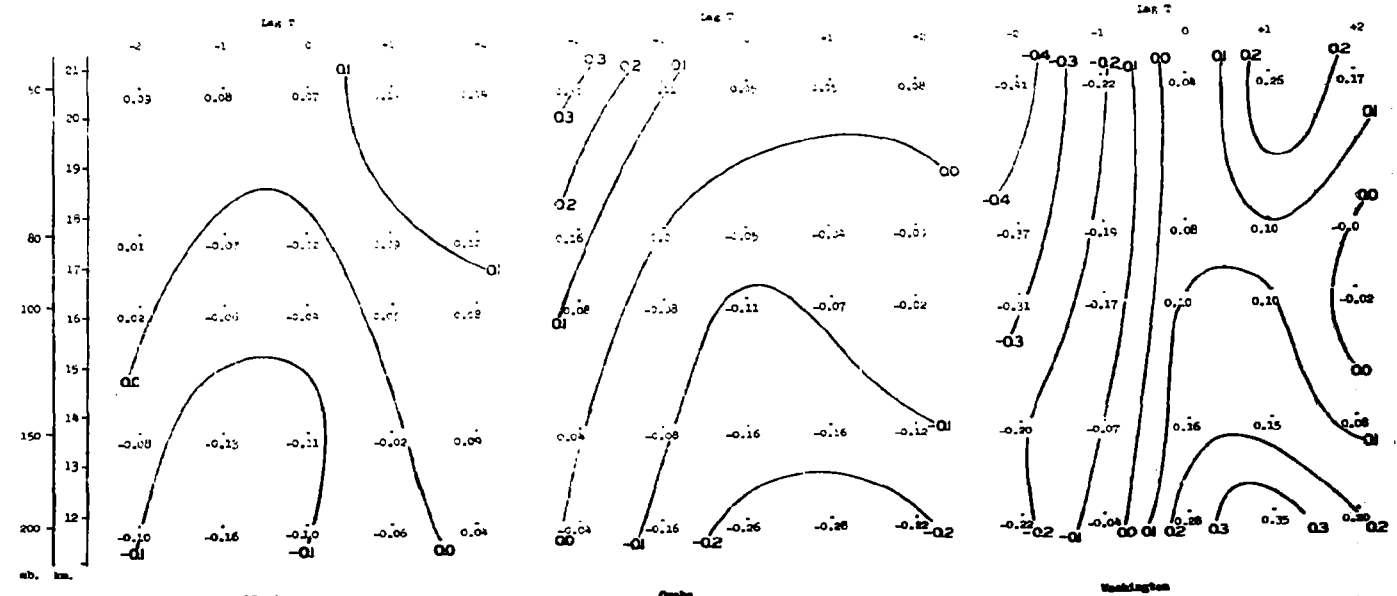

Fig. VI-35

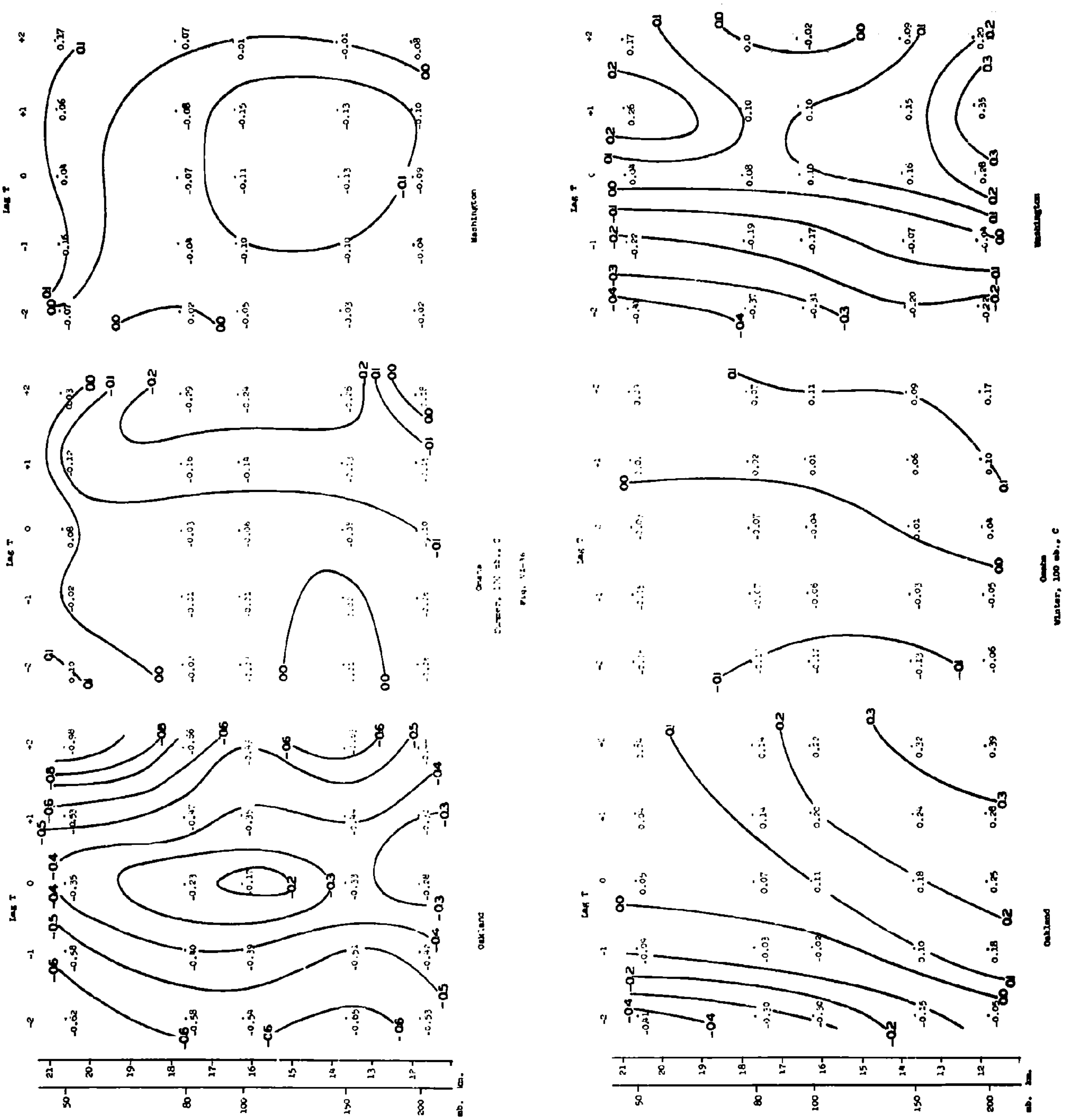

Omaha
Winter, 100 mb., C
Fig. VI-37

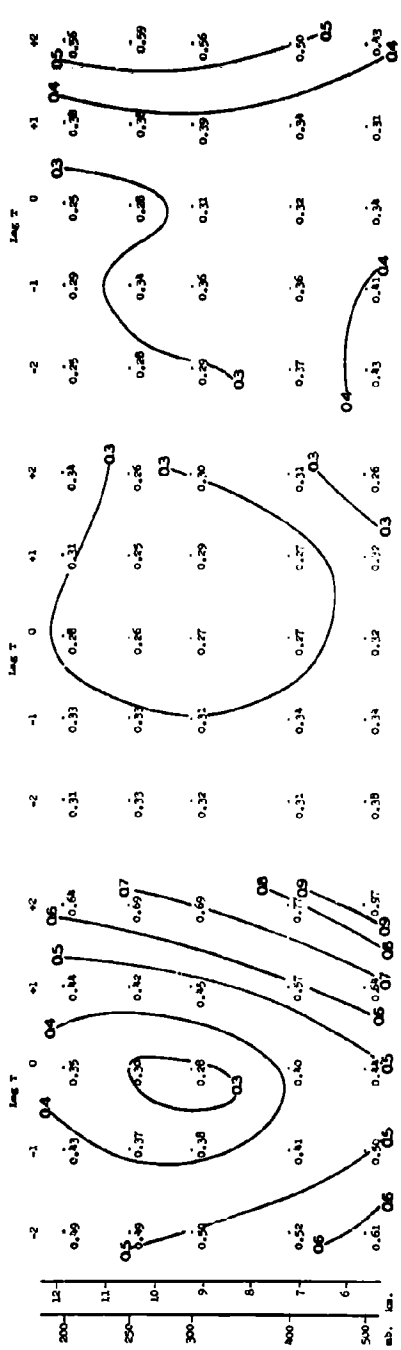

Fig. VI-38

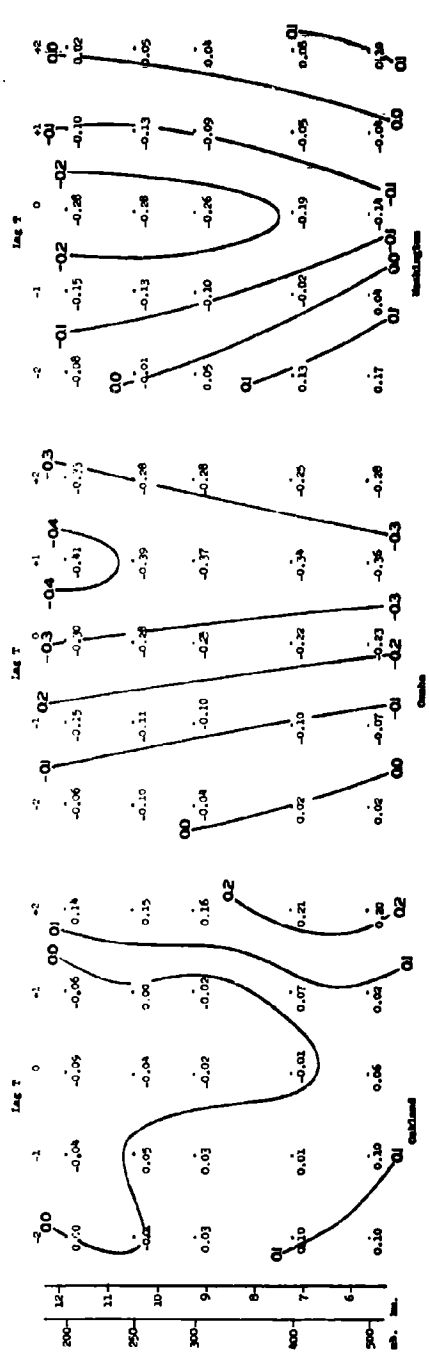

Fig. VI-39

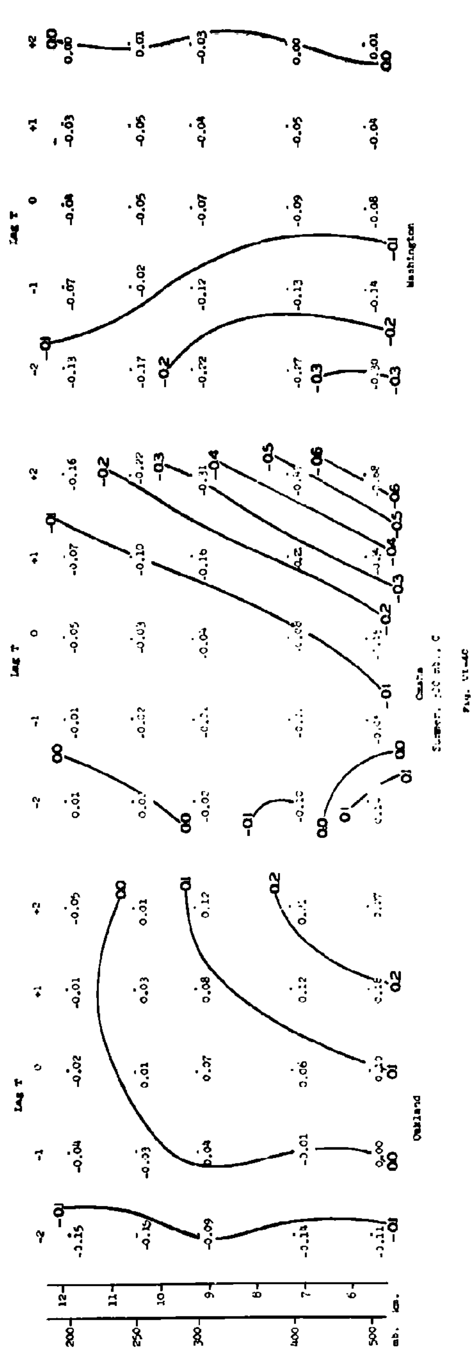

Omaha
Summer, 300 mb., C
Fig. VI-40

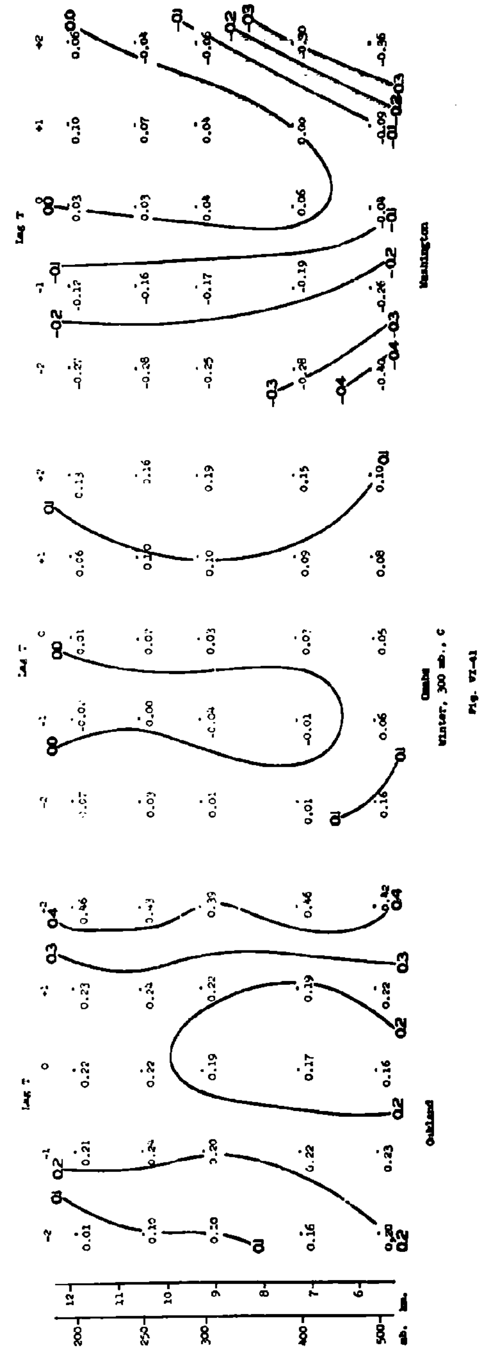

Omaha
Winter, 300 mb., C
Fig. VI-41

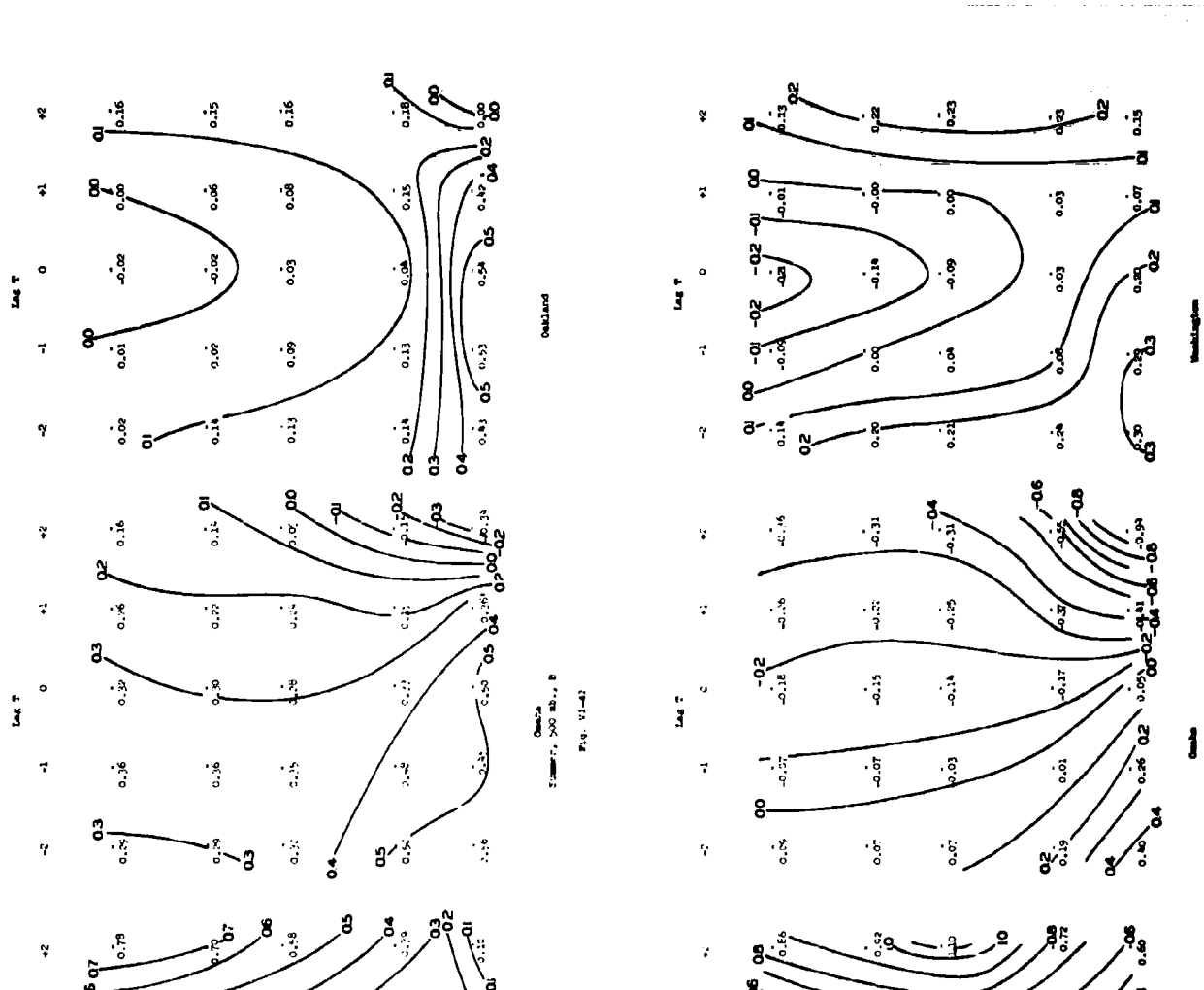
Lag T
Oakland
Omaha
Summer, 900 mb., 8
Fig. VI-42
Washington
Omaha
Winter, 900 mb., 8
Fig. VI-43
Oakland
Washington
mi.
mb.

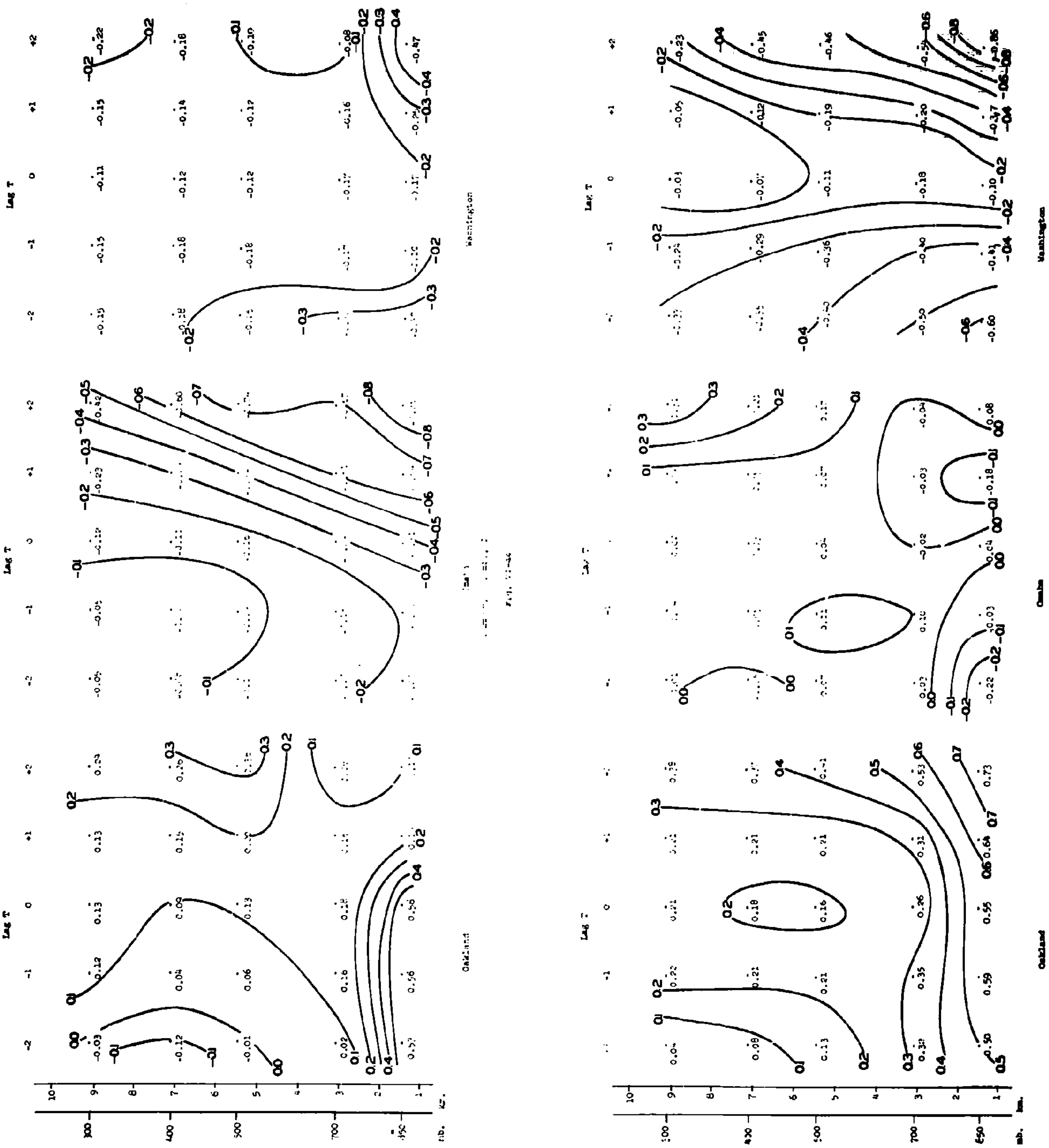

Omaha
Winter, 500 mb., C

Fig. VI-43

F. APPLICATION TO VARIABILITY OF WIND IN THE VERTICAL

1. Preliminary Considerations

The variability of wind in the vertical may be described by using $t = x_1 = x_2 = x_1' = x_2' = 0$ in equations (8) and (3b). Then

$$r_{11} = k\left(1 - \frac{z^3}{\zeta^3}\right)\left(1 - \frac{b_2^2}{L^2}z^2\right)\exp\left[-\frac{z^2}{2}\left(\frac{b_1^2+b_2^2}{L^2} + \frac{1}{D^2}\right)\right],$$

$$r_{22} = k\left(1 - \frac{z^3}{\zeta^3}\right)\left(1 - \frac{b_1^2}{L^2}z^2\right)\exp\left[-\frac{z^2}{2}\left(\frac{b_1^2+b_2^2}{L^2} + \frac{1}{D^2}\right)\right],$$

$$r_{12} = k\left(1 - \frac{z^3}{\zeta^3}\right)\left[A + \frac{b_1 b_2}{L^2}z^2 + (Bb_1+Cb_2)z\right]\exp\left[-\frac{z^2}{2}\left(\frac{b_1^2+b_2^2}{L^2} + \frac{1}{D^2}\right)\right],$$

$$r_{21} = k\left(1 - \frac{z^3}{\zeta^3}\right)\left[A + \frac{b_1 b_2}{L^2}z^2 - (Bb_1+Cb_2)z\right]\exp\left[-\frac{z^2}{2}\left(\frac{b_1^2+b_2^2}{L^2} + \frac{1}{D^2}\right)\right].$$

From the first pair, it is evident that the change of r_{11} and r_{22} with respect to height difference, z, are different from each other. This is because the one involves factor $(1 - b_2^2z^2/L^2)$ while the other involves the factor $(1 - b_1^2z^2/L^2)$. These may be simplified to:

$$r_{11} = k(1-Az^3)(1 - B_2^2z^2)\exp(-C^2z^2/2),$$

$$r_{22} = k(1-Az^3)(1 - B_1^2z^2)\exp(-C^2z^2/2),$$

$$r_{12} = k(1-Az^3)(A_o + B_1B_2z^2 + Ez)\exp(-C^2z^2/2),$$

$$r_{21} = k(1-Az^3)(A_o + B_1B_2z^2 - Ez)\exp(-C^2z^2/2).$$

The first few terms of the series expansions of these correlations become

$$r_{11} = k\left[1 - \left(\frac{b_1^2+3b_2^2}{2L^2} + \frac{1}{2D^2}\right)z^2 - Az^3 + \text{---}\right],$$

$$r_{22} = k\left[1 - \left(\frac{3b_1^2+b_2^2}{2L^2} + \frac{1}{2D^2}\right)z^2 - Az^3 + \text{---}\right].$$

If only the part due to the differentiable part of the wind components (the part in parenthesis on the right) is considered, then from Appendix A-III it follows that

$$\sigma_u'^2 - (\sigma_{u'})^2 = \left(\frac{b_1^2+3b_2^2}{L^2} + \frac{1}{D^2}\right)\sigma_u^2$$

and

$$\sigma_v'^2 - (\sigma_{v'})^2 = \left(\frac{3b_1^2+b_2^2}{L^2} + \frac{1}{D^2}\right)\sigma_v^2$$

where

σ_u = Standard deviation of u component

σ_u' = Rate of change of σ_u with height

$\sigma_{u'}$ = Standard deviation of the component of wind shear.

This implies, since the right sides are unequal, that there are basic differences in the behavior of either (i) the standard deviations of the u and v wind components as a function of height, (ii) the standard deviations of the wind shear components, or (iii) both. The inequality of the right-hand terms is, of course, brought about by the tilt of the wind correlation patterns in the horizontal (isobaric surface) as a function of height differences.

It is not necessary to begin with the specific empirical expression employed in Chapter III to obtain these results. Consider a three-dimensional differentiable function. Then let

$$r(\xi,\eta;\zeta) = a_0(\zeta) + \frac{1}{2!}\left[a_{20}(\zeta)(\xi - b_1\zeta)^2 + 2a_{11}(\zeta)(\xi - b_1\zeta)(\eta - b_2\zeta)\right.$$

$$\left. + a_{02}(\zeta)(\eta - b_2\zeta)^2\right] + \text{---}$$

where the coefficients are functions of ζ, the height difference. The parameter ζ is introduced in such a way that the translation of the center of correlation with height difference is explicit

and is located at $\xi - b_1\zeta = 0$, $\eta - b_2\zeta = 0$. Then rearranging terms to appear as ascending powers of ζ, expanding

$$a_0(\zeta) = 1 + a_0''\zeta^2/2! + ---,$$

and setting $\xi = \eta = 0$

$$r(0,0;\zeta) = 1 + \left[a_0'' + (a_{20}b_1^2 + 2a_{11}b_1b_2 + a_{02}b_2^2)\right]\zeta^2/2! + ---.$$

The quantities a_0'', a_{20}, a_{02}, (and perhaps a_{11}) are negative. The coefficient of ζ^2 is made up of two parts. The first, a_0'', is the way in which the correlation coefficient maximum decays with ζ. The second, the parenthetical terms, is the part due to the shift of the correlation maximum with height difference.

Consider the empirical model used previously, with $a_0'' = -1/(2D^2)$. When the correlation concerned is r_{11}, $a_{20} = 1/(2L^2)$, $a_{11} = 0$, $a_{02} = 3/(2L^2)$ while for r_{22}, $a_{20} = 3/(2L^2)$, $a_{11} = 0$, $a_{02} = 1/(2L^2)$. The reason for the difference in behavior lies not so much in these specific values as in the fact that the values are different from r_{11} to r_{22}.

2. Practical Analysis of Wind Correlations in the Vertical

The preceding outline is unsuited for the detailed analysis of wind component correlations in the vertical since it requires many levels above and below the "master level" to determine the parameters and since some of the parameters indicated as constants herein turn out to be functions of the level difference, (see the earlier part of this Chapter in which these variations were discussed extensively). It is, however, possible to use a series approximation for the correlation in the vertical over a limited range of level differences and to obtain specific

information on the coefficients of the first and second terms. Thus, let:

$$r_{11} = a_0 + a_2 z^2 + a_3 z^3 + a_4 z^4 + \text{---}$$
$$r_{22} = b_0 + b_2 z^2 + b_3 z^3 + b_4 z^4 + \text{---}.$$

Then if the series forms are terminated after the fourth degree term, reasonable estimates of a_0, a_2, b_0, b_2 may be obtained (also a_3 and b_3, but the meaning of these terms is not as useful as the first pairs).

This procedure was carried out for the summer and winter wind component correlations at Washington, D.C., and Wiesbaden, Germany.(4) The results of the determination of the coefficients are given in Table II. (In this table the values pertaining to the north-south wind component are tabulated under column headings that may make it appear that the east-west component is intended. The component intended is given on the line indicating station and season.) In the table the height of the "master level" is indicated in kilometers. The correlation values at the master level ($z = 0$) are, of course, 1 and are not used. The data used were the correlations for height lags of ± 2, ± 4, and ± 6 km, the three values above and below the master level. Values of the four coefficients and the root mean square value of the residuals, $\sqrt{s^2}$, are tabulated. The coefficients are in terms of a 2 km height interval so that the units are $(2 \text{ km})^{-2}$, $(2 \text{ km})^{-3}$, and $(2 \text{ km})^{-4}$ for a_2, a_3, and a_4. The values of a_0 and $\sqrt{s^2}$ are dimensionless.

The value of a_0 is expressed in terms of the standard deviation of wind component and the standard deviation of the observation

TABLE II

ANALYSIS OF WIND COMPONENT CORRELATIONS IN THE VERTICAL

Level	a_0	a_2	a_3	a_4	$\sqrt{s^2}$	σ_*	σ_0	σ_e	σ_1
			Washington, Winter, E-W Component						
8 km	.901	-.0598	.00231	.00182	.009	29.40	27.9	9.2	5.9
10	.862	-.0535	-.00367	.00207	.031	34.28	31.8	12.7	5.6
12	.812	-.0577	-.00215	.00384	.026	32.03	28.9	13.9	5.7
14	.743	-.0605	-.00499	.00313	.038	27.39	23.8	13.5	5.4
16	.574	-.0117	-.00192	-.00056	.043	21.85	16.6	14.3	2.1
18	.467	-.0157	-.00512	.00091	.029	22.36	15.3	16.3	2.0
20	.432	+.0144*	+.00096	-.00252	.024	22.67	14.9	17.1	- *
			Washington, Winter, N-S Component						
8 km	.928	-.0503	.00149	.00119	.018	37.88	36.5	10.1	6.6
10	.882	-.0445	-.00284	.00147	.028	40.36	37.9	13.9	6.3
12	.807	-.0410	-.00258	.00197	.028	30.83	27.7	13.5	6.2
14	.717	-.0116	-.00757	-.00248	.017	23.19	19.6	12.3	3.8
16	.686	-.0810	-.00661	.00540	.079	17.16	14.2	9.6	4.2
18	.420	+.0230*	-.00493	-.00240	.075	13.34	8.6	10.1	0.4*
20	.461	-.0668	+.00060	.00445	.038	11.20	7.6	8.2	2.2
			Washington, Summer, E-W Component						
8 km	.920	-.0532	.00439	.00224	.008	18.94	18.2	5.3	3.8
10	.933	-.0568	.00003	.00245	.005	23.95	23.1	6.2	4.5
12	.889	-.0516	-.00485	.00138	.028	27.30	25.7	9.1	4.4
14	.807	-.0543	-.00915	.00240	.045	23.19	20.8	10.2	4.9
16	.675	-.0553	-.00670	.00352	.058	14.76	12.1	8.4	4.0
18	.477	-.0066	-.00318	-.00090	.045	10.35	7.2	7.5	1.8
20	.497	-.04162	-.00109	.00172	.038	8.17	5.8	5.8	1.4
			Washington, Summer, N-S Component						
8 km	.886	-.0470	.00672	.00093	.010	19.44	18.3	6.6	4.4
10	.916	-.0501	.00162	.00150	.011	27.06	25.9	7.8	5.3
12	.905	-.0617	-.00330	.00258	.032	31.63	30.1	9.8	5.6
14	.782	-.0303	-.00855	-.00011	.042	22.93	20.3	10.7	5.8
16	.678	-.0733	-.00945	.00470	.067	13.60	11.2	7.7	4.4
18	.463	-.0396	-.00844	.00240	.101	8.77	6.0	6.4	2.2
20	.273	-.0313	-.00594	.00193	.058	6.36	3.3	5.4	1.1

TABLE II

(CONTINUED)

Level	a_0	a_2	a_3	a_4	$\sqrt{s^2}$	σ_*	σ_o	σ_e	σ_1
			Wiesbaden, Winter, E-W Component						
8 km	.936	-.0355	.00072	.00093	.002	30.81	29.8	7.8	4.4
10	.928	-.0390	-.00189	.00214	.021	31.93	30.8	8.6	4.7
12	.869	-.0202	-.00136	.00094	.014	24.98	23.3	9.0	3.6
14	.858	-.0357	-.00123	.00178	.003	21.68	20.1	8.2	3.1
16	.871	-.0216	.00102	.00075	.015	20.14	18.8	7.2	2.1
18	.916	-.0468	.00162	.00326	.024	21.00	20.1	6.1	3.2
20	.882	-.0103	.00256	-.00091	.005	20.15	18.9	6.9	1.5
			Wiesbaden, Winter, N-S Component						
8 km	.937	-.0416	.00195	.00080	.002	32.94	31.9	8.3	5.2
10	.913	-.0386	-.00200	.00158	.029	34.55	33.0	10.2	5.1
12	.856	-.0217	-.00206	.00057	.011	26.56	24.6	10.1	4.6
14	.847	-.0435	-.00214	.00206	.003	19.80	18.2	7.7	4.0
16	.842	-.0285	.00015	.00096	.014	15.66	14.4	6.2	2.2
18	.855	-.0501	.00213	.00375	.014	15.17	14.0	5.8	2.4
20	.803	.0023*	.00035	-.00320	.021	14.97	13.4	6.6	- *
			Wiesbaden, Summer, E-W Component						
8 km	.926	-.0310	.00221	.00064	.001	23.99	23.1	6.5	3.6
10	.902	-.0287	-.00228	.00047	.017	28.03	26.6	8.8	3.4
12	.883	-.0298	-.00558	.00050	.010	26.29	24.7	9.0	4.0
14	.881	-.0536	-.00637	.00235	.014	18.83	17.7	6.5	4.4
16	.838	-.0752	-.00400	.00467	.053	13.90	12.7	5.6	3.4
18	.718	-.0320	-.00219	.00040	.035	10.78	9.1	5.7	1.7
20	.746	-.0707	.00004	.00277	.027	9.58	8.3	4.8	1.8
			Wiesbaden, Summer, N-S Component						
8 km	.943	-.0331	.00325	.00051	.004	25.08	24.4	6.0	4.0
10	.930	-.0287	-.00156	.00051	.012	29.66	28.6	7.9	3.6
12	.911	-.0332	-.00454	.00097	.006	26.21	25.0	7.8	4.6
14	.890	-.0452	-.00658	.00147	.013	17.15	16.2	5.7	4.2
16	.851	-.0774	-.00609	.00472	.054	12.78	11.8	4.9	3.4
18	.696	-.0615	-.00623	.00366	.086	8.0	6.7	4.4	2.1
20	.601	-.0578	-.00535	.00262	.020	6.8	5.2	4.3	1.3

*In all cases where $a_2 > 0$, there appear to be discrepancies in the correlations.

errors and the component due to small scale eddies. Thus

$$a_o = k = \frac{\sigma_o^2}{\sigma_*^2} = \frac{\sigma_*^2 - \sigma_e^2}{\sigma_*^2}$$

where: σ_* is the observed standard deviation of wind component, σ_e is the standard deviation of the part due to observation errors and small scale eddies, σ_o is the standard deviation of the wind component in the absence of these effects

$$\sigma_*^2 = \sigma_o^2 + \sigma_e^2$$

The coefficient of the second term of the series is (see Appendix A-III) given by

$$\sigma_1^2 = \left(\frac{\partial \sigma_o}{\partial z}\right)^2 + \sigma_o^2\left(\frac{-2a_2}{a_o}\right) = \left(\frac{\partial \sigma_o}{\partial z}\right)^2 + \sigma_*^2(-2a_2)$$

where σ_1 is the standard deviation of the wind shear component. In this instance, the wind shear concerned is that due to the differentiable part of the wind.

To discuss meaningfully the wind shear vector, it is assumed that the wind shear exists in the derivative sense, $\partial u/\partial z$ and $\partial v/\partial z$. This implies that the wind component is a differentiable function of height. The correlation coefficient of such a function must be quadratic near zero height separation, and hence the form of the series approximation to the correlation coefficients must omit the linear term.

The values of σ_o and σ_e were determined from σ_* and a_o and are tabulated in Table II and illustrated in Fig. VI-46. The shape of the curves of σ_* (and σ_o) are well known and deserve no particular comment. The shape of the curves of σ_e pose some rather interesting problems.

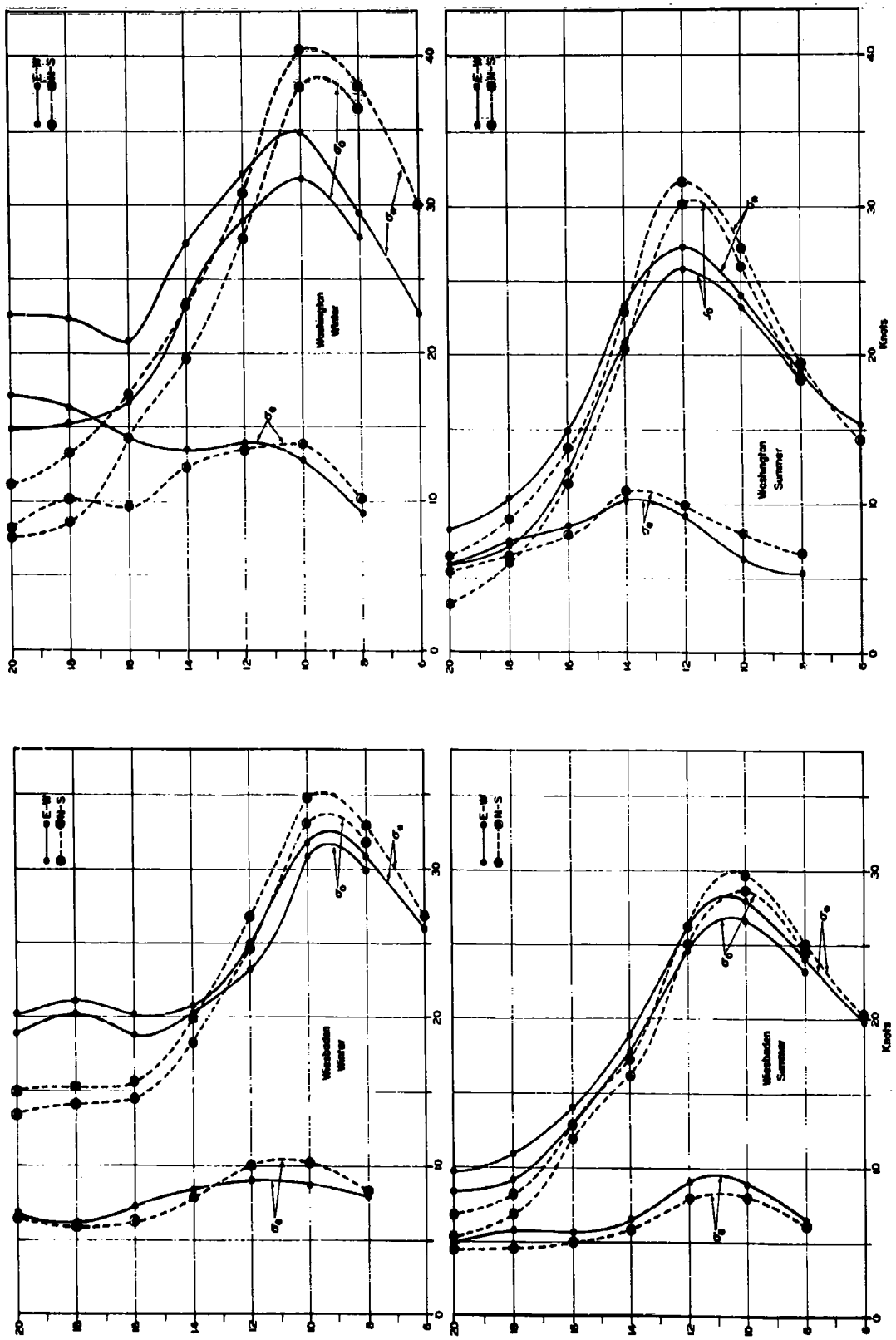

Fig. VI-46 Variation of σ_*, σ_o, and σ_e in the Vertical

In all four cases there is a slight maximum in σ_e just above the level of the maximum σ_o or $\bar{\sigma}_*$. This is even true in the case of Washington, winter, where the behavior of σ_e at the 16 to 20 km levels is anomalous. The value of σ_e is made up of two parts,

$$\sigma_e^2 = \sigma_{e_1}^2 + \sigma_{e_2}^2$$

where σ_{e_1} may be thought of as the part due to the error of observation and σ_{e_2} may be thought of as that part due to small scale eddies. It would seem reasonable to assume that the part due to observation error is either constant or slightly increasing in a monotonic sense with altitude. The value of such a function would appear to be bounded by the smaller values of σ_e just above the maximum of σ_o to be explained mostly by small scale eddies.

If a reasonable value of σ_{e_1} is taken as about 5 kts, then to explain values of σ_e (total) of near 10 kts requires that the eddy part, σ_{e_2}, have a value in the neighborhood of 8 kts.

The correlation values near the 20 km level for Washington are extremely low even for a separation of only 2 km between levels. This shows up in the values of a_o which decrease to near 0.4 at this altitude. The implication is that at these levels the larger part of the observed variability of wind component is made up of observation error and the effects of the small scale eddy components. At these levels, the correlation data showed some pronounced irregularities so that the values of a_2 turned out to be positive. It is presumed that such

values are due to the statistical fluctuations of the data with decreasing number of observations at these altitudes.

The value of the standard deviation of the wind shear component was calculated using the relation above in terms of the standard deviation of wind component and its vertical gradient and the value of a_2 (or b_2) from an empirical fit of the correlation coefficient values. The calculated values of the standard deviation of wind shear are shown in Fig. VI-47 and in Table II. The numerical values are remarkably consistent showing values near 5 kts/km from 8 to 14 km and decreasing somewhat above the 14 km level. (The full curves in Fig. VI-47 represent values for the east pointing component while the dashed curves are for the north pointing component.)

The relative contribution of the two terms that constitute the expression for the standard deviation of the wind shear varies markedly with the level concerned. The term in the vertical gradient of the standard deviation of height contributes the greater part at levels above and below the level of maximum standard deviation of wind component. Near the level of maximum standard deviation of wind component this term becomes small, but through this level the value of a_2 (or b_2) remains nearly constant while its multiplier (σ_0^2) is a maximum so that as a result the value of σ_1 remains nearly constant.

At the 18 and 20 km levels the values of σ_1 are somewhat uncertain. The correlation coefficient values near these levels were low and showed some peculiar variations which caused positive values of a_2 (or b_2) to appear in some instances.

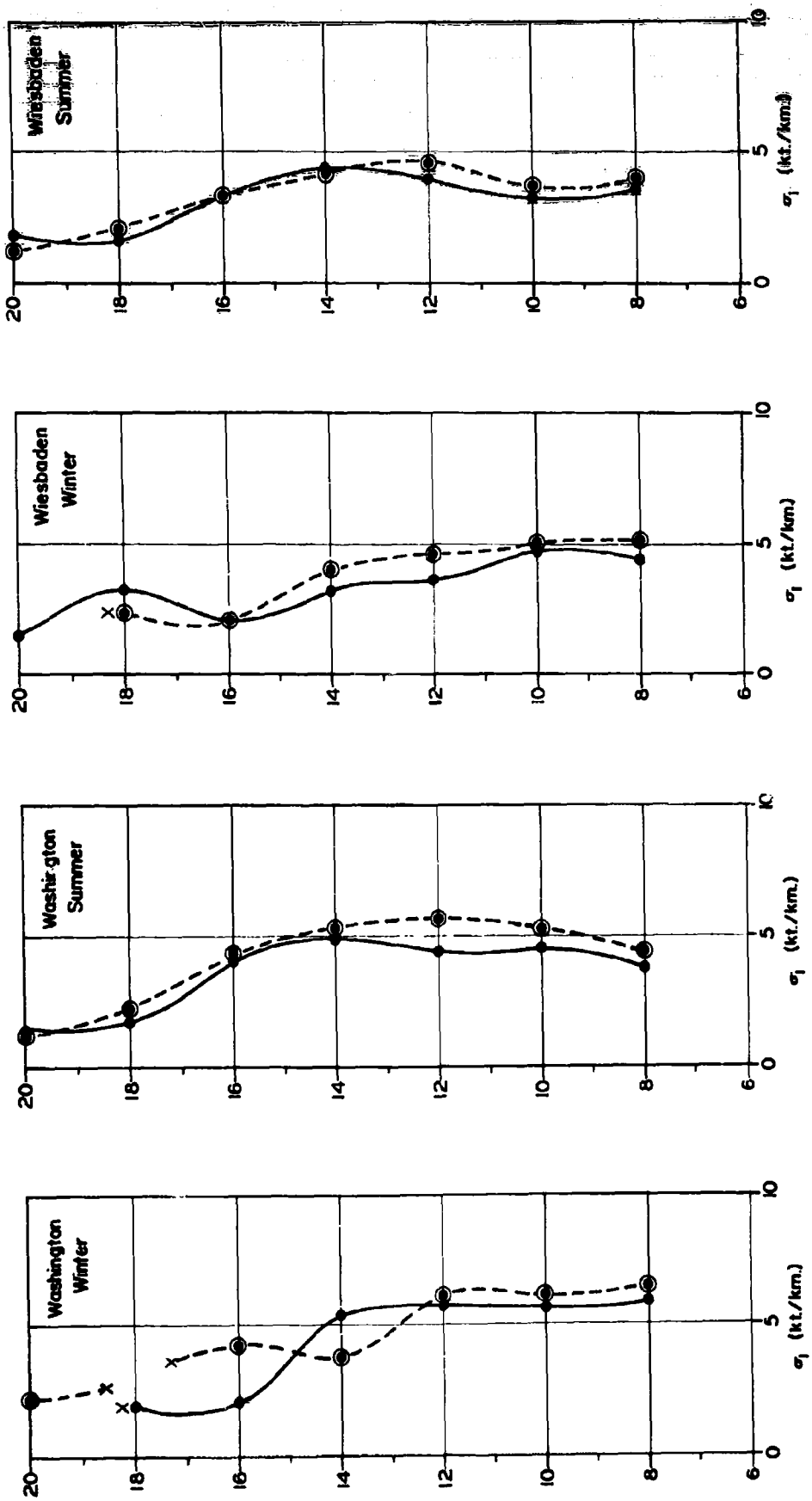

Fig. VI-47 Variation of σ_1 in the Vertical

The preceding analysis is carried out on the assumption that the vertical structure of the wind field is made up of a part that is differentiable on the scale of the spacing of the correlation values (2 km) and that the remaining part is divided into independent random variations, one of these due to observation error and another due to small scale eddies with their velocity components considered as random if separated by as much as 1 km.

The analysis may be pushed a little farther on a conjectured basis by an inspection of the bounds allowed to the wind shear due to the small scale eddies. If these eddies can be considered homogeneous in the vertical, i.e. the vertical gradient of the eddy velocity component standard deviation is negligible, then

$$\sigma_1^2 \cong \sigma_0^2(-2a_2)$$

where now the σ_1 and σ_0 refer to the eddy components. If the eddy velocities are differentiable in the vertical (and we must stick to this assumption or else give up the concept of a wind component shear with a finite second moment), then the eddy component correlation in the vertical must be of the form

$$r = 1 - \tfrac{1}{2}\frac{z^2}{\lambda^2} + \text{---}$$

where λ is a depth parameter and $a_2 = 1/(2\lambda^2)$. Then

$$\sigma_1(\text{eddy}) \cong \sigma_0(\text{eddy})/\lambda(\text{eddy}),$$

$$\sigma_1 \cong \sigma_0/\lambda.$$

Under our previous assumptions, it was found that $\sigma_0(\text{eddy}) \cong 8$ kts. Since it was assumed that the eddy velocity components were essentially independent at 2 km height separation, the

correlation coefficient for z = 2 must be reasonably small. This would indicate a value of λ of not more than about 1 km. The resulting value of σ_1(eddy) is then approximately 8 kts/km. This would lead to an estimate of the total standard deviation of the wind component shear of near 10 kts/km.

The preceding estimates are, of course, conjectured. Until such time as data is available, one cannot truly say what the small scale eddy structure is in the vertical. It is not beyond possibility that it is indeed not differentiable and that a standard deviation of the wind shear simply does not exist.

REFERENCES:

1. Ellsaesser, H. W., Wind Variability, (AWS TR 105-2), Air Weather Service Technical Report (MATS), U.S. Air Force, Wash., D.C., 10 March 1960

2. Durst, C. S., "The Variability of Wind with Time and Distance", Geophysical Memoirs, No. 93, Meteorological Office, Air Ministry, London, 1954

3. Charles, B. N., The U.S. Weather Bureau, Sandia Corporation Co-operative Report in Climatology, (Upper-Wind Statistics from USWB-FCDA Data), SCTM-302-57(51), Sandia Corporation, Albuquerque, New Mexico, 15 pp., December 9, 1957

4. Court, A., Vertical Correlations of Wind Components, Scientific Report No. 1, Contract No. AF19(604)-2060, AFCRC-TN-292, Co-operative Research Foundation, San Francisco 18, Calif., 7 pp. + tables, 19 March 1957, ASTIA No. 117182

* * * PART THREE * * *

CHAPTER VII

WIND VARIABILITY AT SHORTER DISTANCES

A. INTRODUCTION

The data from rawinsonde stations in the synoptic network provides information on the components of the wind correlation tensor over a range of distances from near 200 n mi upward. The effective cutoff at the long distance end is near 3000 n mi, an arbitrary figure depending primarily on the collection of data available for analysis. The lower figure is set by the spacing of the rawinsonde stations in the synoptic network. These limitations, especially the lower distance, implies that the structure of the wind correlation tensor components is determined by the "synoptic" scale disturbances of the wind field. Since data for separation of less than 200 n mi has not been used, the way in which the correlation coefficient r_{11} and r_{22} or $r_{\ell\ell}$ and r_{tt} approach 1 as separation approaches zero is left to conjecture due to the absence of data. The simplest way out of this situation is to assume that the winds are subject to observational error and small scale disturbances that are uncorrelated with the true value of the wind components. This assumption leads to a form of the correlation coefficient which is discontinuous at zero distance. It is undoubtedly true that the rawind observations are subject to observational error so that the correlations computed from them should be discontinuous

at zero distance. The smaller scale disturbances, however, also have a definite correlation structure of their own. If there were data available on winds at distances down to zero, the principle components of the wind correlation tensor (normalized form) should display a transition zone from the structure of the synoptic scale disturbances to a value nearer to unity at zero without so large a discontinuity. The situation is illustrated in Fig. VII-1. If winds at short distance separations are determined by an electronic system such as a doppler navigator which has an appreciable lag constant, a false approach curve for small distances may be obtained due to an entirely different kind of effect that might be classed as another kind of observation error.

The data presented in this Chapter is divided into three major parts. In Section B data on wind correlation tensor components is presented that were obtained from closely spaced observations of the conventional synoptic type. In Section C some data is presented which were obtained from flights on which doppler navigator winds were read at five-minute intervals. In Section D the wind data was obtained from doppler navigator readings of Project Jet Stream flights. Section E is devoted to a discussion of the combined picture of data from all sources.

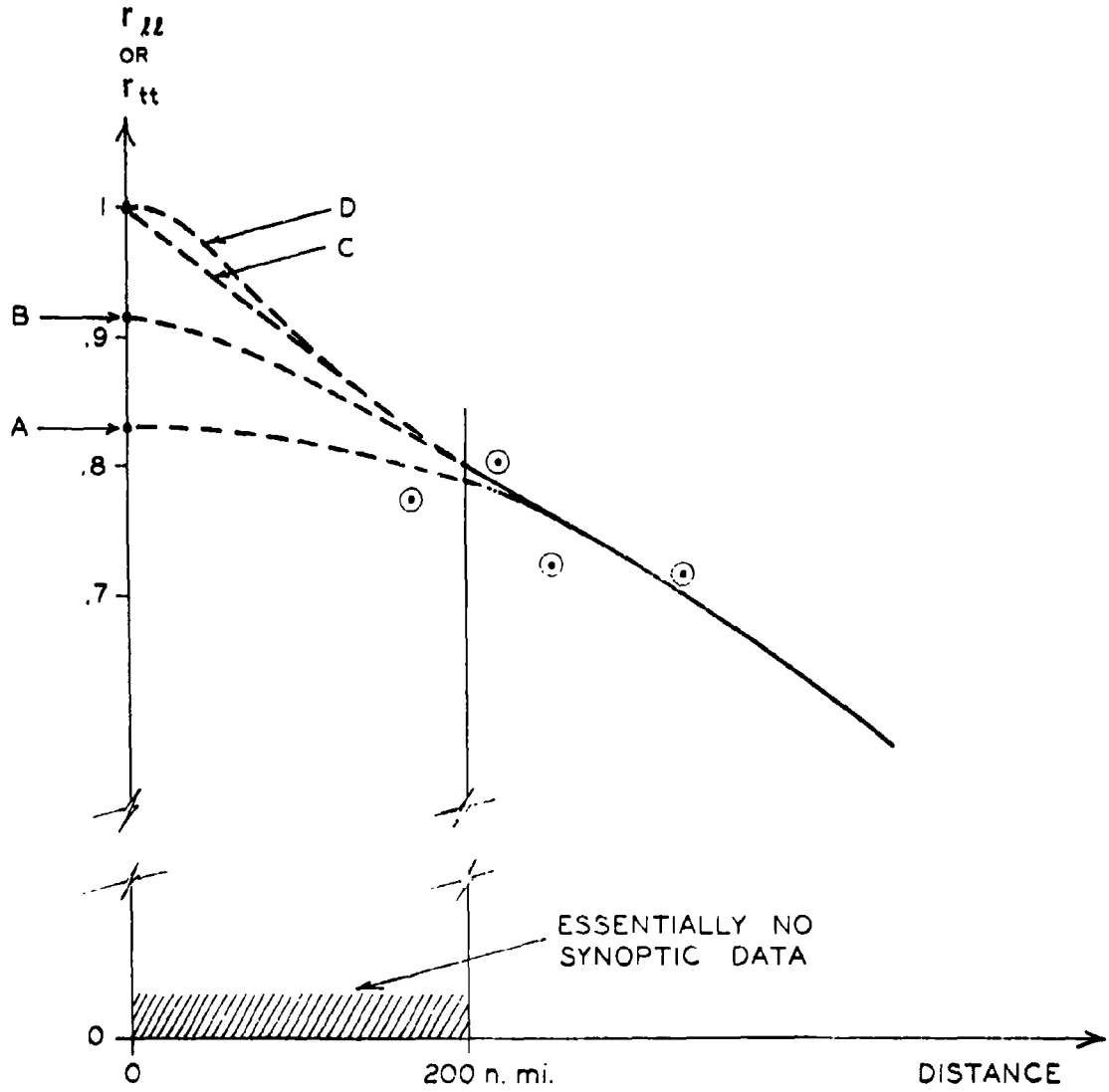

Fig. VII-1: Some possible correlation structures near zero distance. A: The extrapolation assuming lumped errors and smaller scale eddies; B: The extrapolation assuming random errors but accounting for the structure of smaller scale eddies; C: A possible situation if there are no random errors; D: A possible case in which correlations are computed from wind data determined by a linear system with an appreciable lag constant (over smoothing of winds).

B. WIND CORRELATION TENSOR COMPONENTS FROM CLOSELY SPACED RAWINSONDE OBSERVATIONS

The location of the station pairs, their separation, and the years in which the observations were made are given in the following table:

TABLE I

STATION PAIRS, SEPARATION, AND DATA PERIOD

Station Pair	Distance	Period of Data
Portland-Brunswick	21 n mi	1953-1955
Washington-Dahlgren	30	1953-1957
Rome-Albany	76	1950-1951
Merced-Oakland	81	1955-1957
Norfolk-Hatteras	103	1955-1958

One of each station pair is obviously one of the regular synoptic network. The other station made upper wind observations for other purposes. As will be noted from Table II, the number of observation pairs available, the number of simultaneous wind observations is far from the maximum possible. It is only in the case of the last two station pairs that there is reasonable assurance that the winds at both locations are determined by electronic tracking methods.

The correlation coefficients and supplementary data calculated from the data are listed in Table II. Figs. VII-2 through VII-5 show the values of the longitudinal and transverse correlations as a function of observation point separation. The data points shown in black are those from Table II. The remaining data points are from the data with Washington as master station

TABLE II

WIND CORRELATIONS FOR
CLOSELY SPACED STATIONS AND RELATED DATA

Station Pair Season Level	Brunswick Portland Summer 700 mb	Brunswick Portland Winter 700 mb	Washington Dahlgren Summer 700 mb	Washington Dahlgren Winter 700 mb	Rome Albany Summer 700 mb
$\bar{U}_\ell$ (mps)	4.3	0.4	3.0	0.5	7.5
$\bar{U}_t$,	-6.6	-10.8	7.0	14.5	0.8
$\bar{U}_{\ell'}$	3.0	1.5	2.7	0.9	5.8
$\bar{U}_{t'}$	-7.5	-10.1	6.4	14.6	0.0
σ_ℓ	6.3	8.4	5.8	9.5	4.8
σ_t,	4.7	8.5	4.6	7.5	5.4
$\sigma_{\ell'}$	5.8	7.6	5.6	9.6	4.3
$\sigma_{t'}$	5.2	7.5	4.2	6.7	4.8
$r_{\ell\ell}$	0.911	0.899	0.863	0.867	0.751
$r_{\ell t}$	-0.267	0.284	0.069	0.001	0.123
$r_{t\ell}$	-0.048	0.140	-0.138	-0.055	-0.121
r_{tt}	0.755	0.885	0.855	0.817	0.763
$r_{\ell t}$ (at P)	-0.092	0.287	-0.037	0.060	-0.014
$r_{\ell t}$ (at P')	-0.166	0.139	0.075	0.018	0.017
N	50	36	44	46	73

Station Pair Season Level	Rome Albany Winter 700 mb	Oakland Merced Summer 700 mb	Oakland Merced Winter 700 mb	Oakland Merced Summer 500 mb	Oakland Merced Winter 500 mb
$\bar{U}_\ell$ (mps)	9.8	-0.4	-5.3	-5.2	-14.1
$\bar{U}_t$,	1.9	-2.3	-0.8	-4.2	-1.2
$\bar{U}_{\ell'}$	9.3	-2.2	-6.8	-5.4	-13.6
$\bar{U}_{t'}$	-1.0	-1.0	-1.5	-3.7	-1.0
σ_ℓ	6.8	3.6	6.6	6.6	11.2
σ_t,	11.2	3.7	9.0	6.0	13.1
$\sigma_{\ell'}$	8.8	4.0	6.9	6.7	11.2
$\sigma_{t'}$	10.3	4.7	10.5	7.0	13.4
$r_{\ell\ell}$	0.596	0.802	0.842	0.900	0.917
$r_{\ell t}$	0.010	-0.337	0.107	-0.195	0.166
$r_{t\ell}$	-0.180	-0.271	0.077	-0.134	0.150
r_{tt}	0.821	0.686	0.882	0.872	0.907
$r_{\ell t}$ (at P)	0.095	-0.407	0.008	-0.173	0.187
$r_{\ell t}$ (at P')	-0.075	-0.360	0.172	-0.164	0.158
N	21	91	173	89	167

TABLE II

(CONTINUED)

Station Pair Season Level		Norfolk Hatteras Summer 700 mb	Norfolk Hatteras Winter 700 mb	Norfolk Hatteras Summer 500 mb	Norfolk Hatteras Winter 500 mb
$\overline{U}_\ell$	(mps)	3.5	4.8	5.4	7.4
$\overline{U}_t$		4.1	14.0	6.7	19.5
$\overline{U}_\ell'$		2.3	4.2	3.7	6.8
$\overline{U}_t'$		2.9	14.5	4.9	19.0
σ_ℓ	(mps)	5.2	8.5	6.2	13.3
σ_t		5.7	7.9	6.9	16.8
σ_ℓ'		4.3	7.7	5.7	12.6
σ_t'		5.1	7.5	6.2	15.1
$r_{\ell\ell}$		0.771	0.842	0.860	0.926
$r_{\ell t}$		-0.077	-0.203	-0.051	-0.323
$r_{t\ell}$		-0.139	-0.258	-0.151	-0.373
r_{tt}		0.755	0.723	0.819	0.920
$r_{\ell t}$	(at P)	-0.054	-0.282	-0.076	-0.348
$r_{\ell t}$	(at P')	-0.143	-0.250	-0.163	-0.370
N		176	250	174	208

and at the 500 mb level. The data points from Table II are labeled with the first digit of the level to which the values pertain.

The spread of the data points precludes any serious analysis of the data to determine the shape of the curve near zero separation. This is primarily due to the unreliability of the correlation values which occurs for at least two reasons: First, the number of cases available was small in several instances; second, the observations were made using several kinds of equipment and hence the effect of observation errors differ from one station pair to another. There is no readily available North

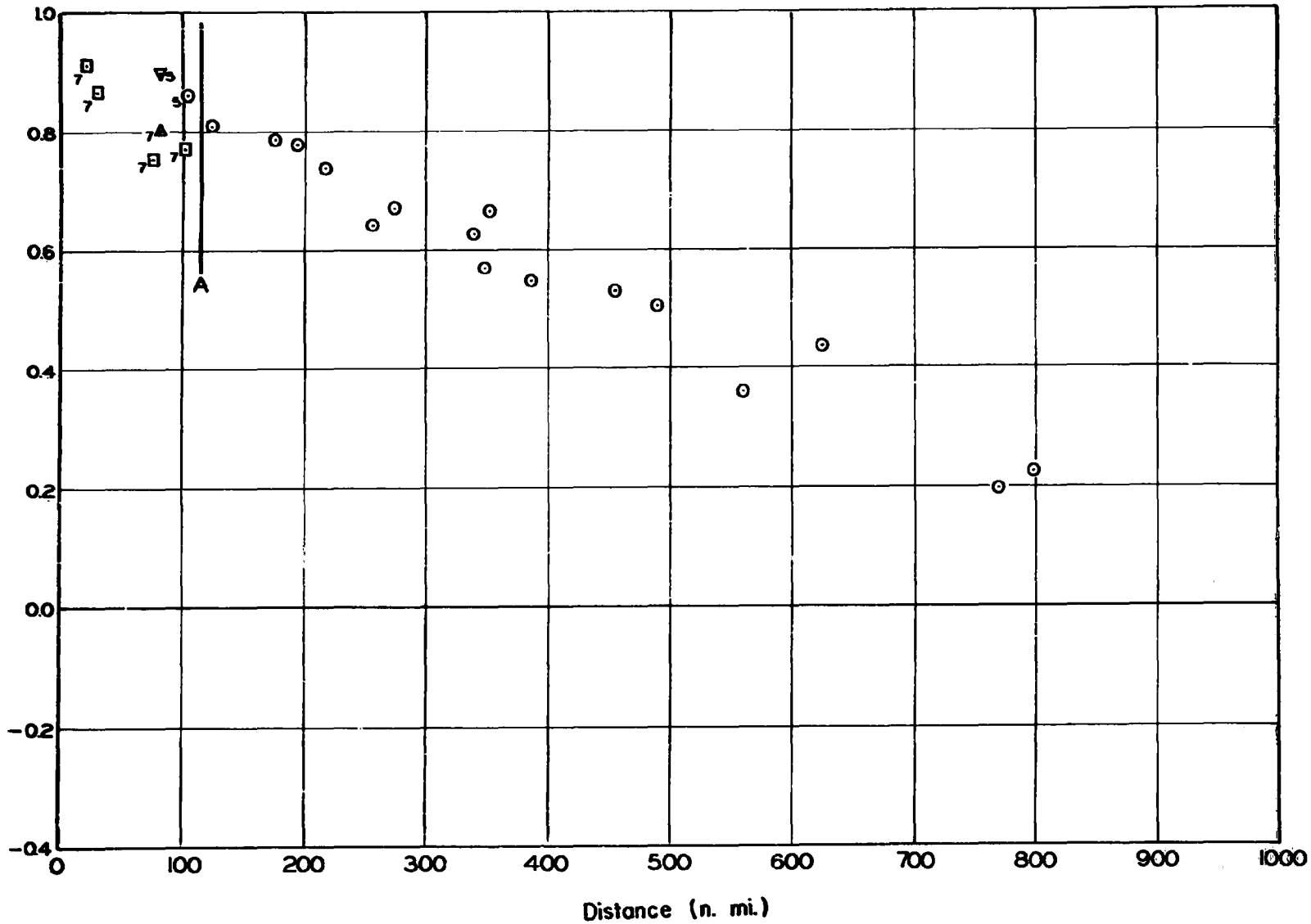

r_{ll}

Fig. VII-2 $r_{\ell\ell}$ as a Function of Distance, Summer Data

Points to the left of A from the preceding table, those to the right from SC-USWB-FCDA data with Washington as master station, 500 mb. Number besides the data points indicates level.

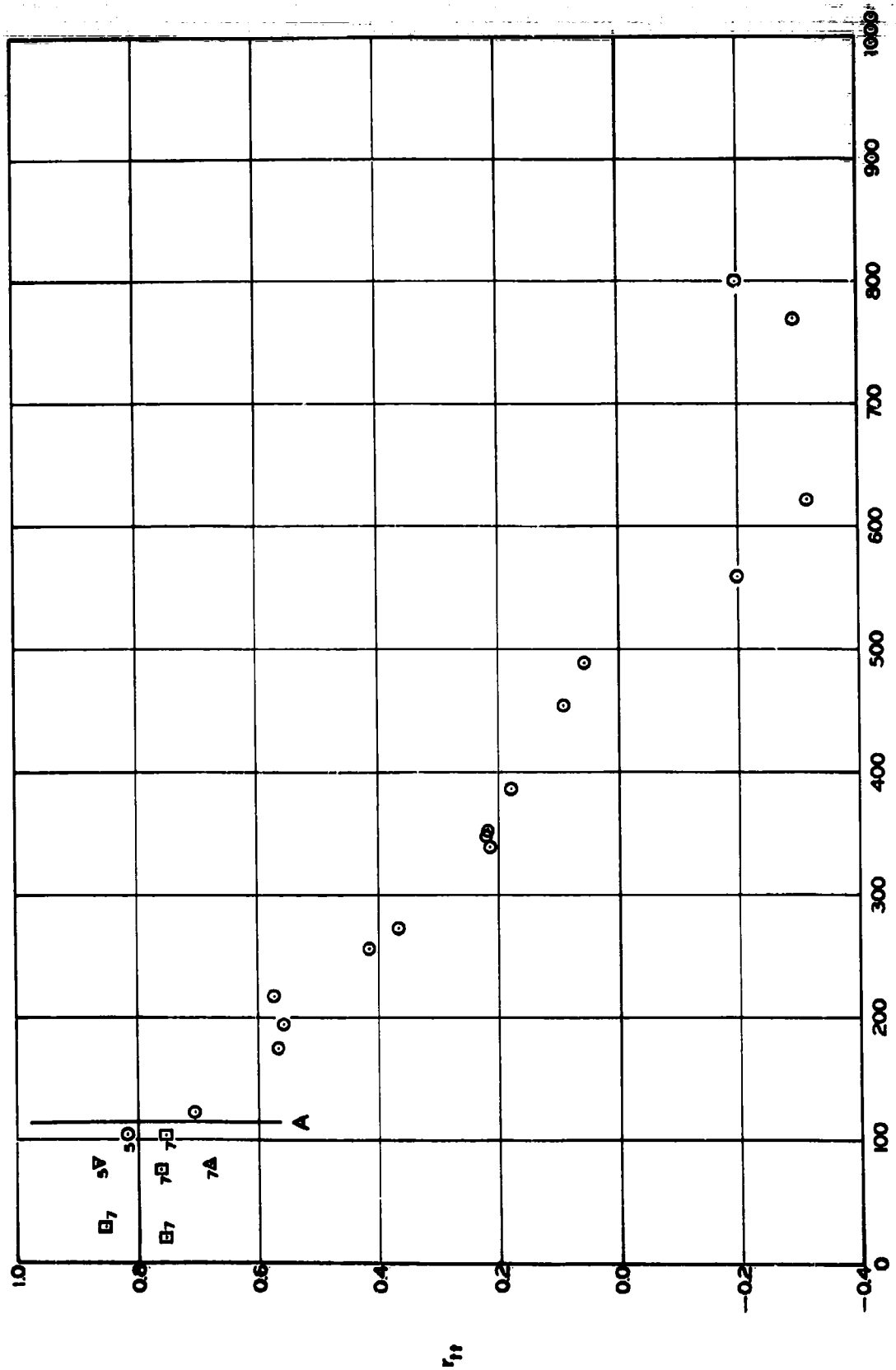

Fig. VII-3 r_{tt} as a Function of Distance, Summer Data

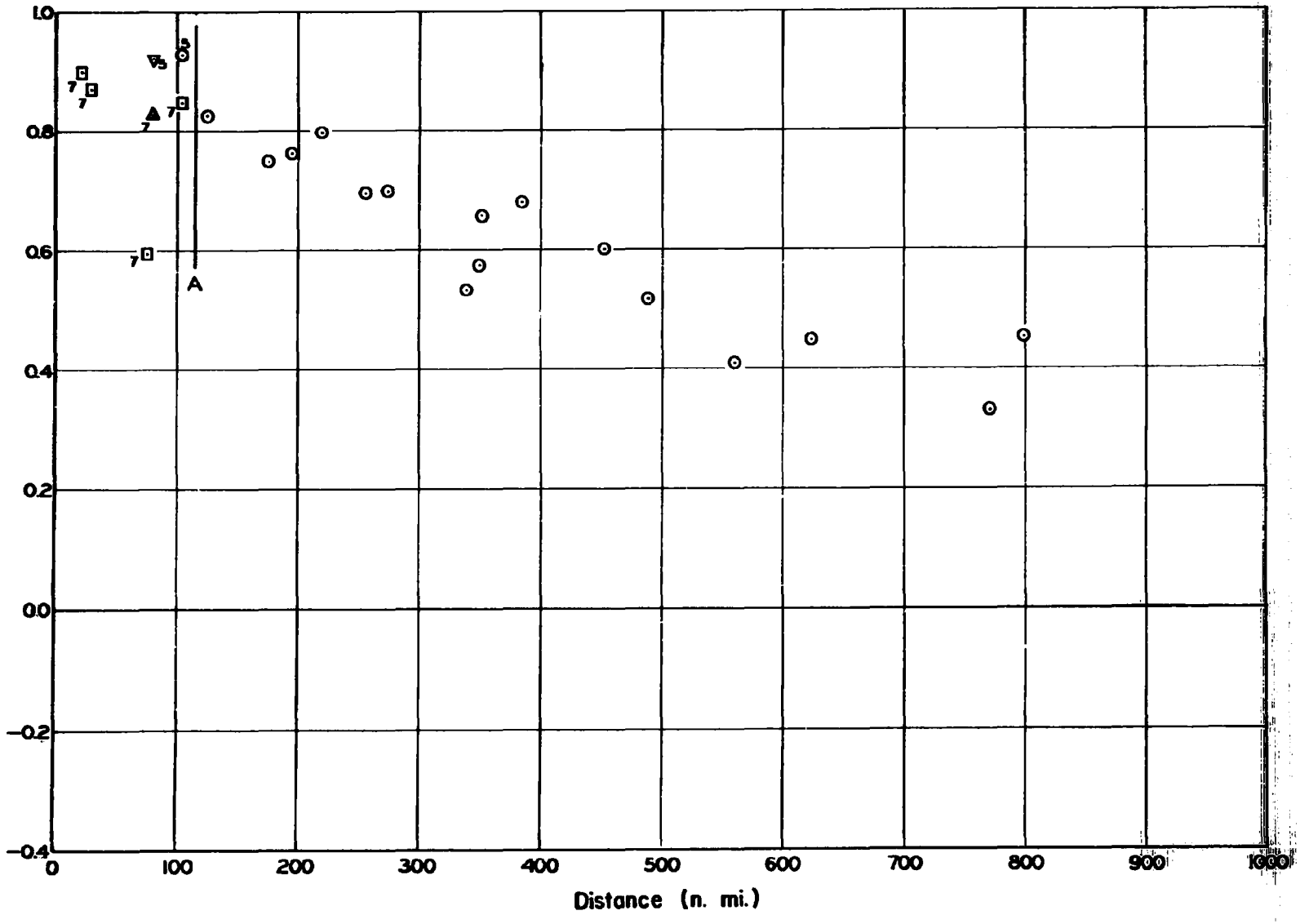

Fig. VII-4 r_{ll} as a Function of Distance, Winter Data

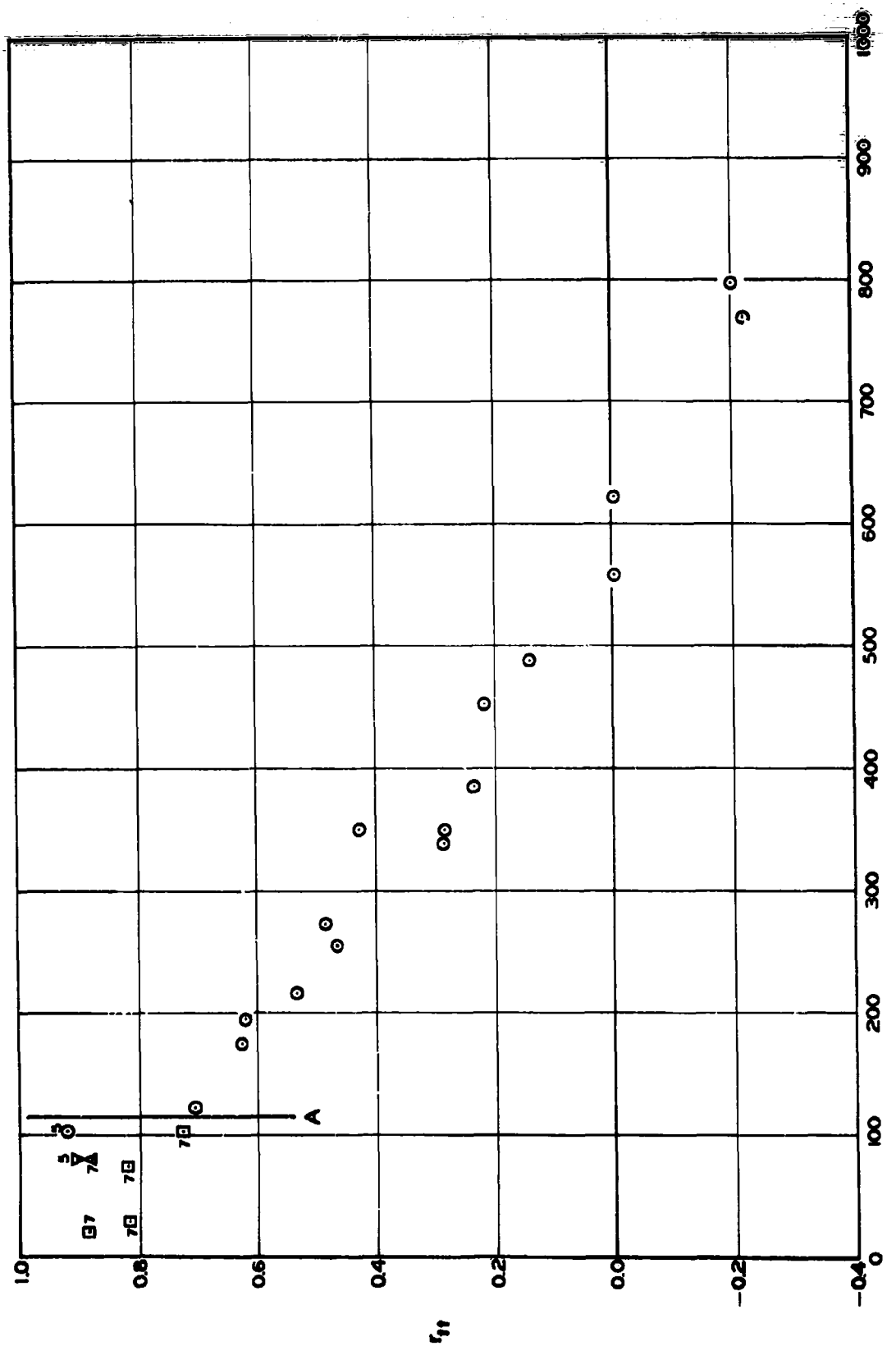

Fig. VII-5 r_{tt} as a Function of Distance, Winter Data

American data available at 700 mb with which to compare the five values of the component correlation coefficients at this level. The values at both 500 mb and 700 mb are shown in Figs. VII-2 through VII-5 compared with the data at 500 mb with Washington as the master station.

To show at least part of the difficulties in a somewhat different way, all of the correlations of Figs. VII-2 through VII-5 are shown in Fig. VII-6. In this case the values of $\log(1-r_{\ell\ell})$ and $\log(1-r_{tt})$ are used as ordinate and the value of log (r) (r = distance) is the abscissa. This method of plotting the data greatly enlarges the region near zero distance. The data points lying to the left of 110 n mi distance are those tabulated in Table II. Superimposed on the data points are the curves for

$$r_{\ell\ell} = k \exp(-r^2/2L^2)$$

and

$$r_{tt} = k(1 - r^2/L^2)\exp(-r^2/2L^2)$$

where L = 525 n mi and values of k = 1.0, 0.9, and 0.8. One would certainly hesitate to estimate the value of k from such a spread of data points, but the general behavior of the points with decreasing values of distance appears to be of this type and certainly $k < 1.0$.

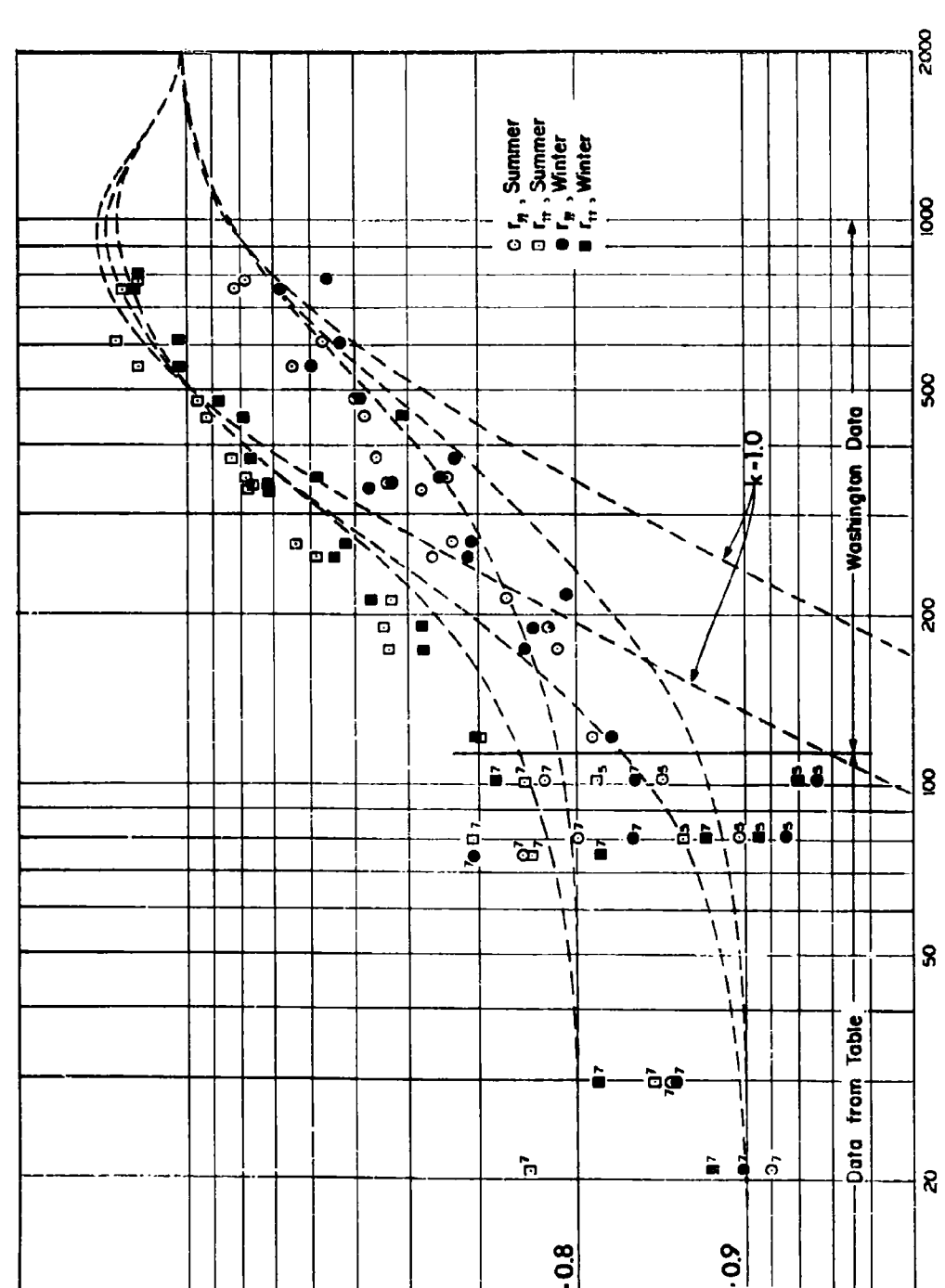

Fig. VII-6 Values of $r_{\ell\ell}$ and r_{tt} for Summer and Winter as a Function of Distance

(This is the same data as in Figures VII-2 through VII-5 plotted in a different form.) See text for significance of curves shown.

C. MEAN SQUARE WIND COMPONENT DIFFERENCES FROM FOURTH WEATHER WING OBSERVATIONS

The Fourth Weather Wing,* in connection with a problem quite different from that at hand, obtained data on wind direction and velocity during flights near 25,000 feet over the northern United States.# The data was obtained by recording the direction and velocity as indicated by the doppler navigator equipment. The meteorological observer tabulated these data at five-minute intervals. The flights concerned were as follows:

Route 1: 19 Jan 60, 1 Feb 60, 21 March 60

Route 2: 10 Jan 60, 2 Feb 60, 23 March 60

Route 3: 21 Jan 60, 3 Feb 60, 26 March 60.

The routes flown were:

Route 1: From near San Francisco to Seattle and thence across the northern states to near Fargo and thence to Dayton.

Route 2: From Dayton Ohio to Kylertown, Pa., Torento Ont., Quebec, Que., Caribou, Maine, then south and southeast (passing southeast of Cape Cod) to Norfolk, Va., and return to Dayton, Ohio.

Route 3: Same as Route 1 only flown in the reverse direction.

The total data recorded consisted of time, true air speed, ground speed, altitude, wind speed and direction, and latitude and longitude.

---

*Abbreviated in the following as 4WW.

#We wish to cxpress our great appreciation of the kindness of 4WW personnel in providing us with a copy of these data and in answering many questions on this program.

1. Check of the Data Quality

The 4WW data was manually recorded by the meteorological observer. For this reason, the tabulations were inspected to determine the extent to which the data were affected by human and other errors.

The first check was on the accuracy of the last digit of the recorded wind speed. Wind speed was tabulated to the nearest whole knot. It seemed reasonable to assume that the last digit of the recorded wind speed would be randomly distributed among the digits 0, 1, ---, 8, 9. Three examples of the distribution of the last digit are shown in Fig. VII-7. In the example for 2 Feb 60 the digit count seems to be reasonably uniform. From example for 21 Jan 60 one would conclude that the observer had a strong tendency to read velocity to the nearest ten knots. On 26 March 60 the digit distribution indicates a tendency to read the instrument to the nearest five knots. Since the digit distribution differed radically from flight to flight, it is impossible to reach any firm conclusion on errors in instrument reading. It is certainly evident that an accuracy of one knot in wind speed is much too low. An error of at least two or three knots due to instrument reading alone would seem more appropriate.

In "eye-balling" the 4WW data, a few cases were found in which the recorded data seemed inconsistent. That is, the wind speed and direction did not tally with the recorded values of true air speed, ground speed, and distance and direction flown.

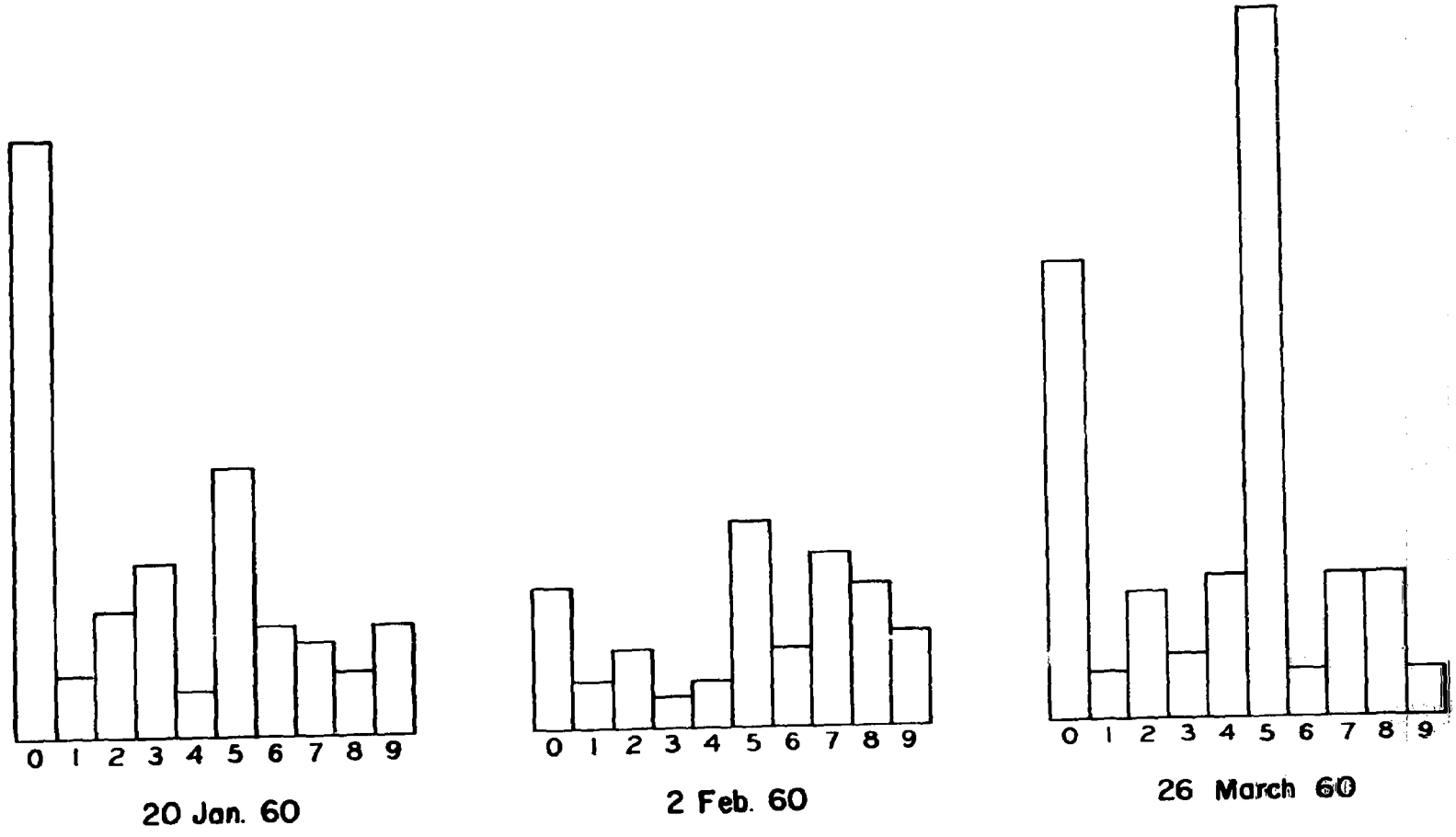

Fig. VII-7 Digit Frequency in Wind Speed Readings, 4WW Data

It was felt that such items of inconsistent data should not be used. To check the data self-consistency, the true air speed was calculated for each five-minute interval using the co-ordinate at the beginning and end of this interval and the winds recorded. The calculated true air speed was then compared with the recorded true air speed. The results are shown in the following Table III:

TABLE III

TRUE AIR SPEED DISCREPANCIES

Day	Mean Difference	Std. Deviation
19 Jan 60	0.02 kts	5.8 kts
20 Jan 60	0.26	4.0
21 Jan 60	0.21	3.6
1 Feb 60	-2.33	3.3
2 Feb 60	1.70	5.5
3 Feb 60	-4.63	5.4
21 March 60	-0.40	1.8
23 March 60	-1.54	4.3
26 March 60	1.34	3.3

There appeared to be no connection between the days on which the wind speed records appeared to be biased toward "0" in the last digit and the days with large standard deviation of the true air speed discrepancy.

In this form of a check on self-consistent data, inconsistencies arise not only from incorrect winds, but many other items of data involved. Specifically, the computation of true air speed was subject to the errors that had been made, not only in

wind speed and direction, but also in ground speed and track. No attempt to correct discrepancies is possible. It is also quite possible that the check may reveal a self-consistent situation when the data items are actually incorrect. One merely hopes that this case occurs infrequently. Rejection of the cases in which the data was found to be inconsistent does not necessarily indicate erroneous wind data. A total of 33 out of approximately 900 data items were rejected on the basis of inconsistency.

2. Treatment of the Data

The data were processed in two ways; first on the basis of distance intervals in terms of ground distance, and second in terms of time lag intervals or essentially in terms of air distance intervals. In the first instance, the distance between observation pairs was computed using the position co-ordinates (latitude and longitude) of the wind data pairs. The difference between longitudinal and transverse wind components at the points was accumulated in classes according to the computed distance. The class intervals used are shown in Table IV. It will be noted that at the lower distances the class intervals overlap somewhat. In the case of distances falling into two class intervals, the data were tabulated in both intervals.

In the case of the distance lags on the basis of time intervals between observations, the true air speed is used to convert time lag to distance lag. Tables V and VI give estimates of the conversion factors involved.

TABLE IV

CLASS INTERVALS BASED ON GROUND DISTANCE SEPARATION

Nominal Separation	Lower Limit	Upper Limit
15 n mi	12.0 n mi	18.0 n mi
19	15.4	22.5
24	19.7	28.6
30	25.2	35.4
38	32.2	44.3
48	41.2	55.4
61	52.8	69.4
77	67.5	87.0
98	86.4	108.9
124	110.6	136.4
156	141.6	170.8
198	181.2	213.8
250	232.0	267.8
316	296.9	335.4
400	380.0	420.0

TABLE V

AVERAGE TIME AIR SPEED AND ITS STANDARD DEVIATION

Flight	Average T.A.S.	Std. Dev.
19 Jan 60	252 kts	3 kts
20 Jan 60	257	7
21 Jan 60	259	6
1 Feb 60	271	3
2 Feb 60	269	8
3 Feb 60	261	4
19 March 60	270	7
23 March 60	266	5
26 March 60	261	7
Composite	262	8

TABLE VI

CONVERSION OF TIME LAG TO AIR DISTANCE LAG (COMPOSITE)

Time Lag	Distance Lag	Std. Dev.
5 min.	22 n mi	1 n mi
10	44	1
15	65	2
20	87	3
25	109	3
30	131	4
40	175	5
50	218	7
60	262	8
80	349	11
100	436	13

The actual ground distance between observation pairs was computed in each instance and the mean and standard deviation of the ground distance were tabulated along with the other data in the case of point pairs based on time lag separation.

The aircraft was not operating at exactly the same altitude during any given day, but altitude changes are relatively minor. For the most part the aircraft flew near 25,000 feet. However, to be certain that the effect of altitude changes between data points was minimized, only data pairs were accepted in which there was less than 1000 feet altitude difference.

In the case of ground distance separation of the data points, the longitudinal and transverse components of the wind were determined as lying along and across the line joining the two points. In this instance, it is immaterial whether or not the aircraft actually flew this track or not. By far the majority

of data points were along straight flight paths, but occasionally there are bends in the track flown, this is particularly true in the case of Route No. 2 (above).

When the time lag (air distance) is used to classify data pairs, the straightness of the flight path assumes a role of some importance. Consequently, to assure that the track between data points was reasonably straight, the track was computed at each point of a pair. When the tracks at the two points differed by more than 10°, the data pair was rejected. It is, of course, possible that the track at two widely separated points could have been the same, but the actual aircraft path between them may be quite sinuous. This sort of situation did not occur in any instance.

3. Results

The results of the calculation of the quantities

$$\overline{\Delta_\ell^2} = \overline{(U_\ell - U'_\ell)^2} \quad \text{and} \quad \overline{\Delta_t^2} = \overline{(U_t - U'_t)^2}$$

from the 4WW data are given in Table VII, for ground distance lags. The values of (U_ℓ, U_t) are for one point on the track and for (U'_ℓ, U'_t) are for a point ahead. The distance between the points is given in the left-hand columns and refers to the nominal separation of the points which were grouped in the class intervals of Table IV. The subscripts ℓ and t refer to longitudinal and transverse components.

The results from all nine flights are shown in Table VII together with a summary in which all of the data have been combined. In each instance the number of data pairs entering into

TABLE VII

VALUES OF MEAN SQUARED WIND COMPONENT DIFFERENCES FROM 4WW DATA; FIXED GROUND DISTANCE LAGS. DISTANCE LAG IN NAUTICAL MILES; MEAN SQUARE VELOCITY DIFFERENCES IN KNOTS SQUARED.

FLIGHT: 19 January 60

Dist. Lag	N	$\overline{\Delta_\ell^2}$	$\overline{\Delta_t^2}$
15	7	7.7	5.3
19	49	15.3	14.9
24	58	17.8	27.7
30	14	33.4	53.9
38	46	25.5	21.3
48	58	53.5	42.1
61	58	53.3	26.6
77	71	99.5	66.9
98	84	129.8	76.9
124	95	227.8	90.8
156	107	260.4	106.7
198	115	375.0	129.3
250	122	622.2	180.6
316	122	928.7	205.6
400	90	1206.2	301.9

FLIGHT: 20 January 60

Dist. Lag	N	$\overline{\Delta_\ell^2}$	$\overline{\Delta_t^2}$
15	17	40.3	51.2
19	50	48.5	62.5
24	48	67.7	87.0
30	18	52.7	33.7
38	58	89.6	99.7
48	55	99.3	163.3
61	70	127.1	228.0
77	78	162.8	306.3
98	97	147.7	444.1
124	113	208.0	684.1
156	129	251.8	955.4
198	147	323.7	1250.8
250	171	422.7	1614.8
316	102	869.0	2841.3
400	56	1482.5	2859.6

FLIGHT: 21 January 60

15	51	76.2	43.1
19	73	63.1	34.3
24	33	52.5	19.3
30	47	134.9	84.9
38	72	112.6	71.8
48	79	146.2	99.1
61	91	120.2	142.6
77	96	218.8	156.4
98	122	278.1	202.6
124	119	395.2	284.5
156	145	544.3	398.4
198	151	837.6	524.6
250	152	1153.0	581.2
316	116	1833.8	803.7
400	43	1215.0	190.9

FLIGHT: 1 February 60

15	8	2.8	13.7
19	44	20.6	14.6
24	55	20.7	16.6
30	6	28.7	17.6
38	41	49.0	35.1
48	43	33.4	30.5
61	55	73.6	52.3
77	61	83.4	59.8
98	67	111.2	67.0
124	78	181.1	96.6
156	75	201.0	103.9
198	93	265.2	120.2
250	97	389.4	138.3
316	98	526.2	57.9
400	88	696.6	117.0

TABLE VII

(CONTINUED)

FLIGHT: 2 February 60

Dist. Lag	N	$\overline{\Delta_\ell^2}$	$\overline{\Delta_t^2}$
15	2	26.1	7.5
19	10	33.4	48.7
24	28	16.0	16.9
30	25	30.0	22.5
38	10	76.6	55.9
48	31	89.5	38.9
61	26	80.4	75.2
77	38	120.6	136.7
98	30	225.0	182.0
124	33	216.2	192.5
156	33	442.2	410.7
198	42	564.2	709.6
250	53	1055.0	737.6
316	43	1244.3	682.1
400	31	739.0	331.5

FLIGHT: 3 February 60

Dist. Lag	N	$\overline{\Delta_\ell^2}$	$\overline{\Delta_t^2}$
15	16	43.8	59.7
19	57	25.2	43.1
24	45	18.7	51.4
30	21	121.1	193.8
38	56	61.1	74.8
48	48	118.3	193.6
61	70	152.3	184.7
77	68	203.0	269.8
98	83	209.4	352.9
124	89	259.4	482.2
156	107	300.5	710.5
198	115	378.6	1119.1
250	129	500.4	1595.0
316	136	684.8	2287.7
400	68	538.0	1541.0

FLIGHT: 21 March 60

15	1	-	-
19	14	23.5	26.7
24	63	11.3	17.2
30	33	18.2	39.6
38	8	26.4	81.1
48	61	32.0	38.6
61	31	60.3	56.9
77	65	44.2	45.8
98	64	52.1	57.1
124	72	70.3	79.1
156	83	75.2	83.0
198	95	86.6	102.6
250	98	97.7	131.5
316	101	124.7	175.3
400	66	223.9	123.2

FLIGHT: 23 March 60

15	27	24.2	20.4
19	49	14.2	21.8
24	34	25.3	30.0
30	45	35.1	78.0
38	54	33.9	73.0
48	55	36.8	144.4
61	69	56.1	193.5
77	79	63.3	289.4
98	86	113.2	376.3
124	99	171.3	548.8
156	102	302.6	649.0
198	120	400.3	665.2
250	129	678.7	867.4
316	74	1076.3	1070.6
400	11	422.1	871.2

TABLE VII

(CONTINUED)

FLIGHT: 26 March 60				FLIGHT: SUMMARY			
Dist. Lag	N	$\overline{\Delta_\ell^2}$	$\overline{\Delta_t^2}$	Dist. Lag	N	$\overline{\Delta_\ell^2}$	$\overline{\Delta_t^2}$
15	69	13.8	27.9	15	198	37.1	34.4
19	82	14.1	22.0	19	428	30.2	31.7
24	20	10.0	50.5	24	384	27.4	36.7
30	71	31.5	53.3	30	280	56.1	69.2
38	87	30.1	42.9	38	432	60.5	63.9
48	90	44.7	57.6	48	520	75.0	94.0
61	90	47.9	60.7	61	560	97.1	127.5
77	114	54.8	60.9	77	670	123.3	171.6
98	142	78.5	59.1	98	775	157.8	227.3
124	137	76.8	73.5	124	835	217.4	332.7
156	162	93.3	80.6	156	943	296.8	478.8
198	167	82.8	87.5	198	1045	412.2	674.4
250	168	100.6	88.7	250	1119	609.6	906.0
316	148	92.0	91.3	316	940	893.8	1193.7
400	8	35.0	23.2	400	461	1140.6	1175.8

the calculation of $\overline{\Delta_\ell^2}$ and $\overline{\Delta_t^2}$ are shown in the column headed N. The value of N differs widely from one distance lag to another in individual flights. This is due to the fact that the data were read at five-minute intervals, but the aircraft, though flown at a reasonably constant true air speed, was influenced by head and tail winds. Thus under different wind conditions the data values accumulate in different class intervals. This effect is especially pronounced when data point separation is less than 40 n mi. Here we are dealing with data points separated in time by one and two five-minute intervals. The class intervals are also narrow in this range so that the effect of head or tail winds becomes pronounced.

There is a tendency for the number of points to decrease abruptly at the 400 n mi class interval. This is due to a combination of many factors which include the large time separation and the effect of the rejection criteria such as data at same altitude for each of a pair.

The data for any one flight represent a kind of space average of the mean square value of the component differences for each day. There is a great variation in the behavior of the mean square component differences from one day to another. This is brought about by several factors of which some are:

i) The natural variability associated with the relatively few samples entering into each individual day's distance lag computations.

ii) The variability of the inherent wind variability from place to place from day to day in the area covered by the flight.

It is felt that the data for individual days is without significance and that only the summary data can be interpreted seriously.

The data for the same quantities for air distance lags is tabulated in Table VIII. In this table, the rows are indicated by the time separation of the wind component pairs. The corresponding distance separation is given in Table VI. The average ground distance separation and its standard deviation, d and σ_d, are also tabulated. In addition to $\overline{\Delta_\ell^2}$ and $\overline{\Delta_t^2}$, the values of $\overline{\Delta_\ell}$ and $\overline{\Delta_t}$ are also shown. (This last pair was not tabulated in the case of the ground distance lags. In Table VII, the data

TABLE VIII

VALUES OF MEAN SQUARE WIND COMPONENT DIFFERENCES FROM 4 WW DATA WITH AIR DISTANCE (TIME) LAGS

Time Lag (min.)	N	$\bar{d}$ (n mi)	σ_d (n mi)	$\overline{\Delta_\ell}$ (knots)	$\overline{\Delta_t}$ (knots)	$\overline{\Delta_\ell^2}$ (knots^2)	$\overline{\Delta_t^2}$ (knots^2)
			FLIGHT:	19 January 60			
5	78	23	6	0.4	-0.4	20.1	26.1
10	68	44	8	0.4	-0.9	50.5	39.0
15	63	66	8	0.7	-1.7	96.4	62.0
20	61	87	10	1.1	-2.3	152.8	81.8
25	57	109	12	1.0	-2.8	228.2	107.1
30	53	131	14	1.3	-3.8	304.1	133.9
40	48	174	18	2.0	-5.7	446.7	180.5
50	44	218	19	3.7	-6.1	523.7	251.1
60	41	258	24	3.7	-6.5	592.3	238.6
80	34	338	30	3.9	-6.1	618.4	326.4
100	32	415	32	6.4	-7.5	1068.0	475.5
			FLIGHT:	20 January 60			
5	84	22	5	-1.1	-1.9	61.9	73.8
10	68	44	8	-1.9	-4.1	119.3	148.9
15	61	64	11	-3.5	-4.9	162.3	278.0
20	52	86	13	-4.5	-6.0	175.1	351.4
25	44	107	15	-5.5	-6.9	267.5	479.8
30	38	127	18	-7.6	-10.3	336.0	714.6
40	27	167	20	-11.9	-16.8	616.9	1437.9
50	21	216	26	-13.5	-17.8	1009.4	1846.8
60	14	248	29	-21.5	-31.3	1398.7	3138.8
80	8	306	14	-51.3	-79.2	2781.4	7632.4
100	4	384	5	-50.4	-107.3	2750.2	11676.5
			FLIGHT:	21 January 60			
5	97	18	3	-0.6	0.6	63.7	34.8
10	84	36	5	-0.5	0.6	98.9	65.8
15	79	54	7	-1.2	1.4	149.2	116.5
20	78	71	10	-1.8	1.2	209.2	152.7
25	75	89	11	-2.1	2.2	266.2	223.0
30	70	106	14	-1.4	2.6	319.1	270.7
40	60	141	19	-0.6	3.3	437.0	374.6
50	52	176	25	-2.7	6.2	628.4	482.6
60	52	211	29	-2.0	4.1	786.5	550.0
80	43	279	38	-2.4	3.8	1234.6	662.7
100	35	346	46	-2.7	7.0	1827.5	888.3

TABLE VIII

(CONTINUED)

Time Lag (min.)	N	$\bar{d}$ (n mi)	σ_d (n mi)	$\overline{\Delta_l}$ (knots)	$\overline{\Delta_t}$ (knots)	$\overline{\Delta_l^2}$ (knots^2)	$\overline{\Delta_t^2}$ (knots^2)
			FLIGHT: 1 February 60				
5	69	22	4	0.8	0.7	20.1	18.1
10	62	43	5	1.2	1.0	45.5	32.8
15	56	64	6	1.7	1.2	77.8	51.0
20	55	84	8	1.9	1.0	129.6	68.7
25	53	105	9	1.9	0.9	172.8	73.1
30	52	126	10	2.4	1.5	216.6	85.8
40	48	168	11	3.9	3.0	294.4	111.4
50	45	210	12	3.9	1.1	403.6	92.3
60	40	252	14	2.0	-0.3	541.6	59.7
80	35	334	17	-0.1	3.6	736.1	108.3
100	31	414	18	-3.3	6.1	801.2	154.0
			FLIGHT: 2 February 60				
5	46	26	4	1.3	-2.1	27.9	25.1
10	32	52	5	4.5	-5.5	76.5	59.7
15	26	78	6	9.4	-7.8	161.1	113.9
20	21	105	7	11.3	-12.5	267.9	267.4
25	18	131	7	11.4	-18.3	404.1	481.3
30	16	156	8	7.7	-26.9	484.0	932.8
40	11	211	6	-1.5	-43.3	567.0	2065.7
50	10	260	5	-3.3	-55.9	801.1	3286.5
60	8	311	7	-9.3	-60.0	539.8	4015.0
80	2	407	0	-10.4	-72.5	115.0	5268.4
100	-	-	-	-	-	-	-
			FLIGHT: 3 February 60				
5	76	20	4	-0.5	0.7	30.3	54.0
10	71	41	6	-1.5	1.3	81.7	135.9
15	65	61	8	-2.7	2.4	133.5	205.7
20	61	81	10	-3.8	3.1	199.2	317.4
25	56	102	12	-6.0	3.9	248.0	438.1
30	49	122	13	-8.6	8.1	312.6	589.4
40	45	162	17	-13.0	1.2	440.5	897.2
50	38	202	19	-17.4	-3.8	580.2	1176.9
60	31	242	21	-22.6	-10.7	904.7	1461.5
80	28	290	86	-25.0	-15.4	1291.1	1920.3
100	26	333	105	-23.7	-17.2	1566.5	2385.2

TABLE VIII

(CONTINUED)

Time Lag (min.)	N	$\bar{d}$ (n mi)	σ_d (n mi)	$\overline{\Delta_\ell}$ (knots)	$\overline{\Delta_t}$ (knots)	$\overline{\Delta_\ell^2}$ (knots^2)	$\overline{\Delta_t^2}$ (knots^2)
			FLIGHT: 21 March 60				
5	75	25	3	0.3	0.8	17.2	23.8
10	66	50	5	0.8	2.1	36.2	41.8
15	61	75	6	1.2	3.6	52.1	51.2
20	53	99	7	1.2	5.0	58.9	77.1
25	47	123	8	1.3	6.3	72.1	121.4
30	45	147	9	2.1	7.9	83.1	150.3
40	40	193	14	3.0	9.6	93.1	191.7
50	35	241	14	4.2	13.0	108.5	285.5
60	31	288	11	7.0	17.1	122.5	390.5
80	27	383	15	10.3	21.2	255.5	563.4
100	27	476	10	14.5	27.7	353.0	870.4
			FLIGHT: 23 March 60				
5	83	20	5	-0.2	0.3	18.9	21.9
10	63	40	9	-1.0	0.5	30.6	67.0
15	54	58	11	-1.0	-0.1	49.8	162.1
20	45	75	13	-2.5	-0.4	64.2	281.3
25	42	95	17	-1.9	-1.1	79.6	423.6
30	37	110	18	-3.0	-2.5	126.2	597.8
40	29	151	26	-0.1	-6.1	263.2	894.8
50	24	190	26	1.8	-4.9	494.5	975.2
60	20	225	25	3.4	-7.4	680.2	1155.1
80	11	282	26	-9.5	-10.0	883.4	825.8
100	6	320	36	-26.4	-5.4	948.0	124.7
			FLIGHT: 26 March 60				
5	105	17	4	-0.1	0.5	13.6	24.1
10	91	34	4	0.0	1.4	30.7	48.0
15	81	52	4	0.4	2.5	41.9	54.4
20	72	69	5	0.3	4.2	70.7	75.6
25	63	86	6	-0.1	5.3	85.8	85.0
30	59	103	6	-0.1	5.2	89.7	91.6
40	56	139	8	1.1	7.7	96.5	133.8
50	47	173	9	-0.3	11.5	115.5	216.5
60	43	209	10	-0.6	12.5	113.7	250.4
80	39	276	14	1.1	15.4	87.6	339.1
100	38	345	16	0.7	18.0	122.7	367.8

TABLE VIII

(CONTINUED)

Time Lag (min.)	N	$\bar{d}$ (n mi)	σ_d (n mi)	$\overline{\Delta_\ell}$ (knots)	$\overline{\Delta_t}$ (knots)	$\overline{\Delta_\ell^2}$ (knots^2)	$\overline{\Delta_t^2}$ (knots^2)
			FLIGHT: SUMMARY				
5	713	21	5	0.0	0.0	31.1	34.0
10	605	42	8	-0.1	0.0	62.9	71.5
15	546	62	11	-0.1	0.2	99.3	120.0
20	498	82	14	-0.5	0.4	141.8	172.8
25	455	102	17	-0.9	0.5	190.9	241.3
30	419	122	20	-1.2	-0.1	235.3	324.3
40	364	162	25	-1.4	-0.5	331.5	492.9
50	316	203	31	-1.9	-0.3	459.2	634.0
60	280	241	35	-2.5	-1.4	570.8	745.4
80	227	312	54	-3.9	-0.3	771.0	908.8
100	199	383	68	-2.8	3.6	969.6	989.7

points were paired together even though the flight path had sharp corners so that a mean value of the longitudinal or transverse wind component difference would be without meaning. In Table VIII, pairs were rejected if the flight path between points was not reasonably straight.)

The number of data pairs for each flight decreases with increasing time lag. This is due to several items, mostly the effect of rejection criteria of which the condition for a reasonably straight flight path is prominent. The effect is easily seen on 20 Jan 60, 2 Feb 60, and 23 March 60 when the flight path formed a loop from Dayton around the northeastern states and return (Route 2).

The values of $\overline{\Delta_\ell^2}$ and $\overline{\Delta_t^2}$ from Table VIII for each flight show the same variation in wind behavior as a function of lag as

those in the previous table and for the same reasons. Only the summary table in which values from all nine flights are combined is considered of any real significance.

The composite values of $\overline{\Delta_\ell^2}$ and $\overline{\Delta_t^2}$ as functions of distance lag are shown graphically in Fig. VII-8. The horizontal scale is ground distance in the case of the values determined from such class intervals and is air distance lag for the data determined from observation time lags. The two pairs of data points appear to agree reasonably well. The agreement would have been even better if the average ground distance had been used for the abscissa for data grouped on the basis of time lags. (Compare distances of Table VI with the average distance of Table VIII.

The central parts of the curves (140 n mi to 200 n mi) seem to be well behaved as far as the mean square of component difference vs distance relative is concerned. At the short distance end, the points for five-minute time lag (22 n mi) appear reasonably placed as an extension of the remaining points. The point pairs from ground distance lag classes seem to jump around unnecessarily. It is easily seen from Table VII that the first five points select samples from the nine flights in a very irregular manner whereas the sampling from the middle group of points is reasonably uniform.

At large distances, the same nonrepresentative sampling may account for the departure of the data points from the trend of the middle points.

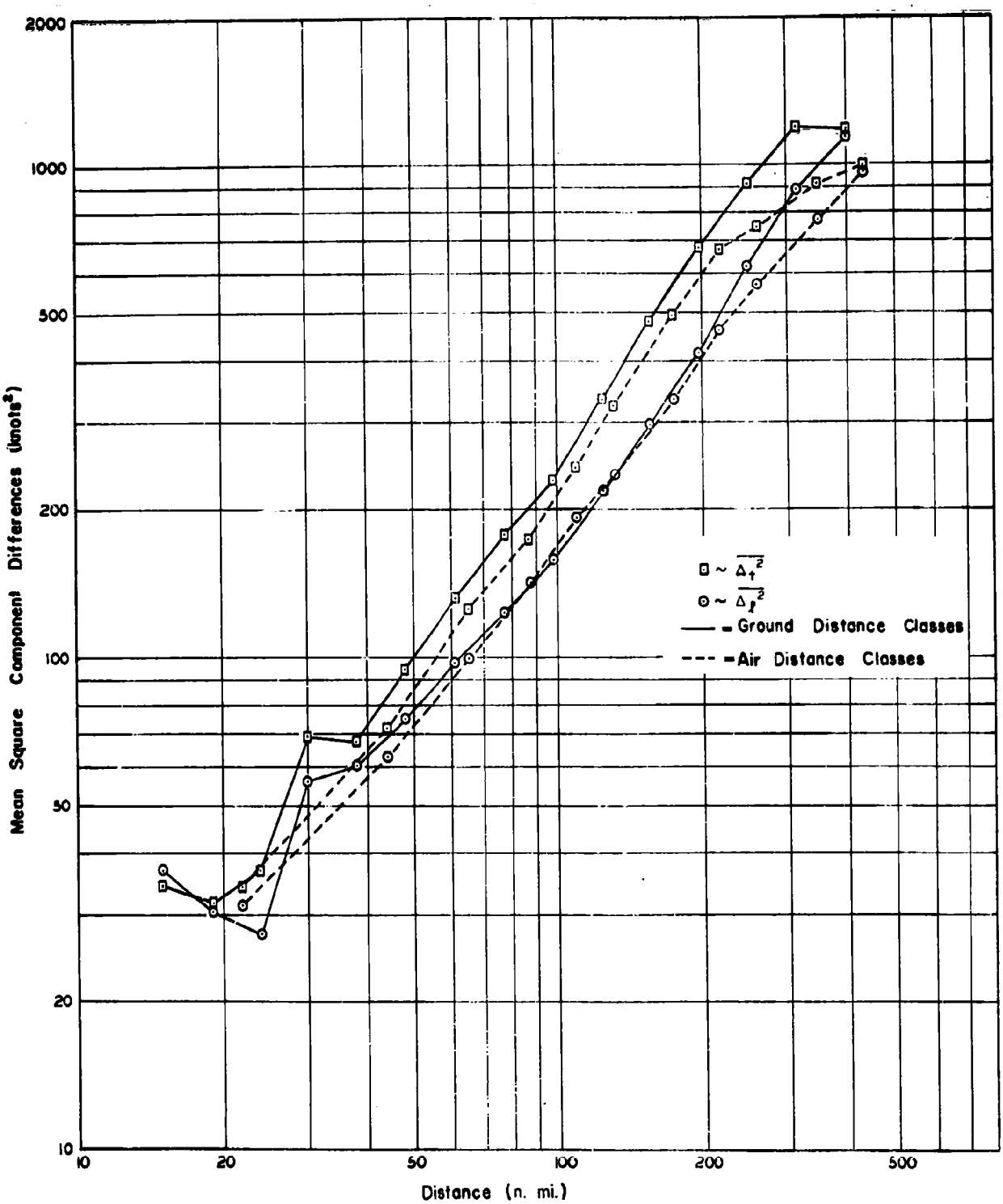

Fig. VII-8 Comparison of Value of Mean Squared Component Differences Based on Ground Distance Classes and Air Distances (time lag) Classes

D. MEAN SQUARE WIND COMPONENT DIFFERENCES FROM PROJECT JET STREAM DATA

1. General Remarks

Early in this study Mr. I. I. Gringorten called our attention to the wind data available from Project Jet Stream.(1) In connection with the Project Jet Stream program, a series of volumes were prepared entitled, "Flight Data Pertaining to Jet Streams, Jet No. XXX, Flown XX Month Year" where the X's, month, and year are appropriately chosen. These volumes contain graphs of the quantities measured and a printout of the data from which the graphs were prepared, together with maps showing the general weather situation, the flight path and some wind data along it, and other pertinent information. The data were obtained from photographic recordings of the aircraft instrumentation and were reduced at the Data Reduction Laboratory of the University of Dayton, Dayton, Ohio. For our purposes, we are interested in the wind data from the doppler navigator equipment.

The frame speed of the camera used to photograph the instrument dials was near two frames per minute. Though the aircraft had a true air speed of near 425 knots compared with 260 knots for the 4WW data, the fact that the data was recorded ten times more frequently makes possible wind comparisons with a distance separation of order of 3 n mi instead of 22 n mi.

Had the flights all been made entirely in the jet stream region, there would be considerable question of the validity of the use of this data to make inferences concerning the turbulent structure of the atmosphere in general at or near the jet stream

level. Fortunately, there were several flights that were required for miscellaneous purposes on which the instrument and recorder were operating and which were either wholly or at least extensively outside the jet stream as such. Only such flights or flight legs were selected for inclusion in this study.

2. The Data

The data used was selected from the flights listed in Table IX. The fact that nearly all the flight legs in Table IX were on a westerly track was quite accidental. The subdivision into several subsections is based on minor changes of track.

The data from Project Jet Stream were handled in a more straightforward manner than the 4WW data. Instead of dealing with a flight along a crooked track, Project Jet Stream data were selected so as to lie along essentially straight flight path segments. Altitude in each segment was carefully maintained and each segment was checked for such constancy of altitude before inclusion in the list of Table IX.

The air distances corresponding to the time lags used are listed in Table X for each JETNO (our numbers 1 through 6). The lag number increases by one unit for simple indexing purposes. The number of time lag intervals corresponding to each lag number is shown in the second column of Table X. These were selected to roughly approximate an exponential form (i.e., that the logarithm of the time lags would be roughly uniformly spaced). The air distances corresponding to each time lag were computed from the mean true air speed and mean interval of time lag for each JETNO. These distances are subject to some dispersion that

TABLE IX

DESCRIPTIVE DATA ON JET FLIGHTS FROM WHICH DATA WAS USED

Jet No.	Flt. No.	Start	End	Date	Winds	Alt. Thsd. Feet	Track	No. of Points	Dist. n mi	Average Time Interval Sec	Avg. Grnd. Dist. (n mi)	Mean TAS kts	S.D. TAS kts
1	24	16h 15m 55s	17h 33m 48s	19-3-57	Head	36	254°	142	426	32.9	3.3	422.6	7.1
		17 34 21	18 01 44		Head	36	244°	51	141	32.9	2.8		
2	24	20 22 17	20 57 10	19-3-57	Tail	38	88°	64	332	32.7	5.3	423.5	17.1
		20 57 42	21 11 52		Tail	38	103°	27	134	32.7	5.1		
3	24	21 18 57	22 04 48	19-3-57	Cross	35	16°	85	316	32.8	3.8	423.4	3.6
4	E22	23 09 04	00 07 54	4-12-57	Q-Head	34	243°	139	423	25.4	3.1	438.6	6.8
		00 08 20	00 28 36		Q-Head		237°	49	142	25.3	3.0		
		00 29 01	00 46 24		Q-Head		226°	42	123	25.4	3.0		
5	E57	00 24 58	00 51 49	29-6-58	Cross	34	252°	65	188	24.4	2.9	432.2	4.2
		00 54 13	01 17 50		to		280°	63	172	24.4	2.8		
		01 18 15	01 41 22		Head		258°	57	158	24.3	2.8		
		01 41 46	01 41 22		"		245°	37	101	24.4	2.8		
		01 57 37	02 06 57		"		262°	24	62	24.3	2.7		
		02 07 22	02 30 28		"		276°	56	149	24.3	2.7		
		02 30 52	02 48 20		"		233°	44	114	24.4	2.6		
		02 48 45	03 38 19		"		250°	132	316	24.4	2.6		
6	35	20 13 19	20 51 07	17-5-57	Q-Head	41	258°	334	126	6.8	0.69	427.6	4.0

REMARKS:
JETNO-1: Flight was north of a jet.
JETNO-2: Along the core of a jet.
JETNO-3: On the north side of a jet.
JETNO-4: Well to the southwest of a jet core.
JETNO-5: A long, cross-country flight with no evidence of a jet stream except beyond flight path at western end.
JETNO-6: Well south of a jet stream; was selected because this short stretch of data were spaced about 7 seconds apart.

arises from two sources, the fact that the true air speed is not really uniform and the fact that the timer actuating the camera shutter did not run exactly uniformly. The largest factor is the true air speed variation, which (Table IX) amounts to approximately 1.0% (standard deviation). (In JETNO-2 it amounts to 4% and JETNO-1 and JETNO-4 to about 1.7%. The case of JETNO-2 is the only situation in which flight was in the jet stream core. This is presumed to account for the higher variability of the true air speed.)

TABLE X

LAG NUMBERS, TIME INTERVALS, AND AIR DISTANCES FOR JET STREAM DATA

Lag No.	No. of Intervals	Distance (n mi) 1	2	3	4	5	6
1	1	3.9	3.8	3.9	3.1	2.9	0.8
2	2	7.7	7.7	7.7	6.2	5.9	1.6
3	3	11.6	11.5	11.6	9.3	8.8	2.4
4	4	15.4	15.4	15.4	12.4	11.7	3.2
5	6	23.2	23.1	23.1	18.6	17.6	4.9
6	8	30.9	30.8	30.8	24.7	23.4	6.5
7	10	38.6	38.5	38.5	30.9	29.3	8.1
8	12	46.3	46.2	46.2	37.1	35.1	9.7
9	16	61.8	61.5	61.6	49.5	46.8	12.9
10	20	77.2	76.9	77.0	61.9	58.5	16.2
11	24	92.7	92.3	92.4	74.2	70.2	19.4
12	28	108	108	108	86.6	81.9	22.7
13	36	139	138	139	111	105	29.1
14	44	169	169	169	136	129	35.6
15	52	201	200	200	161	152	42.1
16	60	232	231	231	186	176	48.5

3. Results

The values of the mean square wind component differences that are obtained from the Project Jet Stream observations are tabulated in Table XI. The tabulated data is somewhat more extensive than that from the 4WW observations since the flight paths were straight and some meaning could be assigned to such items as the mean longitudinal and transverse wind components and their standard deviations.

It is felt that the values of the mean square wind velocity component differences from the individual JETNO's are somewhat unreliable (with the possible exception of JETNO-5). The amount of data entering into each is not only limited in quantity, but also the observations are made in a highly specific atmospheric situation.

Remarks on the wind variability in general are usually understood in the sense of a kind of average of a wide variety of situations. Consequently, a composite of the JETNO-1 through JETNO-5 was prepared and the results tabulated in Table XII. (Here the mean component values and their standard deviation are omitted since they have no significance in the composite picture.)

In spite of the fact that we consider the mean square component differences of the individual JETNO's as unreliable, it is interesting to compare the internal variations with those of the variations of the nine 4WW flights. The values of $\overline{\Delta_\ell^2}$ and $\overline{\Delta_t^2}$ in Table VIII vary widely in this regard; in some instance $\overline{\Delta_\ell^2} < \overline{\Delta_t^2}$ holds and in others the equality is (strongly) reversed.

TABLE XI

DATA ON MEAN SQUARE VELOCITY DIFFERENCES FROM PROJECT JET STREAM DATA

Lag No.	N	$\overline{\Delta_\ell}$	$\overline{\Delta_t}$	$\overline{\Delta_\ell^2}$	$\overline{\Delta_t^2}$	$\overline{U}_\ell$	$\overline{U}_t$	$\overline{U}'_\ell$	$\overline{U}'_t$	σ_ℓ	σ_t	σ'_ℓ	σ'_t
						* * * JETNO-1 * * *							
1	193	-0.4	0.3	1.4	2.1	-73.7	26.7	-74.1	27.0	23.0	22.0	23.3	22.0
2	192	-0.8	0.6	3.3	5.4	-73.4	26.6	-74.2	27.1	22.8	22.0	23.3	22.0
3	191	-1.1	0.9	5.7	8.9	-73.2	26.4	-74.3	27.3	22.6	21.9	23.3	21.9
4	190	-1.5	1.2	8.6	12.7	-72.9	26.2	-74.4	27.4	22.3	21.9	23.3	21.9
5	188	-2.3	1.8	14.5	20.9	-72.4	25.9	-74.7	27.7	21.8	21.7	23.3	21.8
6	186	-3.1	2.5	20.2	29.6	-71.8	25.5	-75.0	28.0	21.3	21.6	23.3	21.8
7	184	-4.0	3.1	26.2	38.2	-71.3	25.2	-75.3	28.3	20.8	21.4	23.2	21.7
8	182	-4.8	3.9	31.1	46.4	-70.8	24.8	-75.6	28.6	20.3	21.1	23.1	21.6
9	178	-6.5	5.6	41.2	54.8	-69.8	23.9	-76.3	29.4	19.3	20.5	22.9	21.2
10	174	-8.2	7.3	48.0	60.6	-68.8	22.9	-77.0	30.3	18.4	19.7	22.7	20.7
11	170	-9.9	9.2	54.2	67.5	-67.8	22.0	-77.7	31.1	17.4	18.9	22.5	20.1
12	166	-11.5	11.0	62.4	72.7	-66.8	21.0	-78.3	32.0	16.5	18.1	22.4	19.5
13	158	-14.6	14.7	83.3	87.9	-65.0	19.2	-79.6	33.9	14.8	16.6	22.2	18.1
14	150	-17.7	17.9	100.3	97.1	-63.4	17.7	-81.2	35.6	13.5	15.7	21.6	17.0
15	142	-21.0	21.2	104.0	82.2	-62.0	15.8	-83.0	37.0	12.4	14.0	20.8	16.3
16	134	-24.2	23.7	120.1	77.0	-60.4	14.6	-84.5	38.4	10.7	13.5	20.4	15.8
						* * * JETNO-2 * * *							
1	91	0.3	-0.2	1.5	7.1	153.7	-2.9	153.9	-3.1	6.0	12.3	5.8	12.1
2	90	0.5	-0.4	4.5	19.0	153.6	-3.0	154.1	-3.4	5.9	12.4	5.7	12.0
3	89	0.7	-0.6	8.0	32.2	153.5	-3.1	154.2	-3.7	5.9	12.5	5.6	11.8
4	88	0.9	-0.8	11.8	46.5	153.4	-3.1	154.3	-3.9	5.9	12.5	5.5	11.6
5	86	1.4	-1.3	20.7	76.1	153.1	-3.1	154.6	-4.4	5.8	12.7	5.3	11.3
6	84	2.0	-1.8	29.1	106.3	152.9	-3.1	154.9	-5.0	5.5	12.8	4.9	10.7
7	82	2.6	-2.5	37.7	133.4	152.6	-3.1	155.2	-5.6	5.3	13.0	4.4	10.0
8	80	3.1	-3.0	46.0	155.4	152.4	-3.2	155.5	-6.1	5.2	13.1	4.1	9.6
9	76	3.7	-4.0	55.8	191.9	152.2	-3.1	155.8	-7.1	5.2	13.5	3.9	8.7
10	72	3.7	-4.9	-53.0	229.9	152.2	-3.1	156.0	-8.0	5.4	13.8	3.9	8.2
11	68	3.5	-5.4	43.8	278.7	152.4	-3.1	155.9	-8.5	5.5	14.2	4.0	8.1
12	64	3.4	-6.1	37.0	318.8	152.3	-2.7	155.7	-8.8	5.6	14.4	4.1	8.3
13	56	4.1	-9.7	38.5	271.1	151.6	0.7	155.8	-9.0	5.7	11.9	4.3	8.8
14	48	4.9	-11.8	52.7	345.3	151.2	2.8	156.1	-9.0	6.0	11.5	4.6	9.5
15	40	5.9	-14.4	58.9	416.4	151.0	5.1	156.9	-9.2	6.6	11.2	4.7	10.4
16	32	7.1	-15.0	22.7	301.7	150.0	8.4	157.1	-6.6	7.0	10.1	5.2	9.7

TABLE XI
(CONTINUED)

Lag No.	N	$\overline{\Delta_\ell}$	$\overline{\Delta_t}$	$\overline{\Delta_\ell^2}$	$\overline{\Delta_t^2}$	$\overline{U}_\ell$	$\overline{U}_t$	$\overline{U}'_\ell$	$\overline{U}'_t$	σ_ℓ	σ_t	σ'_ℓ	σ'_t
						* * *	JETNO-3	* * *					
1	84	0.2	1.2	2.2	3.4	3.3	-110.8	3.5	-109.6	9.0	32.2	9.0	32.4
2	83	0.4	2.5	3.8	6.3	3.1	-111.5	3.6	-109.0	8.8	31.8	9.1	32.2
3	82	0.7	3.7	6.6	10.0	3.0	-112.1	3.6	-108.5	8.8	31.4	9.1	32.0
4	81	1.0	4.9	9.2	14.5	2.8	-112.8	3.7	-107.9	8.7	31.0	9.1	31.8
5	79	1.5	7.3	14.7	24.1	2.4	-114.2	3.9	-106.9	8.5	30.1	9.2	31.5
6	77	2.1	9.7	19.5	35.5	2.0	-115.5	4.0	-105.8	8.2	29.4	9.2	31.2
7	75	2.6	12.1	23.9	48.2	1.6	-116.8	4.2	-104.7	8.0	28.7	9.3	30.8
8	73	3.2	14.7	28.2	59.8	1.3	-118.2	4.5	-103.5	7.8	27.9	9.3	30.3
9	69	4.4	20.1	33.9	72.0	0.7	-120.9	5.1	-100.8	7.7	26.2	9.2	29.1
10	65	5.9	25.5	38.7	77.2	-0.1	-123.5	5.8	-98.0	7.2	24.7	9.0	27.6
11	61	7.6	31.0	49.3	87.0	-1.0	-126.3	6.6	-95.3	6.4	22.9	8.7	26.3
12	57	9.8	36.6	52.1	98.8	-2.2	-129.2	7.6	-92.6	4.9	20.7	8.1	25.1
13	49	13.3	49.2	44.1	101.5	-3.5	-135.5	9.8	-86.3	3.4	14.6	6.5	21.2
14	41	16.2	61.4	42.6	43.6	-4.6	-140.6	11.6	-79.2	2.6	9.6	5.4	15.0
15	33	19.1	69.9	24.6	17.2	-5.3	-143.7	13.8	-73.8	2.2	7.9	3.6	11.1
16	25	19.6	77.6	15.7	31.8	-4.9	-147.4	14.7	-69.8	2.3	5.1	2.4	9.7
						* * *	JETNO-4	* * *					
1	230	0.0	-0.3	3.1	2.8	-13.1	27.3	-13.1	27.0	6.3	24.1	6.4	24.2
2	229	0.1	-0.7	6.9	6.5	-13.2	27.5	-13.1	26.8	6.3	24.1	6.4	24.1
3	228	0.2	-1.1	9.6	11.6	-13.2	27.7	-13.1	26.6	6.3	24.0	6.4	24.0
4	227	0.3	-1.4	11.2	16.6	-13.3	27.8	-13.1	26.4	6.1	23.9	6.4	23.9
5	225	0.4	-2.1	13.9	26.3	-13.5	28.2	-13.0	26.1	6.0	23.7	6.4	23.7
6	223	0.6	-2.8	19.8	34.8	-13.6	28.5	-13.0	25.7	5.9	23.6	6.5	23.5
7	221	0.8	-3.5	24.1	42.6	-13.7	28.8	-12.9	25.3	5.8	23.4	6.4	23.2
8	219	1.1	-4.3	26.5	47.4	-13.8	29.2	-12.8	24.8	5.6	23.2	6.2	22.8
9	215	1.4	-5.9	33.0	49.8	-14.0	29.9	-12.6	24.0	5.5	22.9	6.1	22.0
10	211	1.8	-7.6	37.2	50.5	-14.2	30.6	-12.4	23.1	5.4	22.4	6.0	21.2
11	207	2.1	-8.9	36.2	53.3	-14.3	31.4	-12.2	22.5	5.3	22.0	6.0	21.0
12	203	2.2	-10.0	38.9	57.6	-14.4	32.1	-12.2	22.1	5.4	21.6	6.0	21.0
13	195	2.6	-12.7	37.8	63.2	-14.5	33.5	-11.9	20.9	5.4	20.8	5.9	20.6
14	187	3.2	-15.5	29.2	60.8	-14.6	35.1	-11.4	19.6	5.5	19.7	5.4	20.0
15	179	3.9	-18.4	27.3	52.9	-14.8	36.6	-10.9	18.2	5.5	18.8	5.0	19.4
16	171	4.6	-21.2	34.3	47.5	-15.0	38.0	-10.5	16.7	5.6	18.1	4.7	18.5

TABLE XI
(CONTINUED)

Lag No.	N	$\overline{\Delta_\ell}$	$\overline{\Delta_t}$	$\overline{\Delta_\ell^2}$	$\overline{\Delta_t^2}$	$\overline{U}_\ell$	$\overline{U}_t$	$\overline{U}'_\ell$	$\overline{U}'_t$	σ_ℓ	σ_t	σ'_ℓ	σ'_t
						* * * JETNO-5 * * *							
1	476	-0.1	-0.1	1.3	4.9	-26.6	10.0	-26.7	9.9	19.6	10.7	19.6	10.7
2	475	-0.2	-0.1	3.1	10.1	-26.5	10.0	-26.8	9.9	19.6	10.7	19.6	10.7
3	474	-0.4	-0.2	5.1	15.1	-26.4	10.0	-26.8	9.9	19.6	10.7	19.6	10.7
4	473	-0.5	-0.2	7.2	19.6	-26.4	10.1	-26.9	9.8	19.6	10.7	19.5	10.7
5	471	-0.8	-0.3	11.3	28.1	-26.2	10.1	-27.0	9.8	19.5	10.6	19.5	10.7
6	469	-1.1	-0.4	15.0	33.4	-26.1	10.2	-27.2	9.7	19.4	10.6	19.4	10.6
7	467	-1.3	-0.6	18.8	38.7	-26.0	10.2	-27.3	9.7	19.3	10.6	19.4	10.6
8	465	-1.6	-0.7	22.2	46.3	-25.8	10.3	-27.4	9.6	19.2	10.6	19.3	10.6
9	461	-2.1	-0.9	27.9	62.3	-25.5	10.4	-27.7	9.5	19.1	10.6	19.2	10.5
10	457	-2.6	-1.2	34.1	75.6	-25.3	10.5	-27.9	9.3	19.0	10.5	19.1	10.5
11	453	-3.2	-1.4	40.3	91.5	-25.0	10.6	-28.2	9.2	18.9	10.5	19.0	10.5
12	449	-3.8	-1.6	46.4	111.0	-24.7	10.7	-28.5	9.1	18.7	10.5	18.8	10.4
13	441	-5.0	-1.9	55.6	147.2	-24.2	10.8	-29.1	8.9	18.3	10.6	18.3	10.4
14	433	-6.1	-2.2	58.0	180.0	-23.6	10.9	-29.8	8.7	18.1	10.6	17.9	10.4
15	425	-7.2	-2.5	53.9	198.3	-23.2	11.1	-30.4	8.5	17.9	10.7	17.4	10.4
16	417	-8.4	-2.8	53.4	212.7	-22.6	11.2	-31.0	8.4	17.7	10.8	17.1	10.5

TABLE XII

COMPOSITE OF DATA ON VELOCITY COMPONENT DIFFERENCES FROM JETNO-1 THROUGH JETNO-5

Lag No.	N	$\bar{d}$	σ_d	$\overline{\Delta_\ell}$	$\overline{\Delta_t}$	$\overline{\Delta_\ell^2}$	$\overline{\Delta_t^2}$
1	1074	3.3	0.4	-0.1	0.0	1.8	4.0
2	1069	6.6	0.8	-0.2	0.1	4.1	8.9
3	1064	9.8	1.3	-0.2	0.1	6.6	14.3
4	1059	13.1	1.7	-0.4	0.1	8.9	19.6
5	1049	19.6	2.5	-0.5	0.2	13.4	30.0
6	1039	26.2	3.3	-0.6	0.2	18.5	39.1
7	1029	32.7	4.2	-0.7	0.2	23.2	47.7
8	1019	39.2	5.0	-0.9	0.3	27.0	56.1
9	999	52.2	6.6	-1.2	0.4	33.9	68.8
10	979	65.2	8.3	-1.6	0.5	38.9	79.0
11	959	78.0	9.9	-2.1	0.6	42.7	92.0
12	939	91.1	10.7	-2.5	0.8	47.3	106.1
13	899	116.4	14.6	-3.2	1.0	55.0	123.8
14	859	141.6	17.4	-4.4	0.9	58.1	142.3
15	819	166.8	20.5	-5.5	0.4	55.8	149.7
16	779	191.5	23.2	-6.7	-0.2	58.2	150.9

This inequality is much more consistently valid in the data of Table XI. It is not known whether this is a result of the difference due to different eddy structures at 25,000 and 35,000 feet.

Columns for the mean air distance between points ($\bar{d}$) and its standard deviation (σ_d) are shown in Table XII. The values of mean air distance are the weighted mean values for the individual JETNO's. The standard deviation tabulated should be interpreted with care. It is a value computed on the basis of the five distance values of Table X with weights equal to the number of data pairs. Since the number of data pairs is highly variable,

the "distribution" of distances is far from "normal". Also no account is taken of the variability of true air speed within JETNO's, shutter time variations, etc.

The detailed discussion of the significance of the data from the Project Jet Stream flights is deferred to Section F.

E. RELATION BETWEEN MEAN SQUARE COMPONENT DIFFERENCES AND THE COMPONENTS OF THE WIND CORRELATION TENSOR

The values of the mean square velocity component differences are related to the components of the wind correlation tensor through the following elementary equations. A mean square difference may be expressed as

$$\overline{\Delta^2} = \overline{(U-U')^2} \tag{1}$$

$$= \overline{\left[(U-\overline{U}) - (U'-\overline{U}') + (\overline{U}-\overline{U}')\right]^2}$$

$$= \overline{\left[u-u' + (\overline{U}-\overline{U}')\right]^2}$$

$$= \overline{u^2} - 2\overline{uu'} + \overline{(u')^2} + 2\overline{u}(\overline{U}-\overline{U}') \tag{2}$$

$$-2\overline{u'}(\overline{U}-\overline{U}') + (\overline{U}-\overline{U}')^2$$

where the subscripts are suppressed for the moment and where

$$u = U - \overline{U},\ u' = U' - \overline{U}'$$

If the points P and P′ were fixed (where U and U′, respectively, are measured), then $\overline{u} = \overline{u}' = 0$ (these are the means of the departure from the mean) and if the mean velocity field were uniform, then $\overline{U} = \overline{U}'$ so that $(\overline{U}-\overline{U}')^2 = 0$.

If the mean velocity field is nearly uniform, this last term may be considered negligible. If, in addition, the wind variability at P and P′ is nearly the same, $\overline{u^2} \cong \overline{(u')^2}$, one may write

$$\overline{\Delta^2} \cong 2(\overline{u^2}-\overline{uu'}) = 2\overline{u^2}(1-r_{uu}) \tag{3}$$

where r_{uu} is the correlation coefficient relating U at P to U′ at P′. In the case in which P and P′ are fixed, the means are based on a period of observations in time.

In the case of the 4WW and Project Jet Stream observations, the points P and P′ are not fixed in space but are fixed with respect to each other and the means are taken with respect to space (i.e., means over a flight path). This raises several questions as to the validity and interpretation of the results.

When the flight path is straight, as in the case of the individual Jet Stream Flights, the situation is nearly the same as that for fixed P and P′. In this case P and P′ are fixed with respect to the orientation of P′ with respect to P (i.e., in the direction of the heading). The distance between P and P′ is subject to some variation (when fixed time lags are used) due to variations in the integrated true air speed. These variations are relatively minor. It was seen that for the Jet Stream data, the value of the standard deviation of the true air speed was only 1.0 to 4.0%. The value of the integrated true air speed over a flight path of some length would be less the longer the flight path. Some other factors also influence the air spacing of P and P′ such as the uniformity of the camera shutter trigger, the uniformity of the timing clock, etc. It is assumed that these are relatively minor factors.

The evaluation of the correlation coefficient, r_{uu}, from the values of $\overline{\Delta^2}$ raises the question of determining the value of $\overline{u^2}$, the basic wind component variance. In the case of flight data, the flight is made at a specific level on a specific day and hence in a very particular synoptic situation. The value of $\overline{u^2}$ from such data would be a reflection only of the line of

flight in that situation. Consequently, the value of $\overline{u^2}$ would be most unreliable. To obtain a reliable estimate of $\overline{u^2}$ would require many flights (more or less identical) so that the data on $\overline{u^2}$ from each would be reasonably representative. (Another alternative, flying many aircraft over the world simultaneously to sample the entire field of motion seems (very) unfeasible and not free from objections.) Consequently, it seems unwise to use data on $\overline{\Delta^2}$ to actually compute correlation coefficient values. The values of $\overline{\Delta^2}$, from the few situations at hand begin to approach a "representative sample" (even though poorly) so that one has much more confidence in the composite results of the several flights than in those for a single flight.

When the observations are taken from flight paths on different headings, the question of the structure of the components of the wind correlation tensor arises. It has been shown that the way in which the wind component correlation coefficients vary with distance is a function of the orientation of P′ with respect to P when the components in a fixed direction are used. If we were to use for U and U′ the east pointing wind component, then to adequately study the variation of $\overline{\Delta^2}$, it would be necessary to determine its value not only as a function of the time lags (distance) but also as a function of flight heading. This increases the magnitude of the problem greatly. On the other hand, it has been seen that the wind vector is resolved along and across the flight path, the components of the wind correlation tensor become independent if the orientation of P′ with respect to P (in certain idealized cases which seem to be

verified for synoptic scale disturbances). Consequently, this orientation of the reference frame is used. At least in this case we may look for a connection between the values of $\overline{\Delta^2}$ from synoptic observations and values from aircraft observations where the point separation distances overlap and still make use of what aircraft data are available.

Then the flight path is not straight, as in the case of the 4WW observations, the only interpretation that seems feasible for values of $\overline{\Delta^2}$ is in terms of the longitudinal and transverse wind components. In such a case the values of $\overline{\Delta_\ell^2} = \overline{(U_\ell - U'_\ell)^2}$ and $\overline{\Delta_t^2} = \overline{(U_t - U'_t)^2}$ are compiled in the sense of an ensemble average in which the values over the flight path are considered as a space average. In this case, the values of individual means, their differences, and standard deviations usually associated with a correlation coefficient computation are completely meaningless.

The interpretation of the data on $\overline{\Delta_\ell^2}$ and $\overline{\Delta_t^2}$ is made via equation (3). This requires that certain assumptions are made concerning a meaningful value of $\overline{u^2}$, the wind component variance. It is necessary to assume that such a value exists and that either it is independent of the orientation of P′ with respect to P or that the ensemble averages have been taken with the orientation sufficiently randomized that its value is a suitable mean (and, of course, that its variation with respect to orientation is not too large).

In spite of the lengthy discussion of the conceptual difficulties encountered in using flight observations for estimating

the behavior of $\overline{\Delta_\ell^2}$ and $\overline{\Delta_t^2}$ as a function of the separation of P and P', there are certain outstanding advantages in this method of attack.

First, the values of $(1-r_{uu})$, r_{uu} = correlation coefficient, are particularly suitable for estimating the behavior of r_{uu} for the separation of P' from P near zero. The use of the co-ordinates $(\log(d), \log(1-r_{uu}))$ or equivalently $(\log(d), \log \overline{\Delta^2})$, where d is separation distance, permit a "magnification" of the area near $d = 0$, $r_{uu} = 1$ that increases as this point is approached.

A second, and more important, advantage lies in the fact that the effects of at least certain types of observation error are minimized. It was pointed out in the first section of this Chapter that, when dealing with rawinsonde observations it is expected that for very closely spaced observations one is reduced to the analysis of observation error and that for small enough separation of observation points correlation behavior is almost entirely determined by the size of these errors. In dealing with velocity component differences, one can by no means dismiss observation errors, but the way in which they must be accounted for and the range of their effects are quite different.

Errors that are relatively constant from one observation of a wind component to the next cancel out when the component is observed with the same "instrument" and component differences are used. One is not, then, faced with evaluating the total instrument error, but only the extent to which the error differs from one observation to the next. This has a tendency to reduce the effect of errors by an order of magnitude or so.

In using the wind observations from a device such as the doppler navigator, it is necessary to account for a completely different type of observational error, that of the tendency of the electro-mechanical device to "smooth" the observations. This effect is most prominent when the observations are closely spaced and is of decreasing importance for increasing spacing.

The use of quantity $(U_\ell - U'_\ell)(U_t - U'_t)$ to estimate the structure of the correlation tensor components $\overline{u_\ell u'_t}$ and $\overline{u'_\ell u_t}$, or the correlation coefficients $r_{\ell t}$ and $r_{t\ell}$, is impossible from the flight data at hand. This is due to the fact that these components (correlation coefficients) are quite small in the first place and in the second place are direction sensitive (i.e., they depend on the orientation of P′ with respect to P). To treat these components would require that the flight legs be carefully classed in terms of heading. This had not been done, and the data available makes it impractical.

F. STRUCTURE OF WIND CORRELATION TENSOR COMPONENTS FROM FLIGHT DATA

1. Presentation of Combined Flight and Rawinsonde Data

The composite data on $\overline{\Delta_\ell^2}$ and $\overline{\Delta_t^2}$ from both the 4WW and Project Jet Stream flights together with the values from JETNO-6 and computed values of these quantities from the winter, 300 mb level, SC-USWB-FCDA data are plotted in Fig. VII-9. The ordinate is the logarithm of the $\overline{\Delta_\ell^2}$ or $\overline{\Delta_t^2}$ (knots squared) while the abscissa is the logarithm of the separation of point P' from P (nautical miles).

The first striking feature of this illustration lies in the large scatter of the points of the SC-USWB-FCDA data. This is due to two factors. First, part of the scatter is due to the fact that the values of $r_{\ell\ell}$ and of r_{tt} possess some scatter in themselves. The second, and more important factor, is the fact that the values of $\overline{u_\ell^2}$ and $\overline{u_\ell'^2}$ (or $\overline{u_t^2}$ and $\overline{u_t'^2}$) that were used were those actually observed. These values strongly reflect the fact that the wind variability is variable from place to place (especially with latitude). Thus the values of $\overline{\Delta_\ell^2}$ and $\overline{\Delta_t^2}$ which had been plotted show a much larger scatter than those values of $1-r_{\ell\ell}$ and $1-r_{tt}$.

The data points for $\overline{\Delta_\ell^2}$ and $\overline{\Delta_t^2}$ from the two flight observation sources demand some brief comment. The most striking property that these points display is their tendency to lie parallel to each other. This property will be discussed in more detail later. That they do not lie along the same pair of "parallel" curves (one for $\overline{\Delta_\ell^2}$ and the other for $\overline{\Delta_t^2}$) is due

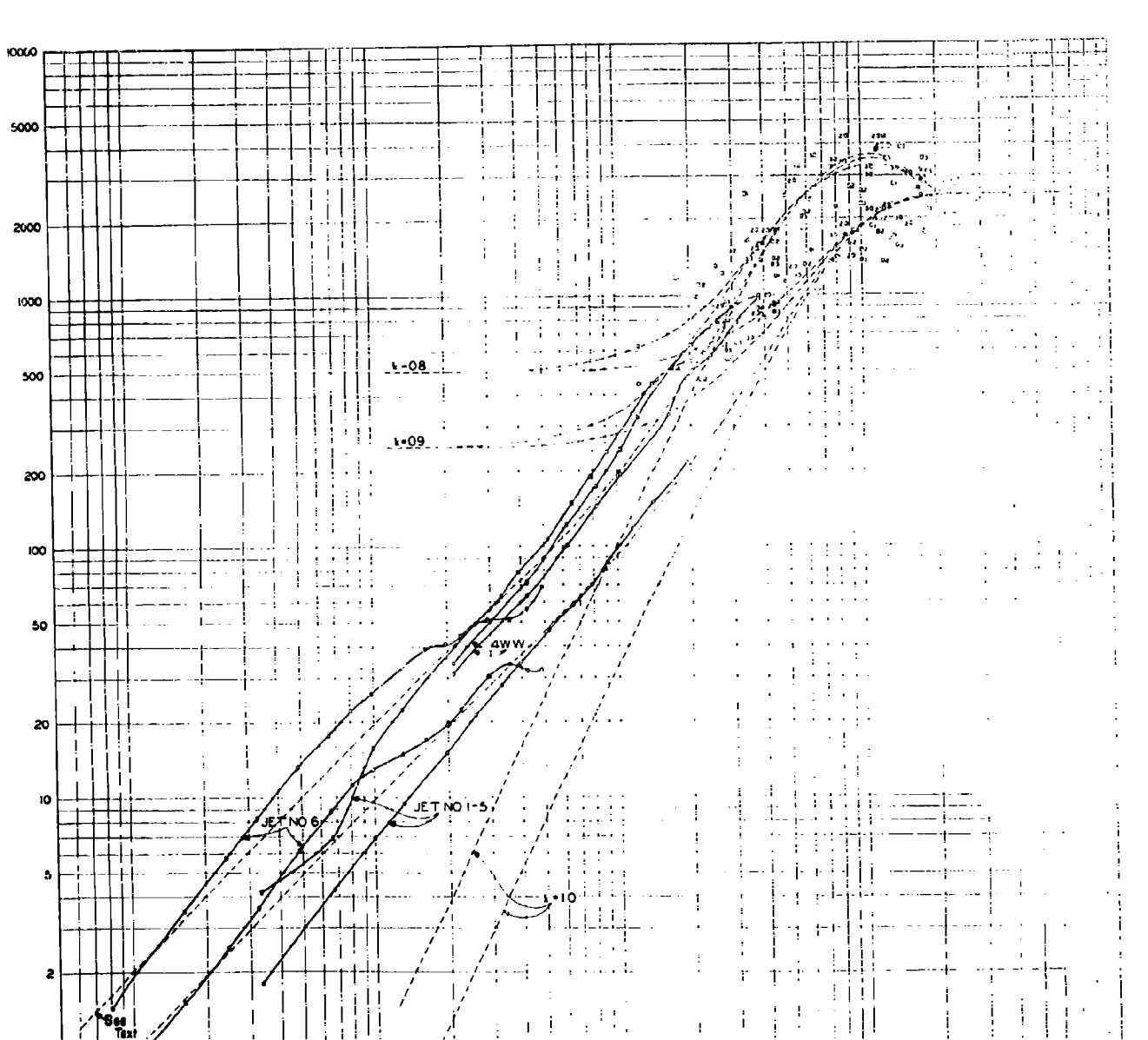

Fig. VII-9 Composite Data on $\overline{\Delta_1^2}$ and $\overline{\Delta_t^2}$

at least in part to the effect of the term in $\overline{u_\ell^2}$ (or $\overline{u_t^2}$) of equation (3), i.e., on the basic wind component variance concerned.

The 4WW observations are made in middle and late winter at near 25,000 feet. The fact that these are winter observations could urge a large value for $\overline{u^2}$. The fact that they were at 25,000 feet would indicate a somewhat smaller value of $\overline{u^2}$ than would be expected near the 35,000-foot level where the Project Jet Stream flights operated.

The composite data from Project Jet Stream reflects very strongly the values from JETNO-5, a long flight made in late June and reflecting essentially summer (low) values of $\overline{u^2}$.

The flight, JETNO-6, shown individually because of the close spacing of P′ to P, was made in late May and so tends to reflect transition conditions from winter to summer. On the other hand, this flight was made at 41,000 feet, very near the level of maximum $\overline{u^2}$.

To summarize, the vertical displacement of the flight data points is strongly dependent on the value of $\overline{u^2}$ that might be considered as prevailing. This value is affected by such a variety of factors, such as season, altitude, heterogeneity of data, etc., that it seems somewhat unreasonable to evaluate the amount of the relative vertical displacement explicitly.

2. Correlation Structure at Shorter Distances

The form that the curves of Fig. VII-9 should take is subject to some conjecture. The empirical form of the correlation coefficient that was used for the synoptic scale data in

previous chapters has been, in simplified form, such as to give

$$\overline{\Delta_\ell^2} = 2\overline{u^2}(1 - e^{-r^2/2L^2})$$

and (4)

$$\overline{\Delta_t^2} = 2\overline{u^2}\left[1 - (1 - r^2/L^2)e^{-r^2/2L^2}\right]$$

where $\overline{u^2}$ is of no significance in detail but represents a mean square component standard deviation. The curves for this pair are shown by the dashed lines in Fig. VII-9, labeled k = 1.0. Obviously, they drop much too rapidly with decreasing distance. As shown previously, if these correlations are modified by introducing an "error" of observation, then they have a horizontal asymptote for small distance values. These are the dashed curves labeled k = 0.9 and k = 0.8 where k is a measure of the ratio of observation error to natural variability. Neither situation is tolerable.

The situation may be described in somewhat different terms by assuming that the wind components are made up of terms additively combined and independent of each other. Thus let

$$u = u_1 + u_2 + \text{---} + u_n$$

so that

$$\overline{uu'} = \overline{u_1 u_1'} + \overline{u_2 u_2'} + \text{---} + \overline{u_n u_n'}.$$

The cross product terms are all zero from the independence assumption. Then

$$r = k_1 r_1 + k_2 r_2 + \text{---} + k_n r_n$$

$$k_1 + k_2 + \text{---} + k_n \leq 1$$

where the k's are constant factors which depend on the relative

contribution of each term to the total one-point wind variability and the r's are the correlation coefficients for each term separately.

For example, suppose that the term in u_1 is due to the "synoptic scale" wind variability as above and that the u_2 term is due to smaller eddies with a correlation structure given by

$$e^{-r/D}$$

where D is a distance parameter that measures the size of the smaller eddies. Then the previous expressions become

$$\overline{\Delta_\ell^2} = 2\overline{u^2}(1 - k_1 e^{-r^2/2L^2} - k_2 e^{-r/D})$$

and* (5)

$$\overline{\Delta_t^2} = 2\overline{u^2}(1 - k_1(1 - r^2/L^2)e^{-r^2/2L^2} - k_2(1 - r/D)e^{-r/D})$$

The fit of this empirical form to the data points leaves something to be desired, but is better than the former alternatives. The main difficulty seems to be that the "shift" from the form of (4) to the form that would predominate at very small separations (where the slope of the curve is near unity) appears prominently in the empirical curves but does not appear in the data points.

---

* The form of the correlations in $\overline{\Delta_t^2}$ is associated with those in the expression for $\overline{\Delta_\ell^2}$ through the continuity equation. See Chapter V, Section B.

G. "MESO SCALE" EDDY STRUCTURE ALOFT

The data on $\overline{\Delta_\ell^2}$ and $\overline{\Delta_t^2}$ shown in Fig. VII-9 clearly indicate that the wind variability at two points is due to at least two factors, first a systematic eddy structure on the "synoptic" scale, i.e., to the traveling disturbances seen on the synoptic charts with an average size of near 600 n mi (as defined by the statistical wind parameter L) and, second, a "tapering off" into eddies of smaller scale and intensity. The Jet Stream data[1] clearly indicate the presence of these smaller scale eddies which are loosely called "meso scale" eddies here. Such eddies are of a size that would be undetected in the present network of rawinsonde observations except for their effect on a single station. The presence of such eddies is evident on the graphs of the Project Jet Stream data which appear in the data volumes. Exerpts from these graphs are shown in Figs. VII-10a and VII-10b.

In these figures, the top curve of data points represents the magnitude of the parallel wind component, the middle curve the perpendicular component, and the bottom curve the temperature (of no immediate concern here). The terms parallel and perpendicular are defined with respect to the direction of the maximum wind speed encountered during the flight. It is evident from the data points that there are small perturbations of the wind velocity components with a magnitude of a few knots and that these perturbations are not entirely random.

To obtain a closer look at the meso scale eddy structure shown in these figures, the "synoptic scale" wind was subtracted from the total wind. This was relatively easy to approximate in

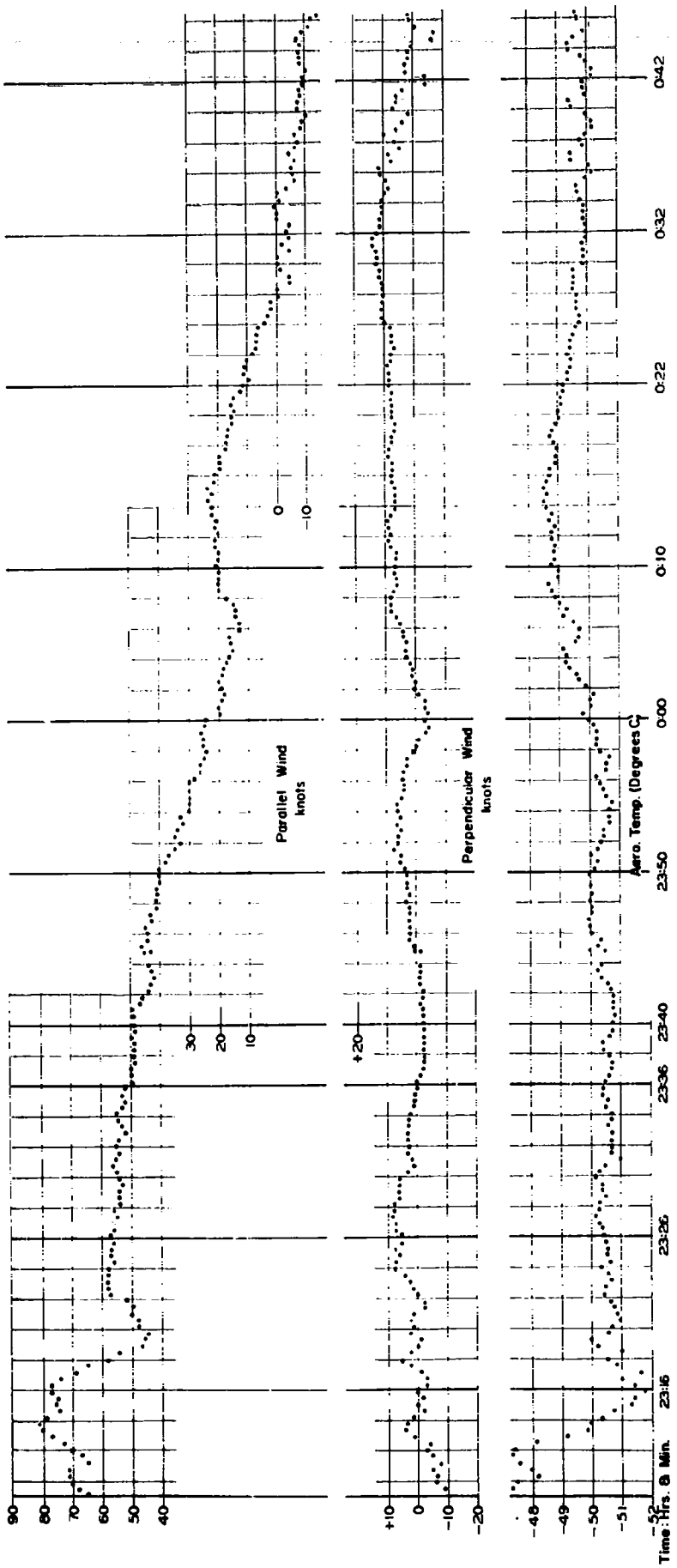

Fig. VII-10a. Wind Components and Temperature; JETNO 4 (Jet E22, Pressure Altitude 34,360 ft.)

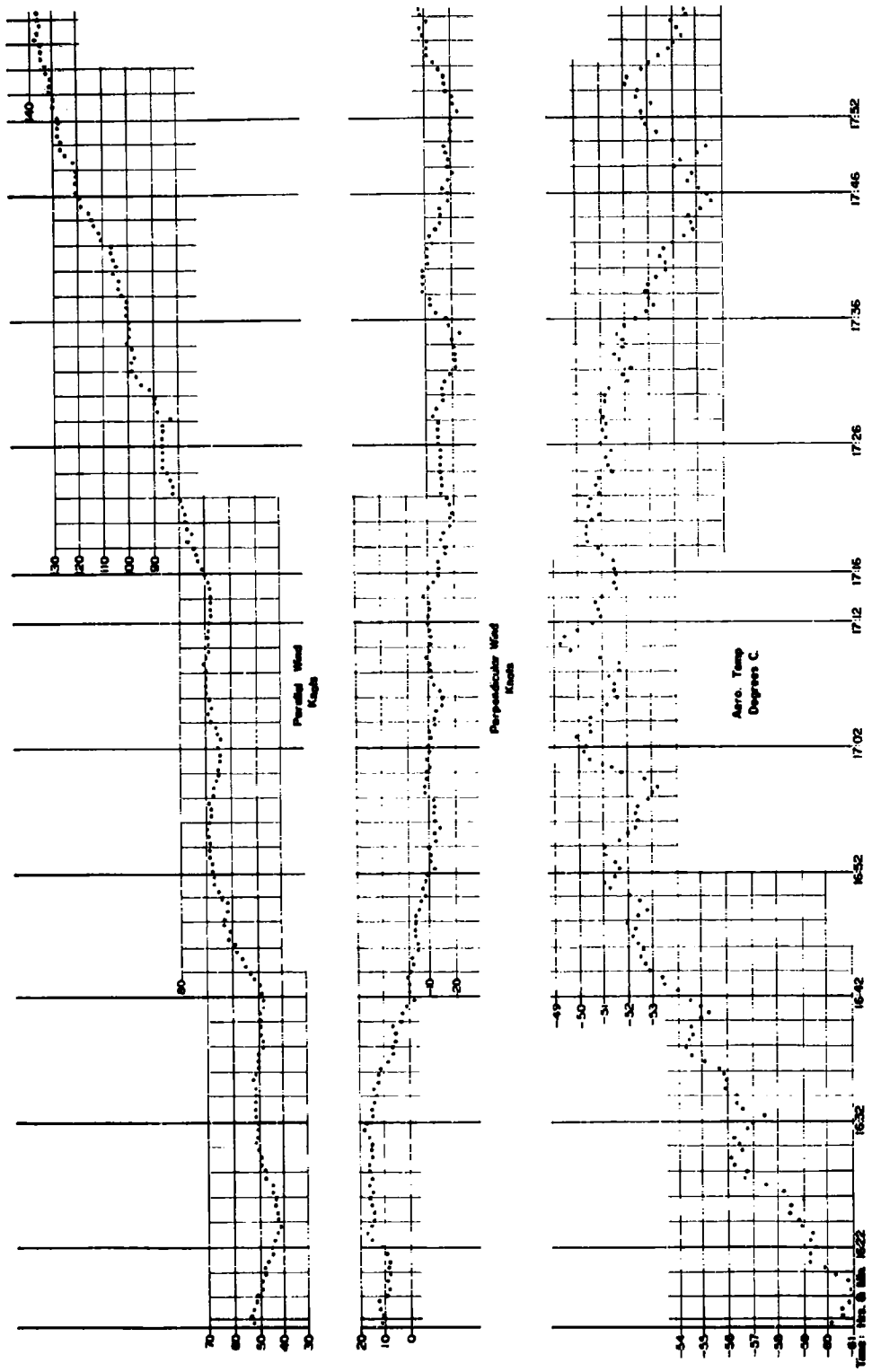

Fig. VII-10b. Wind Components and Temperature, JETNO 1 (Jet E.24, Pressure Altitude 35,720 ft.)

these cases. Each flight is of rather short duration so that it covers only a small part of a "disturbance" on the synoptic scale. Consequently, the synoptic scale wind for each component was approached by fitting the data for each wind component by a quadratic function of time. The residual wind components obtained when these fitted wind component values were subtracted from the observed values is considered as the meso scale wind component. The values of the meso scale eddy components for [illegible] are then given in terms of the parallel and perpendicular components. The organization of these residuals into a sequence of eddy vectors is readily evident.

The two time sequences of the eddy velocity components do not show the structure of the eddies to advantage. The residual values are replotted in Fig. VII-1 in the form of velocity vectors as a function of time along the flight path. The coordinates are rotated with the parallel component as the customary x-direction and the perpendicular component as the y-direction. The relative geographical area is shown in the lower left corner of the figure. The direction of the line of points along which the eddy vectors lie is that of the average heading. The length of the arrow shaft is proportional to the vector velocity, the arrow flies with the eddy wind. The points are spaced along the average flight path at equal intervals. No attempt was made to use real time as a co-ordinate since the departure from the average time interval between observations is quite small. The numbers at the end of each line across the page simply record the point number serially.

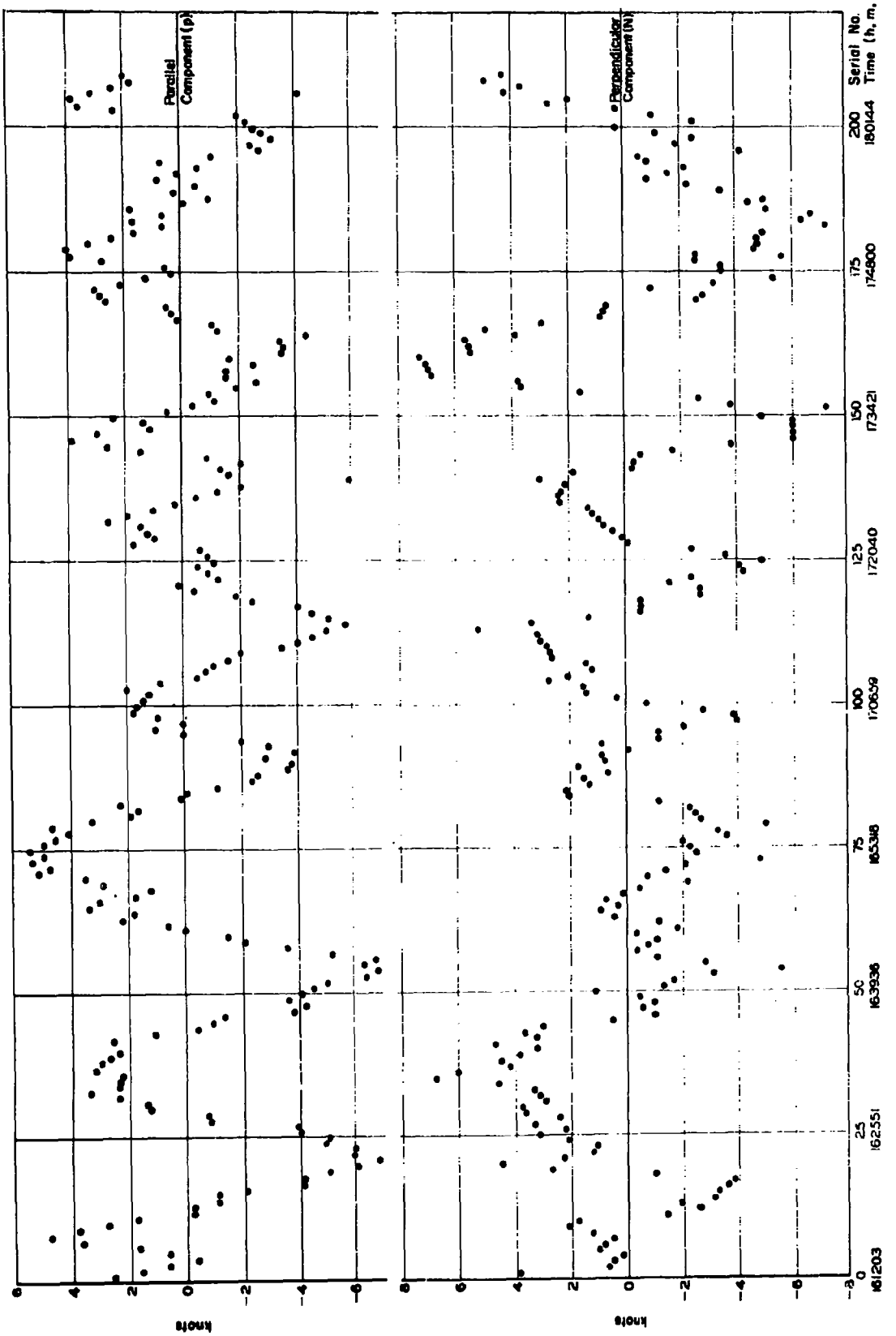

Fig. VII-11 Eddy Velocity Components, JETNO-1

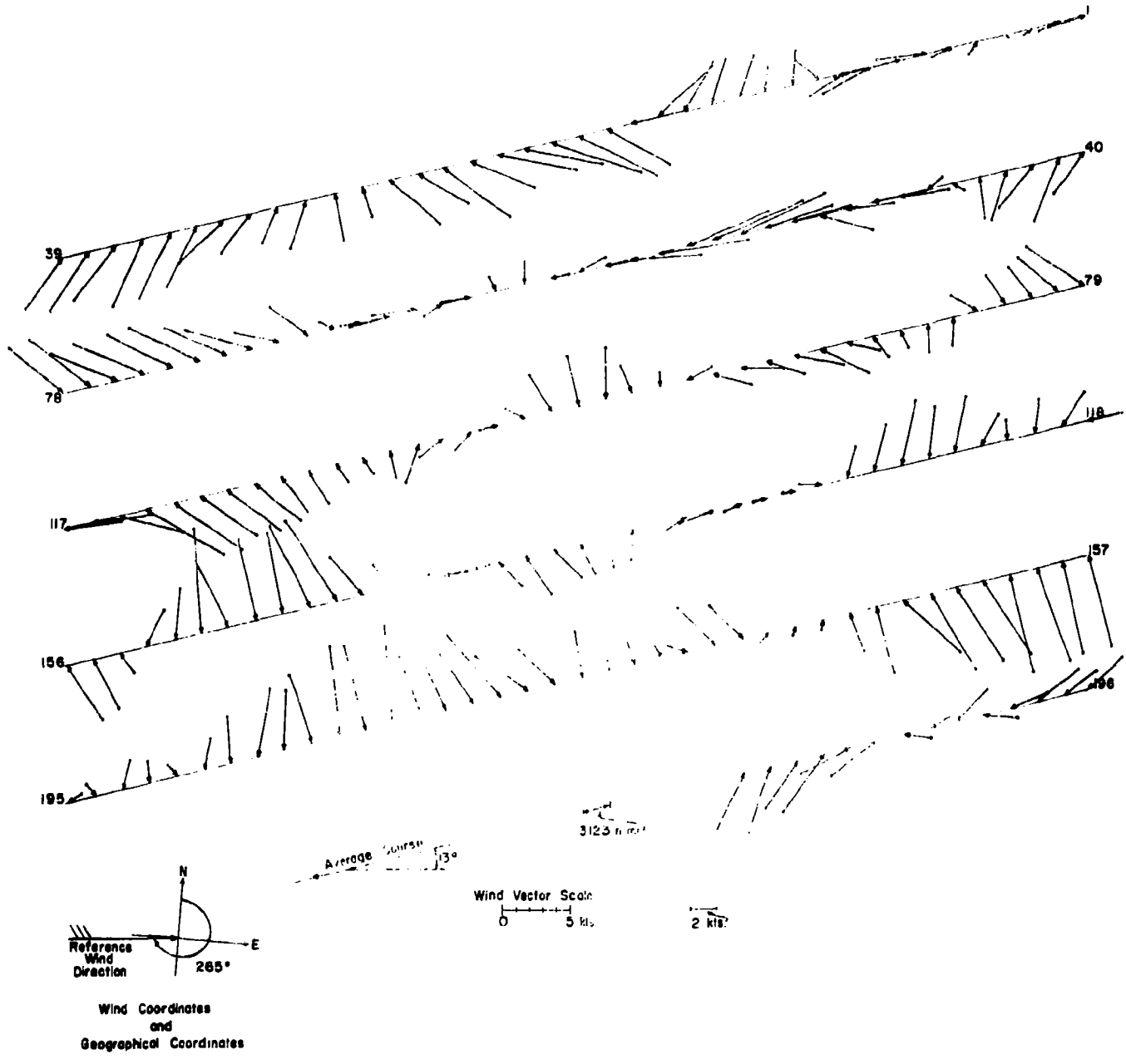

Fig. VII-12 Eddy Velocity Vectors, JETNO-1

These serial numbers and the corresponding time in hours, minutes, and seconds is shown as the abscissa in Fig. VII-11. Several sections are shown displaced vertically, simply to permit a scale large enough to show the eddies clearly but to keep the whole figure to reasonable dimensions.

The data values of Figs. VII-11 and VII-12 are carried somewhat beyond the real limits of accuracy of the tabulated data values. Wind component values were tabulated to the nearest knot while the values plotted in Fig. VII-11 are to the nearest tenth of a knot and those of Fig. VII-12 to the nearest half knot. The irregularities of the points in Fig. VII-12 clearly indicate this. It is also evident that the eddy velocities are of an order of magnitude greater than these irregularities.

The size of the eddies shown in Fig. VII-12 appears to be reasonably regular. By averaging the spacing between reversals of the eddy velocity with respect to the flight path, it amounts to approximately 13 time intervals or about 40 n mi. The magnitude of the eddy components appears to be 3 to 4 knots.

The eddy velocity correlation coefficients for the components of the velocity correlation tensor were computed for JETNO-1 through JETNO-5 and are illustrated in Fig. VII-13. The data itself in tabular form is contained in Appendix B-IV together with the means and standard deviations of the velocity components. (These correlation coefficients are <u>not</u> the same as those appearing in $\overline{\Delta_l^2}$ and $\overline{\Delta_t^2}$ discussed previously. The correlations that appear in such expressions involve the total wind as a

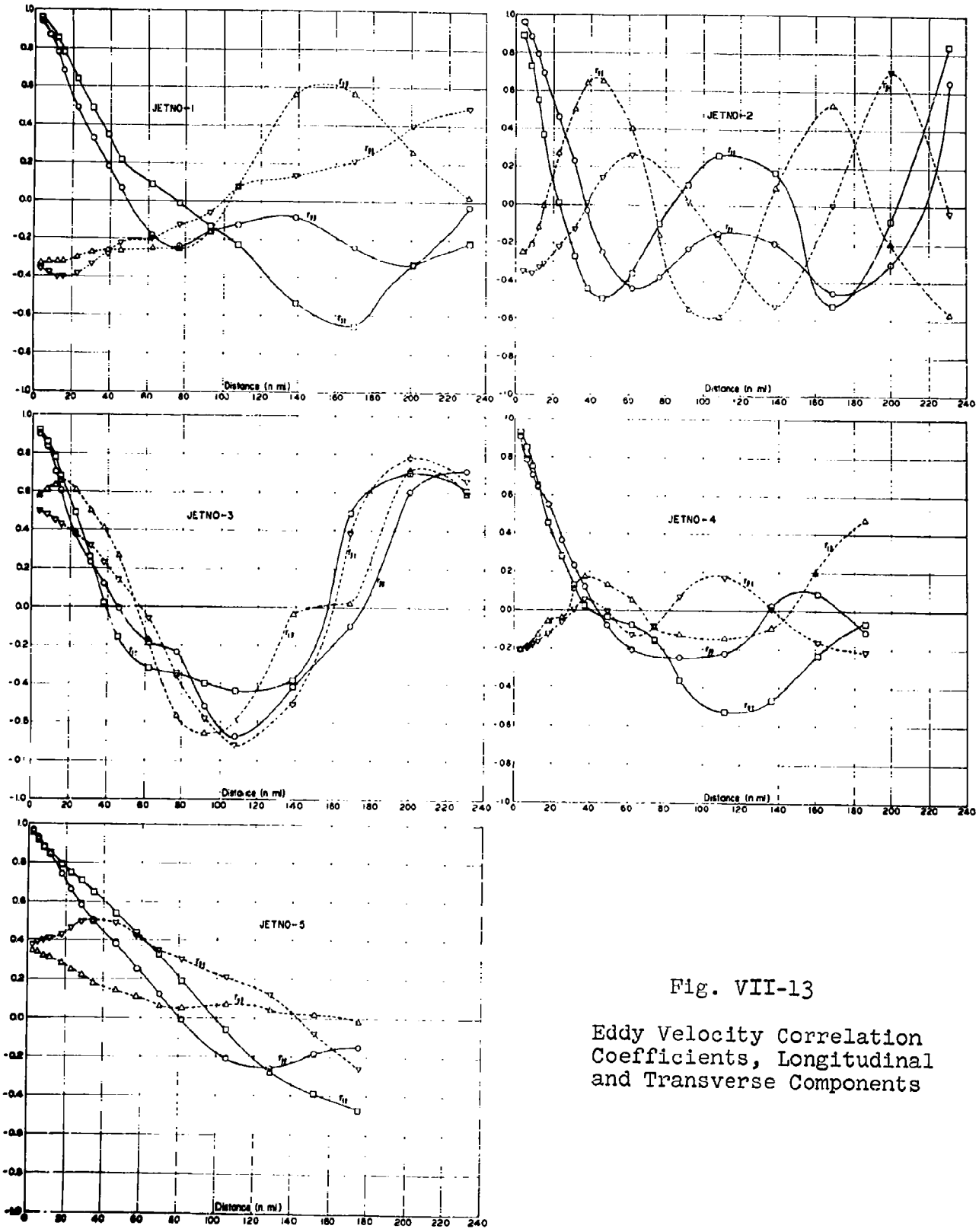

Fig. VII-13

Eddy Velocity Correlation Coefficients, Longitudinal and Transverse Components

function of distance while the correlations here discussed involve the meso scale eddy part of the total wind.)

There are several features in common in the five parts of Fig. VII-13. Some of these are:

i) Both $r_{\ell\ell}$ and r_{tt} decay from the value of unity at zero separation in an exponential manner.

ii) The value of $r_{\ell\ell}$ (as well as that of r_{tt}) decreases to negative values.

iii) Near zero separation, either $r_{\ell\ell}$ or r_{tt} may be the larger.

iv) The values of $r_{\ell\ell}$ and r_{tt} seem to oscillate, or tend toward such behavior for larger separations.

v) The values of $r_{\ell t}$ and $r_{t\ell}$ near zero distance may be appreciably different from zero.

vi) The values of $r_{\ell t}$ and $r_{t\ell}$ also tend to oscillate at larger distances.

Since the values of $r_{\ell t}$ and $r_{t\ell}$ are significantly different from zero, especially at zero distance, and since the values of the standard deviations of the longitudinal and transverse components were also appreciably different, the one-point frequency distribution of the eddy wind must be far from circularly normal. To test whether there was a preferential co-ordinate system oriented in the direction of the maximum eddy wind variability, the reference axes were rotated into this direction and the corresponding correlation coefficients computed. (The rotation was carried out in terms of the covariance forms so that it was not necessary to re-compute from the original data.) The results

are shown in Fig. VII-14 and the values are tabulated in Appendix B-IV together with the accessory quantities.

Since we have used terms and the subscripts corresponding to longitudinal and transverse to refer a co-ordinate system oriented along and at right angles to the two points concerned, the terminology associated with the components in Fig. VII-14 is changed. The terms parallel and normal to the direction concerned will be used and indicated by corresponding first letter subscripts. The six items characterizing the correlation coefficients of Fig. VII-13 are still valid for Fig. VII-14 with the exception of Item v). In place of Item v) above, the discussion of Fig. VII-14 would note that in those cases in Fig. VII-13 where $r_{tt} > r_{ll}$ ($r_{ll} > r_{tt}$) for small distances in Fig. VII-14, the relation is $r_{pp} > r_{nn}$ ($r_{nn} > r_{pp}$).

In discussing the structure characteristics, JETNO-5 will be discussed separately. The data in this case comes from a particularly long flight, the correlations are based on over 400 data pairs, and consequently the correlations represent a sample from a wide variety of conditions (summer). The data entering the correlations of JETNO-1 through JETNO-4 are from short flight legs and represent small samples of only a few eddies each (11 identifiable eddies in the case of JETNO-1, about half this number if a full "wave length" is considered to constitute an eddy).

The characteristics noted regarding the behavior of the correlation coefficients corresponding to the components of the

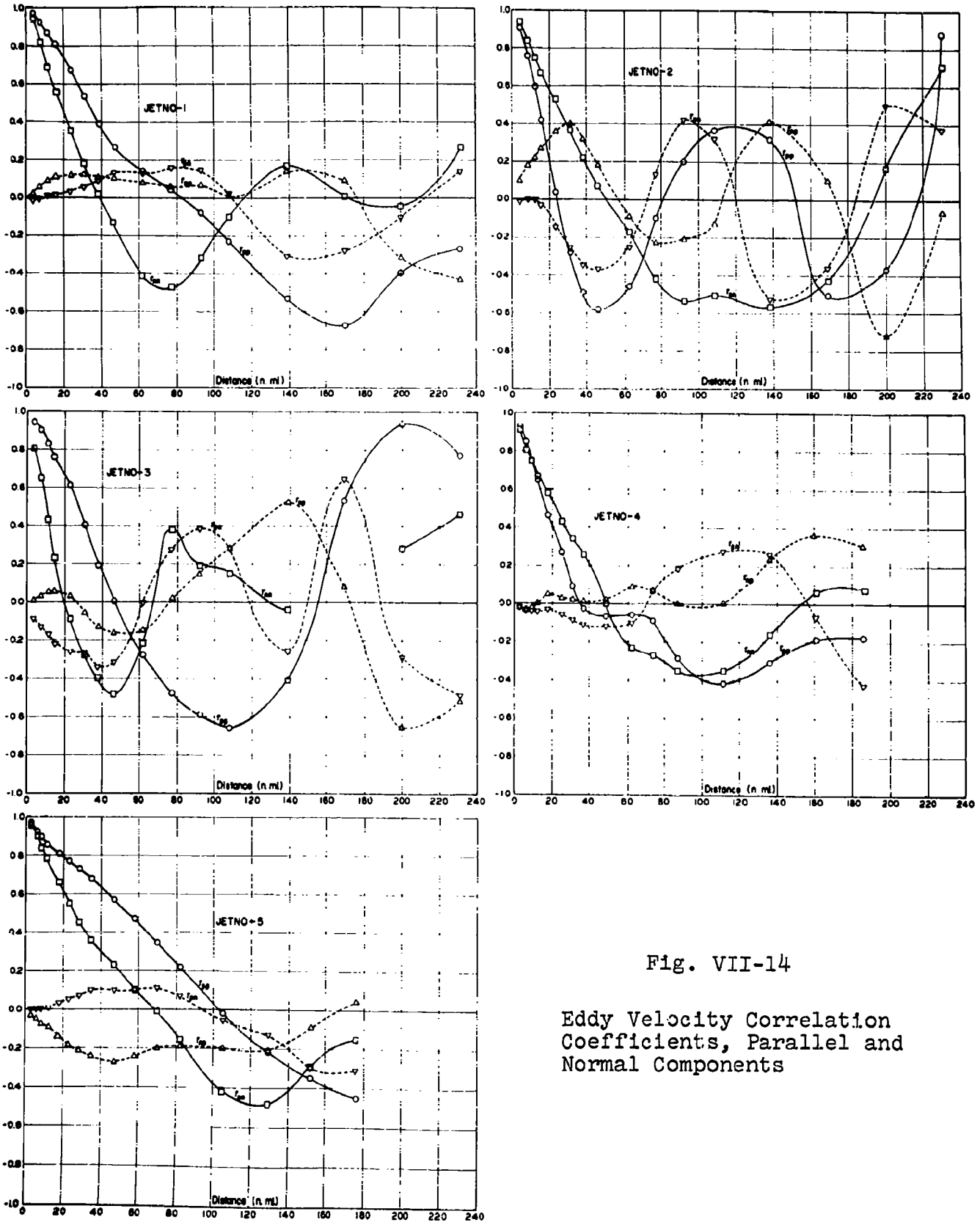

Fig. VII-14

Eddy Velocity Correlation Coefficients, Parallel and Normal Components

correlation tensor for eddy velocities imply several significant items regarding the kinematic structure of the eddy motions.

First, the fact that $r_{\ell t}$ and $r_{t\ell}$ were distinctly non-zero at zero distance and since σ_ℓ and σ_t are quite different, one would conclude that the eddy structures are strongly asymetrical. This is especially true since there was a greater difference between σ_p and σ_n.

Second, since $r_{\ell\ell}$ and r_{tt} (r_{pp} and r_{nn}) (and also the cross correlations) tend to oscillate, it would seem to indicate that eddies of alternate sense of rotation form a reasonably regular pattern (over relatively short distances).

Third, the more rapid decay of the value of r_{tt} as compared with $r_{\ell\ell}$ in discussing the synoptic scale eddies in the atmosphere is strictly the case for eddies with a stream function. If the eddy velocity were determined by a potential function of the same geometrical pattern, the roles of the velocity components would be interchanged. In such a case, the longitudinal component would decay more rapidly than the transverse. The correlations observed are some of one and some of the other type. From this it would seem reasonable to assume that the meso scale eddies are associated with local two dimensional divergence fields that are relatively much stronger than those associated with synoptic scale disturbances.

Fourth, if one uses the distance at which $r_{\ell\ell}$ or r_{tt} (or r_{pp} or r_{nn}) first reaches the zero value as a scale parameter, this scale appears to lie between 20 and 40 n mi.

The case of JETNO-5 is somewhat different from the first four, particularly in that the rate of decrease of correlation with distance is smaller. This would indicate a larger eddy size in general. This flight was made in summer and extended across the continent so that many more eddies were "sampled" under conditions quite different from the flights discussed above.

The effect of the time constant of the doppler navigator system, without doubt, affects the correlations at the smaller distances. In all cases (except JETNO-3 in parallel and normal components) the correlations of like components "pinch together" as the correlations approach 1. It is understood that the time constant of the doppler system is normally about 30 to 45 seconds but that for the flights concerned the value may have been especially reduced to near 15 seconds. Since the data readings were made about 30 seconds apart, the effect of the time constant of the system is without doubt present if the former is the case and is probably present if the latter were true.

REFERENCES:

1. Erdlich, R. M. and R. M. Rados, The Meteorological Measurements and Field Program of Project Jet Stream, Geophysical Research Papers No. 64, Geophysics Research Directorate, A.F.C.R.C., A.R.D.C., U.S.A.F., Bedford, Mass., October, 1959 (The data collections for each flight of Project Jet Stream are not referred to individually.)

CHAPTER VIII

APPLICATIONS

This chapter is devoted to a discussion of some applications of the ideas developed in the preceding chapters. It is not intended to be complete or exhaustive. The reader will, without doubt, have problems at hand to which application of the basic philosophy may be made, if not the specific results.

There are two basic ideas behind the applications which should be made explicit. These are:

1. In spite of the discussions of variation of parameters with season, level, etc., the correlation coefficients that appear are remarkably conservative. They have very nearly the same parameter values over the entire hemisphere (outside the tropics). Consequently, instead of speaking of correlations between properties at, say, Washington and Buffalo, it is possible to speak of correlations of these properties between any two points separated by a distance of 256 n mi and with an azimuth of the line joining them of 343°. Further, if reference directions are suitably chosen it may be possible to ignore the azimuth.

2. The correlation coefficients concerned deal with the properties of a continuum. Consequently, these correlation coefficients must have certain definite properties as functions of space and time separations. They are, for example, non-negative Hermitian functions; they are continuous except for a possible jump discontinuity at zero; etc.

This, of course, comes from the fact that the structure of the correlation coefficients reflect the basic dynamical characteristics of the atmosphere and insofar as these characteristics are unchanged in space and time, so is the structure of the correlation coefficients. In fact, to carry the case further, the correlation coefficients in normalized form do not reflect the background parameter variability which appears in the standard deviations (one-point variances) so that the space and seasonal variations of these basic variabilities may be handled separately.

A. EXTRAPOLATION FROM LIMITED DATA

The term extrapolation is used here in the sense of both extrapolation in space and in time. The term "forecasting" might well be used when extrapolation in time (or time and space) is involved. The forecasting techniques are, of course, the most elementary of the statistical type. For this reason, the term "forecasting" was not used.

1. Single Station

(a) The Basic Relations

In extrapolating information from a single station, an extension of the ideas presented in the preceding chapters is needed. This is the form of the correlation between wind and height on an isobaric surface. The empirical form of this correlation is

$$r_{h\ell} = 0$$

$$r_{ht} = -\frac{r}{L} e^{-r^2/2L^2}$$

where $r_{h\ell}$ = the correlation coefficient relating the height at P to the longitudinal wind component at P′ and r_{ht} = the correlation coefficient relating height as P to the transverse wind component at P′.

That this should be the form of these expressions, consider the geostrophic wind equations in the form

$$\lambda u'_{\ell} = -g\frac{\partial h'}{\partial y'}$$

$$\lambda u'_{t} = g\frac{\partial h'}{\partial x'}$$

where the x-direction is along PP′ and the y-direction is normal

PP′. Then

$$\lambda\overline{(hu'_\ell)} = -\,g\left(\overline{h\frac{\partial h'}{\partial y'}}\right),\quad \lambda\overline{(hu'_t)} = g\left(\overline{h\frac{\partial h'}{\partial x'}}\right).$$

On the right sides, we have (following Appendex A-I)

$$\left(\overline{h\frac{\partial h'}{\partial x'}}\right) = \frac{\partial\overline{(hh')}}{\partial x'} = \frac{\partial(\sigma\sigma' R_{hh})}{\partial x'} = \sigma\frac{\partial\sigma'}{\partial x'}R_{hh} + \sigma\sigma'\frac{\partial R_{hh}}{\partial r}$$

where $r = x' - x$ and it is assumed that R_{hh} is a function of r only (r = distance from P to P′). Further,

$$\left(\overline{h\frac{\partial h'}{\partial y'}}\right) = \frac{\partial(hh')}{\partial y'} = \sigma\frac{\partial\sigma'}{\partial y'}R_{hh}$$

since the y′ direction is perpendicular to the line PP′. If the approximation $R_{hh} = e^{-r^2/2L^2}$ is used, noting that

$$g\sigma_h/\lambda\sigma_u \cong g\sigma_h/\lambda\sigma_v \cong L,$$

and neglecting the gradient of the standard deviation of height, then one obtains the relation above.

In a like manner,

$$r_{\ell h} = 0$$
$$r_{th} = \frac{r}{L}e^{-r^2/2L^2}$$

where the correlations are between the longitudinal and transverse wind components at P and the height at P′.

The preceding relations may be used to extrapolate either wind components or height from a single observation. Thus, if one uses a simple regression form (standardized variables)

$$h' = a_1 u_1 + a_2 u_t + a_3 h,$$
$$u' = b_1 u_1 + b_2 u_t + k_3 h,$$
$$v' = c_1 u_1 + c_2 u_t + c_3 h,$$

then it follows at once* that

$$
\begin{aligned}
h' &= \left[(r/L)\exp(-r^2/2L^2)\right](u_t) + \left[\exp(-r^2/2L^2)\right](h), \\
u'_\ell &= \left[\exp(-r^2/2L^2)\right](u_\ell), \\
u'_t &= \left[(1 - r^2/L^2)\exp(-r^2/2L^2)\right](u_t) \\
&\quad + \left[(-r/L)\exp(-r^2/2L^2)\right](h).
\end{aligned} \tag{1}
$$

(b) Discussion

1) Extension of Geostrophic Relation

The preceding extrapolation relations are interesting in two ways. First, the correlation coefficients r_{ht} and r_{th} may be thought of as a statistical extension of the geostrophic wind equation. It is well known that the numerical value of the height of the isobaric surface does not provide information on wind and conversely. The geostrophic wind equation requires height gradient. On the other hand, every meteorologist knows that if the height of the isobaric surface is known, especially if it departs appreciably from normal, this information alone makes it possible to construct a rough picture of conditions throughout the surrounding area. This is possible through the correlations r_{th} and r_{ht} which are zero at zero separation but which attain a maximum of 0.607 at $r = L$. Thus, in estimating height, knowledge of the transverse wind contributes appreciably to the estimate and in

*Use is made of the correlations r_{hh}, $r_{\ell\ell}$, and r_{tt} which are obtained in the previous chapters.

estimating wind, knowledge of the height contributes much (in this case the most, just where the information on wind, r_{tt}, becomes zero).

ii) Reasonable and Silly Estimates

In the second place, it is a common misconception that a statistical forecast procedure only gives estimates that tend toward the mean and cannot give estimates indicating further departure from the mean. The first and last of the estimates above are examples to the contrary. Just how this comes about is readily seen in the case of the estimate for height, H'. This obviously arises from the first terms of a Taylor expansion of the height of the isobaric surface:

$$H' = H + \frac{\partial H}{\partial x}\Delta x + \text{---}$$

where $\frac{\partial H}{\partial x} = \frac{\lambda}{g}U_t$. If we divorce ourselves of physical ideas and put the emphasis on the observed quantities, one obtains the linear form

$$H' = a_1 H + a_2 U_t$$

where the coefficients a_1 and a_2 are to be determined from the usual statistical methods. The physical method amounts to extrapolation along the tangent to the isobaric surface in the direction concerned. This type of extrapolation is strongly limited in the range of distance used (Δx = r very small). If the distance is excessive, the resulting estimates are ridiculous. On the other hand, the statistical estimate based on the same relations also starts, for small Δx = r, estimating along

the tangent but departs therefrom and eventually estimates the mean value (zero in the case of standard variables). Thus, it may be said that the statistical estimate behaves like the physical estimate if not pushed too far and that in any case is prevented from giving silly answers (see Fig. VIII-1).

The estimate of height, H′, also provides an estimate of the location of the nearest High or Low. This is obtained by simply differentiating the expression for H′ with respect to distance, setting the result equal to zero, and solving for r. This involves only a simple quadratic in distance and may be solved graphically.

iii) Where the Variables are Located

The origin of the estimate for the transverse wind component is not immediately obvious. Were it to have come from a Taylor expansion, the first term in U_t would be present but the next term would have been $\partial U_t/\partial x$, a quantity not readily observed at a point. In place of $\partial U_t/\partial x$ there is the totally foreign term in height, H. To trace the origin of this term it is necessary to go back to the Taylor expansion of height in the "statistical" form

$$H' = a_1 H + a_2 U_t .$$

Note here that a_1 and a_2 are functions of the distance between P (where H and U_t are measured) and P′ (where H′ is estimated). Even in the standard Taylor expansion, where

$$a_1 \equiv 1,$$

$$a_2 = (\lambda/g)(\Delta x) = (\lambda/g)r,$$

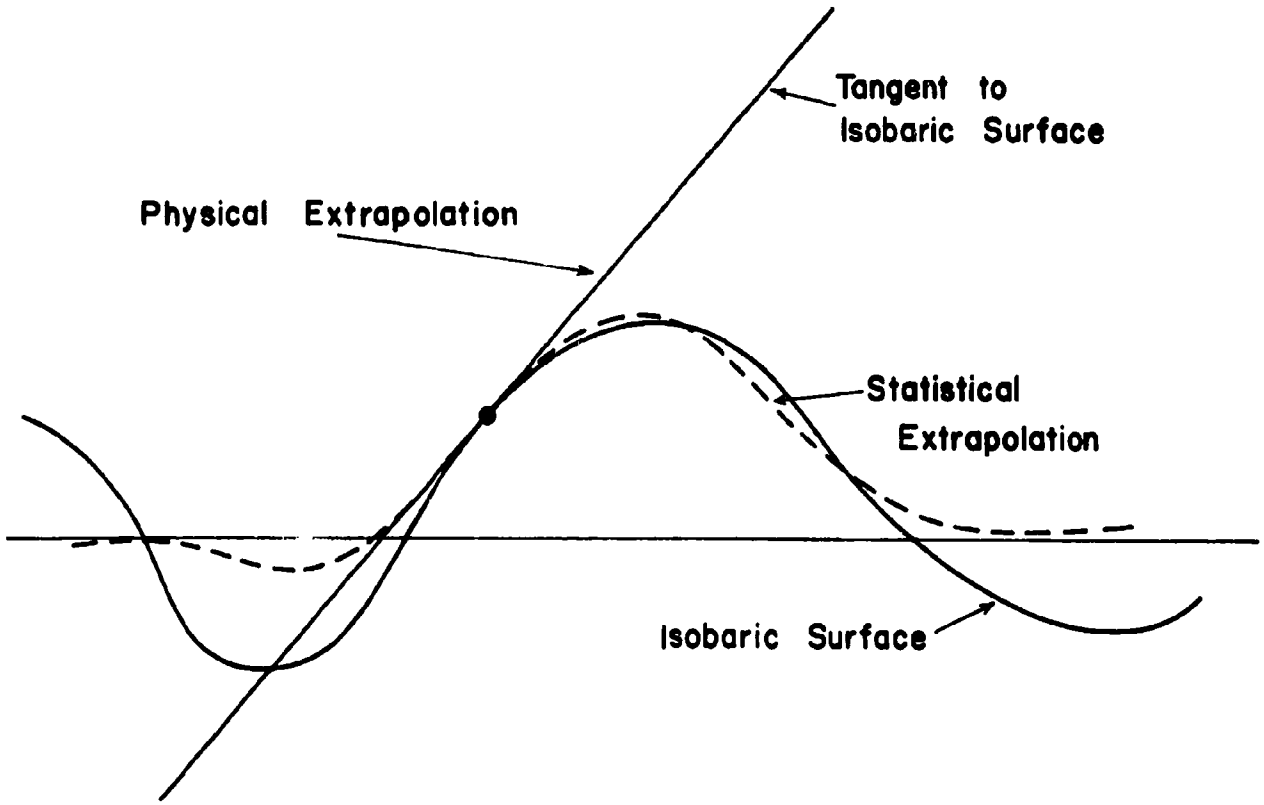

Fig. VIII-1 Physical vs. Statistical Extrapolation

these coefficients are the functions of the variables. When the expression is differentiated with respect to distance to obtain for the transverse wind component,

$$\frac{\lambda}{g}U_t' \cong \frac{\partial a_1}{\partial x}H + \frac{\partial a_2}{\partial x}U_t$$

and so, if new coefficients are introduced to simplify the relation, then

$$U_t' \cong b_1 H + b_2 U_t$$

and the same "observables" are retained. In the physical case, $\partial a_1/\partial x = 0$, which is not the case for a statistical extrapolation. If the extrapolation for height is differentiated with respect to distance, the extrapolation for transverse wind is obtained at once, except for a factor 1/L which would be eliminated in going to the standardized variables since $g\sigma_h/\lambda\sigma_{u_t} \cong L$.

(c) Refinements and Extensions

The simplified estimates of equation (1) using the empirical form of the correlation coefficients may be sharpened somewhat by including the terms in the gradient of the standard deviation of height. These terms were included in the derivation of the covariances from which the correlation coefficients came, but were dropped as being negligible. When this is done, the terms are no longer dependent on distance only, but also depend on the orientation of the line joining the point of observation, P, and the point of estimate, P'.

The time factor may also be included, but in this case it is necessary to go to a standard geographical co-ordinate reference system. Thus

$$h' = a_1 u + a_2 v + a_3 h, \text{ etc.}$$

The idealized correlations have been employed in the sense that when like properties are correlated, the coefficients approach unity as separation approaches zero. It would be more realistic to degrade these coefficients by multiplying by a factor slightly less than one to account for observation errors and small eddy effects.

2. Some Geometrical Problems

(a) A Weather Reconnaissance Problem

Suppose that there are observations of H at P_1, ---, P_n, equally spaced, all lying on a straight line. These data are to be used to estimate H′ at P′ by a linear regression (standardized variables)

$$h' = a_1 h_1 + \cdots + a_n h_n .$$

The normal equations are

$$\begin{aligned} r_{1y} &= a_1 + a_2 r_{12} + \cdots + a_n r_{1n} \\ r_{2y} &= a_1 r_{21} + a_2 + \cdots + a_n r_{2n} \\ &\cdots \qquad\qquad \cdots \\ r_{ny} &= a_1 r_{n1} + a_2 r_{n2} + \cdots + a_n \end{aligned}$$

where r_{yi} is the correlation coefficient between h′ and h_i and r_{ij} is that between h_i and h_j ($r_{ij} = r_{ji}$). The coefficients are given by

$$Ma_i = \begin{vmatrix} 1, & r_{12}, & \cdots, & r_{1(i-1)}, & r_{1y}, & r_{1(i+1)}, & \cdots, & r_{1n} \\ r_{21}, & 1, & \cdots, & r_{2(i-1)}, & r_{2y}, & r_{2(i+1)}, & \cdots, & r_{2n} \\ \cdots & & & & \cdots & & & \cdots \\ r_{n1}, & r_{n2}, & \cdots, & r_{n(i-1)}, & r_{ny}, & r_{n(i+1)}, & \cdots, & 1 \end{vmatrix}$$

where M is the determinate of coefficients

$$M = \begin{vmatrix} 1 , & r_{12}, & ---, & r_{1n} \\ r_{21}, & 1 , & ---, & r_{2n} \\ r_{n1}, & r_{n2}, & ---, & 1 \end{vmatrix}$$

Now let $r_{ij} = \exp\left[-(j-i)^2d^2/2L^2\right]$ where d is the distance between successive points along the line and let P′ be a distance D from the line and opposite point P_j (see Fig. VIII-2), then

$$r_{jy} = \exp\left\{-\left[D^2 + (j-i)^2d^2\right]/2L^2\right\},\ r_{ij} = \exp\left[-D^2/2L^2\right].$$

Thus if j = i, then the column of elements r_{jy} is the same as r_{ij} in M except for the factor $\exp(-D^2/2L^2)$ and $a_j = \exp(-D^2/2L^2)$. If $j \neq i$, then the column of elements r_{jy} is a multiple $\exp(-D^2/2L^2)$ of another column and so $a_j = 0$.

Thus, the whole estimate of H′ at P′ is due to the observation at P_j and all other observations at the other points contribute nothing to the estimate of H′. It would appear that, as far as linear extrapolation of height of an isobaric surface is concerned, the usual system of weather reconnaissance may leave something to be desired.

(b) An Example from Time Series

The example above has its intrinsic properties based on the functional form of the correlation function. Another well-known example from time series analysis is the following. Consider the extrapolation of the value of H from a sequence of values

$$h' = a_1h_1 + a_2h_2$$

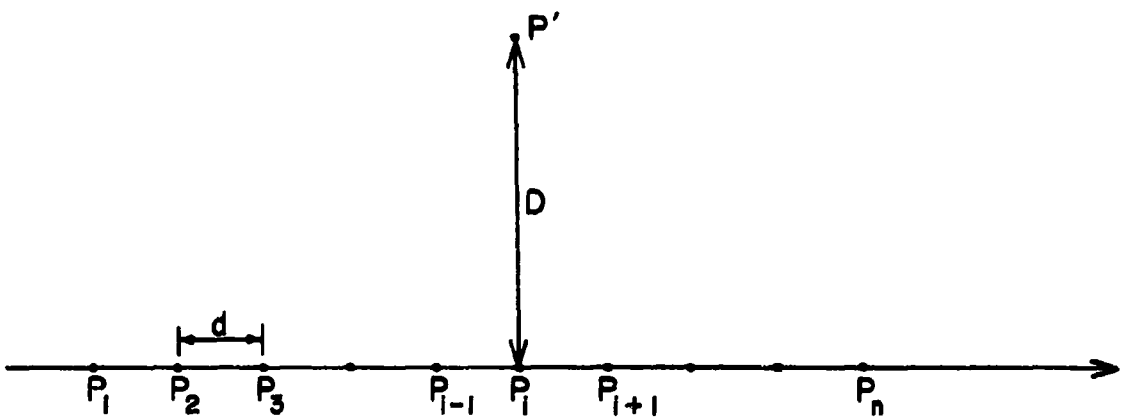

Fig. VIII-2 Geometrical Relations in the Weather Reconnaissance Problem

(standard variables). Then it is well known that the mean square error of estimate is given by

$$s^2 = 1 - a_1 r_{y1} - a_2 r_{y2} = \frac{1 - r_{12}^2 - r_{1y}^2 - r_{2y}^2 + 2r_{1y}r_{2y}r_{12}}{1 - r_{12}^2}.$$

Suppose, now, that

$$r_{12} = e^{-\beta T},$$
$$r_{1y} = e^{-\beta t},$$
$$r_{2y} = e^{-\beta(t+T)},$$

where t = time of estimate following of the observation h_1 and T = time elapsed between the observation h_2 and h_1. Then

$$s^2 = \frac{1 - e^{-2\beta T} - e^{-2\beta t} - e^{-2\beta(t+T)} + 2e^{-\beta(t+t+T+T)}}{1 - e^{-2\beta T}}$$
$$= 1 - e^{-2\beta t}$$

so that the whole estimate of h′ at t units after the observation h_1 is dependent on h_1 and the observation h_2 at T units prior to h_1 contributes no information to the estimate.

The above example has applications of great importance in the time sequence extrapolation of meteorological parameters. It has been proposed that the form of the time lag correlation of wind follows this functional form[1-3]. This form implies that for extrapolation purposes the latest observation contributes all of the available information. There is no doubt that the latest observation contributes by far the most information. From simply the philosophical point of view, i.e. to not close the door too soon, it would seem wise to require the greatest amount of proof before accepting such a correlation function.

The choice of the empirical function to represent the correlations is not a simple one. In Chapter V the problem was discussed in connection with the longitudinal and transverse correlation functions. The choice there was made on the basis of three properties; it must be reasonably simple, it must explain the correlations, and the functions for the longitudinal and transverse correlations must be related in a specific way. Several examples were given which adequately fulfilled the first and last conditions, but where they (all but one) failed was to estimate the minimum value of the transverse correlation coefficient which occurs at a considerable distance. The appearance of the correlation values for the longitudinal correlation coefficient when plotted as a function of distance strongly suggest the simple exponential decay law. In fact it is doubtful whether ordinary test for goodness of fit could distinguish between such a decay and the squared exponential decay selected. For this reason, others have used quite inconcistent empirical expressions in their attempts to fit the data to empirical formulas (Chapter V, references 2-4).

(c) Silent Area Problem

The two examples discussed above both lead to the same conclusion, that the "nearest" data point contributed all of the information to the estimate. The two problems, though they have the same answers, are basically quite different. What is going on will be explored in two dimensions in what might be called the Silent Area Problem.

Suppose that it is required to estimate H′ at P′, that an observation of H_1 at P_1 is available, that no observations may be made between P_1 and P′ (to eliminate the trivial case), and that one other observation of H_2 at P_2 may be made. Where is the best location for P_2 in the sense that the estimate of H′ by a linear regression on H_1 and H_2 has the least error? (See Fig. VIII-3.) In standard variables, the regression is

$$h' = a_1 h_1 + a_2 h_2$$

and the error of estimate (standardized) is

$$s^2 = \frac{1 - r_{12}^2 - r_{1y}^2 - r_{2y}^2 + 2r_{12}r_{1y}r_{2y}}{1 - r_{12}^2}, \qquad (2)$$

$$= 1 - r_{1y}^2 - \frac{(r_{2y} - r_{12}r_{1y})^2}{1 - r_{12}^2};$$

and

$$a_1 = \frac{r_{1y} - r_{12}r_{2y}}{1 - r_{12}^2},$$

$$a_2 = \frac{r_{2y} - r_{12}r_{1y}}{1 - r_{12}^2}.$$

Let $\overline{P_1P'} = D$, $\overline{P_1P_2} = d$, $\overline{P_2P'} = L$, angle $P'P_1P_2 = \theta$.

$$L^2 = d^2 + D^2 - 2Dd\cdot\cos\theta$$

i) <u>"Normal Law" Decay</u>

In the first instance assume that

$$r_{12} = e^{-\alpha^2 d^2/2},$$

$$r_{1y} = e^{-\alpha^2 D^2/2},$$

$$r_{2y} = e^{-\alpha^2 L^2/2},$$

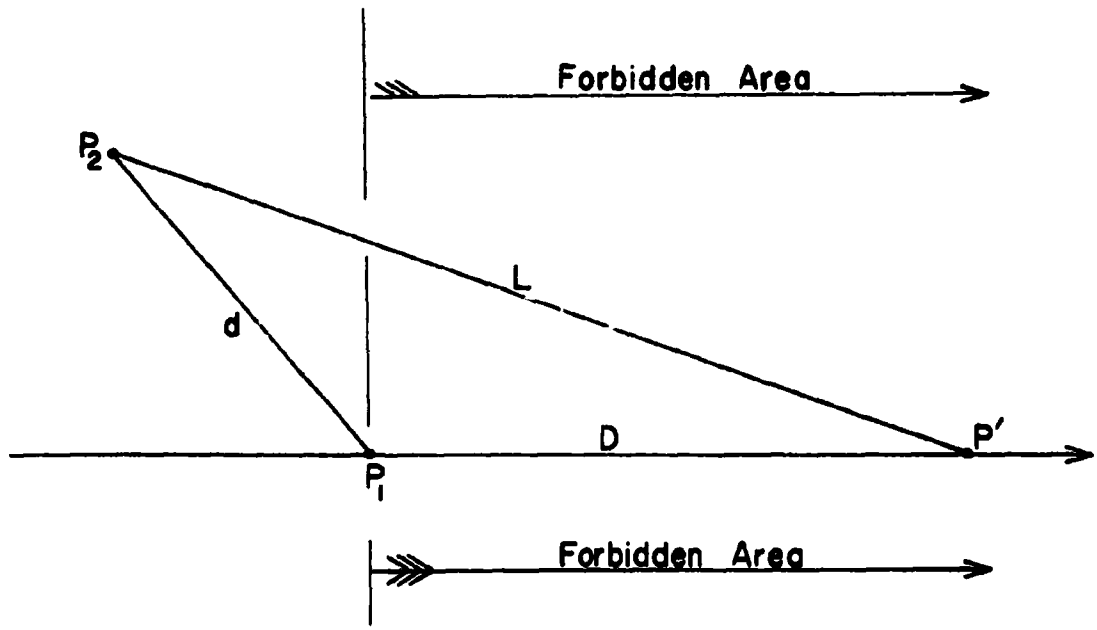

Fig. VIII-3 Geometrical Relations in the Silent Area Problem

(note that the L here is not the size parameter ($1/\alpha$) for which this letter was formerly used). Then

$$s^2 = 1 - e^{-\alpha^2 D^2} - \frac{e^{-\alpha^2(D^2+d^2)}\left(1 - e^{-\alpha^2 Dd\cdot\cos\theta}\right)^2}{1 - e^{-\alpha^2 d^2}}, \qquad (3)$$

$$a_1 = e^{-\alpha^2 D^2/2}\cdot\frac{1 - e^{-\alpha^2(d^2 - Dd\cdot\cos\theta)}}{1 - e^{-\alpha^2 d^2}},$$

$$a_2 = e^{-\alpha^2(D^2+d^2)/2}\cdot\frac{e^{+\alpha^2 Dd\cdot\cos\theta} - 1}{1 - e^{-\alpha^2 d^2}}$$

Along the line $\vartheta = \pm \pi/2$, $a_2 = 0$. This is the line through P_1 perpendicular to P_1P'. Along this line the information at P_2 contributes nothing to the estimate at P' (see section (a) above). On the circle $D\cdot\cos\vartheta = d$, the circle with P_1P' as diameter, P_2 is the closer to P' and consequently all of the estimate comes from P_2. This, however, is the trivial solution.

Consider P_2 lying on a circle of radius d about the point P_1. The factor $(1 - e^{\alpha^2 Dd\cdot\cos\vartheta})^2$ in the expression for s^2 takes on its largest value in the range $+\pi/2 < 0 < 3\pi/2$ (to exclude the trivial solution) when $\vartheta = \pi$. Thus s^2 is least and the smallest error of estimate occurs when P_2 lies on the line $P'P_1$ extended (beyond P_1). (Of course, the error of estimate is less if P_2 lies between P_1 and P', but this is the trivial case.)

ii) Simple Exponential Decay

Consider now the case in which

$$r_{12} = e^{-\beta d}, \quad r_{1y} = e^{-\beta D}, \quad r_{2y} = e^{-\beta L},$$

a simple exponential decay as a function of distance. Then

$$s^2 = 1 - e^{-2\beta D} - \frac{\left(e^{-\beta L} - e^{-\beta(D+d)}\right)^2}{1 - e^{-2\beta d}}.$$

It is at once apparent that the last term is zero when $L = D + d$; i.e. when P_2 lies on P_1P' extended. This is the line along which the observation at P_2 contributes nothing to the estimate at P' and the case corresponds to that in section (b). Let P_2 lie on a circle of radius d centered at P_1. Then from

$$L^2 = D^2 + d^2 - 2Dd\cdot\cos\vartheta = (D+d)^2 = 2Dd(1 + \cos\vartheta)$$

it is seen that as ϑ decreases from π to 0 the value of L decreases and consequently the contribution of the observation at P_2 is more and more effective in reducing the error of estimate at P_1. The decrease of ϑ is stopped at $\vartheta = \pi/2$ to avoid the trivial case. At $\vartheta = \pi/2$, the observation at P_2 makes its largest contribution to the estimate at P' (within the bounds imposed on the problem). Consequently, where the "normal law" decay contributes nothing the "simple exponential" decay contributes the most.

To summarize the situation, the answers to the best location of the second observation are exactly opposite to each other depending on whether the variation of the correlation coefficient is a "normal law" or "simple exponential" decay.

Idealized contours of the root mean square error of estimate are shown in Fig. VIII-4.

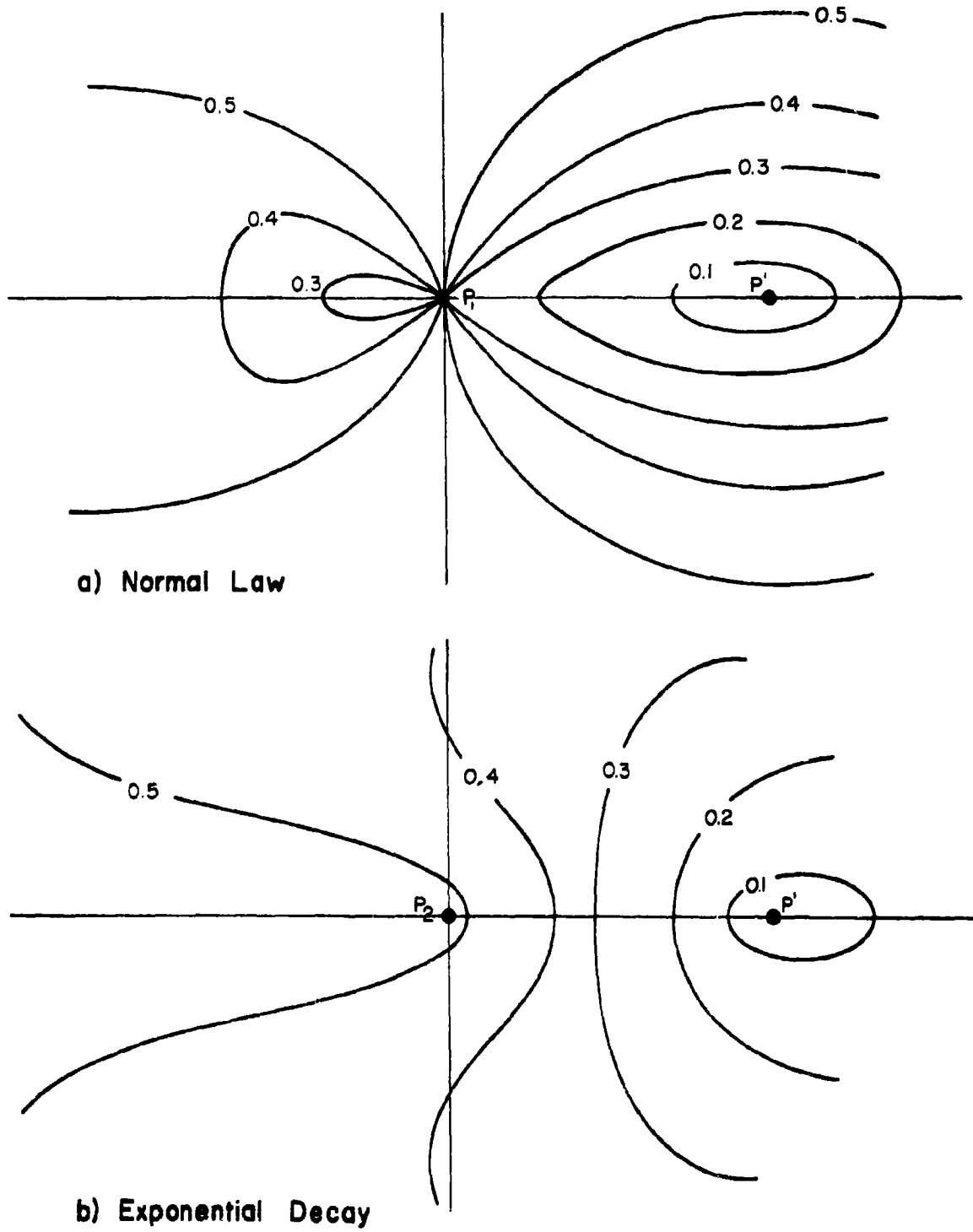

Fig. VIII-4 Contours of $\sqrt{s^2}$ (Schematic) in the Two Examples, k = 1

iii) Some Limit Relations

Equation (2) may be expressed in the form

$$s^2 = 1 - \frac{2r_{1y}r_{2y}}{1 + r_{12}} - \frac{(r_{1y} - r_{2y})^2}{1 - r_{1y}^2}.$$

Now consider $P_2 \rightarrow P_1$ and let

$$r_{2y} = r_{1y} + |\nabla r_{1y}| \cdot d \cdot \cos(\theta - \varphi) + ---$$

where $|\nabla r_{1y}|$ is the magnitude of the gradient of the correlation surface and φ is the direction of the gradient at P_1 (this correlation is thought of as centered at P') while θ is the azimuth of P_2 from P_1. Also let

$$r_{12} = 1 - C|d|^{\gamma} + ---$$

(this correlation surface is thought of as centered at P_1). Then

$$\lim_{d \to 0}\left(\frac{2r_{1y}r_{2y}}{1 + r_{12}}\right) = r_{1y}^2.$$

Now

$$\frac{(r_{1y} - r_{2y})^2}{1 - r_{12}^2} = \frac{|\nabla r_{1y}|^2 d^2 \cos^2(\theta - \varphi) + ---}{2C|d|^{\gamma} + ---}$$

so that

$$\lim_{d \to 0}\left(\frac{(r_{1y} - r_{2y})^2}{1 - r_{12}^2}\right) = \begin{cases} 0 & , \ 0 < \gamma < 2, \\ \dfrac{|\nabla r_{1y}|^2 \cos^2(\theta - \varphi)}{2C}, & \gamma = 2 \ . \end{cases}$$

It then follows that if the field of property (wind component, height of isobaric surface, etc.) is a differentiable function (γ=2), then the value of s^2 has a limit and this limit is less than the value for the case of only a single observation at P_1. If the field of property is not differentiable ($0 < \gamma < 2$), then the information provided by the additional observation at P_2 approaches zero as P_2 approaches P_1.

The situation described in the above is quite ideal. Even in the differentiable case (in the limit $P_2 \rightarrow P_1$) all that one has is two observations to average and thus, perhaps, reduce the error of observation a little. The mathematical formulation above is valid only if it is considered possible to measure gradients with infinitely close observations.

Note that the limit for $\gamma = 2$ is a function of $(\theta - \varphi)$, the orientation of the line $P_1 P_2$ with respect to the line $P_1 P'$. The function s^2 is then discontinuous at the point P_1 and the function value there may range from $1 - r_{1y}^2$ to $1 - r_{1y}^2 - |\nabla r_{1y}|^2$ depending on the direction in which P_2 approaches P_1. If this is along the gradient of the correlation surface, the smaller value is obtained; if perpendicular to the gradient, the larger value is the limit. This corresponds to the directions of maximum and no additional information in part (i) above and generalizes the analysis there into the case where the contours of the correlation surface need not be circular.

Consider the coefficients a_1, a_2 as $P_2 \rightarrow P_1$. Then

$$a_1 = \frac{r_{1y} C|d|^\gamma - |\nabla r_{1y}| \cdot d \cdot \cos(\theta - \varphi) + \cdots}{2C|d|^\gamma + \cdots}$$

$$a_2 = \frac{r_{1y} C|d|^\gamma + |\nabla r_{1y}| \cdot d \cdot \cos(\theta - \varphi) + \cdots}{2C|d|^\gamma + \cdots}$$

so that

$$\lim_{d\to 0}\begin{cases} a_1 = -\infty, & = \frac{r_{1y}}{2}, \\ \theta \neq \varphi \pm \frac{\pi}{2}, & \theta = \varphi \pm \frac{\pi}{2},\ 1 < \gamma \leq 2, \\ a_2 = +\infty, & = \frac{r_{1y}}{2}, \end{cases}$$

$$\lim_{d\to 0}\begin{cases} a_1 = \frac{r_{1y}}{2} - \frac{|\nabla r_{1y}|\cos(\theta-\varphi)}{2C}, \\ \\ a_2 = \frac{r_{1y}}{2} + \frac{|\nabla r_{1y}|\cos(\theta-\varphi)}{2C}, \end{cases} \qquad \gamma = 1 \ ,$$

$$\lim_{d\to 0}\begin{cases} a_1 = \frac{r_{1y}}{2}, & = 0 \ , \\ \theta = \omega \ , & \theta \neq \omega \ , \ 0 < \gamma < 1. \\ a_2 = \frac{r_{1y}}{2}, & = 0 \ , \end{cases}$$

The behavior of the coefficients is highly dependent on the direction of approach, θ, and on the value of γ. The most irregular behavior occurs in exactly the case of most interest, $\gamma = 2$, $\theta = \omega$, $\omega + \pi$.

The reason for this behavior is seen by rearranging the terms of the regression into

$$h' = (a_1+a_2)h_1 + (a_2 d)\frac{h_2-h_1}{d}$$

and nothing that

$$a_1 + a_2 = \frac{r_{1y}|d|^{\gamma} + \cdots}{|d|^{\gamma} + \cdots},$$

$$a_2 d = \frac{|\nabla r_{1y}|d^2\cos(\theta-\varphi) + r_{1y}C|d|^{\gamma+1} + \cdots}{2C|d|^{\gamma} + \cdots}$$

Then

$$\lim_{d\to 0}(a_1+a_2) = r_{1y}, \ 0 < \gamma \leq 2$$

while

$$\lim_{d\to 0}(a_2 \cdot d) = \frac{|\nabla r_{1,\gamma}|}{2C}\cos(\theta-\omega), \quad \gamma = 2,$$
$$= 0, \quad 1 < \gamma < 2.$$

In the limit, the second term of the regression pertains to the directional derivative of the field of property in the direction P_1P_2 while the first term still pertains to the property itself at P_1

$$h' = b_1 h_1 + b_2\left(\frac{\partial h_1}{\partial d}\right)$$

where

$$b_1 = \lim_{d\to 0}(a_1 + a_2), \quad b_2 = \lim_{d\to 0}(a_2 \cdot d).$$

Then $b_1 = r_{1,\gamma}$, $b_2 = 0$ for $0 < \gamma < 2$ so that the situation is unchanged from that considered originally, i.e., for a non-differentiable field of property, the measurement of a property gradient $(\partial h_1/\partial d)$ contributes nothing to the estimate at P'. For $\gamma = 2$, then $b_1 = r_{1,\gamma}$ and $b_2 = (|\nabla r_{1,\gamma}|/2C)\cos(\theta-\omega)$ from which it follows that for a field of differentiable property the estimate at P' is improved by the measurement of the directional derivative of property and that the amount of improvement of the estimate at P' is dependent on the direction in which the derivative is measured, a maximum if on line P_1P', and zero in the direction perpendicular to P_1P'. In the process of taking the preceding limits, explicit expressions for the regression coefficients have been derived for the case of a differentiable field of property in terms of the characteristics of the correlation function of this property.

iv) Observations with Errors

The material in the preceding section is of theoretical interest but the conclusions are not particularly helpful. The relations do tell that, for example, if we are to estimate height at P′ from height at P_1, it would be better to measure the wind component perpendicular to P_1P' at P_1 than make another height measurement anywhere. On the other hand if the field of property is wind component, we cannot measure wind component gradient and the conclusions are silly because as P_2 approaches P_1 the difference in wind component becomes lost in the error of observation or the effect of small scale eddies. To consider these effects, the correlations are degraded by a factor k, $0 < k < 1$ which measures the effect of such "errors". Then (2) becomes

$$s^2 = 1 - k^2 r_{1y}^2 - \frac{k^2(r_{2y} - k r_{12} r_{1y})^2}{1 - k^2 r_{12}^2},$$

$$= 1 - \frac{2k^2 r_{1y} r_{2y}}{1 + k r_{2y}} - \frac{k^2(r_{1y} - r_{2y})^2}{1 - k^2 r_{12}^2},$$

and

$$a_1 = \frac{k(r_{1y} - k r_{12} r_{2y})}{1 - k^2 r_{12}^2},$$

$$a_2 = \frac{k(r_{2y} - k r_{12} r_{1y})}{1 - k^2 r_{12}^2},$$

where the correlation coefficients are still the "theoretical" ones (i.e. without "errors" of observation considered). In the limit as $P_2 \to P_1$ there are no indeterminate expressions and the

relations are

$$s^2 \to 1 - \frac{2k^2}{1+k} r_{1y}^2,$$

$$a_1 \to \frac{k}{1+k} r_{1y},$$

$$a_2 \to \frac{k}{1+k} r_{1y},$$

so the limiting form of the regression is

$$h' = \frac{2k}{1+k} r_{1y} \left(\frac{h_1 + h_2}{2} \right)$$

where h_1 and h_2 are two <u>independent</u> measures at P_1.

The best location of P_2 would minimize s^2 or maximize the term

$$F = \frac{(r_{2y} - k r_{12} r_{1y})^2}{1 - k^2 r_{12}^2}$$

in which the co-ordinates of P_2 appear. To determine the location of P_2 requires a detailed knowledge of the correlation functions concerned. Consequently, the specific examples will be used.

For the "normal law" correlation surface

$$F = F_n = \left[e^{-\alpha^2 L^2/2} - k e^{-\alpha^2 (D^2+d^2)/2} \right]^2 / \left(1 - k^2 e^{-\alpha^2 d^2} \right)$$

$$= e^{-\alpha^2 (D^2+d^2)/2} \left[e^{\alpha^2 D d \cdot \cos\theta} - k \right]^2 / \left(1 - k^2 e^{-\alpha^2 d^2} \right).$$

There will be a line along which $F_n = 0$ given by

$$d \cdot \cos\theta = \frac{\log k}{\alpha^2 D}.$$

This line will be perpendicular to $P_1 P'$ and will cut it a distance $|\log k|/\alpha^2 D$ from P_1 on the side opposite P'. This corresponds to the line through P_1 perpendicular to $P_1 P'$ in the case of $k = 1$. It is the line along which an observation at P_2

contributes no information to the estimate at P′ in addition to that given by the observation at P_1. The point at $\theta = \pi$ where this line intersects P_1P' may be thought of as a point where the errors of observation bring about so much error in estimating the derivative of property that this part of the estimate cancels the advantage of using two independent observations instead of one.

The quadratic term in the expression for F_n (for fixed d) will be a maximum when $\theta = 0$ or π. We consider only $\theta = \pi$ since for $\theta = 0$, P_2 lies between P_1 and P′. Then

$$F_n(d,\pi) = e^{-\alpha^2(D^2+d^2)/2}\left[e^{-\alpha^2 Dd} - k\right]^2/\left(1 - k^2e^{-\alpha^2d^2}\right)$$

and

$$\frac{\partial F_n}{\partial d} = -\frac{\alpha^2 e^{-\alpha^2(D^2+d^2)/2}(e^{-\alpha^2Dd} - k)}{\left(1 - k^2e^{-\alpha^2d^2}\right)^2} \times$$

$$\times \left[d\left(e^{-\alpha^2Dd} - k\right)\left(1 + k^2e^{-\alpha^2d^2}\right) + 2De^{-\alpha^2Dd}\left(1 - k^2e^{-\alpha^2d^2}\right)\right].$$

The best location for P_2 is given by the zero of the factor in square brackets above. This root (located on P_1P' extended) is a true minimum of s^2, a <u>best</u> location for P_2 (see Fig. VIII-5).

In the simple negative exponential form of the correlation surface

$$F = F_e = \frac{\left[e^{-\beta L} - ke^{-\beta(D+d)}\right]^2}{1 - k^2e^{-2\beta d}}$$

where $L^2 = D^2 + d^2 - 2Dd\cdot\cos\theta$. It is seen at once that the numerator of F_e can now never be zero since $L \leq D+d$ and the first term will always be greater than the second term. Consequently, a second observation point even on P_1P' extended will

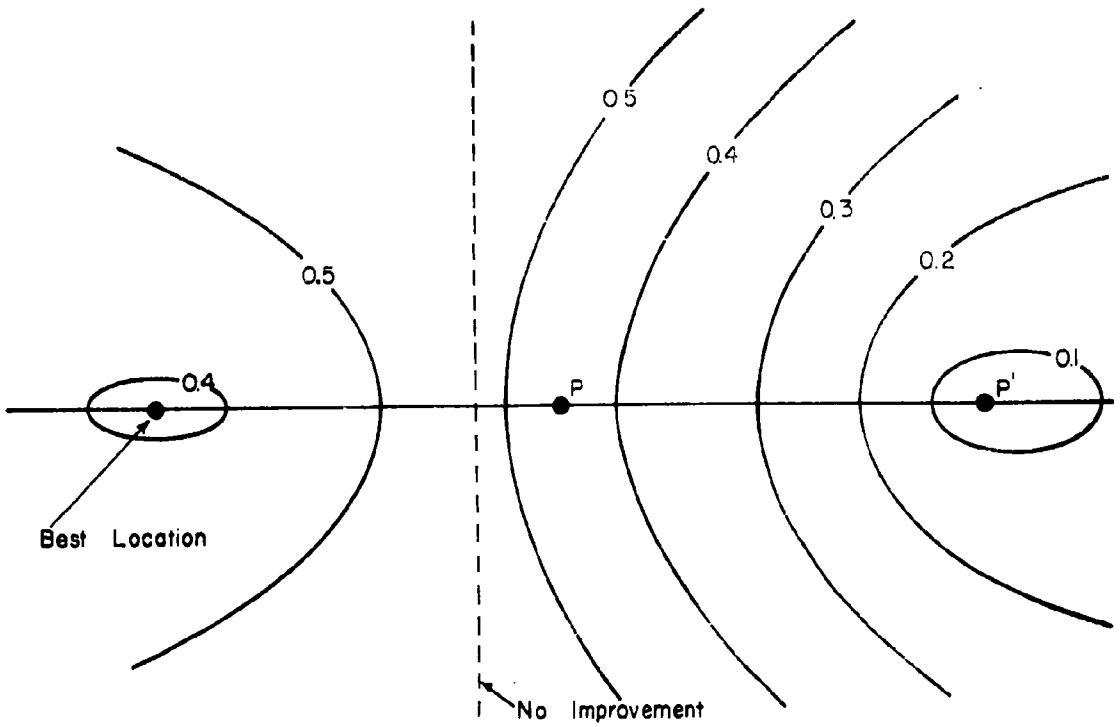

a) Normal Law

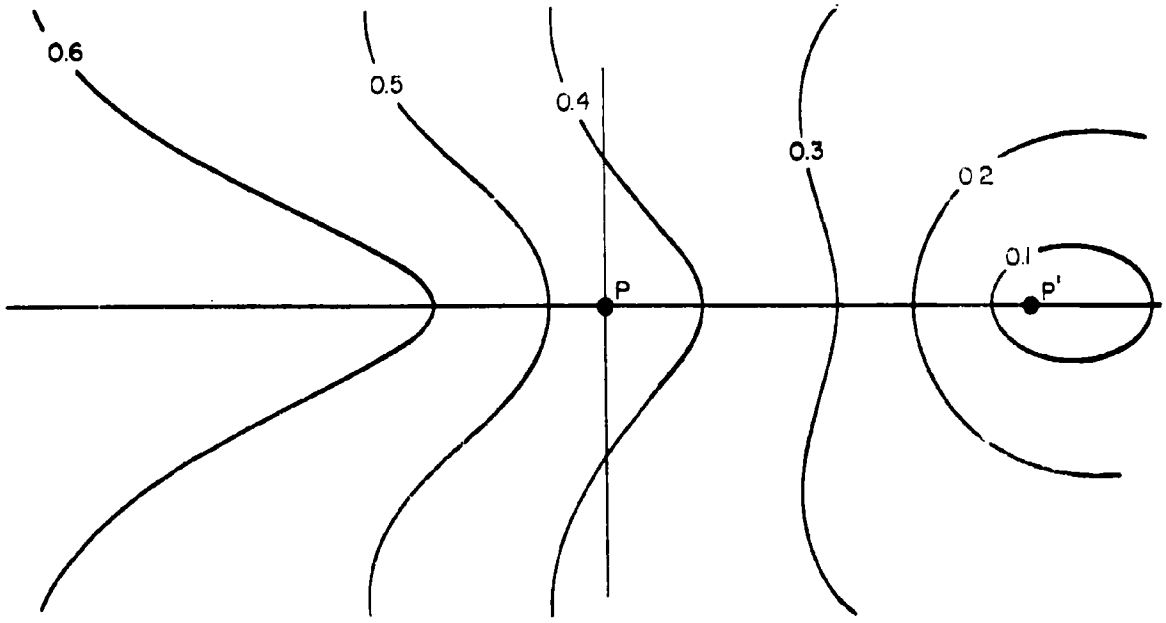

b) Exponential Decay

Fig. VIII-5 Contours of $\sqrt{s^2}$ (Schematic) in the Two Examples, $k < 1$

provide some additional information to improve the estimate at P′. However, the line $P_1 P'$ remains the worst location for a second observation point only now, as P_2 recedes from P_1, the value of s^2 increases from $1 - 2k^2 r_{1,}/(1+k)$ at P_1 to $1 - k^2 r_{1,}$ at large distances.

The situation is shown graphically in Fig. VIII-5 where figures corresponding to those of Fig. VIII-4 are shown but in which $k < 1$. In Fig. VIII-5a it is seen that the knot point at P_1 is no longer present and that the loops that extended to the left of P_1 are now replaced by a center where the estimate at P′ is best. In Fig. VIII-5b the geometrical situation is more or less unchanged as compared with Fig. VIII-4b. Instead of a ridge of constant value for the error of estimate extending to the left of P′ the "ridge" has become somewhat "sloping".

In the case of Figs. VIII-4b and VIII-5b there the line $P_1 P_2$ perpendicular to $P_1 P'$ contains two points (one on each side of P_1) where the location of P_2 is best. This location has not been discussed.

B. WIND SHEAR VECTOR CORRELATIONS

The part of the vertical wind shear that is due to the synoptic scale variability of wind may be obtained from the geostrophic wind shear equations in the form

$$\lambda s_x = \lambda \frac{\partial u}{\partial z} = - \frac{g}{T_o} \cdot \frac{\partial T}{\partial y},$$

$$\lambda s_y = \lambda \frac{\partial v}{\partial z} = \frac{g}{T_o} \cdot \frac{\partial T}{\partial x}.$$

Where T_o is the temperature of the standard atmosphere at the level where the height increment is measured (assumed constant in the horizontal).

These relations are identical to the geostrophic wind equations with the exception that g/T_o now replaces g and temperature now replaces height of the isobaric surface. Note that x and y are to be measured on the isobaric surface so that the gradient of temperature is not in the true horizontal.

These relations may be used to construct the components of the wind shear correlation tensor in terms of temperature correlations in exactly the same way that components of the wind correlation tensor were expressed in terms of the height correlations.

The standard deviations of the wind shear correlations may be expressed as[4]

$$\lambda^2(\overline{s_x^2}) = \left(\frac{g}{T_o}\right)^2\left[|\nabla\sigma_T|^2\sin^2\psi + 2(b_1 + b_2\sin^2\theta_o)\sigma_T^2\right],$$

$$\lambda^2(\overline{s_y^2}) = \left(\frac{g}{T_o}\right)^2\left[|\nabla\sigma_T|^2\cos^2\psi + 2(b_1 + b_2\cos^2\theta_o)\sigma_T^2\right],$$

$$\lambda^2(\overline{s_x s_y}) = -\left(\frac{g}{T_o}\right)^2\left[|\nabla\sigma_T|^2\sin\psi\cos\psi + 2b_2\sin\theta_o\cos\theta_o\right],$$

$$\lambda^2(\overline{s_x^2} + \overline{s_y^2}) = \left(\frac{g}{T_o}\right)^2\left[|\nabla\sigma_T|^2 + \frac{2\sigma_T^2}{L_T^2}\right],$$

where it has been assumed that the temperature correlation function on an isobaric surface may be written in the form

$$R_{TT} = 1 - \left[b_1 + b_2\cos^2(\theta-\theta_o)\right]r^2 + \text{---}$$

where θ is the orientation of P′ with respect to P and r is the distance PP′. The parameter, L_T, is a size parameter which measures the average dimensions of temperature systems on an isobaric surface ($L_T^{-2} \cong 2b_1$).

The above relations have not been used to estimate the standard deviation of the wind shear component due to the fact that data on the temperature correlations are not generally available. If the structure of the temperature correlations in the horizontal were known, the information provided would be useful.

The relations are not as complex as they appear since they contain several small terms. The value of $|\nabla\sigma_T|$ is reasonably small and the value of b_2 may also be small. In the later case,

this amounts to the assumption that two-point temperature correlation contours are essentially circular.

The analysis of the components of the wind shear correlation tensor proceeds exactly as that of the wind component correlation tensor. The tensor terms should have almost the same "structure", i.e. the contours of constant shear correlation tensor component should be nearly coincident with the corresponding wind correlation tensor component if the assumption that the temperature correlations would be like the height correlations is made. This is not necessarily the case.

In the case of the height correlations, the assumption that height was a differentiable function was made. This assumption is somewhat less plausable in the case of temperatures. The nature of the correlation structure is intimately dependent on the character of the field of property (differentiable or not and if not the nature and "density" of its irregularities).

It was seen in Chapter VII that the standard deviations of wind shear may be expressed as

$$\overline{s_x^2} = \left(\frac{\partial \sigma_u}{\partial z}\right)^2 + 2\sigma_u^2 a_2,$$

$$\overline{s_y^2} = \left(\frac{\partial \sigma_v}{\partial z}\right)^2 + 2\sigma_v^2 b_2,$$

where a_2 and b_2 are the coefficients of the second order terms of the correlation of wind component as a function of height:

$$r_{uu} = 1 - a_2 z^2 + \text{---},$$

$$r_{vv} = 1 - b_2 z^2 + \text{---}.$$

From the above

$$\overline{s_x^2} + \overline{s_y^2} = \left(\frac{\partial \sigma_u}{\partial z}\right)^2 + \left(\frac{\partial \sigma_v}{\partial z}\right)^2 + 2(\sigma_u^2 a_2 + \sigma_v^2 b_2)$$

and if, also

$$\sigma_u^2 \cong \sigma_v^2 \cong \sigma^2/2$$

then

$$\overline{s_x^2} + \overline{s_y^2} \cong \left(\frac{\partial \sigma_v}{\partial z}\right)^2 + \frac{2\sigma_v^2}{D_o^2}$$

where D_o is a parameter which describes the "depth" of wind systems. This relation and the one derived from the geostrophic wind shear equations combine to give

$$\lambda^2\left[\left(\frac{\partial \sigma_v}{\partial z}\right)^2 + 2\frac{\sigma_v^2}{D_o^2}\right] \cong \left(\frac{g}{T_o}\right)^2\left[|\nabla \sigma_T|^2 + 2\frac{\sigma_T^2}{L_T^2}\right].$$

This relates the depth of wind disturbances with the size of temperature disturbances on an isobaric surface.

C. "UNIVERSAL" EXTRAPOLATION AND FORECAST METHODS

The usefulness of correlation structure in the extrapolation of weather parameters and in forecasting those parameter values may be illustrated by an analysis of an elementary least squares extrapolation or interpolation problem. Consider observations at P_1, ---, P_n where x_1, ---, x_n are observed and let P' be the point at which an extrapolated value, y, is required and assume that the extrapolation or forecast is to be a linear combination of the x_i's in the usual way. Then

$$y = b_1 x_1 + \text{---} + b_n x_n \tag{4}$$

(standard variables for convenience). The normal equations are

$$\begin{aligned} b_1 \quad &+ b_2 r_{12} + \text{---} + b_n r_{1n} = r_{1y} \\ b_1 r_{21} \; &+ b_2 \quad + \text{---} + b_n r_{2n} = r_{2y} \\ b_1 r_{n1} \; &+ b_2 r_{n2} + \text{---} + b_n r_n \quad = r_{ny} \end{aligned}$$

where $r_{ij} = r_{ji}$ are the correlation coefficients. If these are rewritten in general notation,

$$b_j a_{ij} = gi$$

$$a_{ij} = r_{ij}, \; (r_{ii} = 1), \; g_i = r_{iy}$$

then the solution for the coefficients is

$$b_j = g_i a^{ij}$$

where a^{ij} represents the element in the i'th row and j'th column of the inverse of the matrix of coefficients. Now since

$$y = b_j x_j$$

then

$$y = x_j g_i a^{ij} = g_i (x_j a^{ij}). \tag{5}$$

Consider now what is involved in the various quantities that have been used. First, the values of x_i are the observations made at a number of fixed points, P_1, ---, P_n. Second, the a^{ij} are the elements of the inverse of the matrix a_{ij} which are in turn the n^2 correlation coefficients that relate the observations at the same set of points. These quantities are known a priori from the past record, or from the structure of two-point correlations of the quantities concerned. As soon as the quantities, x_i, are known, then the terms $(x_j a^{ij})$ may be computed. Third, the correlations, $g_i = r_{iy}$, are the two-point correlations relating x_i at P_i with y at P'. In view of the fact that one is dealing with a field property, these correlation coefficients may be considered as known functions of the position of P' with respect to P_i. As a consequence, the location of P' may be considered variable and equation (5) may be considered as a least squares interpolation formula.

In the elementary form considered above, the interpolation aspects of the relationship are emphasized. The same relation may be used as a forecast formula if the time lag relations are included in the structure of the factors $g_i = r_{iy}$.

In the example above only observations x_i at point P_i were considered. This was to simplify the mode of expression. The technique is quite applicable to the case in which several quantities are observed at each P_i. For example, height and two wind components may be used and from these estimates at P' of height or either (or both) wind component may be made. In such an instance there would be n observation points but 3xn

predictors and three equations leading to the prediction of three quantities. In this particular instance the three sets of equations would have a common matrix of coefficients and would differ only in the terms $g_i = r_{i,y}$. Thus once the common inverse elements of (2) are obtained, there would be three sets of multipliers, g_i, one for each of the predicted quantities.

Several applications may be made to problems of practical importance. Some of these are listed below:

1. Checking for Erroneous Observations

In this case the value at P′ is observed and a value interpolated from surrounding observations. If the value observed differs from the interpolated value by more than a preassigned amount, the observation may be rejected as erroneous. Somewhat similar methods are used in actual practice, but are usually not based on the statistical structure of the field of property. For example, a relation of the form $\left[1 + (d/L_o)^2\right]^{-1}$ is used where the value of L_o is allowed to increase as further refinement of the test is required. This formula is acceptable as far as functional form is concerned, but to allow L_o to exceed the value imposed by the correlation coefficient structure amounts to smoothing the data beyond that which could be naturally present. Other smoothing techniques use a form in which the exponent of d/L_o is 4 instead of 2. Such formulas force a smoothing (or rejection) which is quite impossible since it can be easily shown that the exponent cannot exceed 2.

2. A Sage Problem

In transforming data from synoptic observations into values on a three-dimensional grid for the purpose of interceptor missile control, the preceding type of an extrapolation-interpolation-forecast method is unusually useful. It lends itself readily to computer applications in that the only stored elements need be the observation point and grid point co-ordinates together with the simple two-point correlation coefficient formula. Observations fed into the system can be transferred to the grid by direct interpolation-extrapolation and the time element in the g_i's may be used to up-date the information hour by hour (or minute by minute) until new observation information is introduced.

3. Artillery Problems

For Army operations in which data are available over a corps area, the above type of extrapolation provides an easily computerized procedure for arriving at expected parameter values in time and space, not only in the area of observations, but also extending into the surrounding areas. The method is independent of the location of the observation points so that it is applicable to a "fluid" situation in which the observation points may be changing from day to day.

4. Fleet Operations

Extrapolation from observation points that are in a state of continual change may be handled with nearly the same ease as the case of fixed observation points. The major requirement in this situation is merely that the observation must be

accompained by the co-ordinates of the point of observation when introduced into the computing procedure. In the other case (fixed observation points) these co-ordinates were considered as already tabulated in the procedure.

REFERENCES:

1. Durst, C. S., "The Variation of Wind with Time and Distance", Geophysical Memoirs, No. 93, Meteorological Office, Air Ministry, London, 1954

2. Spreen, W. C., The Distribution of the Temporal Wind Variation, (Unpublished), (Paper presented at the 148th Meeting of the A.M.S., Asheville, N. Carolina, 1 November 1956)

3. Ellsaesser, H. W., Wind Variability, (AWS TR 105-2), Air Weather Service Technical Report (MATS), U.S. Air Force, Wash., D.C., 10 March 1960

4. Buell, C. E., The Size of Height Systems on an Isobaric Surface, Report No. KN-61-16(R), AFCRL-404, Scientific Report No. 1, Contract No. AF19(604)-7282, Kaman Nuclear, Colorado Springs, Colorado, July, 1961

APPENDIX A-I

WIND COVARIANCE TENSOR COMPONENTS IN TERMS OF HEIGHT CORRELATIONS AND STANDARD DEVIATIONS

The equations (7) of Chapter III are derived here. The notation used is the same as that of the preceding chapters with additions where necessary. Let the geostrophic wind equations be written as

$$e_{i3k}\lambda_3 u_k = -g\cdot\frac{\partial h}{\partial x_i},\quad i = 1, 2, \tag{1}$$

where $\lambda_3 = \lambda$ = Coriolis parameter, u_k = wind component, g = acceleration of gravity, h = height of the isobaric surface, x_i = horizontal co-ordinate on an isobaric surface, $e_{i3k} = +1$ if i3k are in natural order, -1 if in reverse order, 0 if otherwise. The summation convention on repeated subscripts is being used. Here, and in what follows, the subscript conventions of ordinary cartesian tensors are employed. The reason for this becomes immediately evident since, if the calculations are carried out in component form, the bulk of the expressions is extremely cumbersome.

Since the equations (1) are linear in u_k and h, the symbols u_k and h may be understood to represent mean values, observed values, or departures from the mean. In the following, the symbols will be accepted as departures from the mean to simplify the ideas, means will be considered as taken over a sample of years or seasons or days at a fixed point (geographical location and isobaric level) though this restriction is somewhat stronger than is actually required.

The equations (1) are equally valid at all points so that the equations are understood to refer to a point P as written and to a point P′ if the symbols are suitably modified as in

$$e_{j3\ell}\lambda_3' u_\ell' = -g\cdot\frac{\partial h'}{\partial x_j'},\quad j = 1, 2. \tag{1'}$$

On multiplying equations (1) and (1′) together and taking mean values, indicated by the bar over the symbols,

$$e_{i3k}e_{j3\ell}\lambda_3\lambda_3'\overline{(u_k u_\ell')} = g^2\,\frac{\partial^2\overline{(hh')}}{\partial x_i\,\partial x_j'},\quad i, j = 1, 2, \tag{2}$$

where, on the right of (2), use has been made of the fact that h is a function of x_i and h′ is a function of x_j' only. The correlation function,* R_{hh}, is defined by the relation

$$\sigma\sigma' R_{hh} = \overline{(hh')} \tag{3}$$

where σ is the standard deviation of height at P and σ′ is the standard deviation of height at P′. As pointed out in Chapter III, the correlation function, R_{hh}, is a function of the location of P and P′. On the other hand, σ is a function of the location of P only and σ′ of P′ only. The differentiation of the right-hand side of (2) takes this situation into account:

$$\frac{\partial^2\overline{(hh')}}{\partial x_i\,\partial x_j'} = \sigma\sigma'\frac{\partial^2 R_{hh}}{\partial x_i\,\partial x_j'} + \frac{\partial\sigma}{\partial x_i}\sigma'\frac{\partial R_{hh}}{\partial x_j'} + \sigma\frac{\partial\sigma'}{\partial x_j'}\cdot\frac{\partial R_{hh}}{\partial x_i} + \frac{\partial\sigma}{\partial x_i}\cdot\frac{\partial\sigma'}{\partial x_j'}R_{hh}. \tag{4}$$

The height correlation function may be thought of as primarily a function of the location of P′ with respect to P which involves the location of P itself in a secondary sense. For

---

*The symbol R_{hh} is used instead of the usual symbol for such a correlation coefficient, r_{hh}, since the lower case r will be used later as the radial distance from P to P′.

example, if (r,θ) are the polar co-ordinates of P′ with respect to P and if one expresses the height correlation function in terms of a series of powers of r with coefficients as trigonometric polynomials in θ such as

$$R_{hh} = 1 - \left[a_1 + a_2\cos^2(\theta-\theta_0)\right]r^2 + \text{---} \tag{5}$$

the parameters a_1, a_2, θ_0, would be functions of the location of P itself. The values of these parameters might be thought of as being slowly varying functions of the location of P. Let the co-ordinates of P′ with respect to P, in cartesian form be given by ξ_i where

$$\begin{aligned} x_i' &= x_i^0 + \xi_i, \\ x_i &= x_i^0. \end{aligned} \tag{6}$$

Then

$$\frac{\partial}{\partial x_i} = \frac{\partial}{\partial x_i^0} - \frac{\partial}{\partial \xi_i}, \quad \frac{\partial}{\partial x_i'} = \frac{\partial}{\partial \xi_i}, \tag{7}$$

so that (using (3), (4), and (7)) (2) becomes (dropping the superscript ° as being superfluous)

$$e_{i3k}e_{j3\ell}\lambda_3\lambda_3'\overline{(u_k u_\ell')} = g^2\left\{\frac{\partial\sigma}{\partial x_i}\cdot\frac{\partial\sigma'}{\partial x_j'}R_{hh} + \sigma'\frac{\partial\sigma}{\partial x_i}\frac{\partial R_{hh}}{\partial \xi_j}\right. \tag{8}$$

$$\left. - \sigma\frac{\partial\sigma'}{\partial x_j'}\cdot\frac{\partial R_{hh}}{\partial \xi_i} - \sigma\sigma'\frac{\partial^2 R_{hh}}{\partial\xi_i\,\partial\xi_j'} + \sigma\left[\frac{\partial\sigma'}{\partial x_j'}\cdot\frac{\partial R_{hh}}{\partial x_i} + \sigma'\frac{\partial^2 R_{hh}}{\partial\xi_j\,\partial x_i}\right]\right\}.$$

The final term in brackets of equation (8) involves the fact that the correlation function R_{hh} is a function of the location of the point P. The relative location of P′ with respect to P is not shown by the notation in the derivatives of σ and σ′; the variables locating P and P′ separately are retained to emphasize the functional dependence of these quantities.

As noted by (5), the correlation function has a tendency to have an axis of symmetry. If such a direction is taken as that of θ_o, then it is convenient to express R_{hh} in terms of co-ordinates (r,s), $s = r\cdot\cos(\theta-\theta_o)$ (see Fig. III-2). Let λ_i denote a unit vector in the direction of θ_o and let ν_i be the unit vector in the direction PP'. Then $s = \xi_i\lambda_i$, $r^2 = \xi_i^2 = r^2\nu_i^2$, and then

$$\frac{\partial R_{hh}}{\partial \xi_i} = \frac{\partial R_{hh}}{\partial r}\nu_i + \frac{\partial R_{hh}}{\partial s}\lambda_i \tag{9}$$

and

$$\frac{\partial^2 R_{hh}}{\partial \xi_i\,\partial \xi_j} = \left(\frac{\partial^2 R_{hh}}{\partial r^2} - \frac{1}{r}\cdot\frac{\partial R_{hh}}{\partial r}\right)\nu_i\nu_j + \frac{1}{r}\cdot\frac{\partial R_{hh}}{\partial r}\delta_{ij} \tag{10}$$

$$+ \frac{\partial^2 R_{hh}}{\partial s^2}\lambda_i\lambda_j + \frac{\partial^2 R_{hh}}{\partial r\,\partial s}(\nu_i\lambda_j + \nu_j\lambda_i)$$

where

$$\delta_{ij} = 1 \text{ if } i = j \text{ and } \delta_{ij} = 0 \text{ if } i \neq j.$$

First, the expressions (9) and (10) are substituted into (8), then the identity

$$e_{i3k}e_{j3\ell}\overline{(u_k u_\ell')} = \delta_{ij}\overline{(u_k u_k')} - \overline{(u_j u_i')}$$

is used to obtain the wind component covariances on the left-hand side without the awkward triple-subscript expressions present, and finally the derivatives of the standard deviations of height are replaced by

$$\frac{\partial\sigma}{\partial x_i} = |\nabla\sigma|\mu_i, \quad \frac{\partial\sigma'}{\partial x_j'} = |\nabla\sigma'|\mu_j'$$

where $|\nabla\sigma|$, $|\nabla\sigma'|$ are the magnitudes of the gradient of the standard deviation of height and μ_i, μ_i' are the unit vectors

in the direction of this gradient at P and P′ respectively. The above three steps are performed with no conceptual difficulties, but the algebra is admittedly tedious. The final result is

$$\frac{\lambda\lambda'}{g^2}\overline{(u_i u_j')} = \sigma\sigma'\left[\left(\frac{\partial^2 R_{hh}}{\partial r^2} - \frac{1}{r}\cdot\frac{\partial R_{hh}}{\partial r}\right)\nu_i\nu_j + \frac{\partial^2 R_{hh}}{\partial s^2}\lambda_i\lambda_j + \frac{\partial^2 R_{hh}}{\partial r\,\partial s}(\nu_i\lambda_j + \nu_j\lambda_i)\right] \tag{11}$$

$$+ \frac{\partial R_{hh}}{\partial r}\left[\sigma|\nabla\sigma'|\nu_j\mu_i' - \sigma'|\nabla\sigma|\nu_i\mu_j\right]$$

$$+ \frac{\partial R_{hh}}{\partial s}\left[\sigma|\nabla\sigma'|\lambda_j\mu_i' - \sigma'|\nabla\sigma|\lambda_i\mu_j\right] - |\nabla\sigma||\nabla\sigma'|R_{hh}\mu_j\mu_i'$$

$$+ \delta_{ij}\left\{-\sigma\sigma'\left[\frac{\partial^2 R_{hh}}{\partial^2 r} + 2\frac{\partial^2 R_{hh}}{\partial r\,\partial s}\nu_k\lambda_k + \frac{\partial^2 R_{hh}}{\partial s^2}\right]\right.$$

$$+ |\nabla\sigma||\nabla\sigma'|R_{hh}\mu_k\mu_k' - \frac{\partial R_{hh}}{\partial r}\left[\sigma|\nabla\sigma'|\nu_k\mu_k' - \sigma'|\nabla\sigma|\nu_k\mu_k\right]$$

$$\left. - \frac{\partial R_{hh}}{\partial s}\left[\sigma|\nabla\sigma'|\lambda_k\mu_k' - \sigma'|\nabla\sigma|\lambda_k\mu_k\right]\right\}.$$

The terms of (11) are underscored in the same way as those of Chapter III, equations (7). The significance of the underscoring is, briefly,

Terms remaining if $R_{hh} = R_{hh}(r)$ and $|\nabla\sigma| \equiv 0$

Additional terms if $R_{hh} = R_{hh}(r,s)$, $|\nabla\sigma| \equiv 0$

Additional terms if $R_{hh} = R_{hh}(r)$, $|\nabla\sigma| \not\equiv 0$

Interaction terms when both $R_{hh} = R_{hh}(r,s)$, $|\nabla\sigma| \not\equiv 0$

When $R_{hh} = R_{hh}(r)$, $|\nabla\sigma| \equiv 0$, the wind covariance tensor is given by

$$\frac{\lambda\lambda'}{g^2}\overline{(u_i u_j')} = \sigma\sigma'\left[\left(\frac{\partial^2 R_{hh}}{\partial r^2} - \frac{1}{r}\cdot\frac{\partial R_{hh}}{\partial r}\right)\nu_i\nu_j - \delta_{ij}\frac{\partial^2 R_{hh}}{\partial r^2}\right]. \tag{12}$$

This tensor form is that of a two-dimensional isotropic turbulence. This situation is discussed in some detail in Chapter III.

When $R_{hh} = R_{hh}(r)$, $|\nabla\sigma| \neq 0$, the wind covariance tensor becomes

$$\frac{\lambda\lambda'}{g^2}(\overline{u_i u_j'}) = \sigma\sigma'\left(\frac{\partial^2 R_{hh}}{\partial r^2} - \frac{1}{r}\cdot\frac{\partial R_{hh}}{\partial r}\right)\nu_i\nu_j + \frac{\partial R_{hh}}{\partial r}\left[\sigma|\nabla\sigma'|\nu_j\mu_i' - \sigma'|\nabla\sigma|\nu_i\mu_j\right]$$
$$- |\nabla\sigma||\nabla\sigma'|R_{hh}\mu_j\mu_i' + \delta_{ij}\left\{-\sigma\sigma'\frac{\partial^2 R_{hh}}{\partial r^2} + |\nabla\sigma||\nabla\sigma'|R_{hh}\mu_k\mu_k'\right.$$
$$\left. - \frac{\partial R_{hh}}{\partial r}\left[\sigma|\nabla\sigma'|\nu_k\mu_k' - \sigma'|\nabla\sigma|\nu_k\mu_k\right]\right\} \qquad (13)$$

where the effect of curvature or unequal spacing of the contours of σ = constant is retained by the distinction between σ and σ', μ_i and μ_i', etc. The last term in braces may be considered as quite small. The expression (13) resembles the covariance tensor for a two-dimensional cylindrical or axisymmetric turbulence, except that the factor in brackets in the second term on the right contains a negative sign instead of a plus sign.

If one considers $R_{hh} = R_{hh}(r,s)$, $|\nabla\sigma| \equiv 0$, then the wind covariance tensor is given by

$$\frac{\lambda\lambda'}{g^2}(\overline{u_i u_j'}) = \sigma\sigma'\left\{\left[\left(\frac{\partial^2 R_{hh}}{\partial r^2} - \frac{1}{r}\cdot\frac{\partial R_{hh}}{\partial r}\right)\nu_i\nu_j + \frac{\partial^2 R_{hh}}{\partial s^2}\lambda_i\lambda_j\right.\right. \qquad (14)$$
$$\left. + \frac{\partial^2 R_{hh}}{\partial r\,\partial s}(\nu_i\lambda_j + \nu_j\lambda_i)\right]$$
$$\left. - \delta_{ij}\left[\frac{\partial^2 R_{hh}}{\partial r^2} + 2\frac{\partial^2 R_{hh}}{\partial r\,\partial s}\nu_k\lambda_k + \frac{\partial^2 R_{hh}}{\partial s^2}\right]\right\}$$

which is precisely the form of a two-dimensional homogeneous, axisymmetrical turbulence.

THE COVARIANCE TENSOR IN LONGITUDINAL AND TRANSVERSE COMPONENTS

To obtain the covariance tensor in terms of longitudinal and transverse co-ordinates, the rotation

$$u_\ell = u_i \nu_i$$

$$u_t = u_i e_{i3k} \nu_k$$

is used. Let the direction of ν_i be θ, of λ_i be θ_o, and of μ_i and μ_i' be ψ and ψ'. Then multiplying (11) by $\nu_i \nu_j$ and carrying out the consequent subscript summations

$$\frac{\lambda\lambda'}{g^2}(\overline{u_\ell u_\ell'}) = -\sigma\sigma'\left[\frac{1}{r}\cdot\frac{\partial R_{hh}}{\partial r} + \frac{\partial^2 R_{hh}}{\partial s^2}\sin^2(\theta-\theta_o)\right] \tag{15}$$

$$+ |\nabla\sigma||\nabla\sigma'|R_{hh}\left[\cos(\psi-\psi') - \cos(\theta-\psi)\cos(\theta-\psi')\right]$$

$$- \frac{\partial R_{hh}}{\partial s}\left\{\sigma|\nabla\sigma'|\left[\cos(\theta_o-\psi') - \cos(\theta-\theta_o)\cos(\theta-\psi')\right]\right.$$

$$\left. -\sigma'|\nabla\sigma|\left[\cos(\theta_o-\psi) - \cos(\theta-\theta_o)\cos(\theta-\psi)\right]\right\}.$$

To obtain $(\overline{u_t u_t'})$, multiply (11) by $e_{i3k}\nu_k e_{j3s}\nu_l$ and carry out the summations to obtain

$$\frac{\lambda\lambda'}{g^2}(\overline{u_t u_t'}) = -\sigma\sigma'\left[\frac{\partial^2 R_{hh}}{\partial r^2} + 2\frac{\partial^2 R_{hh}}{\partial r\,\partial s}\cos(\theta-\theta_o) + \frac{\partial^2 R_{hh}}{\partial s^2}\cos^2(\theta-\theta_o)\right] \tag{16}$$

$$+ |\nabla\sigma||\nabla\sigma'|R_{hh}\left[\cos(\psi-\psi') - \sin(\theta-\psi)\sin(\theta-\psi')\right]$$

$$- \frac{\partial R_{hh}}{\partial r}\left[\sigma|\nabla\sigma'|\cos(\theta-\psi') - \sigma'|\nabla\sigma|\cos(\theta-\psi)\right]$$

$$- \frac{\partial R_{hh}}{\partial s}\left\{\sigma|\nabla\sigma'|\left[\cos(\theta_o-\psi') - \sin(\theta-\theta_o)\sin(\theta-\psi')\right]\right.$$

$$\left. - \sigma'|\nabla\sigma|\left[\cos(\theta_o-\psi) - \sin(\theta-\theta_o)\sin(\theta-\psi)\right]\right\}.$$

The covariance $(\overline{u_\ell u_t'})$ is obtained by multiplying (1) by $\nu_i e_{j3k}\nu_k$

and is given by

$$\frac{\lambda\lambda'}{g^2}(\overline{u_\ell u_t'}) = \sigma\sigma'\left[\frac{\partial^2 R_{hh}}{\partial s^2}\cos(\theta-\theta_o)\sin(\theta-\theta_o) + \frac{\partial^2 R_{hh}}{\partial r\,\partial s}\sin(\theta-\theta_o)\right] \qquad (17)$$

$$- |\nabla\sigma|\,|\nabla\sigma'|R_{hh}\cos(\theta-\psi')\sin(\theta-\psi) - \sigma'|\nabla\sigma|\frac{\partial R_{hh}}{\partial r}\sin(\theta-\psi)$$

$$+ \frac{\partial R_{hh}}{\partial s}\left[\sigma|\nabla\sigma'|\cos(\theta-\psi')\sin(\theta-\theta_o) - \sigma'|\nabla\sigma|\cos(\theta-\theta_o)\sin(\theta-\psi)\right].$$

The covariance $(\overline{u_t u_\ell'})$, from multiplying (11) by $e_{i3k}\nu_k\nu_j$ is given by

$$\frac{\lambda\lambda'}{g^2}(\overline{u_t u_\ell'}) = \sigma\sigma'\left[\frac{\partial^2 R_{hh}}{\partial s^2}\sin(\theta-\theta_o)\cos(\theta-\theta_o) + \frac{\partial^2 R_{hh}}{\partial r\,\partial s}\sin(\theta-\theta_o)\right] \qquad (18)$$

$$- |\nabla\sigma|\,|\nabla\sigma'|R_{hh}\cos(\theta-\psi)\sin(\theta-\psi') + \sigma|\nabla\sigma'|\frac{\partial R_{hh}}{\partial r}\sin(\theta-\psi')$$

$$+ \frac{\partial R_{hh}}{\partial s}\left[\sigma|\nabla\sigma'|\cos(\theta-\theta_o)\sin(\theta-\psi') - \sigma'|\nabla\sigma|\sin(\theta-\theta_o)\cos(\theta-\psi)\right].$$

If now we use the approximations

$$L_\ell \cong \frac{\sigma g}{\lambda\sigma_\ell} \cong \frac{\sigma' g}{\lambda'\sigma_\ell'},\quad L_t \cong \frac{\sigma g}{\lambda\sigma_t} \cong \frac{\sigma' g}{\lambda'\sigma_t'}$$

where L is a size parameter, and if we assume that $\psi \cong \psi'$ and $|\frac{\nabla\sigma}{\sigma}| \cong |\frac{\nabla\sigma'}{\sigma'}|$, then (15) through (18) may be expressed in terms of correlation coefficients. Thus

$$\frac{r_{\ell\ell}}{L_\ell^2} \cong -\left[\frac{1}{r}\cdot\frac{\partial R_{hh}}{\partial r} + \frac{\partial^2 R_{hh}}{\partial s^2}\sin^2(\theta-\theta_o)\right] + \left|\frac{\nabla\sigma}{\sigma}\right|^2 R_{hh}\sin^2(\theta-\psi), \qquad (15a)$$

$$\frac{r_{tt}}{L_t^2} \cong -\left[\frac{\partial^2 R_{hh}}{\partial r^2} + 2\frac{\partial^2 R_{hh}}{\partial r\,\partial s}\cos(\theta-\theta_o) + \frac{\partial^2 R_{hh}}{\partial s^2}\cos^2(\theta-\theta_o)\right] \tag{16a}$$

$$+ \left|\frac{\nabla\sigma}{\sigma}\right|^2 R_{hh}\cos^2(\theta-\psi),$$

$$\frac{r_{lt}}{L_\ell L_t} \cong \left[\frac{\partial^2 R_{hh}}{\partial s^2}\cos(\theta-\theta_o) + \frac{\partial^2 R_{hh}}{\partial r\,\partial s}\right]\sin(\theta-\theta_o) \tag{17a}$$

$$- \left|\frac{\nabla\sigma}{\sigma}\right|^2 R_{hh}\sin(\theta-\psi)\cos(\theta-\psi)$$

$$- \left|\frac{\nabla\sigma}{\sigma}\right|\left[\frac{\partial R_{hh}}{\partial r}\sin(\theta-\psi) + \frac{\partial R_{hh}}{\partial s}\sin(\theta_o-\psi)\right],$$

$$\frac{r_{tl}}{L_\ell L_t} \cong \left[\frac{\partial^2 R_{hh}}{\partial s^2}\cos(\theta-\theta_o) + \frac{\partial^2 R_{hh}}{\partial r\,\partial s}\right]\sin(\theta-\theta_o) \tag{18a}$$

$$- \left|\frac{\nabla\sigma}{\sigma}\right|^2 R_{hh}\sin(\theta-\psi)\cos(\theta-\psi)$$

$$+ \left|\frac{\nabla\sigma}{\sigma}\right|\left[\frac{\partial R_{hh}}{\partial r}\sin(\theta-\psi) + \frac{\partial R_{hh}}{\partial s}\sin(\theta_o-\psi)\right].$$

In the case of (17a) and (18a), it is seen that the terms are grouped in pairs which may be separated in the expressions

$$\frac{r_{\ell t}+r_{t\ell}}{L_\ell L_t} = \frac{S}{L_\ell L_t} = 2\left(\frac{\partial^2 R_{hh}}{\partial s^2}\cos(\theta-\theta_o) + \frac{\partial^2 R_{hh}}{\partial r\,\partial s}\right)\sin(\theta-\theta_o) \tag{19}$$

$$-2\left|\frac{\nabla\sigma}{\sigma}\right|^2 R_{hh}\sin(\theta-\psi)\cos(\theta-\psi),$$

$$\frac{r_{\ell t}-r_{t\ell}}{L_\ell L_t} = \frac{D}{L_\ell L_t} = -2\left|\frac{\nabla\sigma}{\sigma}\right|\left[\frac{\partial R_{hh}}{\partial r}\sin(\theta-\psi) + \frac{\partial R_{hh}}{\partial s}\sin(\theta_o-\psi)\right]. \tag{20}$$

The underscoring of the terms in equations (15a), (16a), (19) and (20) correspond to that previously used on the terms of equation (11). The principle terms appear only in (15a) and

(16a), but each of these includes one group of terms due to the fact that R_{hh} may depend on s and a term that depends on the fact that $|\nabla\sigma| \not\equiv 0$. The expression for S contains terms for each of the latter types. The expression for D contains one term due to the fact that $|\nabla\sigma| \not\equiv 0$ and another term in the interaction between $|\nabla\sigma|$ and $R_{hh}(r,s)$. Thus in (20) the expression for D vanishes if $|\nabla\sigma| \equiv 0$. Note further that (20) is the only one of the four expressions in which $|\frac{\nabla\sigma}{\sigma}|$ appears to the first power. If $L\cdot|\frac{\nabla\sigma}{\sigma}|$ is reasonably small, one might say that (20) contains the primary effect of $|\nabla\sigma| \not\equiv 0$ and that this effect appears to "higher order" in the other expressions. If we let

$$R_{hh} = \exp\left[-\tfrac{1}{2}(\alpha^2 r^2 + \beta^2 s^2)\right]$$

where $$\alpha^2 = \frac{1}{L_1^2},\ \beta^2 = \frac{1}{L_2^2} - \frac{1}{L_1^2}$$

$$R_{hh} = 1 - \left[\frac{1}{L_1^2}\left(\frac{r^2}{2}\right) + \left(\frac{1}{L_2^2} - \frac{1}{L_1^2}\right)\left(\frac{s^2}{2}\right)\right] + \text{---}$$

$$= 1 - \left[\frac{1}{L_1^2} + \left(\frac{1}{L_2^2} - \frac{1}{L_1^2}\right)\cos^2(\zeta - \theta_o)\right]\frac{r^2}{2} + \text{---}$$

which introduces elliptical contours of R_{hh} = constant. Then

$$\frac{1}{r}\cdot\frac{\partial R_{hh}}{\partial r} = -\alpha^2\cdot\exp\left[-\tfrac{1}{2}(\alpha^2 r^2 + \beta^2 s^2)\right]$$

$$\frac{\partial^2 R_{hh}}{\partial r^2} = -\alpha^2(1 - \alpha^2 r^2)\exp\left[-\tfrac{1}{2}(\alpha^2 r^2 + \beta^2 s^2)\right]$$

$$\frac{\partial^2 R_{hh}}{\partial r\,\partial s} = \alpha^2\beta^2 rs\cdot\exp\left[-\tfrac{1}{2}(\alpha^2 r^2 + \beta^2 s^2)\right]$$

$$\frac{\partial^2 R_{hh}}{\partial s^2} = -\beta^2(1 - \beta^2 s^2)\exp\left[-\tfrac{1}{2}(\alpha^2 r^2 + \beta^2 s^2)\right]$$

$$\frac{\partial R_{hh}}{\partial s} = -\beta^2 s\cdot\exp\left[-\tfrac{1}{2}(\alpha^2 r^2 + \beta^2 s^2)\right]$$

so that

$$r_{\ell\ell} = L_\ell^2\alpha^2\left\{\left[1 + \frac{\beta^2}{\alpha^2}\cdot\sin^2(\theta-\theta_o) + \frac{1}{\alpha^2}\left|\frac{\nabla\sigma}{\sigma}\right|^2\sin^2(\theta-\psi)\right]\right.$$

$$\left. - \frac{r^2\beta^4}{\alpha^2}\sin^2(\theta-\theta_o)\cos^2(\theta-\theta_o)\right\}\cdot\exp\left[-\tfrac{1}{2}(\alpha^2r^2 + \beta^2s^2)\right],$$

$$r_{tt} = L_t^2\alpha^2\left\{\left[1 + \frac{\beta^2}{\alpha^2}\cos^2(\theta-\theta_o) + \frac{1}{\alpha^2}\left|\frac{\nabla\sigma}{\sigma}\right|^2\cos^2(\theta-\psi)\right]\right.$$

$$\left. - \alpha^2r^2\left[1 + \frac{\beta^2}{\alpha^2}\cos^2(\theta-\theta_o)\right]^2\right\}\cdot\exp\left[-\tfrac{1}{2}(\alpha^2r^2 + \beta^2s^2)\right]$$

$$S = -L_\ell L_t\alpha^2\left\{\frac{1}{\alpha^2}\left[\left|\frac{\nabla\sigma}{\sigma}\right|^2\sin 2(\vartheta-\psi) + \beta^2\sin 2(\theta-\theta_o)\right]\right.$$

$$\left. -\beta^2r^2\left[1 + \frac{\beta^2}{\alpha^2}\cos^2(\theta-\theta_o)\right]\sin 2(\theta-\theta_o)\right\}\cdot\exp\left[-\tfrac{1}{2}(\alpha^2r^2 + \beta^2s^2)\right],$$

$$D = -2L_\ell L_t\alpha^2r\left|\frac{\nabla\sigma}{\sigma}\right|\left\{\sin(\theta-\psi) - \frac{\beta^2}{\alpha^2}\cos(\theta-\vartheta_o)\sin(\vartheta_o-\psi)\right\} \times$$

$$\times \exp\left[-\tfrac{1}{2}(\alpha^2r^2 + \beta^2s^2)\right].$$

Since $\lim_{r\to 0} r_{\ell\ell} = 1$, $\lim_{r\to 0} r_{tt} = 1$,

$$\left[L_\ell^2\alpha^{2\ -1}\right] = 1 + \frac{\beta^2}{\alpha^2}\sin^2(\theta-\vartheta_o) + \frac{1}{\alpha^2}\left|\frac{\nabla\sigma}{\sigma}\right|^2\sin^2(\theta-\psi),$$

$$\left[L_t^2\alpha^{2\ -1}\right] = 1 + \frac{\beta^2}{\alpha^2}\cos^2(\theta-\vartheta_o) + \frac{1}{\alpha^2}\left|\frac{\nabla\sigma}{\sigma}\right|^2\cos^2(\theta-\psi),$$

which indicate a slight dependence of L_ℓ and L_t on the orientation angle θ, the azimuth of P′ relative to P. Then

$$r_{\ell\ell} = \left[1 - \frac{L_\ell^2\beta^4r^2}{4}\sin^2 2(\theta-\theta_o)\right]\exp\left[-\tfrac{1}{2}(\alpha^2r^2 + \beta^2s^2)\right], \qquad (21)$$

$$r_{tt} = \left[1 - L_t^2\alpha^4r^2\left(1 + \frac{\beta^2}{\alpha^2}\cos^2(\theta-\vartheta_o)\right]\exp\left[-\tfrac{1}{2}(\alpha^2r^2 + \beta^2s^2)\right]. \qquad (22)$$

From (21) and (22), the effect of the ellipticity of the height correlation contours introduces some modifications.

These would have complex effects on the shape of the contours of equal correlation coefficient. The exponential term, of course, preserves the over-all ellipticity of the height correlation contours, but the trigonometric terms in the first factor would induce some additional irregularities at the larger distances. These would appear at those distances where the correlations are small and where the numerical values of the observed correlations are uncertain. The effects appear to be due primarily to the ellipticity of the height correlation contours, $\beta \neq 0$. The effect of the gradient of the standard deviation of height are hidden in the factors L_ℓ and L_t.

The effects of non-homogeneity ($|\nabla\sigma| \neq 0$) and lack of isotropy ($\beta \neq 0$) appear clearly as the reason for $S \neq 0$ and $D \neq 0$. When only the dominant terms are retained, $L_\ell L_t \cong L^2$,

$$S = -\left[L^2\left|\frac{\nabla\sigma}{\sigma}\right|^2 \sin 2(\theta-\psi) + L^2\beta^2 \sin 2(\theta-\theta_0)\right]\cdot\exp\left[-\tfrac{1}{2}(\alpha^2 r^2 + \beta^2 s^2)\right], \quad (23)$$

$$D = -2rL\left|\frac{\nabla\sigma}{\sigma}\right|\cdot\sin(\theta-\psi)\cdot\exp\left[-\tfrac{1}{2}(\alpha^2 r^2 + \beta^2 s^2)\right]. \quad (24)$$

From (23) the effect of $|\nabla\sigma|$ and β are combined to form an expression

$$S = -A\cdot\sin 2(\theta-\varphi)\cdot\exp\left[\tfrac{1}{2}(\alpha^2 r^2 + \beta^2 s^2)\right],$$

where

$$A^2 = L^4\left\{\left[\beta^2\cos 2\theta_0 + \left|\frac{\nabla\sigma}{\sigma}\right|^2\cos 2\psi\right]^2 + \left[\beta^2\sin 2\theta_0 + \left|\frac{\nabla\sigma}{\sigma}\right|\sin 2\psi\right]^2\right\},$$

$$\tan\varphi = \frac{\beta^2\sin 2\theta_0 + \left|\frac{\nabla\sigma}{\sigma}\right|^2\sin 2\psi}{\beta^2\cos 2\theta_0 + \left|\frac{\nabla\sigma}{\sigma}\right|^2\cos 2\psi}.$$

The function S is discontinuous at $r = 0$ and that the contours of constant S form a four-leafed clover pattern with $S = 0$ on the directions $\theta = \varphi + k\frac{\pi}{2}$, $k = 0, 1, 2, 3$, and with values of S alternating sign in the quadrants between them. The extreme values of S are at the discontinuity point. The magnitude of the discontinuity at $r = 0$ is due to both the gradients of the standard deviation of height and the "ellipticity" of the contours of the height correlation.

The expression for D in (24) is dominated by the factor in gradient of the standard deviation of height. If the height field were homogeneous, this expression would be zero. The expected contours of constant D form a pattern of two centers, one of positive value and the other of negative value separated by a line along which $D = 0$ that lies in the direction of ψ, the direction of the gradient of the standard deviation of height. The extreme values are approximately $\pm 2L^2\left|\frac{\nabla\sigma}{\sigma}\right| \cdot e^{-2}$ and are located at a distance of $r = L$.

APPENDIX A-II

SPECIAL CONSIDERATIONS REGARDING THE DETERMINATION OF L AND k FROM THE UNIVERSITY OF WISCONSIN DATA

The University of Wisconsin wind component correlation tensor data requires special consideration. The majority of the data on wind correlations has been calculated from the actually-observed winds, or at least from data that purports to closely approximate such winds. The University of Wisconsin correlations were calculated from basic height data using height differences between points 10° latitude or longitude (generally) apart. These height differences were multiplied by the appropriate constants to convert them into geostrophic wind components. Consequently, the correlations are not between geostrophic wind components at two points, but between average geostrophic wind components over two (sizable) intervals. The correlations thus calculated tend to be larger than the correlations that would be obtained were it possible to use geostrophic wind components at a point. The amount of the difference between such averaged components and point components is an increasing function of the length of the interval over which the averaging is done.

The correction for the fact that average instead of point winds are used may be derived in the following manner. Let u_a, u_a' be the components of the averaged geostrophic wind, let u, u' be the components of the true geostrophic wind, let the averaging interval be of lengths η and ξ centered at P and P′

respectively. Then

$$u_a = -\frac{g}{\lambda}\cdot\frac{h\,\frac{\eta}{2} - h - \frac{\eta}{2}}{\eta} = -\frac{g}{\lambda}\cdot\frac{1}{\eta}\int_{-\eta/2}^{\eta/2}\frac{\partial h}{\partial y}\,dy = \frac{1}{\eta}\int_{-\eta/2}^{\eta/2} u\,dy,$$

$$v_a = \frac{g}{\lambda}\cdot\frac{h\,\frac{\xi}{2} - h - \frac{\xi}{2}}{\xi} = \frac{g}{\lambda}\cdot\frac{1}{\xi}\int_{-\xi/2}^{\xi/2}\frac{\partial h}{\partial x}\,dx = \frac{1}{\xi}\int_{-\xi/2}^{\xi/2} v\,dx.$$

Then

$$\overline{u_a u_a'} = \frac{1}{\eta\eta'}\int_{-\eta/2}^{\eta/2}\int_{-\eta'/2}^{\eta'/2}\overline{(uu')}\,dy\,dy'.$$

As long as P and P′ are separate, the covariance of the averages (left side) is nearly the same as the average of the covariances (right side)

$$\overline{u_a u_a'} \cong \overline{uu'}$$

However, when P′ coincides with P, this approximation is no longer valid. (Actually it becomes valid as P′ approaches P, but in using grid data, this situation is seldom encountered.) In this case $\eta = \eta'$ but the double integral form is maintained since on the right the points at which u and u′ are determined are independently distributed on the interval $(-\eta/2, +\eta/2)$ about P.

Now let
$$\begin{aligned}\overline{uu'} &= \sigma_u\sigma_u' r_{uu} \\ &= \sigma_u(y)\sigma_u'(y')r_{uu}(y,y') \\ &= \sigma_u(y)\sigma_u'(y')r(y'-y).\end{aligned}$$

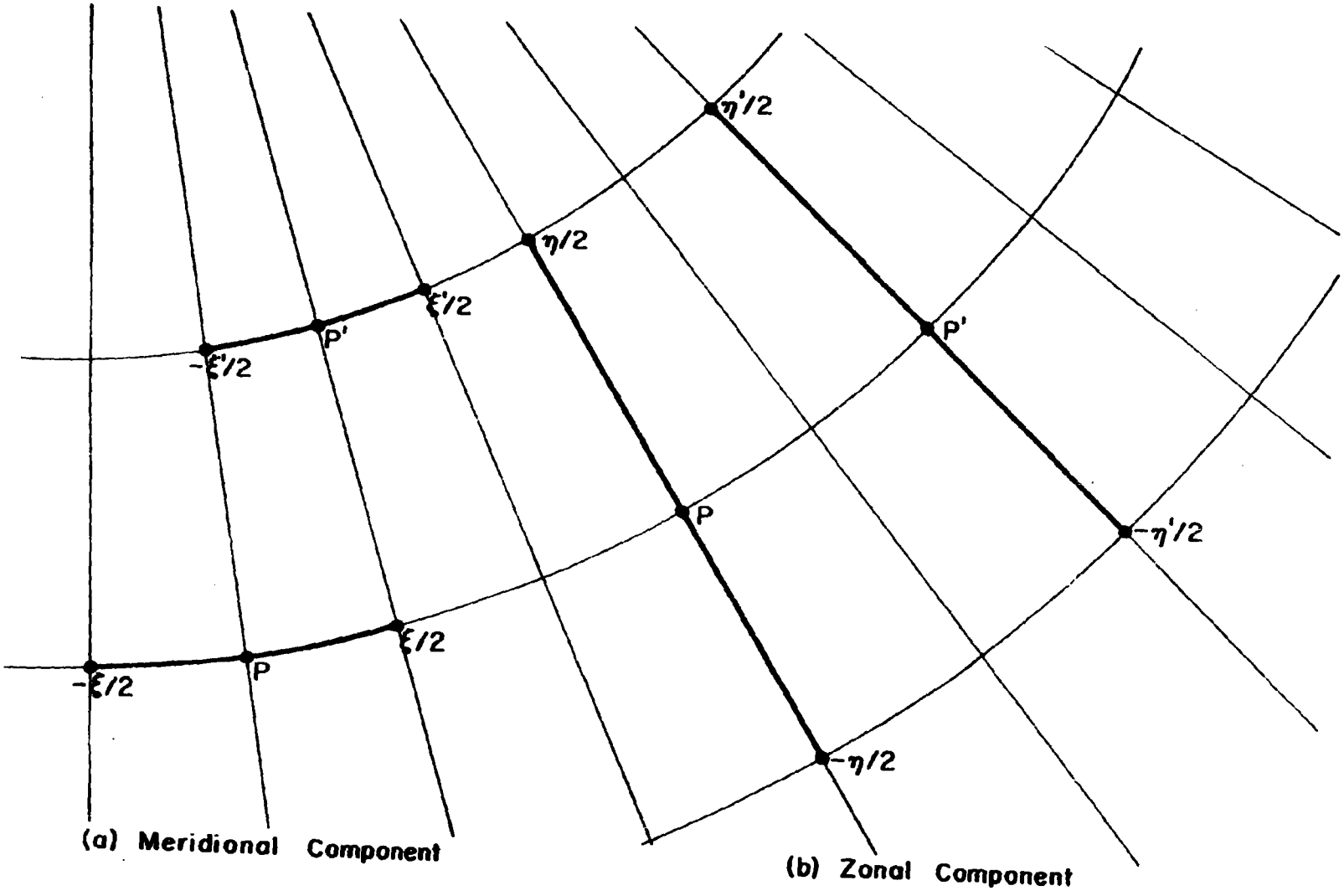

Fig. A-II-1 Geometry of Relations Connecting Averaged and Point Geostrophic Wind Component

Substituting this expression into the integral and using mean values for σ_u and σ_u', one has, approximately

$$(\overline{u_a^2}) \cong \frac{\overline{u^2}}{\eta^2} \int_{-\eta/2}^{+\eta/2} \int_{-\eta/2}^{\eta/2} r_{uu}(y'-y)\, dy\, dy'.$$

Changing variables to $Z = y' - y$

$$(\overline{u_a^2}) = \frac{\overline{u^2}}{\eta^2} \int_{-\eta/2}^{\eta/2} \left[\int_{-y-\eta/2}^{-y+\eta/2} r_{uu}(Z) dZ \right] dy.$$

Note that $r_{uu}(Z)$ is the <u>transverse</u> wind component correlation function. A rough approximation for this function appears to be

$$r_{uu}(= r_{tt}) \cong (1 - \alpha^2 Z^2) e^{-\alpha^2 Z^2/2}.$$

On making this substitution and integrating

$$\overline{u_a^2} = \overline{u^2} \cdot \frac{2}{\alpha^2 \eta^2} \left(1 - e^{-\alpha^2 \eta^2/2}\right) = \overline{u^2} \left[f(\alpha\eta) \right].$$

Table I gives values of $f(\alpha\eta)$ as a function of $\alpha\eta$.

TABLE I

VALUES OF $f(\alpha\eta)$.

$\alpha\eta$	$\left[f(\alpha\eta)\right]^{-1}$
0.0	1.00
0.2	1.012
0.4	1.041
0.6	1.082
0.8	1.128
1.0	1.289

We have seen that $L=\alpha^{-1}$ has values in the range of 500 to 600 n mi. If the length of the averaging interval is 10° latitude, then $\alpha\eta$ is in the range 0.8 to 1.0 and the standard deviation of the average is from 10% to 30% higher than the standard deviation of the point average.

In the case of the meridional wind component, the value of $\alpha\eta$ is, of course, modified by the factor $\cos\varphi$. Consequently, at 60° north, the underestimate of the standard deviation by using an average geostrophic wind is much less for the meridional rather than the zonal component. (From the above table, if L = 8° latitude, the excess is 4% for the meridional component as compared with 13% for the zonal component where the grid point spacing is the full 10° of latitude.)

In the applications to wind component correlations in transverse and longitudinal form, this correction appears in the standard deviations (variances):

$$\overline{u_\ell^2} = (\overline{u^2})\cos^2\theta + 2(\overline{uv})\sin\theta\cos\theta + (\overline{v^2})\sin^2\theta$$

$$\overline{u_t^2} = (\overline{u^2})\sin^2\theta - 2(\overline{uv})\sin\theta\cos\theta + (\overline{v^2})\cos^2\theta$$

as correcting the first and last terms on the right. If several approximations are made, $\overline{u^2} \cong \overline{v^2} >> \overline{uv}$, then

$$\overline{u_\ell^2} \cong (\overline{u_\ell^2})_a \left[\frac{\cos^2\theta}{f(\alpha\eta)} + \frac{\sin^2\theta}{f(\alpha\eta\cos\varphi)}\right] = (\overline{u_\ell^2})_a \cdot G_1$$

$$\overline{u_t^2} \cong (\overline{u_t^2})_a \left[\frac{\sin^2\theta}{f(\alpha\eta)} + \frac{\cos^2\theta}{f(\alpha\eta\cos\varphi)}\right] = (\overline{u_t^2})_a \cdot G_2$$

where θ is the orientation angle of P′ with respect to P (measured

counterclockwise from east), $(\overline{u_\ell^2})_a$ and $(\overline{u_t^2})_a$ are the variances computed from the averaged geostrophic winds, and in which we have written $\eta\cos\varphi$ as the length of the averaging interval for the meridional component which effectively designates η as measured in degrees (in the one case degrees of latitude and in the other case degrees of longitude).

It is readily seen that the correction factor as a function of θ, oscillates between $1/f(\alpha\eta)$ and $1/f(\alpha\eta\cos\varphi)$. The correction applied to the correlations appears in the forms

$$r_{\ell\ell} = (r_{\ell\ell})_a\sqrt{G_1 G_1'} \qquad r_{t\ell} = (r_{\ell t})_a\sqrt{G_2 G_1'}$$

$$r_{\ell t} = (r_{\ell t})_a\sqrt{G_1 G_2'} \qquad r_{tt} = (r_{tt})_a\sqrt{G_2 G_2'}$$

in which $(r_{\alpha\beta'})_a$ indicates the value computed from average components and the prime on G_1 or G_2 refers to the point P′.

The implications of the preceding analysis to the University of Wisconsin correlation data lies principally in the interpretation of the value of k. This parameter was previously described as containing the effects of smaller scale eddies and observation error. In connection with the correlations derived from the University of Wisconsin data, it must be interpreted in terms of the differences between averaged and point geostrophic wind components, and, of course, the fact that averaged geostrophic components instead of real wind components are used.*

---

*Of course, winds are observed by techniques that make use of an average of some kind, altitude, time, etc. The point becomes important for practical purposes when the averaging interval reaches a size comparable with the definition required for the study at hand.

The values for $L^{=\alpha^{-1}}$ derived from the location of the zeros, minima, etc. of the correlation functions are not involved in this correction for using averaged winds since the numerical values of the correlations are not involved direction.

APPENDIX A-III

REPRESENTATION OF THE CORRELATION COEFFICIENT

A. CONDITIONS IMPOSED FROM SYMMETRY

Let H be an observed quantity, a function of a single variable, H(x), and let the values considered by the departure from a suitable mean value. Let r(h,x) be the correlation coefficient of H with itself at two points, x and x + h. Assume that r(h,x) has an infinite series expansion in powers of h with coefficients which are functions of x. Then

$$r(h,x) = a_0(x) + a_1(x)h + a_2(x)\frac{h^2}{2!} + \text{---} + a_n(x)\frac{h^n}{n!} + \text{---}$$

The correlation values at x and x + h must be the same as those at (x+h)-h and (x+h)

$$r(h,x) = r(-h,x+h)$$

and

$$r(-h,x+h) = a_0(x+h) - a_1(x+h)h + a_2(x+h)\frac{h^2}{2!} + \text{---}$$
$$+ a_n(x+h)\frac{(-h)^n}{n!} + \text{---}$$

If, now, the coefficients also have series expansions in powers of h,

$$r(-h,x+h) = a_0 + a_0'h + a_0''\frac{h^2}{2!} + \text{---} + a_0^{(j)}\frac{h^j}{j!} + \text{---}$$
$$- h(a_1 + a_1'h + a_1''\frac{h^2}{2!} + \text{---} + a_1^{(j-1)}\frac{h^{j-1}}{(j-1)!} + \text{---})$$
$$+ \frac{h^2}{2!}(a_2 + a_2'h + a_2''\frac{h^2}{2!} + \text{---} + a_2^{(j-2)}\frac{h^{j-2}}{(j-2)!} + \text{---})$$
$$- + - \text{---}$$
$$+ \frac{(-h)^n}{n!}(a_n + a_n'h + a_n''\frac{h^2}{2!} + \text{---} + a_n^{(j-n)}\frac{h^{j-n}}{(j-n)!} + \text{---})$$
$$+ \text{---}.$$

On collecting terms in like powers of h from this second expression and equating these to the coefficients of the first expansion in powers of h, one obtains the system of equations:

$$a_0 = a_0,$$

$$a_1 = -a_1 + a_0',$$

$$\frac{a_2}{2!} = \frac{a_2}{2!} - a_1' + \frac{a_0''}{2!},$$

$$\frac{a_3}{3!} = -\frac{a_3}{x!} + \frac{a_2'}{2!} - \frac{a_1''}{2!} + \frac{a_0'''}{3!},$$

$$\frac{a_4}{4!} = \frac{a_4}{4!} - \frac{a_3'}{3!} + \frac{a_2''}{2!2!} - \frac{a_1'''}{3!} + \frac{a^{iv}}{4!},$$

--- ---

It is seen at once that the even subscripted terms are independent but that the odd subscripted terms depend on the preceding even subscripted terms. Thus

$$a_1 = \tfrac{1}{2}\cdot a_0',$$

$$\frac{a_3}{3!} = \frac{a_2'}{2!} - \frac{1}{24}\cdot a_0''',$$

$$\frac{a_5}{5!} = \tfrac{1}{2}\cdot\frac{a_4'}{4!} - \frac{1}{24}\cdot\frac{a_3'''}{2!} + \frac{a_0^{v}}{2\cdot 5!},$$

$$\frac{a_7}{7!} = \tfrac{1}{2}\cdot\frac{a_6'}{6!} - \frac{1}{24}\cdot\frac{a_4'''}{4!} + \frac{1}{2\cdot 5!}\cdot\frac{a_2^{v}}{2!} - \frac{17}{4\cdot 7!}\cdot a_0^{vii},$$

--- ---

Since as a rule one is interested in the case of $a_0 = 1$, then

$$r(h,x) = 1 + \frac{a_2}{2!}\cdot h^2 + \tfrac{1}{2}\cdot\frac{a_2'}{2!}\cdot h^3 + \frac{a_4}{4!}\cdot h^4 + \left(\tfrac{1}{2}\cdot\frac{a_4'}{4!} - \frac{1}{24}\cdot\frac{a_2'''}{2!}\right)h^5$$

$$+ \frac{a_6}{6!}\cdot h^6 + \left(\tfrac{1}{2}\cdot\frac{a_6'}{6!} - \frac{1}{4!}\cdot\frac{a_4'''}{4!} + \frac{a_2^{v}}{4\cdot 5!}\right)h^7 + \text{---}.$$

It is seen that, if the "shape" of the correlation function changes from place to place (i.e., the coefficients are indeed

non-trivial functions of x, $a_n \neq$ constant, n = 2, 3, ---) then the correlation function expansion contains odd powers of h and the correlation curve is not symmetrical with respect to h = 0.

The situation is somewhat more general than indicated in the above. If it is assumed that

$$r(h,x) = 1 - A(x)|h|^{\alpha} - |h|^{\alpha}\omega(h,x), \quad 0 < \alpha \leq 2$$

where

$$\omega(h,x) = b_1(x)h + b_2(x)\frac{h^2}{2!} + \text{---}$$

then the condition

$$r(h,x) = r(-h,x+h)$$

requires that

$$A = A,$$

$$b_1 = -b_1 + A',$$

$$\frac{b_2}{2!} = \frac{b_2}{2!} - b' + \frac{A''}{2!},$$

$$\frac{b_3}{3!} = -\frac{b_3}{3!} + \frac{b_2'}{2!} - \frac{b_1''}{2!} + \frac{A'''}{3!},$$

--- ---

These are the same equations as obtained before with $a_0 = 1$, $a_1 = 0$, $a_2/2! = -A$, $a_3/3! = -b_1$, $a_4/4! = -b_2$, etc.

Consequently, the correlation function need not approach a_0 (or 1) as a quadratic ($1 - h^2/2\lambda^2 + \text{---}$) but may approach its limit value in any of the permissible ($0 < \alpha \leq 2$) ways. When the field of variable correlated is not homogeneous (i.e., when the coefficients of the expansion are not constant, independent of x) then the correlation function will contain "odd" power terms and will not be symmetrical with respect to the value h = 0.

A somewhat different aspect of this property is discussed in the next section in the case of a differentiable field of property being correlated.

B. EXPANSION FOR AN ANALYTIC FUNCTION

If H(x) possess a power series expansion (is an analytic function), then

$$H(x+h) = H + H'h + H''\frac{h^2}{2!} + \text{---} + H^{(n)}\frac{h^n}{n!} + \text{---}$$

and the covariance of H is given by

$$\overline{H(x)H(x+h)} = (\overline{H^2}) + (\overline{HH'})h + (\overline{HH''})\frac{h^2}{2!} + \text{---} + (\overline{HH^{(n)}})\frac{h^n}{n!} + \text{---}$$

where it is assumed that the means appearing as coefficients exist. In terms of the correlation coefficient

$$\overline{H(x)H(x+h)} = \sigma(x)\sigma(x+h)r(h,x)$$

$$= \sigma_o(\sigma_o + \sigma_o'h + \sigma_o''\frac{h^2}{2!} + \text{---})(1 + a_1h + a_2\frac{h^2}{2!} + \text{---}).$$

Multiplying the two series and equating the coefficients with those of the other expansion above,

$$\overline{H^2} = \sigma_o^2,$$

$$(\overline{HH'}) = a_o\sigma_o^2 + \sigma_o\sigma_o',$$

$$\overline{(HH'')}/2! = a_2\sigma_o^2/2! + a_1\sigma_o\sigma_o' + \sigma_o\sigma_o''/2!,$$

$$\overline{(HH''')}/3! = a_3\sigma_o^2/3! + a_2\sigma_o\sigma_o'/2! + a_1\sigma_o\sigma_o''/2! + \sigma_o\sigma_o'''/3!,$$

--- ---

From the first and second equations, it is seen at once that $a_1 = 0$ (as before). The left-hand terms may be developed as follows:

$$(\overline{H^2}) = \sigma_o^2$$

$$\overline{HH'} = \sigma_o\sigma_o' = \tfrac{1}{2}(\sigma_o^2)'$$

$$(\overline{HH''}) + (\overline{H'H'}) = \tfrac{1}{2}(\sigma_o^2)'', \quad (\overline{HH''}) = -\sigma_1^2 + \tfrac{1}{2}(\sigma_o^2)''$$

where $(\overline{H'H'}) = \sigma_1^2$. Continuing,

$$(\overline{HH'''}) + (\overline{H'H''}) = -(\sigma_1^2)' + \tfrac{1}{2}(\sigma_0^2)''', \quad (\overline{H'H''}) = \tfrac{1}{2}(\sigma_1^2)'$$

so that

$$(\overline{HH'''}) = -\frac{3}{2}(\sigma_1^2)' + \tfrac{1}{2}(\sigma_0^2)'''.$$

Further

$$(\overline{HH^{iv}}) = \sigma_2^2 - 2(\sigma_1^2)'' + \tfrac{1}{2}(\sigma_0^2)^{iv}$$

$$(\overline{HH^{v}}) = \frac{5}{2}(\sigma_2^2)' - \frac{5}{2}(\sigma_1^2)''' + \tfrac{1}{2}(\sigma_0^2)^{v}$$

--- ---

where $(\overline{H''H''}) = \sigma_2^2$, etc.

Substituting the values for the covariances $(\overline{HH^{(n)}})$ and solving for the a_n's, one obtains

$$\frac{a_2}{2!} = \tfrac{1}{2}\left(-\frac{\sigma_1^2}{\sigma_0^2} + \frac{(\sigma_0')^2}{\sigma_0^2}\right),$$

$$\frac{a_3}{3!} = -\tfrac{1}{4}\cdot\frac{(\sigma_1^2)'}{\sigma_0} + \tfrac{1}{2}\cdot\frac{\sigma_0'\sigma_0''}{\sigma_0^2} + \tfrac{1}{2}\cdot\frac{\sigma_1^2}{\sigma_0^2}\left(\frac{\sigma_0'}{\sigma_0}\right) - \tfrac{1}{2}\left(\frac{\sigma_0'}{\sigma_0}\right)^3,$$

--- ---.

The expressions for the coefficients become quite complex when the conditions for homogeneity are not satisfied, i.e., $\sigma_0' \neq 0$, etc.

The above terms are a generalization of the well-known case for a homogeneous analytic random function that is simply expanded in the form

$$r(h,x) = \sum_0^\infty (-1)^n \left(\frac{\sigma_n}{\sigma_0}\right)^2 \frac{h^{2n}}{(2n)!}$$

where

$$\sigma_n^2 = (\overline{H^{(n)}H^{(n)}}).$$

If the expansion of the correlation function is written as

$$r(h,x) = 1 - \tfrac{1}{2}\cdot\frac{h^2}{L^2} + \text{---}$$

then

$$\frac{1}{L^2} = \frac{\sigma_1^2}{\sigma_o^2} - \frac{(\sigma_o')^2}{\sigma_o^2}$$

or

$$\sigma_1^2 = \frac{\sigma_o^2}{L^2} + \left(\frac{d\sigma_o}{dx}\right)^2.$$

If H represents height on an isobaric surface, then H' would represent a wind component (with appropriate factors) and one obtains the well-known relation between the standard deviation of wind and the standard deviation of height where L plays the role of the parameter that describes the size of height disturbances.

If H represents a wind component, say the east pointing component, u, and x is in the vertical direction, then σ_1 is the standard deviation of the east pointing component of the wind shear. The value of L^2 may be obtained from the radius of curvature of the correlation of wind with height at h = 0 (this corresponds to a "depth" of wind systems). It is seen that the standard deviation of wind shear is made up of two parts, one is the combination of the standard deviation of wind divided by a depth parameter, the other is due to the non-homogeneity of wind with height. Note that in the above application one is finding the standard deviation of wind shear due to the differentiable part of the wind. It is necessary to consider the relation

$$r^* = k_o(1 - h^2/2L^2 + ---)$$

in finding L and to note that

$$k_o = 1/(1 + \overline{e^2}/\sigma_u^2)$$

where $\overline{e^2}$ is the mean square value of the observation error and the non-differentiable part of the wind (i.e., the part due to small eddies of depth less than a depth commensurate with the averaging depth of wind observations).

APPENDIX A-IV

GAUSS' PROCEDURE

In the case of the parameters A, B, C, D, E, and F of the equations on page V-27, a simple least squares procedure is impossible. As a consequence, an iterative method of solution is used. The major steps of the procedure are outlined here.

The equations consist of pairs which may be represented schematically as follows:

$$y_1 = F_1(r,\theta;A_1,---,A_6),$$
$$y_2 = F_2(r,\theta;A_1,---,A_6).$$

The estimates on the right are considered equally important in the determination of the parameters A_1, ---, A_6 (corresponding to A, ---, F respectively). Consequently, the sum of the squares of the residuals from the two equations together are minimized. Thus

$$\sum\left[(y_1-F_1)^2 + (y_2-F_2)^2\right] = \text{Minimum.}$$

The usual procedure of differentiating with respect to the parameters and setting these derivatives to zero leads to the equations

$$\sum\left[(y_1-F_1)\frac{\partial F_1}{\partial A_i} + (y_2-F_2)\frac{\partial F_2}{\partial A_i}\right] = 0,\ i = 1,\ ---,\ 6.$$

This produces six equations in the six parameters, A_1, ---, A_6. The parameter values are involved in complex expressions which cannot be solved simply; i.e., each of the six equations is so complex that it cannot be solved for the parameter values in the usual explicit form.

Consequently, an iterative method of solution is used. This is obtained by using the Taylor expansion of the functions F_1 and F_2.

$$F_1 = F_1^{(o)} + \frac{\partial F_1}{\partial A_1}\Delta A_1 + \text{---} + \frac{\partial F_1}{\partial A_6}\Delta A_6 + \text{---},$$

$$F_2 = F_2^{(o)} + \frac{\partial F_2}{\partial A_2}\Delta A_2 + \text{---} + \frac{\partial F_2}{\partial A_6}\Delta A_6 + \text{---},$$

where $F_1^{(o)}$ and $F_2^{(o)}$ indicate that the function is evaluated at the initial parameter values $A_1^{(o)}$, ---, $A_6^{(o)}$. It is assumed that the derivatives are evaluated at the same point, but this is not shown specifically to keep notation complications within reason. When this substitution is made and the terms rearranged, the preceding equations become:

$$\left[\overline{\left(\frac{\partial F_1}{\partial A_1}\right)^2} + \overline{\left(\frac{\partial F_2}{\partial A_1}\right)^2}\right]\Delta A_1 + \left[\overline{\left(\frac{\partial F_1}{\partial A_1}\cdot\frac{\partial F_1}{\partial A_2}\right)} + \overline{\left(\frac{\partial F_2}{\partial A_1}\cdot\frac{\partial F_2}{\partial A_2}\right)}\right]\Delta A_2 + \text{---}$$

$$+ \left[\overline{\left(\frac{\partial F_1}{\partial A_1}\cdot\frac{\partial F_1}{\partial A_6}\right)} + \overline{\left(\frac{\partial F_2}{\partial A_1}\cdot\frac{\partial F_2}{\partial A_6}\right)}\right]\Delta A_6 = \left[\overline{\left((F_1 - y_1)\frac{\partial F_1}{\partial A_1}\right)} + \overline{\left((F_2 - y_2)\frac{\partial F_2}{\partial A_1}\right)}\right],$$

$$\text{---} \qquad\qquad \text{---}$$

$$\left[\overline{\left(\frac{\partial F_1}{\partial A_6}\cdot\frac{\partial F_1}{\partial A_1}\right)} + \overline{\left(\frac{\partial F_2}{\partial A_6}\cdot\frac{\partial F_2}{\partial A_1}\right)}\right]\Delta A_1 + \left[\overline{\left(\frac{\partial F_1}{\partial A_6}\cdot\frac{\partial F_1}{\partial A_2}\right)} + \overline{\left(\frac{\partial F_2}{\partial A_6}\cdot\frac{\partial F_2}{\partial A_2}\right)}\right]\Delta A_2 + \text{---}$$

$$+ \left[\overline{\left(\frac{\partial F_1}{\partial A_6}\right)^2} + \overline{\left(\frac{\partial F_2}{\partial A_6}\right)^2}\right]\Delta A_6 = \left[\overline{\left((F_1 - y_1)\frac{\partial F_1}{\partial A_6}\right)} + \overline{\left((F_2 - y_2)\frac{\partial F_2}{\partial A_6}\right)}\right].$$

The bars inside the square brackets are to call attention to the fact that these expressions are summed over the data values. The higher order terms on the left, indicated by ---, are neglected. All of the coefficients are evaluated at the initial parameter estimate, $A_1^{(o)}$, ---, $A_6^{(o)}$. The set of equations is then solved

for $\Delta A_1^{(0)}$, ---, $\Delta A_6^{(0)}$. These determine the new estimates, $A_1^{(1)} = A_1^{(0)} + \Delta A_1^{(0)}$, ---, $A_6^{(1)} = A_6^{(0)} + \Delta A_6^{(0)}$. The coefficient values are then recomputed from the new parameter values, $A_1^{(1)}$, ---, $A_6^{(1)}$ and further increments are obtained:

$$A_1^{(2)} = A_1^{(1)} + \Delta A_1^{(1)}, \quad ---, \quad A_6^{(2)} = A_6^{(1)} + \Delta A_6^{(1)}.$$

The process is continued until the additional increments are considered sufficiently small or until some other convergence criterion is satisfied.

In the particular case at hand, the iterative sequence was stopped when $\Delta A/A \leq 10^{-2}$. This insured a reasonably small amount of computation and in view of the small change in the residuals this degree of accuracy was considered sufficient.

The residuals were calculated directly from the initial expression to be minimized. In using such an iterative procedure, the indirect estimate from the calculated coefficients and the non-homogeneous terms of the normal equations do not provide a legitimate estimate of the sum of squares of the residuals.

DISTRIBUTION LISTS

(One copy each distributed except as indicated)

Code	Organization
	LIST G-A
1-1	Science Advisor Department of State Washington 25, D.C. (U)
1-6	Office of Secretary of Defense (DDR and E, Tech. Library) Washington 25, D.C. (U)
2-2	Institute of Technology Library MCLI-LIB, Building 125, Area B Wright-Patterson Air Force Base, Ohio
2-4	Hq. USAF (AFCSA, Secretary) Washington 25, D.C.
2-6	Hq. USAF (AFRDR) Washington 25, D.C.
2-8	AFCRL, OAR (CRIPA) Stop 39 (20) L. G. Hanscom Field Bedford, Massachusetts
2-9	ARL (ARA-2) Library AFL 2292, Building 450 Wright-Patterson Air Force Base, Ohio
2-10	ESD (ESRDG) L. G. Hanscom Field Bedford, Massachusetts
2-14	ASD (ASAPRD-Dist) Wright-Patterson Air Force Base, Ohio
2-16	ACIC (ACDEL-7) 2d and Arsenal St. Louis 18, Missouri (U)
2-19	NAFEC LIBRARY BRANCH, Building 3 Atlantic City, New Jersey Attention: RD-702
2-107	AWS (AWSSS/SIPD) Scott AFB, Illinois
2-119	A. U. (Library) Maxwell AFB, Alabama
2-33	Hq. AFCRL, OAR (CRIP, J. R. Marple) L. G. Hanscom Field Bedford, Massachusetts
3-8	Dept. of the Army (SIGRD-8-B-5) Washington 25, D.C.
3-9	Technical Documents Center Evans Signal Labs. Belmar, New Jersey
4-20	Technical Reports Librarian U.S. Naval Postgraduate School Monterey, California (U)
4-25	Director U.S. Naval Research Laboratory Code 2027 Washington 25, D.C.

DISTRIBUTION LISTS (CONTINUED)

Code	Organization
	LIST G-A
4-41	ONR (Geophysics Code N-416) Office of Naval Research Washington 25, D.C.
5-9	Documents Expediting Project (UNIT X) Library of Congress Washington 25, D.C. (U)
5-14	Superintendent of Documents Government Printing Office Washington 25, D.C. (U)
5-65	ASTIA (TIPAA) (10) Arlington Hall Station Arlington 12, Virginia
5-18	National Research Council 2101 Constitution Avenue Washington 25, D.C. (U)
5-23	NASA Attention: Library, Code AFET-LA Stop 85 Washington 25, D.C.
5-26	Librarian Boulder Laboratories National Bureau of Standards Boulder, Colorado (U)
5-28	Library National Bureau of Standards Washington 25, D.C. (U)
5-46	Director of Meteorological Research U.S. Weather Bureau Washington 25, D.C. (U)
5-53	Library U.S. Weather Bureau Suitland, Maryland (U)
6-87	Director, USAF Project RAND The Rand Corporation 1700 Main Street Santa Monica, California Thru: A. F. Liaison Office
6-90	Dr. William W. Kellogg Rand Corporation 1700 Main Street Santa Monica, California (U)
7-8	Mr. Malcolm Rigby American Meteorological Society P.O. Box 1736 Washington 13, D.C. (U)
7-35	Institute of Aerospace Sciences, Inc. 2 East 64th Street New York 21, New York (U)
8-5	Library Geophysical Institute University of Alaska P.O. Box 938 College, Alaska (U)

Code	Organization
	LIST G-A
8-41	Dr. Joseph Kaplan Department of Physics University of California Los Angeles, California (U)
8-47	Professor Fred L. Whipple Harvard College Observatory 60 Garden Street Cambridge 38, Massachusetts (U)
8-48	Dr. David Fultz Department of Geophysical Sciences University of Chicago Chicago 37, Illinois (U)
8-365	Dr. A. M. Peterson Stanford University Stanford, California (U)
8-366	Professor Clarence Palmer Institute of Geophysics University of California Los Angeles 24, California (U)
9-5	Technical Information Office European Office, Aerospace Research Shell Building, 47 Cantersteen Brussels, Belgium (U)
9-11	Dr. John F. Gabites Officer in Charge of Research New Zealand Meteorological Service P.O. Box 722 Wellington, New Zealand
9-116	Defence Research Member (2) Canadian Joint Staff 2450 Massachusetts Avenue, N.W. Washington 8, D.C.
	Hq. AFCRL-OAR (Remaining Copies) (CRZWD, Irving I. Gringorten) L. G. Hanscom Field Bedford, Massachusetts
	LIST G-E
2-20	AFCRL, OAR (CRZW) 1065 Main Street Waltham, Massachusetts
2-21	AFCRL, OAR (CRZH) L. G. Hanscom Field Bedford, Massachusetts
5-22	1st Weather Wing APO 915 San Francisco, California
5-24	3rd Weather Wing Offutt AFB, Nebraska
5-25	8th Weather Group Randolph AFB, Texas
5-32	2nd Weather Group Langley AFB, Virginia

DISTRIBUTION LISTS (CONTINUED)

Code	Organization
	LIST G-E
5-33	Climatic Center USAF Annex 2, 225 D Street, S. E. Washington 25, D.C.
5-35	2nd Weather Wing APO 633 New York, New York
5-36	4th Weather Wing 421 First National Bank Building Colorado Springs, Colorado
5-37	9th Weather Group Scott AFB, Illinois
5-42	4th Weather Group Andrews AFB Washington 25, D.C.

Code	Organization
	SUPPLEMENTAL LIST
	Michigan State University Department of Statistics East Lansing, Michigan ATTENTION: Project Director AF 19(628)-355
	University of California at Berkeley Statistical Laboratory Berkeley, California ATTENTION: Project Director AF 19(604)-8051
	Dr. C. L. Godske Professor of Theoretical Meterology University of Bergen Bergen, Norway
	Dr. R. Sneyers Institut Royal Meterologique de Belgique Avenue Circulaire 3 Uccle-Bruxelles 18, Belgium

AD

TWO-POINT VARIABILITY OF WIND, by C. E. Buell, July, 1962, (In three Volumes) 152 p., 205 p., 165 p., resp., incl. tables, illus. Final Report, Contract No. AF19(604)7282, Project 8624, Task 86242, Geophysics Research Directorate, Air Force Cambridge Research Laboratories, Office of Aerospace Research, United States Air Force, Bedford, Mass. (Prepared by Kaman Nuclear, Colorado Springs, Colo.) AFCRL-62-889(I), (II), and (III).

The variability of wind at two points is treated in terms of the components of the wind correlation tensor reduced to correlation coefficient form. It is shown that two of the components are of major importance and are quite distinct from each other, the longitudinal correlation coefficient and the transverse correlation coefficient. The remaining two components are relatively less important. Wind correlation data from several sources are assembled and analyzed. Such data cover the four seasons, levels from 850 mb to 100 mb, representative locations in the northern hemisphere, and time lags from -2 days to +2 days. A simple empirical form is used to describe the behavior of the correlation tensor components. It is found that for zero time lag the correlations may be described in terms of two parameters, one which measures the effect of observation error and the small scale eddies, the other a scale parameter which measures the size of the synoptic scale wind systems. When the time lag is not zero or when the two points are not on the same isobaric surface, even the simplest description of the correlations requires additional parameters that measure the rate of decay of correlation maximum with time, the tilt of the axis of the

(over)

UNCLASSIFIED

1. Wind Variability (meteorology) - Northern Hemisphere
2. Wind Variability (meteorology) - Applications
3. Wind Variability (meteorology) - Synoptic Scale
4. Wind Variability (meteorology) - Meso Scale
5. Wind Variability (meteorology) - Tensor Components

I. C. E. Buell

AD

TWO-POINT VARIABILITY OF WIND, by C. E. Buell, July, 1962, (In three Volumes) 152 p., 205 p., 165 p., resp., incl. tables, illus. Final Report, Contract No. AF19(604)7282, Project 8624, Task 86242, Geophysics Research Directorate, Air Force Cambridge Research Laboratories, Office of Aerospace Research, United States Air Force, Bedford, Mass. (Prepared by Kaman Nuclear, Colorado Springs, Colo.) AFCRL-62-889(I), (II), and (III).

The variability of wind at two points is treated in terms of the components of the wind correlation tensor reduced to correlation coefficient form. It is shown that two of the components are of major importance and are quite distinct from each other, the longitudinal correlation coefficient and the transverse correlation coefficient. The remaining two components are relatively less important. Wind correlation data from several sources are assembled and analyzed. Such data cover the four seasons, levels from 850 mb to 100 mb, representative locations in the northern hemisphere, and time lags from -2 days to +2 days. A simple empirical form is used to describe the behavior of the correlation tensor components. It is found that for zero time lag the correlations may be described in terms of two parameters, one which measures the effect of observation error and the small scale eddies, the other a scale parameter which measures the size of the synoptic scale wind systems. When the time lag is not zero or when the two points are not on the same isobaric surface, even the simplest description of the correlations requires additional parameters that measure the rate of decay of correlation maximum with time, the tilt of the axis of the

(over)

UNCLASSIFIED

1. Wind Variability (meteorology) - Northern Hemisphere
2. Wind Variability (meteorology) - Applications
3. Wind Variability (meteorology) - Synoptic Scale
4. Wind Variability (meteorology) - Meso Scale
5. Wind Variability (meteorology) - Tensor Components

I. C. E. Buell

AD

TWO-POINT VARIABILITY OF WIND, by C. E. Buell, July, 1962, (In three Volumes) 152 p., 205 p., 165 p., resp., incl. tables, illus. Final Report, Contract No. AF19(604)7282, Project 8624, Task 86242, Geophysics Research Directorate, Air Force Cambridge Research Laboratories, Office of Aerospace Research, United States Air Force, Bedford, Mass. (Prepared by Kaman Nuclear, Colorado Springs, Colo.) AFCRL-62-889(I), (II), and (III).

The variability of wind at two points is treated in terms of the components of the wind correlation tensor reduced to correlation coefficient form. It is shown that two of the components are of major importance and are quite distinct from each other, the longitudinal correlation coefficient and the transverse correlation coefficient. The remaining two components are relatively less important. Wind correlation data from several sources are assembled and analyzed. Such data cover the four seasons, levels from 850 mb to 100 mb, representative locations in the northern hemisphere, and time lags from -2 days to +2 days. A simple empirical form is used to describe the behavior of the correlation tensor components. It is found that for zero time lag the correlations may be described in terms of two parameters, one which measures the effect of observation error and the small scale eddies, the other a scale parameter which measures the size of the synoptic scale wind systems. When the time lag is not zero or when the two points are not on the same isobaric surface, even the simplest description of the correlations requires additional parameters that measure the rate of decay of correlation maximum with time, the tilt of the axis of the

(over)

UNCLASSIFIED

1. Wind Variability (meteorology) - Northern Hemisphere
2. Wind Variability (meteorology) - Applications
3. Wind Variability (meteorology) - Synoptic Scale
4. Wind Variability (meteorology) - Meso Scale
5. Wind Variability (meteorology) - Tensor Components

I. C. E. Buell

AD

correlation maximum in the vertical, and the downstream displacement of the correlation maximum with time. Parameters to measure the gradient of the basic one point wind variability and the departure of the systems from circular form are required to adequately describe the behavior of the minor wind correlation tensor components.

Several applications of the methods of correlation analysis are discussed.

The structure of the longitudinal and transverse components of the wind correlation tensor are extended down to a distance of the order of a mile through the use of wind data from aircraft.

UNCLASSIFIED

UNCLASSIFIED

AD

correlation maximum in the vertical, and the downstream displacement of the correlation maximum with time. Parameters to measure the gradient of the basic one point wind variability and the departure of the systems from circular form are required to adequately describe the behavior of the minor wind correlation tensor components.

Several applications of the methods of correlation analysis are discussed.

The structure of the longitudinal and transverse components of the wind correlation tensor are extended down to a distance of the order of a mile through the use of wind data from aircraft.

UNCLASSIFIED

UNCLASSIFIED

AD

correlation maximum in the vertical, and the downstream displacement of the correlation maximum with time. Parameters to measure the gradient of the basic one point wind variability and the departure of the systems from circular form are required to adequately describe the behavior of the minor wind correlation tensor components.

Several applications of the methods of correlation analysis are discussed.

The structure of the longitudinal and transverse components of the wind correlation tensor are extended down to a distance of the order of a mile through the use of wind data from aircraft.

UNCLASSIFIED

UNCLASSIFIED

AD

correlation maximum in the vertical, and the downstream displacement of the correlation maximum with time. Parameters to measure the gradient of the basic one point wind variability and the departure of the systems from circular form are required to adequately describe the behavior of the minor wind correlation tensor components.

Several applications of the methods of correlation analysis are discussed.

The structure of the longitudinal and transverse components of the wind correlation tensor are extended down to a distance of the order of a mile through the use of wind data from aircraft.

UNCLASSIFIED

UNCLASSIFIED